Prof. Dr. G. PERSOONE

BELGIAN NATIONAL R-D PROGRAM

ON THE ENVIRONMENT

WATER

Sea Project

MATHEMATICAL MODEL

Annual Report

December 1974

IV

First Part

Laboratorium voor
Biologisch Onderzoek
van Waterverontreiniging
en Marikultuur
Jozef Plateaustraat, 22
B - 9000 GENT
Tel. 091/25.73.71 (post 4106)

Office of the Prime Minister

Interministerial Commission for Science Policy

MATHEMATICAL MODEL

Annual Report

December 1974

IV

First Part

BELGIAN NATIONAL R-D PROGRAM

ON THE ENVIRONMENT

WATER

Sea Project

MATHEMATICAL MODEL

Annual Report

December 1974

IV

First Part

Office of the Prime Minister

Interministerial Commission for Science Policy

é. t. a. b. é. t. y. p.
quai de Longdoz, 72
4000 LIÈGE
Tél. 42.59.21

TABLE OF CONTENTS

Chapter I - Hydrodynamic models and their implications in the transient and and residual circulations, mud deposition and soil erosion, chemical and ecological dynamics in the Southern Bight of the North Sea

I.- The Southern Bight model in the North Sea modelling effort 10
II.- The hydrodynamic submodels 16
1.- Tidal and storm surge model (transient state) 16
2.- Residual circulation model 19
3.- Results of computations 22
III.- Mud deposition in the Southern Bight 31
IV.- Ecosystems dynamics in the Southern Bight 34
V.- Dispersion and sedimentation around a dumping ground 37
VI.- Bottom erosion 45
1.- Introduction 45
2.- Mass conservation law for the sediment bed 46
3.- The boundary condition at the bed-fluid interface 47
4.- The density distribution in a cohesive sediment bed 51
5.- The interface mass flux continuity 53
6.- The solution for the erosion flux 56
7.- An approximate expression of the erosion flux 59
8.- Comparison with experiment 60

Chapter II - I. A mathematical model of microbial and chemical oxidation-reduction processes in the Scheldt estuary

Introduction 69
1.- Experimental results 72
2.- General principles of the model 72
3.- Mathematical resolution 77
4.- Results and discussion 80

II. Determination of Cu, Pb, Cd, Zn in sea water by anodic stripping voltammetry. A first approach to the problem of the speciation of heavy metals in sea water

Introduction 86
1.- Determination of Cu, Cd, Pb, Zn in sea water 88
2.- Preliminary comparison between ASV and atomic absorption 104

III. Mass transfer in disturbed sediments

Introduction 109
1.- Experimental 111
2.- Results 113
3.- Kinetic model for dissolved silica 118
4.- Kinetic model of nitrogen diagenesis 122

IV. Sorption by some North Sea sediments 138

Chapter III - Data acquisition and processing

I. Automatic acquisition of meteorological and oceanographic data : further developments and first results

Introduction 159
1.- The data acquisition system 160
2.- The sensors 163
3.- First results 166

II. Present state and prospects of data processing

1.- Data treatment : an overview 173
2.- Present state of the data base and its associated software . . 174
3.- Guidelines for the building of the data base and processing software 179
4.- Requirements for the portability of the storage format and of the software 180
5.- General description of the software 182
6.- The data storage standard format 182
Appendix I - Specification of the wind field for real-time processing and forecasting 184
Appendix II 192

Chapter IV - Study of the contamination of fish and shell fish

1.- Heavy metals 195
2.- Pesticides and P.C.B. 206

Chapter V - Inventory of the water- and sediment pollution

I. Coastal zone 210

1.- Emissions 210
2.- Immixture (mixing zone in the sea) 213
3.- Organisms on the breakwaters 217

II. Rivers 225

1.- Hydrographic basin of the river Meuse 225
2.- Hydrographic basin of the river Scheldt 233
3.- Hydrographic basin of the river Yser 240
4.- Hydrographic basin of the river Rhine 240

III. General conclusions 242

1.- Progress of works 242
2.- General synthesis of the results 243
3.- Further studies 244

IV. Appendix - List of record cards 245

Chapter VI - Physiological effects of some pollutants

1.- Phytoplankton 247
2.- Invertebrates 257
3.- Vertebrates 271
4.- General conclusions 293

Chapter I

Hydrodynamic models and their implications in the transient and residual circulations, mud deposition and soil erosion, chemical and ecological dynamics in the Southern Bight of the North Sea

by

Jacques C.J. NIHOUL

Based on work by ADAM Y., DE BACKER J.L., LAMBERMONT J., LEBON G., NIHOUL J.C.J., RONDAY F.C.
Geophysical Fluid Dynamics Groups, Universities of Liège and Louvain.

This chapter is a synthesis of recent advances of the Math. Modelsea programme prepared as a working document for internal circulation and for presentation to the International Council for the Exploration of the Sea. The material is taken from recent progress reports and published papers and books. References should be made to the original publications.

I.- *THE SOUTHERN BIGHT MODEL IN THE NORTH SEA MODELLING EFFORT*

Based on :

- Math. Modelsea (1974), I.C.E.S. Hydrography Committee, C.M. 1974 - C : 1;
- NIHOUL J.C.J. (1975a), Modelling of Marine Systems, Elsevier Publ., Amsterdam;
- NIHOUL J.C.J. (1975b), Application of Mathematical Models to the Study, Monitoring and Management of the North Sea, in "Ecological Modelling in a Resource Management Framework", Resources for the Future, Washington D.C.

Mathematical models of the North Sea have been developed in most of the bordering countries. The national efforts are now coordinated by the Joint North Sea Modelling Group initiated by JONSIS (the Joint North Sea Information System) reporting to I.C.E.S. (the International Council for Exploration of the Sea). Data are provided by international surveys called JONSDAP (Joint North Sea Data Acquisition Program).

In an earlier stage, the models tended to address separately the Physics, the Chemistry and the Biology of the North Sea. Now, the development of computing facilities allowing more ambitious programs, these models are progressively integrated in a common, general, interdisciplinary model with the purpose of understanding the North Sea environment, predicting its evolution, — taking into account the constraints of modern society — , and assisting its management.

The distinction, between complex research models and simple, oriented management models, is avoided. Management models are regarded as "subsets" of the general multipurpose model, derived from it to answer specific questions with the degree of sophistication which the objectives, on the one hand, the reliability of data, on the other hand, recommend.

The different stages in the elaboration of the mathematical model and of its submodels are shown in figure 1.

1.-

The mathematical description of the system is confronted with the data base constituted from existing or newly acquired data (*e.g.* Jonsdap campaigns, Belgian five years' survey of the Eastern part of the Southern Bight, ...). The data base provides information for :

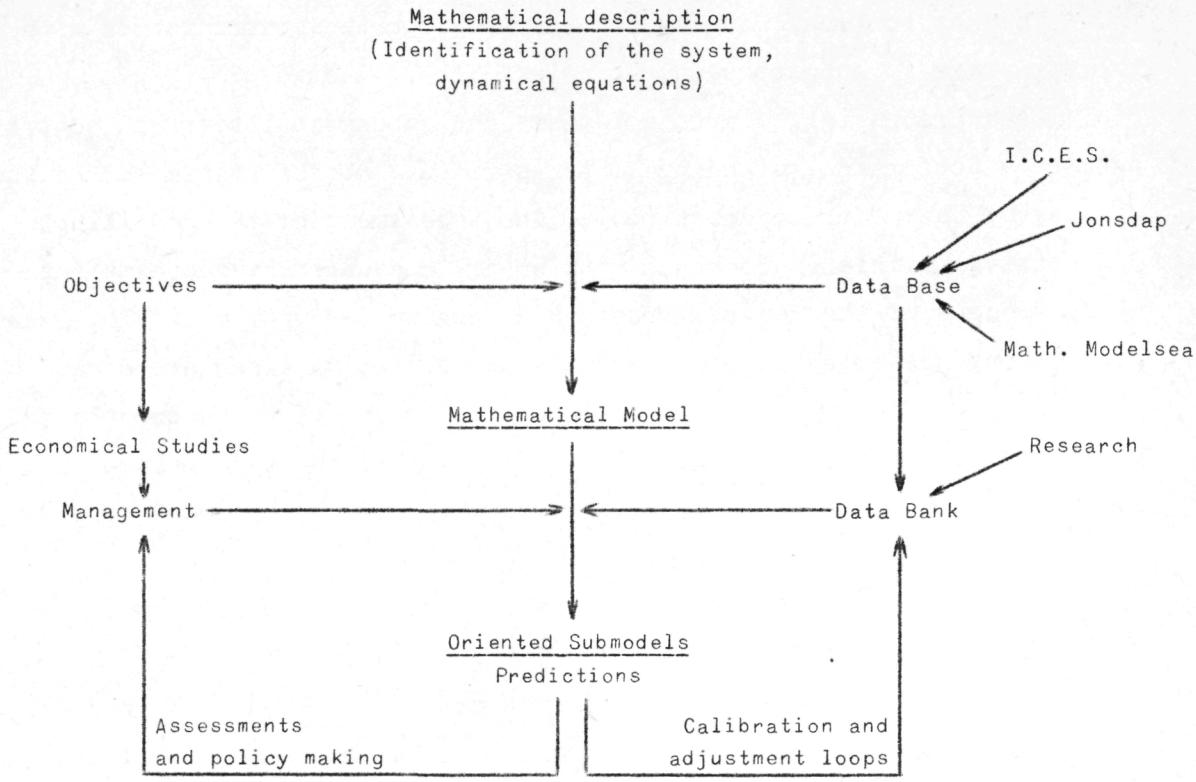


fig. 1.

i) a correlation study suggesting variables which are not significantly interrelated and between which interactions may be disregarded,

ii) an orders of magnitude study indicating variables and processes which can be neglected,

iii) a sensitivity analysis evaluating the degree of refinement which is required in the specification of state variables and interaction laws,

iv) a dialogue with the users of the model allowing a more precise definition of the objectives and indicating the degree of sophistication which is required to produce reliable predictions answering the questions put to the model without unnecessary expensive complexity.

2.-

The mathematical model which emerges from the confrontation with the data base is submitted to the scientific reflection.

Data processing, simulation tests and fundamental research contribute to a better understanding of the structure of the system and of the ability of the model to describe it. The assessment of the modelling prospective efficiency combined with specific management requests determines subsets of the general model which can be used for reliable, speedy predictions answering limited purposes and assisting immediate decisions.

The calibration, adjustment and exploitation of the submodels feed back information in the general model whose development, combined with new requests from management objectives, gives birth to second generation submodels with increased reliability.

A continuous interaction between research and application is thus achieved in the guiding framework of mathematical modelling.

To proceed from a general mathematical description to a tractable mathematical model and later to more limited submodels one can :

1) reduce the *support*, *i.e.* the extent of the system in physical space and time either by :
   i) narrowing the field of investigation or
   ii) averaging over one or several space coordinates or over time,

2) reduce the *scope*, *i.e.* the dimensions of the system in state space either by
   i) closing the system at a limited number of state variables (allowing for the global effect of other less essential parameters in adjustable coefficients) or
   ii) averaging over suitably defined compartments of which only the aggregate properties, not the details, are described.

The operating models of the North Sea can all be regarded as reduced size versions of an interdisciplinary three-dimensional model on which one or several simplifications were performed as described above.

i) Integration over depth and reasonable hypotheses on the vertical density distribution have allowed the development of two-dimensional models of tides and storm surges.

ii) Further time integration (over a time sufficiently long to cover several tidal periods and thus cancel to a large extent tidal oscillations and transitory wind currents) has given the residual circulation model where the results of tidal computations are used to calculate the forcing due to non-linear tidal interactions.

iii) Tidal and residual models have been exploited to evaluate the dispersion and the advection of marine constituents and to elaborate dispersion models adapted to the study of coastal discharges of pollutants and off-shore dumpings.

iv) The hydrodynamic models have revealed distinctive marine regions where different current regimes prevail and which appear as natural boxes for the elaboration of completely space integrated time dependent chemical and ecological box models.

Chemical and ecological models have also been simplified by restricting attention to the aggregate properties of compartments such as dissolved substances, suspensions, bottom sediments, phytoplankton, zooplankton, heterotrophic bacteria, fish, ...

The Southern Bight model developed in Belgium demonstrated that in this shallow area of extremely variable depth, the dispersion of pollutants was dominated by the shear effect associated with the vertical variations of very intense tidal currents. The predictions of the size and the shape of patches of pollutants after a release were found in excellent agreement with the observations.

The presence of residual gyres was identified as a major factor in the sedimentation pattern and the existence of ecological niches where distinct ecosystems prevail.

In particular, the gyre discovered off the eastern Belgian coast succeeded in explaining the observed accumulation of mud and heavy metals in the bottom sediments along the coast by the entrainment and prolonged residence of highly turbid waters from the Scheldt estuary.

The model showed that the gyre created, in that region, outer-lagoon conditions characterized by high nutrient concentrations and phytoplankton biomass but little zooplankton grazing and intensive

recycling of nutrients by bacteria (revealing a rather unhealthy short-circuited food chain where additional releases of nutrients might create the conditions of entrophication).

A nutrient cycle box model was elaborated with special emphasis on the coastal gyre region. On that basis, models were derived to simulate the translocation of pollutants (such as heavy metals) from the water column, through the food chain, to the consumable fish. The predicted concentrations in fish were found in good agreement with the measured concentrations in sampled specimens.

Applications and assistance to management

The Southern Bight model can predict with great accuracy the elevation of the water surface produced by tides and storm surges, the dispersion, sedimentation — and eventual recirculation by strong turbulence — of suspended material as well as the final deposition of sediments on the bottom. It can simulate the effect of coastal engineering works (dredging, construction of a harbour, ...) and can give full assistance to management in this respect.

By revealing the existence of distinctive regions where different circulation regimes prevail, the model identified ecological regions which are the natural boxes for adjacent box models describing the dynamics of the Bight's ecosystems. These models can evaluate the fluxes of carbon, nitrogen, ... , pollutants, ... through the food chain and provide an estimate of the anticipated fish population and level of pollution. In this respect the model can assist Public Health decision. Equivalently, it can elaborate on Public Health tolerances to determine acceptable upper bounds for the pollutants' concentrations in coastal waters or sediments.

The model can predict the dispersion pattern of pollutants both in the water column and in the sediments. By evaluating the extent of the dammage produced by a given coastal or off-shore release, the model can thus appreciate the opportunity of authorizing or penalizing dumpings in the sea and assist management decision. Furthermore, determining the transfer functions which relate the intensity of the source (the amount

released) and the final concentrations in the sea, the model, working backwards from Public Health tolerances, can set up for management the problem of optimizing, subject to economical constraints, the tolerable inputs and the locations of sources of pollution, coastal outfalls and sea dumpings.

II.- THE HYDRODYNAMIC SUBMODELS

Based on :
- Math. Modelsea (1974), I.C.E.S. Hydrography Committee, C.M. 1974 - C : 1;
- NIHOUL J.C.J. (1975a), Modelling of Marine Systems, Elsevier Publ., Amsterdam;
- NIHOUL J.C.J. and RONDAY F.C. (1975), Tellus, 27, 5;
- RONDAY F.C. (1975), Ph. D. Dissertation, Liège University.

The models used in this study are depth averaged models which are the most popular (and economical) in shallow barotrophic areas. Let

$$x_3 = - h(x_1, x_2)$$

be the equation of the bottom and

$$x_3 = \zeta(x_1, x_2, t)$$

the equation of the sea surface; the axes $\mathbf{e}_1$ and $\mathbf{e}_2$ pointing to the east and to the north respectively. The transport of water $\mathbf{U}$ integrated over the depth is cleared of turbulent fluctuations whose dispersing effects are taken into account with an "eddy" viscosity. This "eddy" viscosity combines the effects of shear and turbulence [Nihoul (1975a)]. The mean current $\overline{\mathbf{u}}$ over the depth is also often introduced :

$$\mathbf{U} = \overline{\mathbf{u}}\, H = \frac{1}{H} \int_h^{\zeta} \mathbf{u}\, dx_3 \tag{1}$$

where $H = h + \zeta$

is the instantaneous depth.

1.- Tidal and storm surge model (transient state)

1.1.- Equations of motion

The basic equations can be written [*e.g.* Nihoul (1975a)] :

$$\frac{\partial H}{\partial t} + \nabla . \mathbf{U} = 0 \tag{2}$$

$$(3)\quad \frac{\partial U}{\partial t} + \nabla . (H^{-1}\, U\, U) + f\, e_3 \wedge U = H[\xi - \nabla(\frac{p_a}{\rho} + g\, \zeta)] + a\, \nabla^2 U - \frac{D}{H^2} \|U\|\, U + C_{10}\, V\, \|V\|$$

where f is the Coriolis parameter, ξ the astronomical tide producing force per unit mass, p_a the atmospheric pressure, a the appropriate "eddy" viscosity, V the wind speed at the anemometer level (10 meters), C_{10} the experimental drag coefficient at the sea surface and D the bottom friction coefficient.

The order of magnitude of the shear effect viscosity is $a_{sh} \sim 50\ m^2/s$. Nihoul (1975a) shows that the turbulent contribution is weak. For long waves the diffusive term can be easily estimated : in the most irregular part of the North Sea

$$a\, \frac{\partial^2 U}{\partial x_1^2} \sim 50 . \frac{10}{(2\ 10^4)^2} \sim 10^{-6}\ m^2.s^{-2} .$$

This term is thus much smaller than the Coriolis, pressure and inertial terms (10^{-3} to $10^{-4}\ m^2.s^{-2}$) and will be neglected in the models.

1.2.- Boundary conditions

The North Sea is limited by coasts and by open sea boundaries; two kinds of conditions must be used :

i) along the coast

One assumes

$$\frac{\partial U}{\partial n} = 0$$

where n is the normal unit vector pointing outward. For a zonal coast one imposes $U_2 = 0$, and for a meridian coast $U_1 = 0$.

ii) along an open sea boundary

Equations for long waves are hyperbolic, one must impose either the sea level or the water transport along an open sea boundary. This information is supplied by experiments or by numerical predictions from other models characterized by coarser grids.

1.2.1.- For the Strait of Dover

It is difficult to have experimental current data in the Straits of Dover. Moreover the current is very sensitive to variations of the depth. For these reasons sea level data are used as boundary conditions. A linear interpolation for the sea level can provide good conditions across the Straits.

1.2.2.- For the Skagerrak

From numerical experiments the tidal influence of the Skagerrak on the North Sea system is weak. Small errors in the estimation of the sea level across this open sea boundary will not perturbe too much the whole area.

1.2.3.- For the North Atlantic Entrance

The bathymetry near the 60th parallel is characterized by a large plateau with a mean depth of 180 meters and by a deep channel of 400 meters. Along this open sea boundary amplitude and phase of tides and storm surges are known only at coastal stations (The Liverpool Tidal Institute uses now pressure gauges along the continental shelf; but these data are not yet available).

i) for tidal waves

Taylor (1922) and Godin (1966) studied the propagation of tides in rectangular bays. They found that far from the reflection area the wave has the character of a Kelvin wave. The behaviour of the tidal wave in the northern part of the North Sea is thus similar to a Kelvin wave. In this model one assumes a constant phase for the tide along a line perpendicular to the British coast.

To calculate the phase along the open sea boundary *for the plateau* the following relation is used *for the M_2 tide*

$$\phi_r = \phi_{ref} \pm \frac{r}{\sqrt{gh}} \frac{360}{T_{M_2}} \text{ in degrees ,}$$

where T_{M_2} is the period of the M_2 tide, r the distance between the open sea boundary and the reference phase line, + r if the open sea

boundary line is below the reference line, $-r$ if the open sea boundary line is above the reference line. ϕ_{ref} is the phase at a tidal coastal station. This formula gives us the value of ϕ at the Norwegian Trench. A linear interpolation between ϕ_{NT} and the phase at the Norwegian tidal coastal station is used across the Norwegian Channel.

As the tidal wave has the character of a Kelvin wave at the Northern entrance the amplitude profile of the sea elevation is assumed exponential : only one boundary condition is required to define it completely. At the west side, the amplitude is approximately equal to 1.2 m , the Kelvin wave profile gives an amplitude at the Norwegian Trench $A \sim 0.48$ m ; at the east side of the boundary, the amplitude is 0.4 m and the Kelvin wave profile gives also 0.48 m at the separation "point" between the plateau and the Norwegian Channel. One can thus assume a Kelvin profile for the tidal waves.

ii) storm surges

The estimation of the cross profile of the sea level for a storm surge is very difficult. Until results from data pressure sensors are available, one makes a linear interpolation between coastal stations.

2.- Residual circulation model

2.1.- Equations of the model

The mean flow U_0 is obtained from the time-averaged equations [*e.g.* Nihoul (1975a), Nihoul and Ronday (1975)] :

$$f\, e_3 \wedge U_0 = - H_0\, \nabla\left(\frac{p_a}{\rho} + g\, \zeta_0\right) - K\, H_0^{-1}\, U_0 + \Theta_0 \qquad (4)$$

where $K = D\, \| \overline{u}_1 \|_0$

is the new friction coefficient and is function of the amplitude of the non stationary current field. For the North Sea $\overline{u}_1$ is of the order of 1 m/s in the average; thus

$$K \sim D\, \| \overline{u} \|_0 \sim 2\ 10^{-3} \text{ m/s} .$$

$$\Theta_0 = \tau_w + \tau_t$$

is the new stress which combines the average wind stress

$$\tau_w = (C_{10}\, V \,\|V\|)_0$$

and the "tidal stress" calculated by averaging the non stationary equations

$$\tau_t = - [g\, \zeta_1\, \nabla\zeta_1 + \nabla . (H^{-1}\, U\, U)]_0 \tag{5}$$

For the residual circulation the geostrophic wind is calculated by means of atmospheric pressure data. The surface wind is derived from the geostrophic wind by classical empirical formulas. The mean surface stress over a period of one year is equal to

$$\tau_w = 0.2\ 10^{-4}\ m^2/s^2 \ .$$

The continuity equation for the mean flow allows the definition of a stream function ψ

$$U_{0,1} = - \frac{\partial \psi}{\partial x_2} \qquad\qquad U_{0,2} = \frac{\partial \psi}{\partial x_1} \tag{6}$$

Dividing equation (4) by H_0 and taking the curl in order to eliminate the surface elevation, one obtains :

$$K\, \nabla^2 \psi - \frac{\partial \psi}{\partial x_1} \left(f \frac{\partial H_0}{\partial x_2} + \frac{2K}{H_0} \frac{\partial H_0}{\partial x_1} - \beta \right) + \frac{\partial \psi}{\partial x_2} \left(f \frac{\partial H_0}{\partial x_1} - \frac{2K}{H_0} \frac{\partial H_0}{\partial x_2} \right)$$

$$= H_0\, \omega_3 + \frac{\partial H_0}{\partial x_2}\, \Theta_1 - \frac{\partial H_0}{\partial x_1}\, \Theta_2 \tag{7}$$

where $\omega_3 = (\nabla \wedge \Theta_0)_3$

$\beta = \frac{df}{dy}$ is the beta factor introduced by Rossby in order to take into account the variability of the Coriolis term with the latitude.

The stream function ψ can be split in three parts :

$$\psi = \psi_{stress} + \psi_{interaction} + \psi_{leak}$$

ψ_{stress} induces a circulation directly related to the stress Θ ;
$\psi_{interaction}$ creates a circulation which depends on the gradient of the depth; ψ_{leak} gives the contribution of exterior flows to the model.

2.2.- Boundary conditions

The North Sea is limited by coasts and by open sea boundaries. Two kinds of conditions must be used.

i) along coasts

One assumes that the water transport across the coast is zero. The stream function ψ is then a constant along a coast.

ii) along open sea boundaries

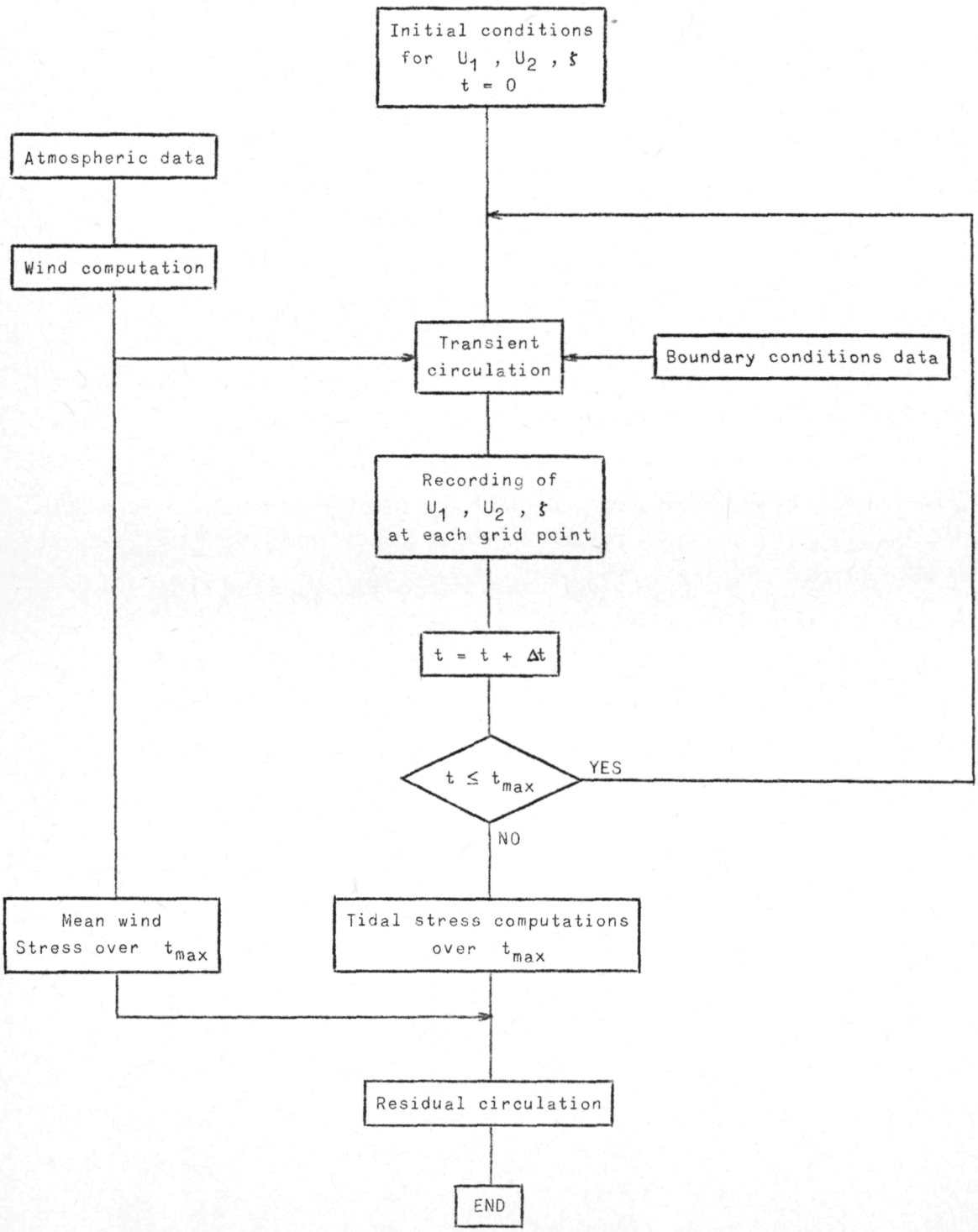
Estimates of water fluxes across open sea boundaries

The inflow of water from the North Atlantic is estimated at 23000 km^3/year [Kalle (1949)]. For the flow through the Straits of Dover Cartwright's (1961) figures give 7400 km^3/year . This value is many times higher than the former estimates [Carruthers (1935)], but this value is now accepted as being nearly correct. Wyrtki (1954) showed that the water balance of the Baltic Sea is complicated. Over short periods of time different authors have found either an outflow or an inflow according to atmospheric conditions. In view of these complexities, the figures of 200 km^3/year given by Leavastu (1963) for a long period of observation seem to provide a reasonable guide to the long-term mean inflow. Due to the lack of precise long-term measurements across the Skagerrak one imposes a stream function at the two sides of the channel with a difference proportional to the net inflow. Inside this open sea boundary it is assumed that the current is unidirectional : in this model this condition implies $\frac{\partial \psi}{\partial n} = 0$ where n is the normal to the boundary.

The most important rivers are the Meuse, the Rhine and the Scheldt which provide a new inflow of 63 km^3/y . The other inputs come from German estuaries (60 km^3/y) and from S.W. Norway. If one assumes that rain (inflow) is balanced by evaporation (outflow) and a steady state water budget, one obtains 30789 km^3/y for the water outflow in the North Atlantic. Observations reveal that the outflow is mainly concentrated in the region of the Trench. In this model one imposes an inflow between the Scottish coast and the third east meridian and an outflow from that meridian to the Norwegian coast. In these two sections a uniform distribution of the flow is assumed.

3.- Results of computations

The procedure of computations for the transient and residual circulation is given on the following flow chart :



The equations for the residual circulation are solved by classical methods.

3.1.- Transient circulation

The current regime in the North Sea is mostly tidal. The most important partial tide is the lunar semi-diurnal. Coastal tidal data are well known and come from the *Table des constantes harmoniques de Monaco*.

Currents and sea elevations are not purely harmonical function of time due to non linear terms in the equations of motion. These non linearities appear in shallow areas : the Belgian, Dutch, German, Danish coast are characterized by shallow waters. In order to compare the amplitude and phase of the M_2 tide at coastal stations, a Fourier analysis of the sea-level is carried out. The comparison between observed and calculated amplitudes and phases for coastal stations shows a very good agreement. Some discrepancies appear along the British coast for the amplitude due to very sharp depth variations. Near Lowestoft (Suffolk) some differences exist for the phase of the tide because this region is submitted to the influences of the North Atlantic and Dover Strait tidal forces. A slight error in the estimation of sea levels along open sea boundaries strongly modifies the phase of the tide in these regions. The approximation of the coastline by a rectangular grid introduces also errors : the wave phase is thus very sensitive to the position of the numerical grid.

Cotidal and corange lines are given in figures 2 and 3. The agreement is good. Due to the small number and low quality of sea level measurements in the inner part of the North Sea one can conclude that the present model gives better results than those provided by Proudman and Doodson (1924).

Tidal currents measured and calculated are also compared; the agreement is very satisfactory. Measurements should be concentrated along the open sea boundaries with some measurements in the central part of the grid to verify the quality of the model. Results from computations agree with measurements (the error is of the order of the experimental

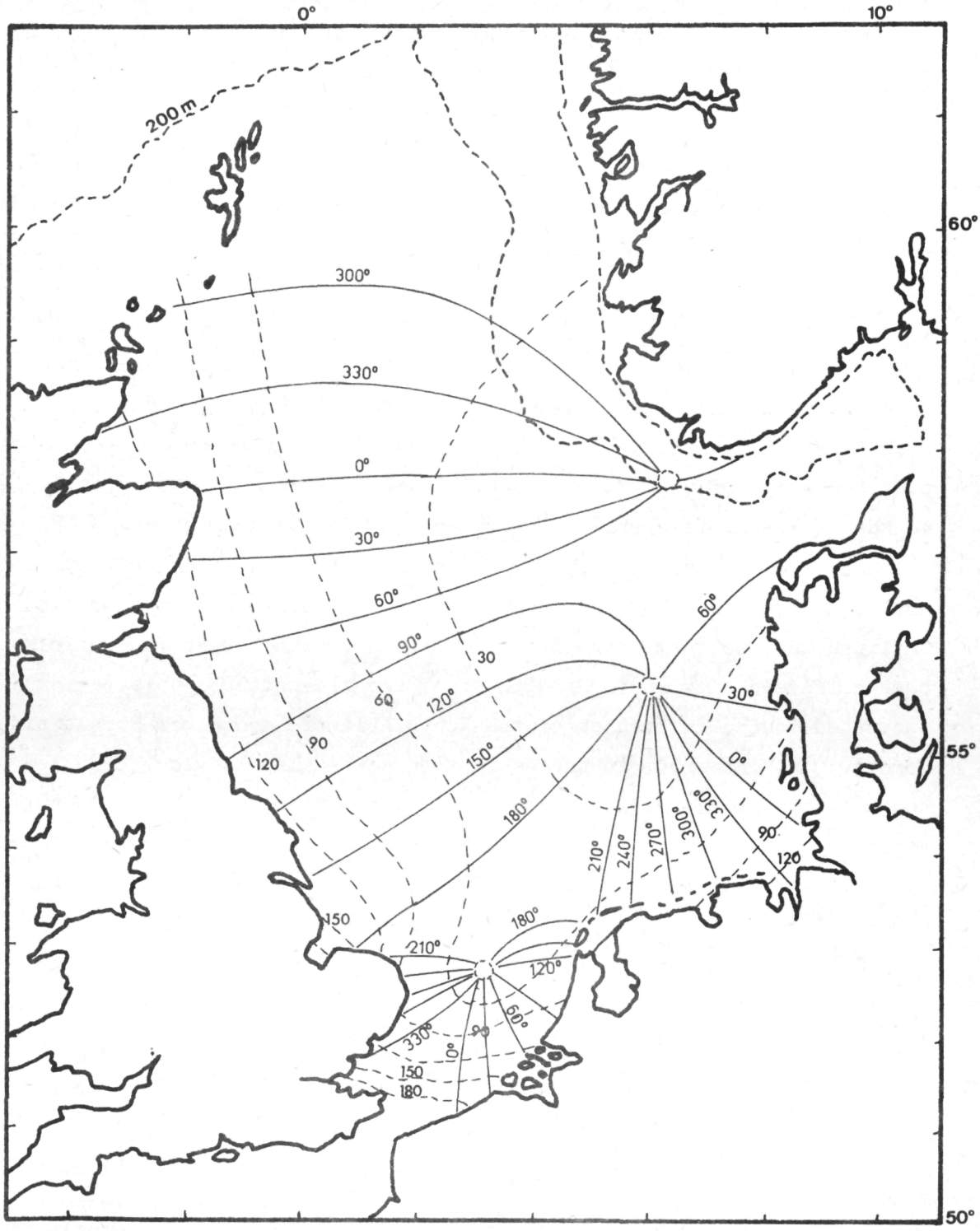


fig. 2.

Lines of equal tidal phases and amplitudes in the North Sea according to the mathematical model.

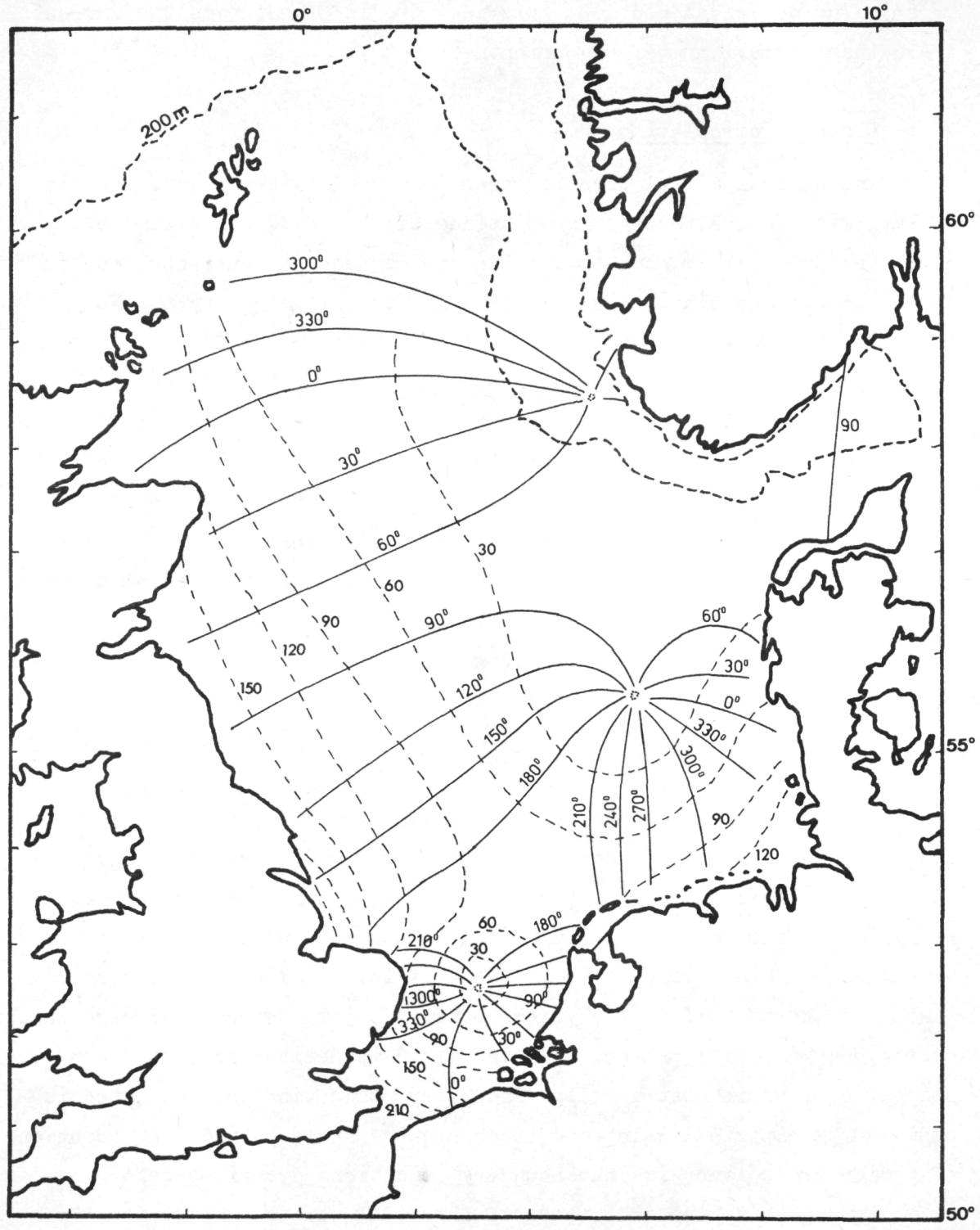


fig. 3.

Lines of equal tidal phases and amplitudes in the North Sea according to observations (after Proudman and Doodson, 1924).

error). The numerical model can provide more information on the current field than a small number of currentmeter stations.

3.2.- Residual circulation

The general circulation in oceans is mostly wind-driven. One can explain with such a theory the existence of the different well-known currents (Gulf Stream, Equatorial, Counter-equatorial currents, etc.). The long-term circulation in the North Sea is influenced by the North Atlantic current which enters the North Sea through the Straits of Dover and through the Channel between the Orcades and Shetland Isles. The influence of the Baltic sea is weak but provides water with a low content of salt (< 34 ‰). From oceanographic measurements (T , S , O_2) it is possible to determine the general distribution of the different water masses [Böhnecke (1922), Laevastu (1963)] (see figure 4).

In winter the North Sea water has no haline and no thermal stratifications except in the Norwegian Channel and near the coast line. The barotropic model can be used. In summer the haline stratification remains weak but a thermal stratification exists in the northern and central part of the bassin. The barotropic model may give approximate results during that period of time.

One assumes here that the water is vertically homogeneous, and a barotropic model is used. Böhnecke (1922) and Laevastu (1963) observed that the circulation pattern remained unchanged all around the year. The difference between summer and winter circulations is determined by the size of the areas of influence (spatial modification of vortex).

To understand from a physical point of view the residual circulation over a one-year time period, the wind field is derived from the mean atmospheric pressure distribution. The geostrophic wind so calculated is modified by empirical relations to obtain the surface wind. The equations of motion are solved with the boundary conditions described before.

To emphasize the importance of the tidal stress, one first solves the equations for the residual circulation without explicitly taking the tidal stress into account (figure 5). The wide stream coming from the North Channel flows down the British coast as far as East Anglia. The

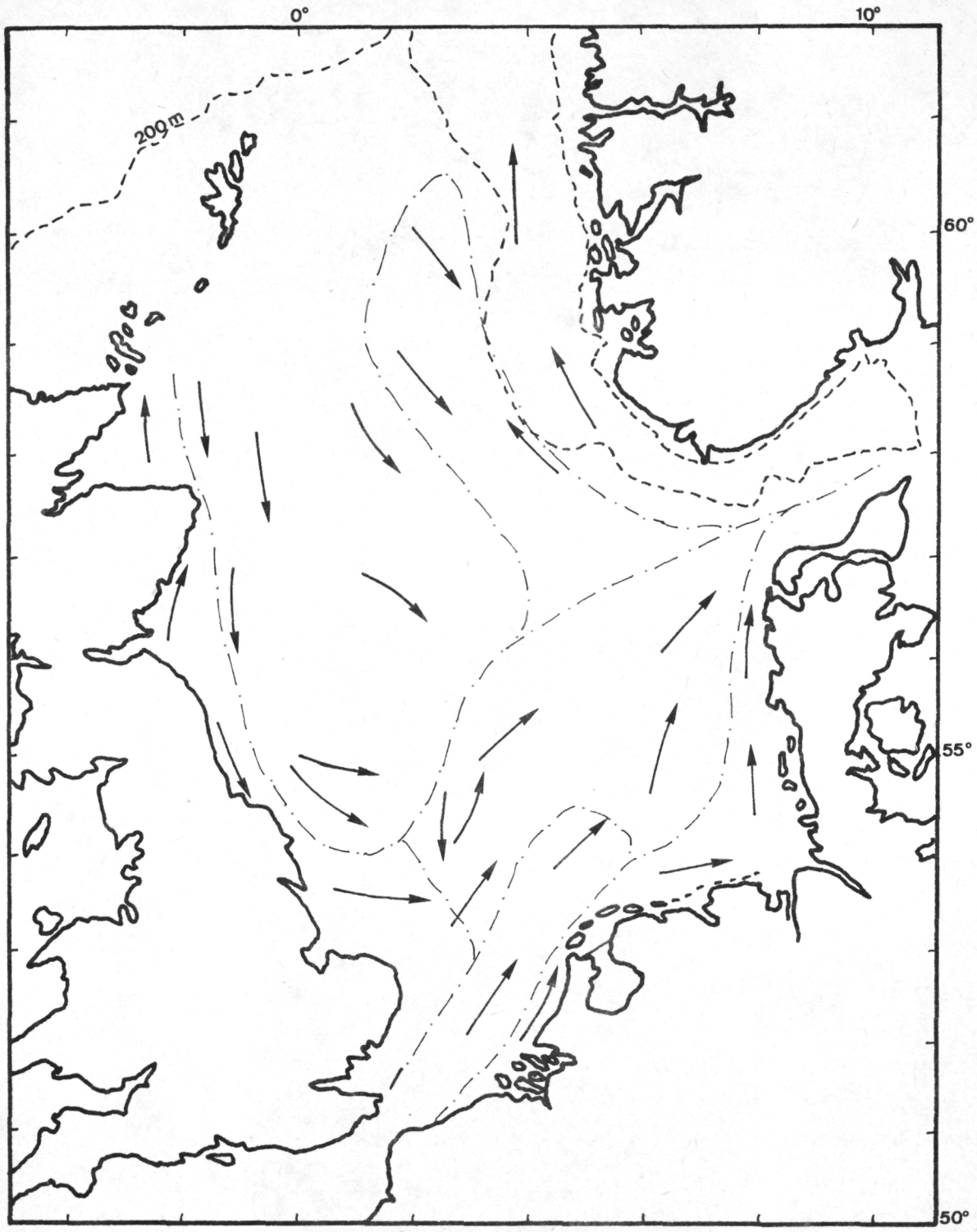


fig. 4.
Water masses in the North Sea according to Laevastu (1963).

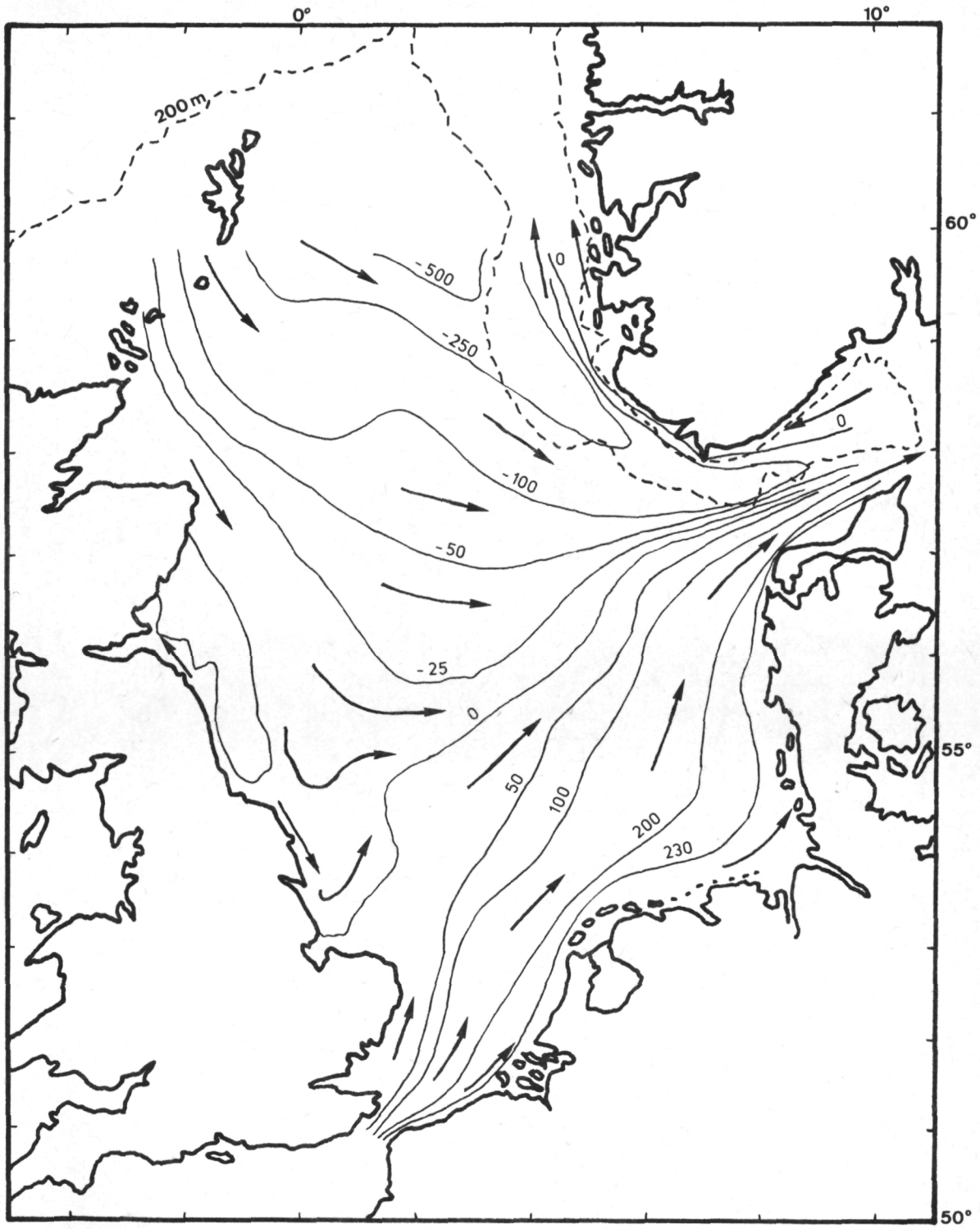


fig. 5.
Residual circulation calculated without tidal stress.
ψ = const (in 10^3 m^3/s)

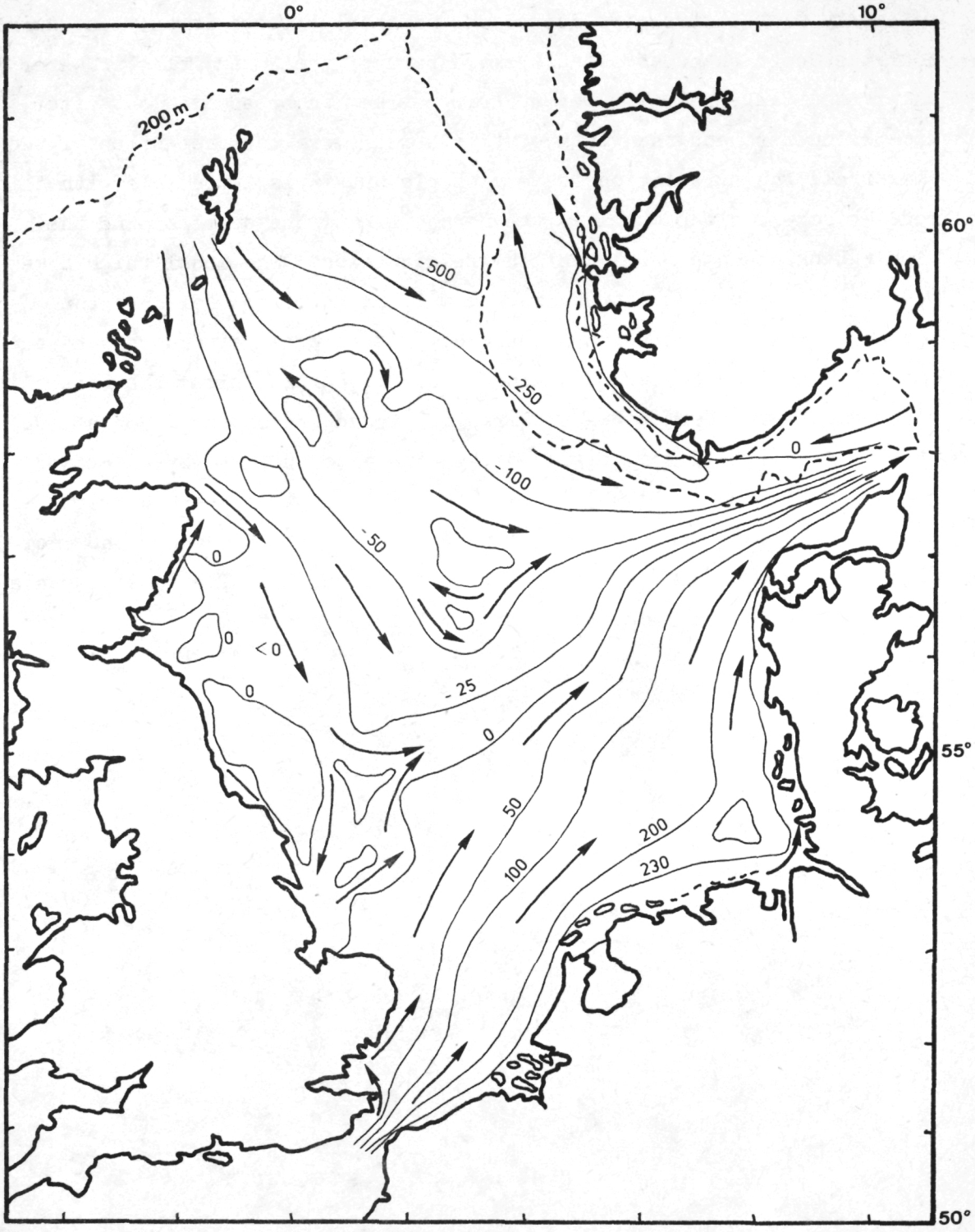


fig. 6.
Residual circulation calculated with the tidal stress.
ψ = const (in 10^3 m^3/s)

intensity of the stream is decreasing southerly; there is only one swirl near the Scottish coast line. A small part of the North Atlantic water enters the Skagerrak. The Dover Strait stream is broadening out after some kilometers and the width of this stream remains constant until the Skagerrak. The circulation is very simple but it is impossible with this model to explain the swirl in the German Bight, the swirl around the Dogger Bank and the swirl near the Belgian coast. The model which takes into account the tidal stress is the only one able to reproduce the actual residual circulation (figure 6). The general pattern remains but important modifications appear in different regions. Along the British coast and in the German Bight swirls exist and are observed for a long time [*e.g.* Hill (1973)]. Figure 6 exhibits also another vortex around the Dogger Bank; Ramster (1965) proves its existence with sea-bed drifters. Other swirls exist in the central part of the North Sea where the residual current was very weak in the former model (figure 5). The model reveals also a south westerly current near the Belgian coast.

III.- MUD DEPOSITION IN THE SOUTHERN BIGHT

Based on :

- Math. Modelsea (1974), I.C.E.S. Hydrography Committee, C.M. 1974 - C : 1;
- NIHOUL J.C.J. (1975c), Effect of the tidal stress on mud deposition in the Southern Bight of the North Sea, Proc. 2d Annual Meeting of the European Geophysical Society, Trieste 20-26 Sept. 1974.

During 1972 and 1973, some 1200 samples were analysed, taken at regular intervals, mostly with a Van Veen sampler, in the Southern Bight of the North Sea. As described by Gullentops (1974) : "The Southern Bight is strikingly free of muddy sediments, indicating that currents and here also wave turbulence are high enough to allow only temporary decantation but no final deposition. Only in front of the Meuse-Rhine mouth, increased fluvial input of suspension material influences the bottom sediments. The big exception is the low energy triangle in front of the eastern Belgian coast in which muddy sedimentation is developing to a considerable extent due to local affluents as the Yser, but mostly to the suspension material dragged out of the Scheldt estuary and trapped in this area.

"ERTS-A remote sensing documents proved this fact strikingly, showing a suspension plume in front of the Rhine mouth and a huge turbid area in front of the eastern Belgian coast connected with an extremely turbid Scheldt estuary.

"The mud area could *in globo* be explained by the tendency to form an outerlagoon, behind the prelittoral ridges, in which increased suspended matter arrival tends to be preserved by the current pattern, is flocculated and aggregated by biological activity and preserved from net erosion by weakened wave activity."

The observations [Elskens (1974)] show the eastern Belgian coast to be a privileged zone of mud accumulation in relation to the whole network studied.

Figure 7 [Nihoul (1975a)] shows the residual currents pattern derived from the simple classical model in which the Reynolds stress, the shear

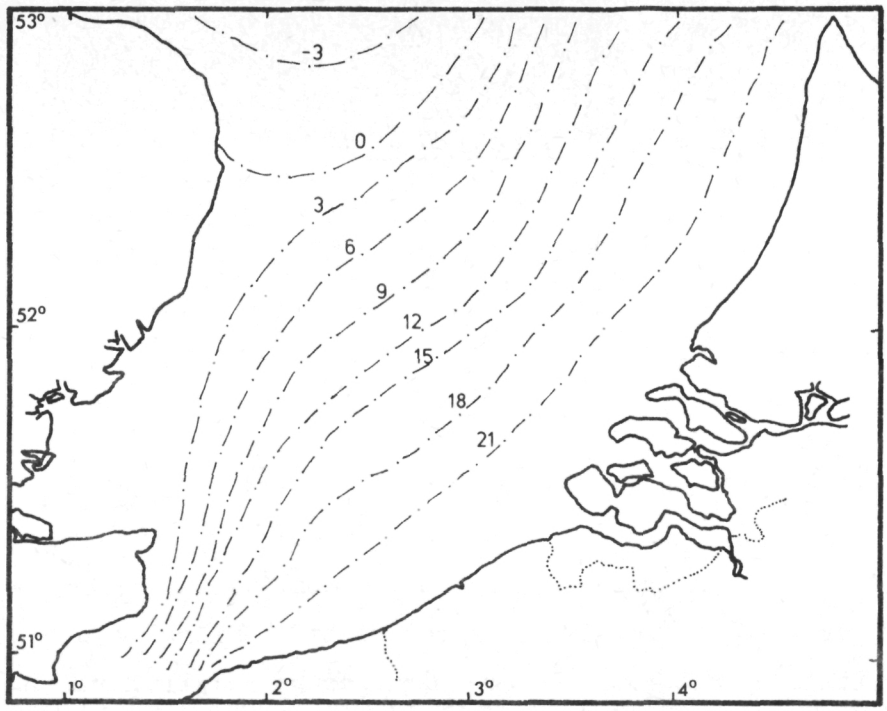


fig. 7.
Residual circulation in the Southern Bight without tidal stress.
Streamlines ψ = const (in 10^4 m^3/s)

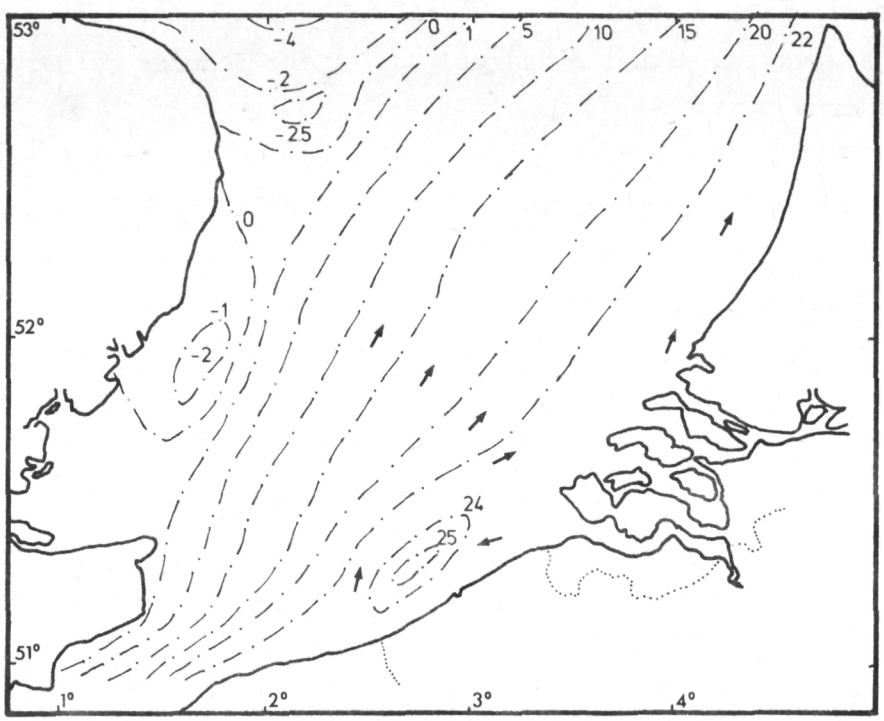


fig. 8.
Residual circulation in the Southern Bight with the tidal stress.
Streamlines ψ = const (in 10^4 m^3/s)

stress *and* the tidal stress are approximated by a diffusion term. Such a pattern – although it reproduces the expected North bound flow from the Straits of Dover – cannot explain the observations of deposited sediments.

On the contrary, the new model described in section II predicts the existence of a residual gyre off the Belgian coast which, increasing the residence time of the water masses and in particular the entrained water from the Scheldt estuary, fully explains the observed sedimentation pattern (figure 8).

IV.- ECOSYSTEMS DYNAMICS IN THE SOUTHERN BIGHT

Based on :

- Math. Modelsea (1974), I.C.E.S. Hydrography Committee, C.M. 1974 - C : 1;
- NIHOUL J.C.J. (1975d), Mesoscale secondary flows. Implications in the chemical and biochemical dynamics of the Southern Bight, Proc. Liège 6th Colloquium on Ocean Hydrodynamics, Liège, April 28 - May 2, 1974.

An extensive survey of chemical and ecological variables in the eastern part of the Southern Bight was made during the years 1971, 1972, 1973 and 1974 in the scope of the Belgian National Program on the Environment, Sea Project. On the basis of these informations, the survey region was divided into three zones where different conditions prevail (figure 9).

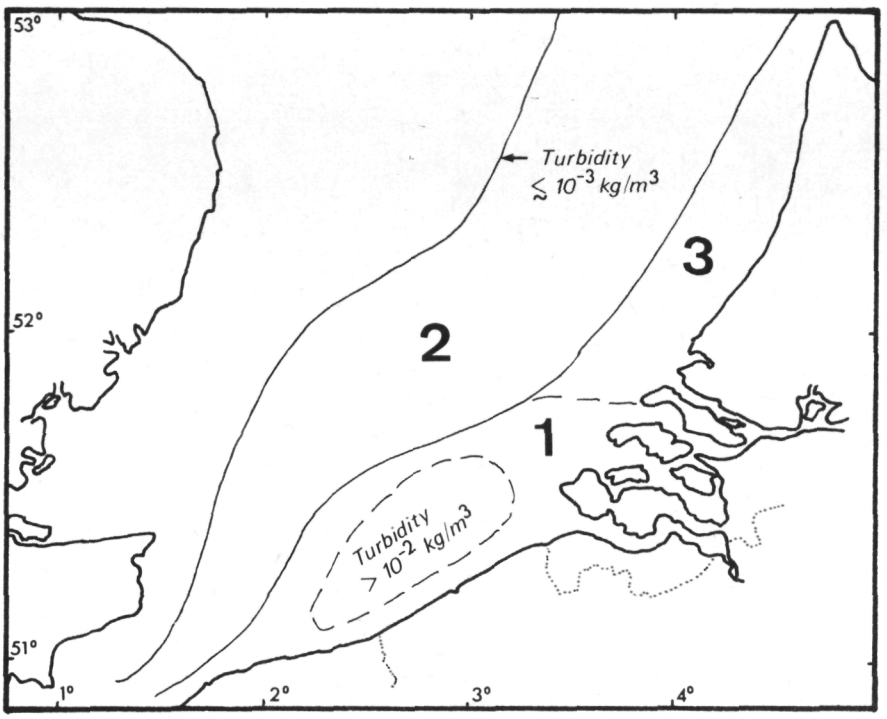


fig. 9.

Three zones in the Southern Bight where a different pattern of residual circulation is predicted by the model and which also appear from the observations as three distinct boxes.

One can see that the different zones correspond to different residual circulation regimes.

i) Zone 1, off the Belgian coast corresponds to the residual gyre. Water from the Scheldt estuary is to a large extent entrained in the gyre before it can escape to the north. An island of high turbidity ($> 10^{-2}$ kg m^{-3}) is observed in the region where closed stream lines are predicted by the model. Bottom sediments in zone 1 are characterized by large areas of mud which can be explained by the tendency to form — as shown by the residual current model — an outerlagoon "in which increased suspended matter arrival tends to be preserved by the current pattern, is flocculated and aggregated by biological activity and preserved from net erosion by weakened wave activity" [Math. Modelsea (1974)].

ii) Zone 2 corresponds to fairly parallel stream lines showing off the north-bound flow of the branch of the Gulf Stream which penetrates the North Sea through the Straits of Dover. The turbidity in zone 2 is considerably lower and no systematic silt deposition occurs.

iii) Zone 3 corresponds to water masses under direct influence of the Meuse-Rhine estuary. The rivers' outfall is in a sense prolonged into the Sea by a residual flow parallel to the Dutch coast, to the north.

The lagoon conditions which result from the residual circulation in zone 1 is responsible for striking differences between the dynamics of the ecosystems in that region and in zone 2.

The high turbidity of the water in zone 1 causes light extinction and reduces primary productivity. The dominance of microplankton in that region (as compared to nannoplankton in zone 2) with a higher half saturation constant could affect productivity in the same way. Taking into account, also, that the depth is smaller in the coastal region, one should expect the integrated production (over depth) to be considerably smaller in zone 1. Observations reveal however that — although there are differences in the annual variations — the yearly average is about the same in the two regions [Podamo (1974)].

This result is obviously related to the much higher nutrient concentration and the much larger specific phytoplankton biomass (measured

by chlorophyll a) observed in zone 1 where lagoon conditions prevail [Podamo (1974)].

Additional information is provided by the ratio phaeophytin a/ chlorophyll a which is systematically larger than one in zone 1 and smaller than one in zone 2; indicating that, in zone 1, most of the phytoplankton cells are dead cells. Zooplankton grazing, on the other hand, is more important in zone 2 than in zone 1, where planktonic and benthic heterotrophic bacteria seem to play the essential role.

A picture thus emerges of a fairly well balanced ecosystem in zone 2 and a rather unhealthy one in zone 1 where intensive phytoplankton production occurs but not, as it should, to provide first level food in the food chain. The phytoplankton crop is harvested only to a small extent. Most of it is left to rot and most of the recycling of nutrients occurs at the dead phytoplankton level under the action of bacteria.

The dynamics of the ecosystems thus reflects the residual circulation patterns and the outerlagoon situation created by the residual gyre in zone 1.

V.- *DISPERSION AND SEDIMENTATION AROUND A DUMPING GROUND*

Based on :

- NIHOUL J.C.J. (1974), Diffusion of turbidity by shear effect and turbulence in the Southern Bight of the North Sea, Proc. Symp. on Turbulent Diffusion in Environmental Pollution, Charlottesville, April 8-14 1973, Advances in Geophysics, 18 A, 331;
- NIHOUL J.C.J. (1975a), Modelling of Marine Systems, Elsevier Publ., Amsterdam;
- NIHOUL J.C.J. and ADAM Y. (1974), Programme national sur l'environnement physique et biologique, C.I.P.S., N 36.

Dumpings in the sea — even though the dumped material may not be toxic as such — create, in many cases, an important pollution problem associated with the local increase of turbidity and the deposition of sediments on the bottom. Solid particles in suspension affect the transparency of the water and may reduce photosynthesis. Silt deposits on the other hand may affect benthic communities and may be in shallow areas prejudiciable to eggs and larvae.

In shallow seas, one is particularly interested in the mean sediments concentration in the water column and in the concentration of bottom sediments.

The equation describing the evolution of the mean concentration of suspensions is derived from the three-dimensional dispersion equation by integration over depth. The average over depth of the quadratic advection terms gives two contributions; the first one contains the product of the means, the second one the mean product of the deviations around the means.

The structure of the latter is analogous to that of the Reynolds stress and experiments reveal that it is indeed responsible for an enhanced dispersion comparable to — but often more important than — the turbulent dispersion. This effect is called the "shear effect" because it is associated with the existence of a vertical velocity gradient.

The shear effect has been described by several authors in pipes, channels and estuaries where, after integration over the cross section, the flow — steady or oscillating — is essentially in one direction [Taylor (1953), (1954); Elder (1959); Bowden (1965)].

In the shallow waters of the Southern Bight, it is generally sufficient to consider the mean concentrations over the depth but, out at sea, no further averaging is possible and the dispersion mechanism is fundamentally two-dimensional. A generalized model was thus developed to account for the rotation of the tidal velocity vector and also include the sedimentation and partial recirculation of the solid suspensions [Nihoul (1974), (1975)].

If $\bar{c}$ and C denote respectively the mean specific mass of suspensions (the depth-averaged mass of suspensions per unit volume) and the specific mass of bottom deposits (the mass of deposited sediments per unit bottom surface) the equations governing the evolution of $\bar{c}$ and C following a dumping at sea can be written [Nihoul and Adam (1974)] :

$$\frac{\partial \bar{c}}{\partial t} + \bar{\mathbf{u}} \cdot \nabla \bar{c} = H^{-1} \nabla \cdot H[\gamma \frac{H}{\bar{\bar{u}}} \bar{\mathbf{u}}(\bar{\mathbf{u}} \cdot \nabla \bar{c})] - H^{-1} \bar{c} \sigma (1 - \frac{\bar{u}^2}{u_c^2}) + \nabla \cdot (\nu \nabla \bar{c}) \tag{8}$$

$$\frac{\partial C}{\partial t} = \bar{c} \sigma (1 - \frac{\bar{u}^2}{u_c^2}) \tag{9}$$

where $\bar{\mathbf{u}}$ is the depth averaged advection velocity, H is the total depth, γ the shear effect coefficient, σ the sedimentation velocity, ν the turbulent diffusivity and where u_c denotes the critical value of $\bar{u}$ above which disruption of the bottom layer by turbulence reverses the sedimentation flux and recirculates sediments in the water column.

It can be shown that the expression for the sedimentation-erosion flux is a first approximation valid for mean velocities $\bar{u}$ never too large compared to the critical value u_c . For larger values of the ratio $\frac{\bar{u}}{u_c}$ more sophisticated formulas must be used and in particular one must take into account that the velocity $\bar{u}$ may exceed a second critical value u_e for which erosion of consolidated bottom sediments may occur. This problem is discussed in the next section.

Knowing the currents and the surface elevations ζ (from atlases or hydrodynamic models), knowing the depth h and thus the total depth

$H = h + \zeta$, the sedimentation velocity of the dumped particles, the turbulent diffusivity and the critical velocity u_c , one can solve equations (8) and (9) and predict as a function of time the evolutions of the patch of suspensions and of the bottom deposits.

Off the Belgian coasts, several dumpings take place periodically in the vicinity of 51° 30' N ; 3° E . These dumpings have been simulated on IBM 370-58 to evaluate their effect on the water turbidity and the deposition of sediments.

The tidal currents which dominate in the area are determined by numerical models and atlases of coastal currents. The critical velocity is estimated at $u_c \sim 0.8$ m/s and is exceeded during a fraction of the tidal cycle. The shear effect coefficient calculated using the vertical velocity profile valid in that region is found to be $\gamma \sim 0.45$. The sedimentation velocity is taken for the particular example chosen as $\sigma \sim 10^{-3}$ m/s .

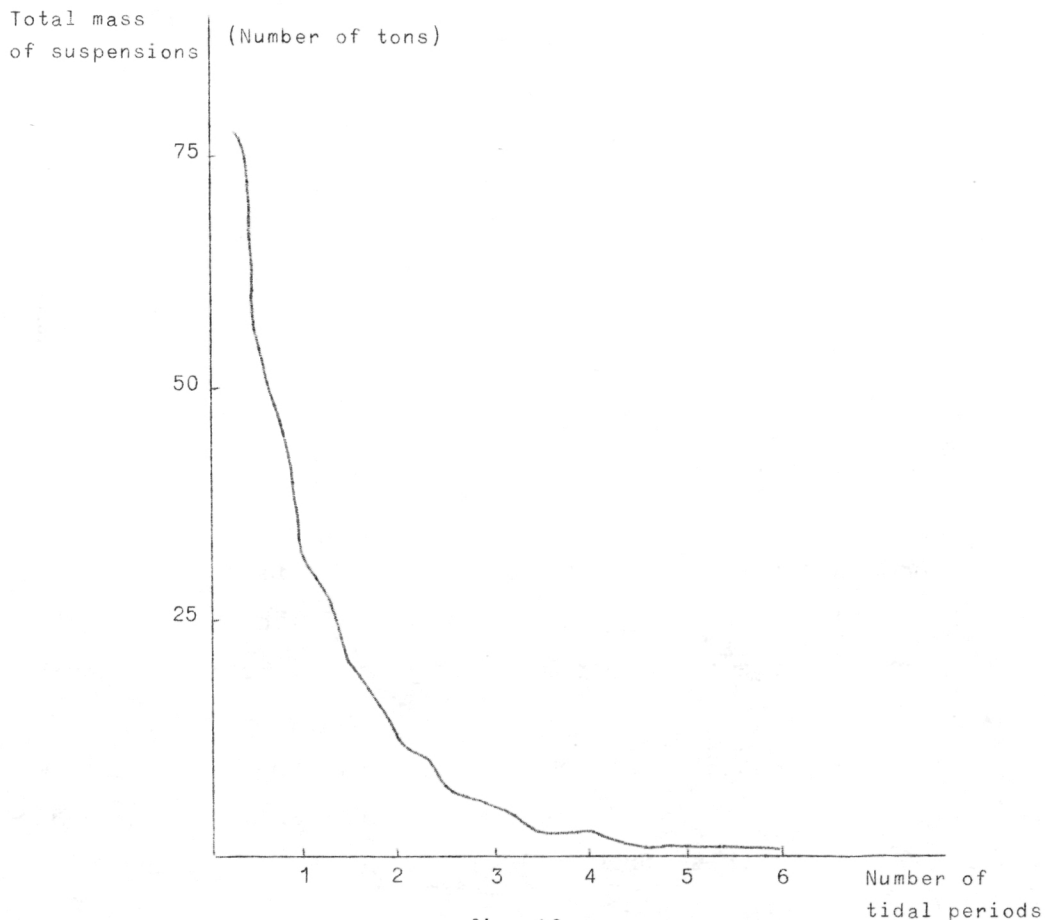


fig. 10.

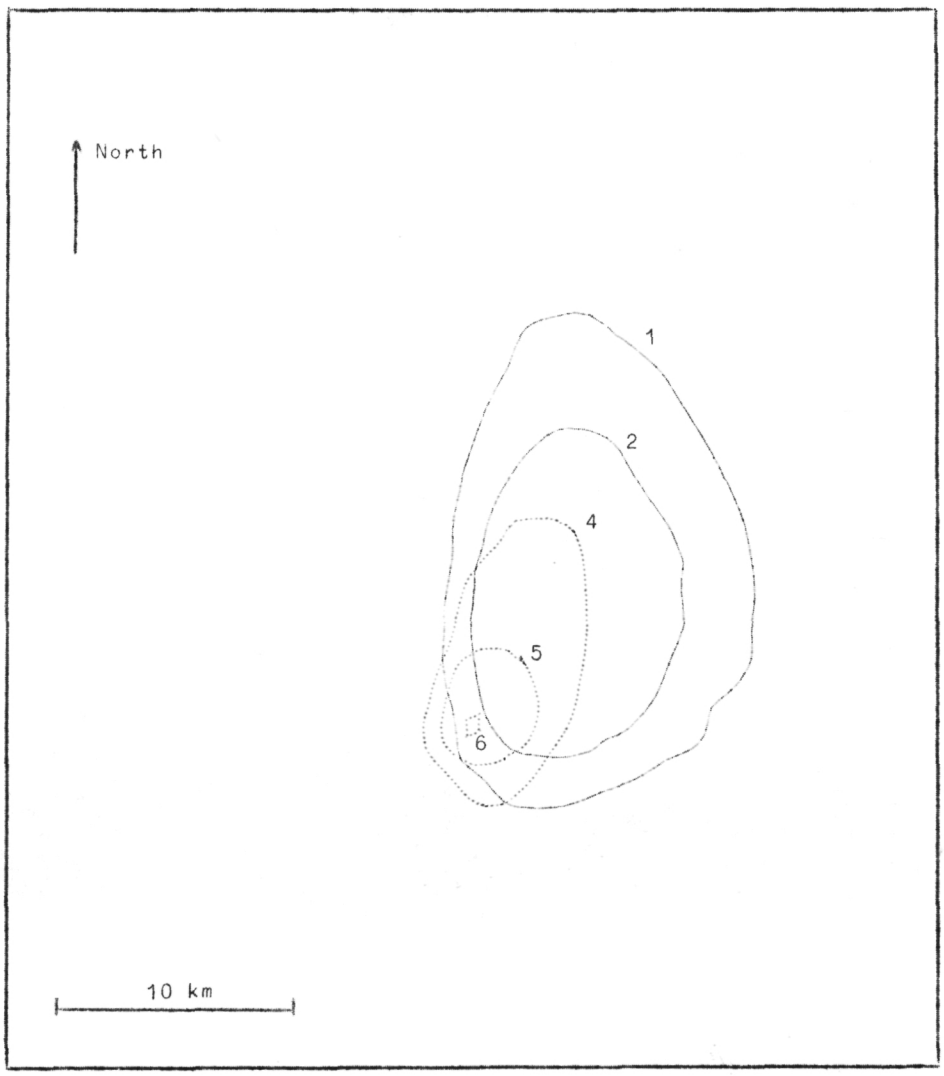


fig. 11.
Isoconcentrations $\frac{1}{4}$ tidal period after the release.

Figure 10 shows the evolution with time of the total mass of suspensions in the water column. Figures 11 and 12 show the evolution over a tidal period of the curves of equal concentrations of suspensions and deposits.

Curves 1, 2 and 3 correspond respectively to concentrations of 1 mg/m^3 , 10 mg/m^3 and 100 mg/m^3 of suspensions. (No curve 3 can actually be seen on these figures because such high concentrations only

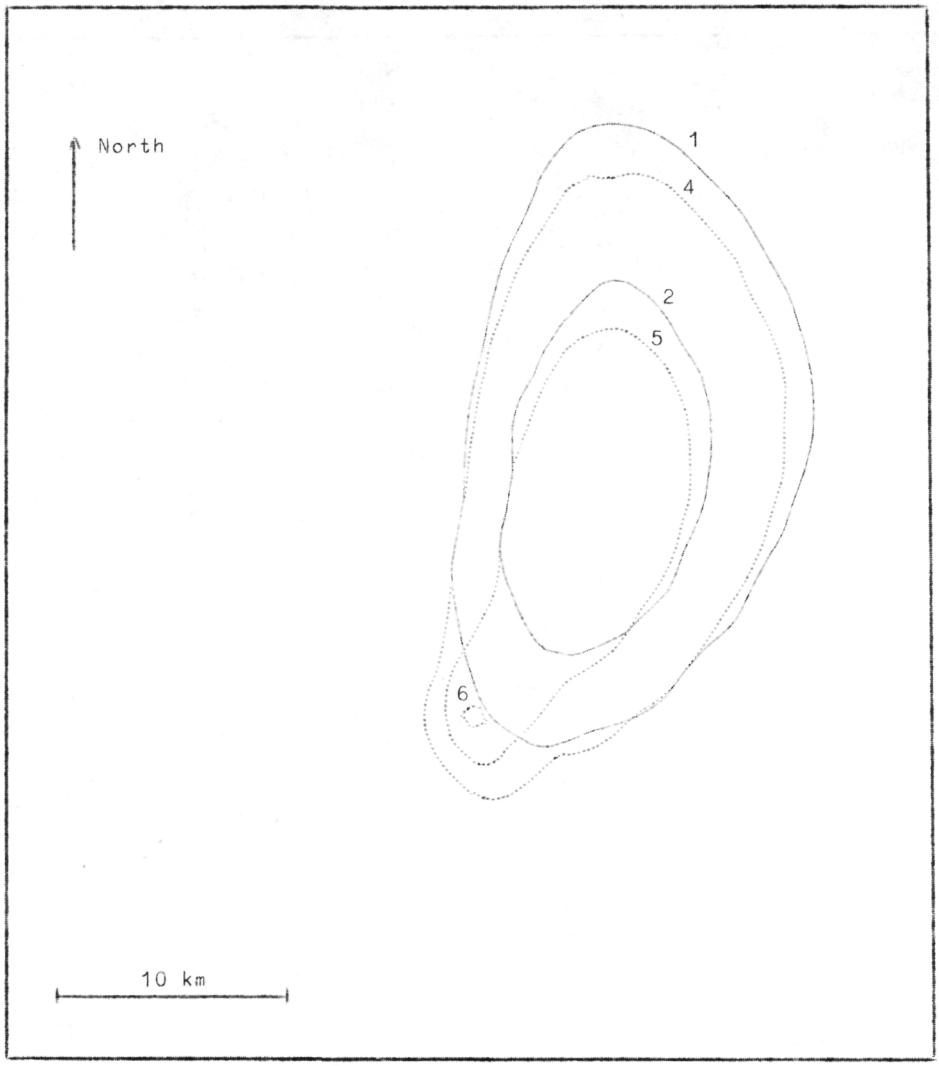


fig. 12.
Isoconcentrations $\frac{1}{2}$ tidal period after the release.

appear around the point of dumping in the first few hours following it and are no longer visible after a quarter of the tidal period.)

Curves 4, 5 and 6 correspond respectively to concentrations of 10 mg/m^2 , 100 mg/m^2 and 500 mg/m^2 of deposited sediments. (Curve 6 or its southern part on figures 13 and 14 may be regarded as locating the dumping ground.)

The results of the numerical simulation are in excellent agreement with the observations. The essential points are :

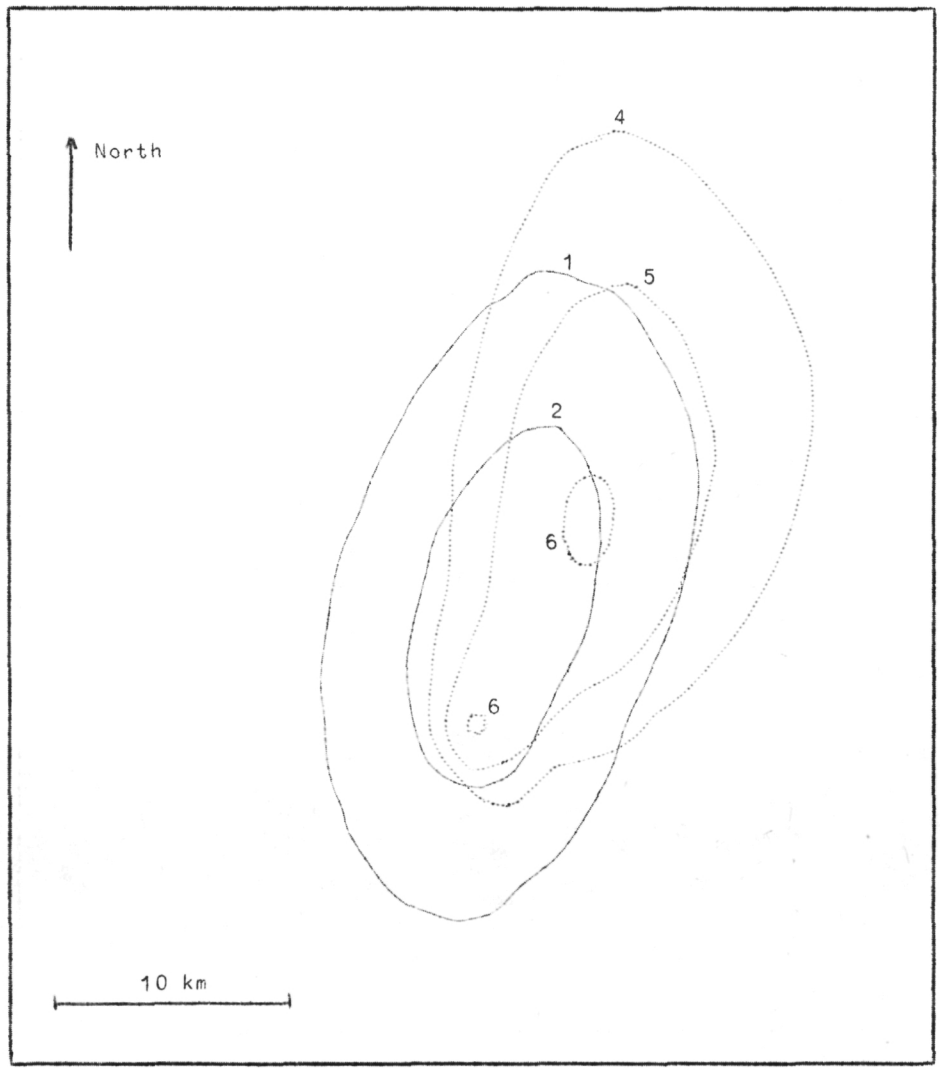


fig. 13.
Isoconcentrations $\frac{3}{4}$ tidal period of the release.

i) a rapid decrease of the total quantity of suspensions despite a periodic recirculation of depositing sediments associated with the stronger tidal currents (the partial recirculation is reflected by the regular bumps in the curve of overall decay);

ii) a strongly anisotropic dispersion characteristic of the shear effect and manifested by the elongation of the isoconcentration curves along the great tidal axis;

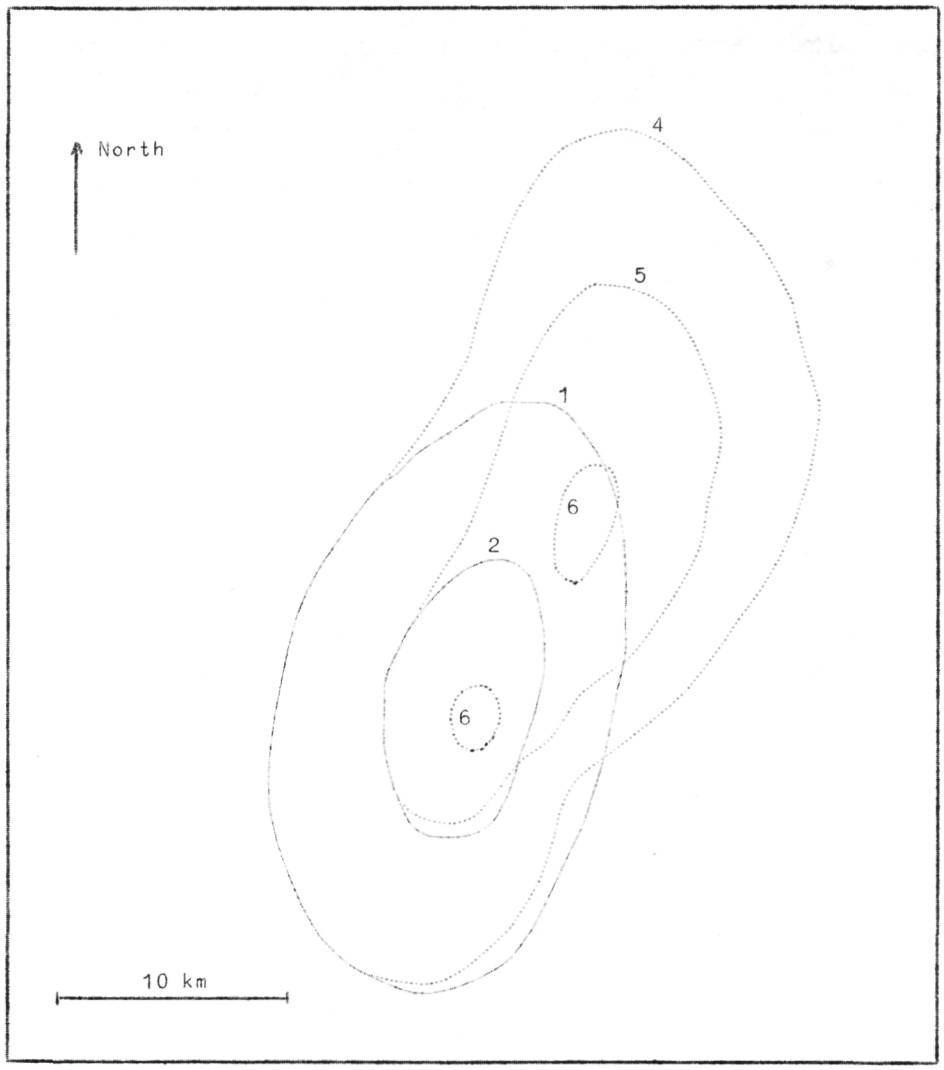


fig. 14.
Isoconcentrations 1 tidal period after the release.

iii) the tendency of the curves of equal concentrations of suspensions to take, *after one tidal period*, quasi-elliptical forms roughly centered at the dumping point. This final shape can be predicted by a simplified model where the evolution equations are, to begin with, integrated over a tidal period [Nihoul (1975a)];

iv) the division of curve 6 (500 mg/m^2) in two and the appearance of a second zone of high sediments-concentration to the north-east of the dumping area. This factor, combined with a general north-east bound

residual current in the area, can be associated with the observed progressive displacement of the deposited dumped material towards the north-east.

VI.- BOTTOM EROSION

Based on :

- LAMBERMONT J. and LEBON G. (1974), Erosion of cohesive soils, Programme national sur l'environnement physique et biologique, C.I.P.S., N 40.

1.- Introduction

Sedimentation means the transport of matter through a solution due to an external force field. Thereby sediment layers are built up at the bottom region of rivers, estuaries and oceans. Depending on the friction velocity or shear stress acting at the layer, deposition or erosion occurs.

Knowledge of the erosion flux under varying flow conditions is important in such diverse areas as estuary maintenance, channel design and pollution dispersal in rivers and oceans.

The results provided by mathematical marine models are only truthworthy when correct boundary inputs are known [Nihoul (1975a)], *i.e.* when the erosion flux is related to the fluid flow.

Many investigations have been carried out on the transport of sand beds (which is not a pollutant) but relatively little has been done on muds. Particularly in pollution studies it is mandatory to have information on the settling and scouring rates of fine grained particles [McCave (1972)].

In this section we concentrate on the physical behaviour of the visco-plastic sediment layer and derive the expression for the erosion flux by considering the action of the turbulent flow.

In § 2, the mass conservation law for a sediment bed is formulated. In § 3, the boundary condition at the bed-fluid interface is discussed; use is made of the experimental data of Migniot (1968). The density distribution is discussed in § 4 and the interface mass flux continuity in § 5. In § 6, the analytic solution for the stationary erosion flux is obtained which for a fine grained sediment can be simplified (§ 7). In § 8, the theory is shown to describe very accurately the experimental studies performed by Partheniades (1965).

2.- Mass conservation law for the sediment bed

Consider a dynamically smooth and isotropic viscoplastic sediment layer (sea bed) in a gravitational field acted on by a two-dimensional turbulent fluid flow.

For simplicity we consider a two component non charged chemically non reacting system, for example water and a single component fine grained sediment as clay.

The solid particle or sediment mass flux $\mathbf{J}^s$ with respect to the barycentric velocity $\mathbf{v}$ of the bed is defined by

$$\mathbf{J}^s = \rho^s(\mathbf{v}^s - \mathbf{v}) \tag{10}$$

where ρ^s and $\mathbf{v}^s$ are the solid particle density and velocity.

The mass conservation equation for the sediment component reads

$$\frac{\partial \rho^s}{\partial t} = - \nabla . (\rho^s \mathbf{v}^s) \quad . \tag{11}$$

Substituting (10) into (11) gives :

$$\frac{\partial \rho^s}{\partial t} = - \nabla . \mathbf{J}^s - \nabla . (\rho^s \mathbf{v}) \quad . \tag{12}$$

We shall neglect temperature gradients in the sediment layer.

Further we consider throughout the layer constant diffusion D^s and sedimentation S^s coefficients. The sediment mass flux with respect to the barycentric velocity is in this case given by :

$$\mathbf{J}^s = - D^s \nabla \rho^s + S^s \rho^s \mathbf{g} \quad . \tag{13}$$

Substituting (13) in (12) results in

$$\frac{\partial \rho^s}{\partial t} = D^s \nabla^2 \rho^s - S^s \mathbf{g} . \nabla \rho^s - \nabla . (\rho^s \mathbf{v}) \quad . \tag{14}$$

These equations are formally the same as for a fluid. However, the sediment layer differs from a fluid — the latter cannot by definition support a shear stress at equilibrium — in that it shows viscoplastic behaviour, *i.e.* possesses a yield stress. That is to say, under an

applied shear stress less or equal to the yield shear stress, it behaves like an elastic solid while above this stress it shows a rate of deformation which is a function of the difference between the applied and yield stresses. The yield stress is a function of the solid component density which varies through the depth of the sediment layer.

Introducing a coordinate system wherein the z axis points downwards normal to the interface between the fluid and flat sediment layer, we consider a sediment layer in which the solid particle density depends only on z and t. The fluid flow above it is turbulent and two-dimensional. Apart from a hydrostatic pressure the fluid exerts then only a shear stress to the top of the sea or river bed.

Consequently plastic shear deformation in the sediment layer is, if it occurs, parallel to the x-y plane. A reasonable approximation inside the layer is then to assume that the barycentric velocity component in the z direction is negligibly small while its other two components are functions of z and t only. Under these restrictions (14) reduces to :

$$\frac{\partial \rho}{\partial t} = D \frac{\partial^2 \rho}{\partial z^2} - S\, g_z \frac{\partial \rho}{\partial z} \tag{15}$$

wherein we have omitted the superscript s.

The z component of (13) is

$$J_z = - D \frac{\partial \rho}{\partial z} + S\, \rho\, g_z \,. \tag{16}$$

3.- The boundary condition at the bed-fluid interface

According to Migniot (1968) the shear stress whereby erosion finds place is uniquely related to the yield stress. Tentatively we shall assume this to be true. Thus for a given sediment layer, with solid particle density ρ_c at the top, erosion finds place when the shear stress exerted on it by the fluid reaches a certain critical value.

To make this statement explicit let us reproduce the experimental results found by Migniot.

The yield shear stress τ_y is, for a great variety of muds, experimentally found to be related to the solid density ρ by

$$\tau_y = n\,\rho^m \tag{17}$$

where n and m are constants depending on the soil. When τ_y is expressed in N/m^2 and ρ in g/ℓ Migniot found m to be close to 5 for all cohesive soils examined while n varies from 10^{-12} to 10^{-15}, depending on the particular sediment.

The yield stress at the top of the sediment layer, where $\rho = \rho_c$, is thus

$$\tau_y = n\,\rho_c^m \quad . \tag{18}$$

Further it is found experimentally that the critical friction velocity U_* acting at the sediment layer, whereby erosion finds place is related to the yield stress by :

$$\begin{cases} U_{*c}(\text{cm/s}) = \tau_y^{1/4}(\text{dynes/cm}^2) & \text{for } \tau_y \leq 15 \text{ dynes/cm}^2 \\ U_{*c}(\text{cm/s}) = 0.5\,\tau_y^{1/2}(\text{dynes/cm}^2) & \text{for } \tau_y \geq 15 \text{ dynes/cm}^2 \end{cases} \tag{19}$$

In M.K.S. units, one has :

$$\begin{cases} U_{*c}(\text{m/s}) = 0.01778\,\tau_y^{1/4}(\text{N/m}^2) & \text{for } \tau_y \leq 1{,}5 \text{ N/m}^2 \\ U_{*c}(\text{m/s}) = 0.016\,\tau_y^{1/2}(\text{N/m}^2) & \text{for } \tau_y \geq 1{,}5 \text{ N/m}^2 \end{cases} \tag{20}$$

Figure 15, taken from Migniot (1968), shows how the relations (20) compare with the experimental points obtained for a number of sediments.

There is a remark to be made here. We infer from the experiments performed by Migniot that τ_y appearing in (19) is the average shear yield stress of the bed in the upper region (say 1 to 10 cm) of the layer. The contact with the fluid will lower the solid particle density and thus by (13) also the yield stress at the top of the sediment layer by a factor G, which we expect to have a value between 1 and 5 .

Taking this into account we obtain from (17) and (20) :

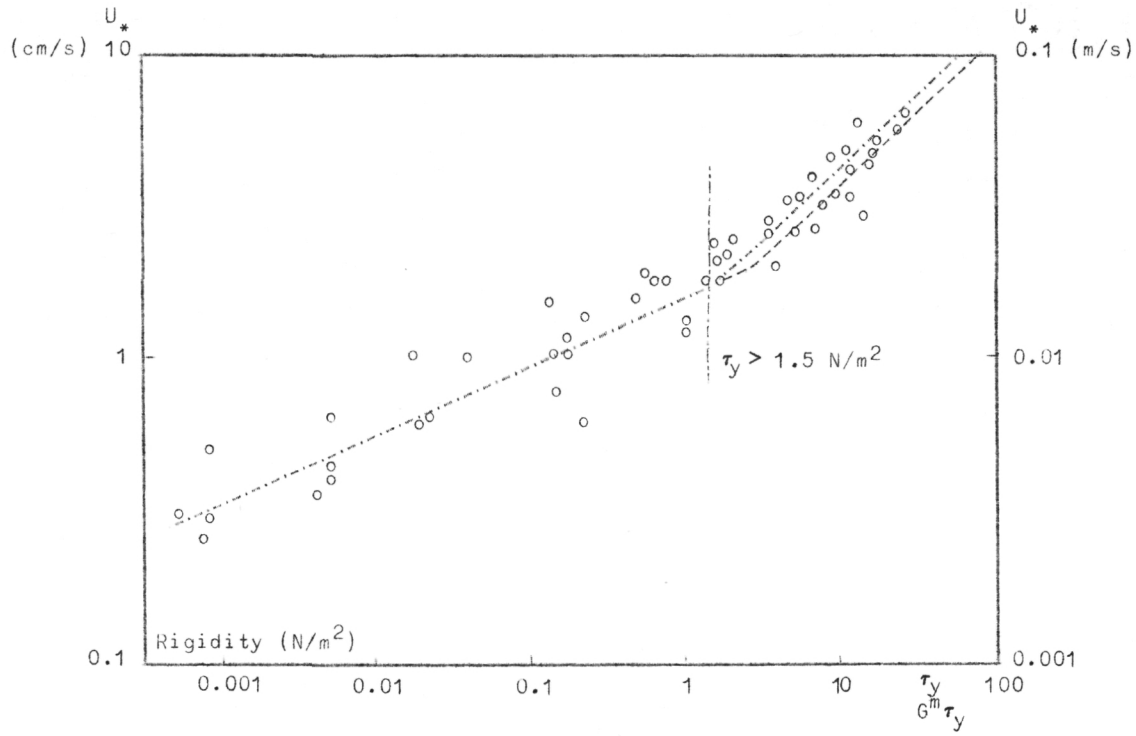


fig. 15.

Critical friction velocity U_* versus yield stress τ_y in upper sediment bed region (after Migniot). The yield stress at the top of the sediment bed $G^m\tau_y$ is also shown.

(21)
$$\begin{cases} U_{*_c}(m/s) = 0.0178\ G^{m/4}\tau_y^{1/4}\ (N/m^2) & \text{for } \tau_y \leq \dfrac{1.5}{G^m}\ N/m^2 \\ U_{*_c}(m/s) = 0.016\ G^{m/2}\ \tau_y^{1/2}\ (N/m^2) & \text{for } \tau_y \geq \dfrac{1.5}{G^m}\ N/m^2 \end{cases}$$

where τ_y is now the yield shear stress at the top of the bed. It is clear from (20) and (21) that Migniot's figure (fig. 15) describes correctly the relation (21) when the absciss in that figure is replaced by $G^m\tau_y$.

The relations (21) may be written as :

(22) $$U_{*_c} = p_i\ \tau_y^{q_i} \qquad (i = 1,2)$$

where $i = 1$ in region 1, defined for $\tau_y \leq \dfrac{1.5}{G^m}\ N/m^2$, and $i = 2$ in region 2, defined for $\tau_y \geq \dfrac{1.5}{G^m}\ N/m^2$.

The critical friction velocity is related to the shear stress exerted by the fluid whereby erosion finds place by :

(23) $$U_{*c} = \sqrt{\frac{\tau}{\rho_v}}$$

wherein ρ_v is the fluid density in the viscous sublayer.

Combining (18), (22) and (23) one finds the relation between the shear stress whereby erosion finds place and the instantaneous value of the solid particle density at the top of the bed, ρ_c, *i.e.*

(24) $$\tau = E_i \, \rho_c^{B_i} \qquad (i = 1,2)$$

where $$E_i = \rho_v \, p_i^2 \, n^{2q_i} \qquad B_i = 2\,mq_i \; .$$

The relations (20), (21), (22) and hence (24) have been determined under quasi-stationary experiments and may consequently not apply to rapidly varying bed shear stress.

Partheniades (1965) has criticized the existence of a relation between a critical friction velocity or shear stress whereby erosion occurs and the yield stress at the top of the bed. From experiments he found that dissolving iron oxides into a sediment layer does not noticeably change the macroscopic shear stress but changes the bed stress whereby erosion occurs. In what follows it will become clear that it is only essential that a relation of the type (24) exists while a relation as (22) need not be true. That is to say, we demand that the instantaneous physico-chemical composition at the top of the sediment bed determines uniquely the bed shear stress whereby scouring (erosion) occurs. Let us observe that the bed shear stress necessary for erosion depends also on the particle density in the viscous sublayer via ρ_v appearing in (24). However the variation of ρ_v with particle density is rather small. This agrees with the observation of Partheniades that the erosion rate is practically independent of the average particle density in the fluid for the range up to 12 g/ℓ attained in his experiments.

Suppose that after some time during which a sediment layer has built up by deposition, the shear stress is rather suddenly raised, say, due to the occurence of a storm. It is clear from (24) that in a short time the sea bed will be eroded to the depth where the solid concentration corresponds to the critical density. During such change one expects

a high scouring rate or even the formation of mud pebbles entering the fluid. This has indeed been observed [Migniot (1968), Partheniades (1972)].

We focus our attention on the calculation of the erosion flux which occurs from there on, when the applied shear stress is either constant (steady state) or changes quasi-stationary. Thereto (15) has to be solved under the appropriate initial and boundary conditions.

4.- The density distribution in a cohesive sediment bed

The initial condition of the sediment layer depends strictly speaking on the whole previous deposition and erosion history.

Nevertheless one can form a reasonable good idea of the solid particle density through the sediment layer from experiments in the ultracentrifuge where processes are speeded up enormously. Figure 16, taken from Fujita (1962), shows how the solid particle density distribution ρ changes in a centrifuge with inner radius r_1 and outer radius

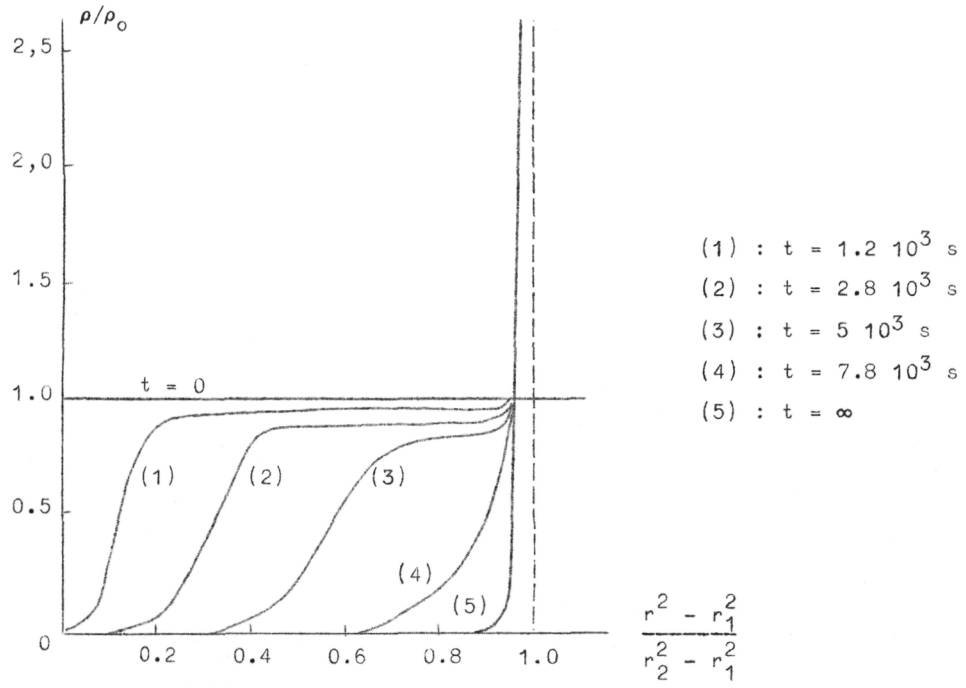


fig. 16.
Variation of density distribution in the ultra centrifuge (after Fujita).

r_2 . The (constant) angular velocity is ω and initially the two components fluid is homogeneous with a sediment density ρ_0 .

The important thing to observe is that for a rather long time one observes a sediment density distribution having a "plateau" region and that the change in plateau density value varies only slowly with time. Migniot (1968) who performed experiments on the settling of solid particles in a gravitational field found also the distribution with a near "plateau" region.

Guided by these results we assume a solid particle density distribution as shown in figure 17 and assume that the density ρ_p at the

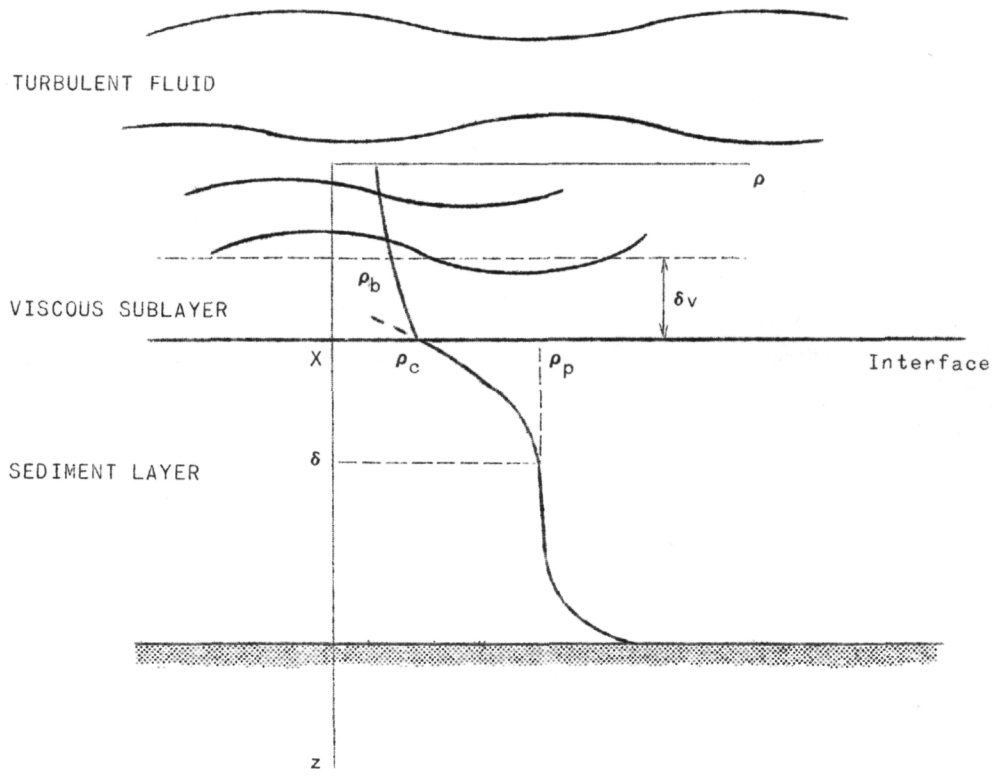


fig. 17.
Density distribution in the sediment bed.

"plateau", at $z = \delta$, remains constant during erosion. The density at the fluid-bed interface at $z = X$, is denoted by ρ_c . As long as erosion occurs its value is determined by (24), *i.e.* by the shear stress acting at the interface.

The vertical profile shown in figure 17 corresponds with the experimentally observed dissolved silica concentration in the North Sea [Wollast and Van Der Borght (1974)].

For $X \leq z \leq \delta$ a parabolic sediment density distribution of the following form may be assumed :

$$\rho = \rho_p + (\rho_c - \rho_p)\left(1 - \frac{z - X}{\delta - X}\right)^2 \qquad X \leq z \leq \delta \tag{25}$$

which satisfies

$$\begin{aligned} &\rho = \rho_c && && \text{at} && z = X \\ &\rho = \rho_p && \text{and} && \frac{\partial \rho}{\partial z}(\delta, t) = 0 && \text{at} && z = \delta \end{aligned} \tag{26}$$

5.- The interface mass flux continuity

In (25), X and δ are, of course, unknown functions of the time. To determine them with (15) we need one additional boundary condition. Thereto we set up the mass balance equation at the interface. Denote by J_+^* the sediment flux *with respect to the moving interface* in the sediment layer arbitrarily close to $X(t)$ and by J_-^* its value in the fluid arbitrarily close to $X(t)$.

By definition one has :

$$J_-^* = \rho_c^s \left(\mathbf{v}_-^s - \frac{dX}{dt}\right) \quad ; \quad J_+^* = \rho_c^s \left(\mathbf{v}_+^s - \frac{dX}{dt}\right) \tag{27}$$

where $\mathbf{v}_+^s$ and $\mathbf{v}_-^s$ are the velocities of the sediment contaminant in the sediment layer and fluid respectively and $\frac{dX}{dt}$ is the velocity of the interface.

The z components of these fluxes are :

$$J_{-z}^* = \rho_c^s \left(v_-^s - \frac{dX}{dt}\right) \quad , \quad J_{+z}^* = \rho_c^s \left(v_+^s - \frac{dX}{dt}\right) . \tag{28}$$

The sediment flux, in the sediment layer arbitrarily close to the interface, with respect to the barycentric or center of mass velocity $\mathbf{v}_+$ is by definition :

(29) $$\mathbf{J} = \rho_c^s \, (\mathbf{v}^s - \mathbf{v}_+)$$

Its z component is

(30) $$J_z = \rho_c^s \, (v^s - v_+) \, .$$

Combining (28) and (30) one obtains for the erosion flux counted positi e downwards

(31) $$J_z = J^*_{+z} + \rho_c^s \, (\frac{dX}{dt} - v_+) \simeq J^*_{+z} + \rho_c^s \, \frac{dX}{dt} \, .$$

The approximation expresses that the barycentric velocity in the sediment layer is negligible compared to $\frac{dX}{dt}$.

As there are no sources or sinks at the bed-fluid interface the normal sediment flux across it measured with respect to the interface velocity must be continuous, so that

$$J^*_{-z} = J^*_{+z} \equiv J_{z,v} \, .$$

Hence (31) can be written, omitting the superscript s ,

$$J_z = J_{z,v} + \rho_c \, \frac{dX}{dt} = \sigma \, \rho_c - D \, \frac{\partial \rho}{\partial t} \, (X,t) \, .$$

Here, (16) has been used and we have put $\sigma = s \, g_z$ where σ is the settle particle velocity in the sediment layer.

To determine the flux $J_{z,v}$ which crosses from the fluid to the sediment layer we calculate the diffusion and the sedimentation fluxes through the viscous sublayer.

The flow in the viscous sublayer is laminar-like in that the mean velocity profile is identical to the linear velocity profile of a plane parallel laminar flow with zero pressure gradient [Monin (1965)]. Nevertheless the flow is three-dimensional and unsteady [Kline *et al.* (1967)] . Streaks were observed by them to waver and oscillate and to pass sometimes rapidly to the outer edge of the boundary layer. The continuous formation and break up of low speed streaks fluctuations, which increase the diffusion coefficient to a higher value than the molecular one, presumably become more frequent and larger with increasing Reynolds number.

We denote the solid particle density (mass of sediment per unit fluid volume) at the top of the viscous sublayer, where it meets the logarithmic boundary layer, by ρ_b (see fig. 17).

The diffusion flux through the viscous sublayer with respect to the interface velocity, counted positive downwards, may be expressed by

$$\hat{J}_{z,diff} = - L (\rho_c - \rho_b) \tag{33}$$

wherein the transport coefficient L is defined by

$$L = \frac{D_v}{\delta_v} > 0 \tag{34}$$

where D_v is the diffusion coefficient and δ_v the thickness of the sublayer.

In (33) we have assumed that the solid particle density varies linearly through the viscous sublayer.

In addition to this diffusion flux there is a sediment flux through the viscous sublayer. Its average, counted positive downwards is

$$\hat{J}_{z,sed} = \frac{1}{\delta_v} \int_0^{\delta_v} J_{z,sed}\, dz = \frac{1}{\delta_v} \int_0^{\delta_v} \sigma_v\, \rho\, dz = \frac{1}{2}\, \sigma_v\, (\rho_b + \rho_c) \tag{35}$$

The total flux through the sublayer, counted positive downwards, is found by adding (33) and (35) :

$$J_{z,v} = L (\rho_b - \rho_c) + \frac{1}{2}\, \sigma_v\, (\rho_b + \rho_c) \,. \tag{36}$$

The viscous sublayer thickness appearing in (34) is related to the critical friction velocity U_{*c}, the fluid kinematic viscosity and the fluid density ρ_v [Monin (1965)] :

$$\delta_v = \alpha_v \frac{\nu}{U_{*c}} = \alpha_v\, \nu \sqrt{\frac{\rho_v}{\tau}} \tag{37}$$

where τ is the critical shear stress acting at the interface between fluid and sediment layer and α_v is a universal constant of order unity.

Hence

$$L = \frac{D_v\, U_{*c}}{\alpha_v\, \nu} = \frac{D_v}{\alpha_v\, \nu}\, \rho_v^{-\frac{1}{2}}\, \tau^{\frac{1}{2}} \,. \tag{38}$$

The relation (32) with $J_{z,v}$ given by (36) and the L appearing herein by (38) determine the additional boundary condition to (26). With them we shall proceed to solve the differential equation (15); its solution is approximated by assuming the parabolic distribution given by (24) and yields the erosion flux.

6.- The solution for the erosion flux

Integration of (15) between $z = X$ and $z = \delta$ results in

$$\int_{X(t)}^{\delta(t)} \frac{\partial \rho}{\partial t}\, dz = -\sigma \int_{X(t)}^{\delta(t)} \frac{\partial \rho}{\partial z}\, dz + D \int_{X(t)}^{\delta(t)} \frac{\partial^2 \rho}{\partial z^2}\, dz$$

$$\int_{X(t)}^{\delta(t)} \frac{\partial \rho}{\partial t}\, dz = -\sigma\,(\rho_p - \rho_c) + \frac{2\,D}{\delta - X}\,(\rho_c - \rho_p) \tag{39}$$

where we have made use of $\frac{\partial \rho}{\partial z}(\delta,t) = 0$ and

$$\frac{\partial \rho}{\partial z}(X,t) = -\frac{2}{\delta - X}\,(\rho_c - \rho_p) \tag{40}$$

which follows from (25).

Now by Leibnitz's rule we have

$$\frac{d}{dt} \int_{X(t)}^{\delta(t)} \rho(z,t)\, dz = \int_X^{\delta} \frac{\partial \rho}{\partial t}\, dz + \rho(\delta,t)\, \frac{d\delta}{dt} - \rho(X,t)\, \frac{dX}{dt}\,. \tag{41}$$

Combining (39) and (41) and using (26) gives

$$\frac{d}{dt} \int_X^{\delta} \rho\, dz = \rho_p\, \frac{d\delta}{dt} - \rho_c\, \frac{dX}{dt} + \sigma\,(\rho_c - \rho_p) + \frac{2\,D}{\delta - X}\,(\rho_c - \rho_p)\,. \tag{42}$$

We proceed to evaluate the left hand side of this equation by means of (25). We find

$$\int_X^{\delta} \rho\, dz = \frac{\delta - X}{3}\,(2\,\rho_p + \rho_c)\,. \tag{43}$$

We have pointed out that it is a good approximation to assume that ρ_p is constant, see figure 16. For a *steady* erosion flux which requires a constant applied shear stress at the top of the viscoplastic sediment layer one finds from (24) that ρ_c is constant. Hence

$$(44) \qquad \frac{d}{dt}\int_{\chi}^{\delta} \rho \, dz = \left(\frac{d\delta}{dt} - \frac{dX}{dt}\right)\left(\frac{2\,\rho_p + \rho_c}{3}\right) .$$

Thus for this case (42) reduces to :

$$(45) \qquad \frac{2\,\rho_p + \rho_c}{3}\left(\frac{d\delta}{dt} - \frac{dX}{dt}\right) = \rho_p \frac{d\delta}{dt} - \rho_c \frac{dX}{dt} + \sigma\,(\rho_c - \rho_p) + \frac{2\,D}{\delta - X}(\rho_c - \rho_p) .$$

In addition to this relation we obtain a second one when (40) is substituted in (32) :

$$(46) \qquad J_z = J_{z,v} + \rho_c \frac{dX}{dt}$$

$$(47) \qquad = \sigma\,\rho_c + 2\,D\,\frac{\rho_c - \rho_p}{\delta - X} .$$

In the stationary state J_z and $J_{z,v}$ are constant. Hence it follows from (46) that $\frac{dX}{dt}$ must be constant. It follows now from (47) that $\delta - X$ must also be constant.

Thus

$$(48) \qquad \frac{d\delta}{dt} = \frac{dX}{dt} .$$

Whence for the stationary state we obtain from (45)

$$(49) \qquad (\rho_c - \rho_p)\frac{dX}{dt} = \sigma\,(\rho_c - \rho_p) + \frac{2\,D}{\delta - X}(\rho_c - \rho_p) .$$

Eliminating $\frac{2\,D}{\delta - X}(\rho_c - \rho_p)$ between (47) and (49) gives

$$(50) \qquad \frac{dX}{dt} = \sigma - \frac{J_{z,v}}{\rho_p} .$$

Substituting this result in (46) gives for the stationary erosion flux :

$$(51) \qquad J_z = \rho_c\,\sigma + \left(1 - \frac{\rho_c}{\rho_p}\right) J_{z,v} .$$

The erosion flux, J , for the stationary state counted as *positive upwards, i.e.* $J = -J_z$, is finally found when (36) is substituted into (51). One has :

$$(52) \qquad J = -\rho_c\,\sigma + \left(\frac{\rho_c}{\rho_p} - 1\right)\left[L\,(\rho_b - \rho_c) + \frac{1}{2}\sigma_v\,(\rho_b + \rho_c)\right]$$

wherein

(53) $$\rho_c = \left(\frac{\tau}{E_i}\right)^{1/B_i}$$

as follows from (24). L which is also a function of τ is given by (38).

The equation (52) has been derived under the assumption that erosion occurs. The auxiliary condition herefore is as follows : when the instantaneous solid particle density at the top of the bed is ρ_c then erosion finds place if and only if the bed shear stress is larger or equal to the critical value τ determined by (53).

This loading condition can also be referred to the initial bed state. Consider a fluid flow such that no erosion finds place. (Either sediment deposition finds place or no deposition and no erosion.) Denote the sediment density at the top of the sediment bed in this state by ρ_1 . The minimum shear stress necessary for the onset of erosion follows from (24) as

(54) $$\tau_1 = E_1 \rho_1^{B_1} \quad .$$

For a shear stress which is smaller but arbitrarily close to τ_1 no erosion occurs. Thus (52) gives the steady state erosion flux for $\tau \geq \tau_1$.

It is clear that the analysis implies that when the bed shear stress is decreased, erosion will cease at once.

Scouring will reoccur under this lower shear stress when the density at the top of the bed diminishes until a value is reached which corresponds with the new ρ_c determined by (53). The lowering of the density during the period when no erosion occurs is due to the diffusion of water into the sediment bed. From the other side deposition will counteract by increasing the bed density. However the experiments of Partheniades show that the latter effect is negligible, because lowering of the shear stress results, in a very short time during which settling is negligible, in a lower scouring rate determined by (52). Settling will only occur when the bed stress is lowered to a minimum value which is close to the value τ_1 at which scouring is first observed for a fresh sediment bed.

7.- An approximate expression of the erosion flux

A simplification of the relation (52) is possible when the defloccu-lated solid particle diameter is very small. During stationary erosion the solid particles break continuously from the bed. Thus unlike deposition during which the particles are flocculated, the diameter of the particles passing during erosion through the viscous sublayer to the bulk fluid is likely to be very small. Therefore the settle velocity in the viscous sublayer approaches a negligible value. This is in accordance with the observations that single clay particles can be carried in suspension by Brownian motion.

The settling velocity σ_v during erosion we expect therefore to be much smaller than $L = \frac{D_v}{\delta_v}$.

The latter is of the order 10^{-9} m/s (the molecular diffusion $D_v \simeq 10^{-11}$ m^2/s while $\delta_v \simeq 0.01$ m).

Hence, for fine grained cohesive soils

$$L \gg \sigma_v \quad , \quad L \gg \sigma \; . \tag{56}$$

The solid particle density at the top of the sediment layer ρ_c is during erosion related to the bed shear stress τ by the relation (53). The condition

$$\frac{\rho_c}{\rho_p} \ll 1 \tag{57}$$

is therefore expected to be satisfied for sufficiently small bed shear stresses. Under the conditions (56) and (57), (52) reduces to :

$$J_i = \frac{L}{E_i^{1/B_i}} \left(\tau^{1/B_i} - \rho_b \, E_i^{1/B_i}\right) \quad \text{for} \quad \tau \geq \tau_1 \quad (i = 1,2) \; . \tag{58}$$

As $J_1 = 0$ for $\tau = \tau_1$ we have

$$\tau_1^{1/B_i} = \rho_b \, E_1^{1/B_i} \; .$$

Hence we may write

$$J_i = \frac{L}{E_i^{1/B_i}} \left(\tau^{1/B_i} - \tau_i^{1/B_i}\right) \quad \text{for} \quad \tau \geq \tau_i \quad (i = 1,2) \; . \tag{59}$$

Thus

$$J_1 = \frac{L}{E^{1/B_1}} \left(\tau^{1/B_1} - \tau_1^{1/B_1}\right) \tag{60}$$

for region 1. One may introduce a bed shear stress τ_2 whereby the flux in region 2 would be zero if only region 2 would be present. That is to say, when only the straight line describing the second region in figure 15 is considered with the understanding that this line is prolonged to cut the absciss. Hence

$$J_2 = \frac{L}{E^{1/B_2}} \left(\tau^{1/B_2} - \tau_2^{1/B_2}\right) \tag{61}$$

in region 2 .

Substituting (34), (37) into (59) yields for the erosion flux

$$J_i = A_i \left(\tau^{1/B_i} - \tau_i^{1/B_i}\right)\tau^{\frac{1}{2}} \quad \text{for} \quad \tau \geq \tau_i \quad (i = 1,2) \tag{62}$$

where

$$A_i = \frac{D_v}{\alpha_v \nu \rho_v^{\frac{1}{2}} E_i^{1/B_i}} \,. \tag{63}$$

The constants appearing herein differ in the first region $(i = 1)$ and second region $(i = 2)$ according to (21) - (24).

It is interesting to observe that for $B_i = 1$, (62) reduces to the bed-load relation derived by Bagnold (1956), see also Monin (1965), for a sand bed. The quantity A_1 is there not determined from the theory but taken from an experimental graph where it is plotted against sand particle diameter.

Of course, the equations we have derived should apply equally to the flow of air over a dust layer, at least when the latter has similar properties as the sediment layer we considered above.

8.- Comparison with experiment

Partheniades (1965), (1972), conducted laboratory erosion experiments in an open rectangular channel. We quote him for the following facts.

"The experiments were conducted in an open flume with recirculating water at ocean salinity. The bed material, sampled from the San Francisco Bay and known as Bay mud, contained approximately equal amounts of silt and clay and some traces of fine sand and organic matter. It is a highly plastic soil with a liquid limit of 99 % and a plasticity index (PI) of 55 % . The clay proportion consists predominantly of montmorillonite and illite. Figure 18 shows the erosion rate as function of the average bottom shear stress. Series I correspond with a bed remolded at its field moisture of 110 % with a shear strength of about 20 p.s.f. ($\simeq$ 1000 N/m^2) at ultimate failure and 11 p.s.f. at yield point. The minimum bed shear strength at which erosion was first observed was about 0.002 p.s.f. ($\simeq$ 0.1 N/m^2) . The bed in series II was formed by releveling that of series I. However, due to some unavoidable water entrainment, it displayed a higher water content and lower shear strength. The observed increase of the resistance to erosion was attributed to cementation due to iron oxides dissolved in the water. The fact that the increased interparticle bonds were not reflected in the macroscopic shear strength of the bed indicates that the soil cohesion, as determined by conventional shear strength tests, is not a representative or a unique measure of the soil resistance to erosion".

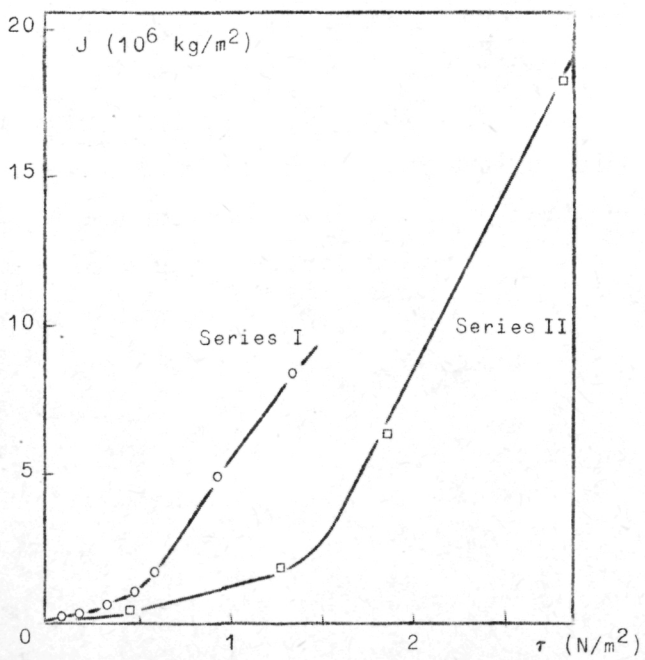


fig. 18.
Variation of erosion rates J with bottom shear stress τ (after Partheniades).

We have commented that a unique relation between the critical shear stress and yield stress is not essential for the theory. The essential thing is that the instantaneous physico-chemical composition at the top of the sediment layer (at the sediment-fluid interface) determines uniquely the shear stress whereby erosion finds place.

To apply the relation (62) to the experiments performed by Partheniades we shall assume that the Bay mud has properties which correspond closely to the data given by Migniot for the Provins clay. For that mud $m = 5$ and $n \simeq 10^{-13}$.

The shear stress whereby erosion occurs is related to the yield stress at the top of the sediment layer by

$$\tau = \rho_v \, p_1^2 \, \tau_y^{2q_i} \tag{64}$$

as follows from (22) and (23).

Series I

There is a clear change in the nature of series I, figure 18, for a bed shear stress of about $\tau_c = 0.011$ lb/ft^2 $= 0.53$ N/m^2 . Using this value in (64) and $\rho_v \simeq 1000$ kg/m^3 and the values $p_1 = 0.0178 \, G^{5/4}$, $q_1 = 0.25$ found by Migniot for the first region [for completeness we shall carry the correction factor introduced in (21) along], we find for the corresponding yield stress $\tau_y = \frac{2.7}{G^5}$ N/m^2 .

By inspection of figure 15 it is seen that this value corresponds very well to the intersecting point of the two straight lines if the line for the higher yield stress range (region 2) is drawn through the experimental points of the Provins clay. The equation for this second line is ($m = 5$) :

$$U^* = p_2 \, \tau_y^{q_2} = 0.0139 \, G^{5/2} \, \tau_y^{0.5} \, .$$

Accordingly, we shall use the values :

$$\begin{cases} p_1 = 0.0178 \, G^{5/4} \quad , \quad q_1 = 0.25 \\ p_2 = 0.0139 \, G^{5/2} \quad , \quad q_2 = 0.5 \end{cases} \tag{65}$$

With (65) it follows from (64) that the two regions are separated at the bed shear stress $\tau = 0.53\ N/m^2$.

From (65) and (24) it follows that

(66) $$B_1 = 2.5 \quad , \quad B_2 = 5 \ .$$

The erosion relation (62) becomes now

(67) $$J_1 = A_1 (\tau^{0.4} - \tau_1^{0.4})\ \tau^{0.5} \quad \text{for} \quad 0.12\ N/m^2 \le \tau \le 0.53\ N/m^2$$

(68) $$J_2 = A_2 (\tau^{0.2} - \tau_2^{0.2})\ \tau^{0.5} \quad \text{for} \quad \tau \ge 0.53\ N/m^2$$

The initial critical bed shear stress reported by Partheniades whereby erosion occurs is $\tau_1 = 0.0025\ lb/ft^2 = 0.12\ N/m^2$.

Using the experimental values

$$J_1 = 0.435\ g/ft^2.h = 1.3 \times 10^{-6}\ kg/m^2.s \quad \text{for} \quad \tau = 0.53\ N/m^2$$

and

$$J_2 = 2.46\ g/ft^2.h = 7.37 \times 10^{-6}\ kg/m^2.s \quad \text{when} \quad \tau = 0.025\ lb/ft^2 = 1.197\ N/m^2$$

obtained from figure 18; we determine the constants in (67) and (68) as

(69)
$$\tau_1 = 0.12\ N/m^2 \quad , \quad \tau_1^{0.4} = 0.43 \quad , \quad A_1 = 4.96 \times 10^{-6}$$
$$\tau_2 = 0.39\ N/m^2 \quad , \quad \tau_2^{0.2} = 0.83 \quad , \quad A_2 = 33 \times 10^{-6}$$

The calculated curve in figure 18 shows that with these values, (67) and (68) give a remarkable good description of the erosion flux observed in series I. In particular one notes that the change in slope is predicted by the theory.

To confirm the theory we must however check if, with the A's given by (69), the diffusion coefficient in the viscous sublayer calculated with (63) corresponds in order of magnitude with the molecular diffusion coefficient $10^{-10} - 10^{-11}\ m^2/s$.

For the two regions we obtain from (24), taking $\rho_v = 1000\ kg/m^3$:

(70) $$E_1 = 10^{-7}\ G^{5/2} \quad , \quad E_2 = 1.93 \times 10^{-14}\ G^5 \ .$$

Using $\alpha_v \simeq 10$, $\nu = 10^{-5}\ m^2/s$ we find from (63) :

$$D_v = 2.4 \times 10^{-11}\ G\ m^2/s \quad \text{in region 1 ,}$$

$$D_v = 1.9 \times 10^{-11}\ G^2\ m^2/s \quad \text{in region 2 .}$$

These diffusion coefficients are of the same order. For a correction factor $G = 5$, the average diffusion coefficient in region 2 is about four times that in region 1. As the turbulent fluctuations in the viscous sublayer become presumably more frequent with increasing shear stress it must be expected that the diffusion coefficient becomes larger.

Series II

Partheniades reports that the increased resistance against erosion in series II is believed to be caused by dissolved iron oxides.

Figure 18 shows that a strong increase in the erosion rate occurs for this II bed by a shear stress of about $\tau = 0.031\ lb/ft^2 = 1.48\ N/m^2$.

According to (64) this corresponds with a yield stress of

$$\tau_y\ G^5 = 21.8\ N/m^2 \qquad (m = 5) .$$

This value should correspond with the yield stress whereby the dependence of U_* on $\tau_y\ G^m$ changes strongly. However, from figure 15, we see that this value is much too high. In conclusion we may say that the physical properties of the bed in series II have changed so much that Migniot's data are not applicable.

Nevertheless we have made an attempt to fit series II. By trial we found that if the value of B_1 and B_2 in (62) are lowered, a slightly better fit could be obtained. In particular for $B_1 = 1$ and $B_2 = 2$ and $m = 5$, it follows from (24) that $q_1 = 0.1$ and $q_2 = 0.2$.

By fitting two points in the first region of series II (figure 18) and another point in region 2 we obtain for A_1 , A_2 in (62) in M.K.S. units :

(70) $$A_1 = 1.7 \times 10^{-6} \quad , \quad A_2 = 19.9 \times 10^{-6} .$$

By using $D_{v_1} = 1.7 \times 10^{-11}\ m^2/s$ we find now from (63) and (24) that :

$$p_1 = 0.036 .$$

With these values the yield stress at the top of the sediment bed which separates region 1 from region 2 follows from (64) as $\tau_y = 2.2\ N/m^2$. This value corresponds nicely with the breaking point observed by Migniot (fig. 15). The value of p_2 can now be determined from the relation

$$U_* = p_1\ \tau_y^{q_1} = p_2\ \tau_y^{q_2}$$

which holds true at the breaking point where region 1 and 2 meet, as follows from (22). We obtain $p_2 = 0.033$.

The diffusion coefficient in region 2 follows now from (70), (63) and (24) as $D_{v_2} = 370 \times 10^{-11}$ which is 100 times larger than for series 1. The equations for the erosion flux in series II are in M.K.S. units :

$$J_1 = 1.7 \times 10^{-6}\ (\tau - 0.34)\ \tau^{\frac{1}{2}} \qquad 0.34\ N/m^2 \leq \tau \leq 1.48\ N/m^2$$

$$J_2 = 19.9 \times 10^{-6}\ (\tau^{0.5} - 1.12)\ \tau^{\frac{1}{2}} \qquad \tau \geq 1.48\ N/m^2 .$$

These give a good description as shown in figure 18.

References

BAGNOLD, R.A., (1956). *Phil. Trans. Roy. Soc. London, A 249.*

BÖHNECKE, G., (1922). Salzgehalt und Strömungen der Nordsee. Veröff. Inst. Meeresk. Univ. Berl., Neue Folge A., *Geog.-Naturwiss. Reihe N° 10,* 1-34.

BOWDEN, K.F., (1965). *J. Fluid Mech., 21,* 83.

CARRUTHERS, J.N., (1935). The flow of water through the Straits of Dover, *Fishery Investigations,* Series N° 2, 1-67.

CARTWRIGHT, D.E., (1961). *J. Institute Navigation, 14,* 130-151.

ELDER, J.W., (1959). *J. Fluid Mech., 5,* 544.

ELSKENS, I., (1974). *Some aspects of the dynamic behaviour of metallic and other pollutants in the water column and the associated sectors,* Part 4, Sediments, in Math. Modelsea I.C.E.S. Hydrography Committee, C.M. 1974 - C : 1, 439-450.

FUJITA, H., (1962). *Mathematical Theory of Sedimentation Analysis*, Academic Press, N.Y.

GODIN, G., (1966). *The tides in the Labrador Sea, Davis Strait and Baffin Bay*, Marine Science Branch Manuscript Report Series, N° 2, Ottawa.

GULLENTOPS, F., (1974). *Detrital Sedimentology in the Southern Bight of the North Sea*, in Math. Modelsea, I.C.E.S. Hydrography Committee, C.M. 1974 - C : 1, 55-80.

HILL, H.W., (1973). *Currents and water masses*, in *North Sea Science*, edited by E. Goldberg, MIT University Press, 17-42.

KALLE, K., (1949). *Die natürlichen Eigenschaften der Gewässer*, in *Handbuch der Seefischerei Nordeuropas*. Vol. 1, Part 2, edited by Schweizerbart, Stuttgart.

KLINE, S.J., REYNOLDS, W.C., SCHRAUB, F.A. and RUNSTADLER, P.S., (1967). *J. Fluid Mech., 30*, 741.

LEAVASTU, T., (1963). *Serial Atlas of Marine Environment*, Amer. Geoph. Soc. Publ.

McCAVE, I.N., (1972). *Transport and Escape of Fine Grained Sediment from Shelf Area*, in *Shelf Sediment Transport Process and Pattern*, Dowclen-Hutchinson and Ross Publ.

MIGNIOT, C., (1968). *La Houille Blanche, 7*, 591.

MONIM, A.S. and YAGLOM, A.M., (1965). *Statistical Fluid Mechanics*, MIT Press, Cambridge, Mass.

NIHOUL, J.C.J., (1974). *Advances in Geophysics, 18 A*, 331.

NIHOUL, J.C.J., (1975a). *Modelling of Marine Systems*, Elsevier Publ., Amsterdam.

NIHOUL, J.C.J., (1975b). *Application of Mathematical Models to the Study, Monitoring and Management of the North Sea*, in *Ecological Modelling in a Resource Management Framework*, Resources for the Future, Washington D.C.

NIHOUL, J.C.J., (1975c). *Effect of the tidal stress on mud deposition in the Southern Bight of the North Sea*, Proc. 2nd Annual Meeting of the European Ceophysical Society, Trieste 20-26 Sept. 1974.

NIHOUL, J.C.J., (1975d). *Mesoscale secondary flows. Implications in the chemical and biochemical dynamics of the Southern Bight of the North Sea*, Liège 6th Coll. Ocean Hydrodyn., *Mém. Soc. Roy. Sci. Liège.*

NIHOUL, J.C.J. and ADAM, Y., (1974). Programme national sur l'environnement physique et biologique, C.I.P.S., *N 36*.

NIHOUL, J.C.J. and RONDAY, F.C., (1975). *Tellus*, *27*, 5.

OTTO, L., (1970). *The mean residual transport in the Southern North Sea*, I.C.E.S., C.M. 1970 - C : 21.

PARTHENIADES, E., (1965). *J. Hydraulics Div.*, *91*, HY 1 4204

PARTHENIADES, E., (1972). *Results of recent investigations on erosion and deposition of cohesive sediments*, in *Sediments*, edited by Hsich Wen Shen, Fort Collins, U.S.A.

PODAMO, J., (1974). *Aspects of dynamic biology in the Southern Bight of the North Sea*, in Math. Modelsea, I.C.E.S. Hydrography Committee, C.M. 1974 - C : 1.

TAYLOR, G.I., (1922). *Proc. London Math. Soc.*, *20*, 148.

TAYLOR, G.I., (1953). *Proc. Roy. Soc.*, *A 219*, 186.

TAYLOR, G.I., (1954). *Proc. Roy. Soc.*, *A 223*, 446.

WOLLAST, R. and VAN DER BORGHT, (1974). *Model of mass transfer in a benthic boundary layer submitted to physical and biological perturbations*, Nato Science Committee Conf., Les Arcs, France.

WYRTKI, K., (1954). *Deutsche Hydrog. Zeit*, *7*, 91.

YALIN, M.S., (1972). *Mechanics of Sediment Transport*, Pergamon Publ., Oxford.

Chapter II

I

A mathematical model of microbial and chemical oxidation-reduction processes in the Scheldt estuary

by

G. BILLEN and J. SMITZ

Based on work by Y. ADAM[3], G. BILLEN[1,2], M. HOENIG[1], Cl. JOIRIS[1], J. LEFEVRE[2], Y. RUNFOLA[3], J. SMITZ[3].

1. Laboratoire de Chimie industrielle, U.L.B.
2. Laboratorium voor Ekologie en Systematiek, V.U.B.
3. Groupe de Mécanique des Fluides géophysiques, U. Lg.

Introduction

The deterioration of chemical and biological properties of natural waters by domestic pollution is not the direct consequence of the presence of an organic load in the water, but is rather the result of heterotrophic bacterial activity which modifies oxidation-reduction characteristics of the water while degrading this charge. Because other oxidants than oxygen can be used by heterotrophic microorganisms (anaerobic respirations), a complete oxidation-reduction budget is necessary to describe correctly the evolution of the chemical composition of the water under microbiological influence. The classical models of river pollution, using oxygen as the only chemical state variable, are confronted with serious difficulties as soon as anaerobic microbial metabolisms occur.

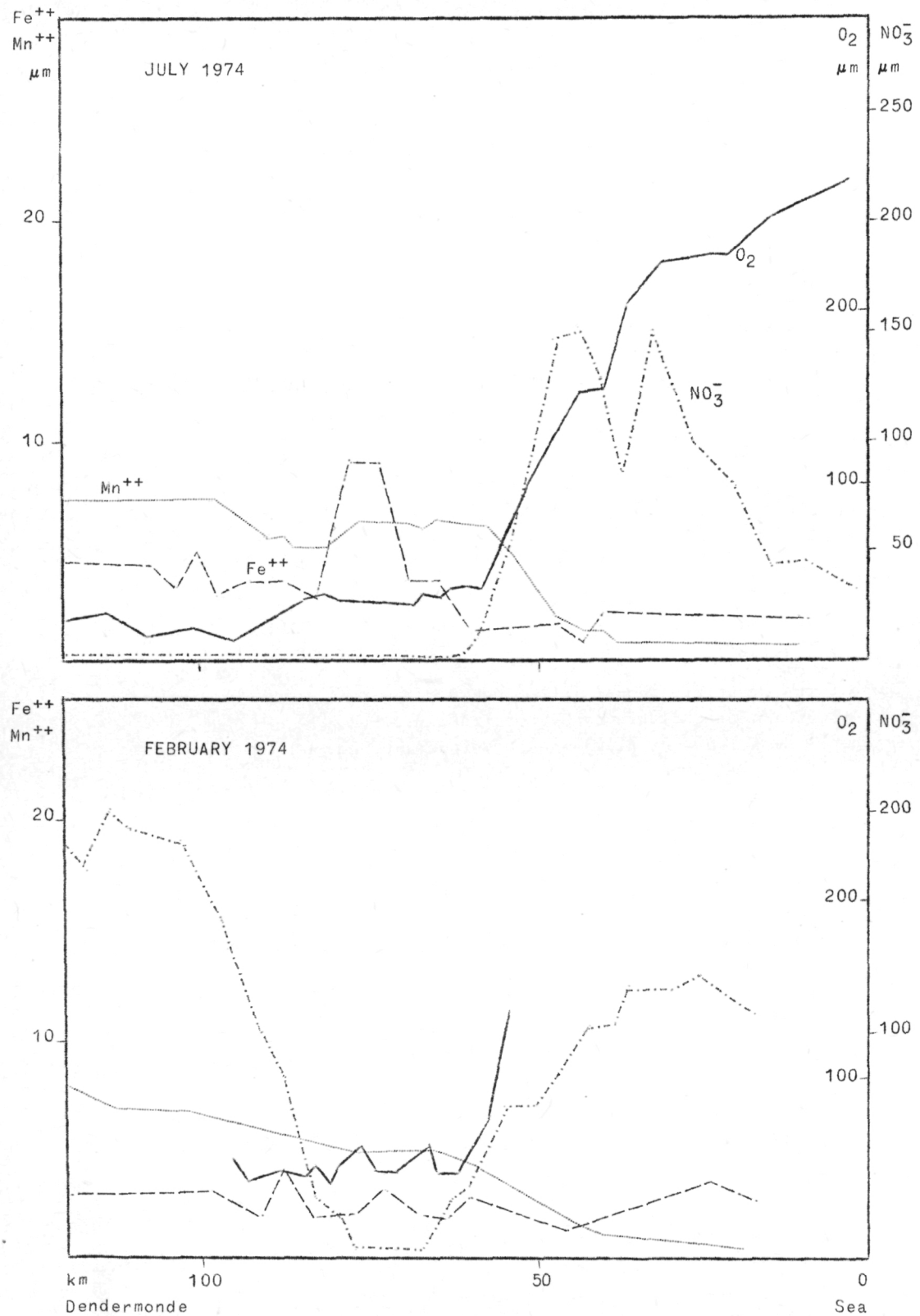


fig. 1.
Longitudinal profiles of oxidation-reduction compounds in the Scheldt Estuary.

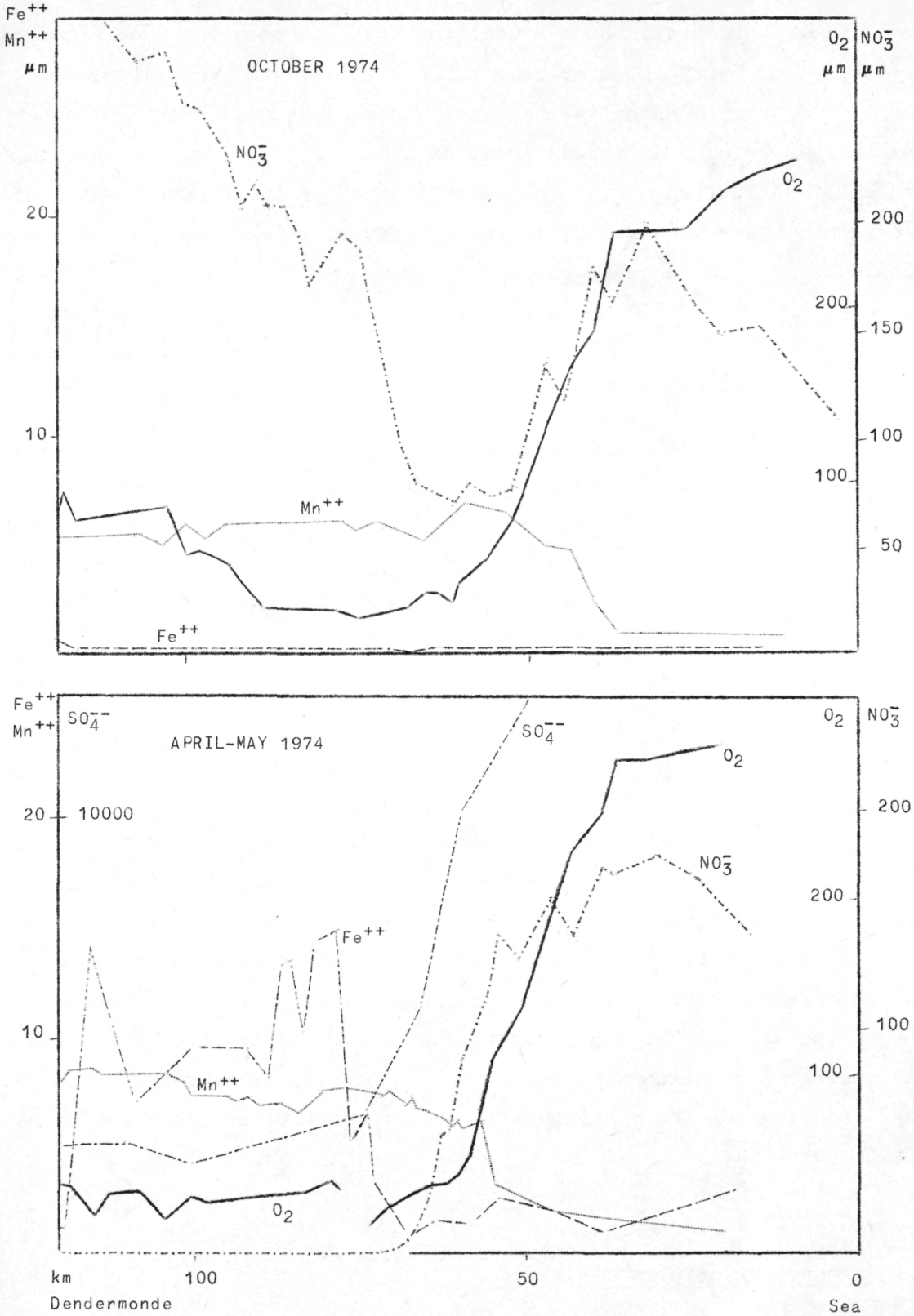


fig. 1.

Longitudinal profiles of oxidation-reduction compounds in the Scheldt estuary.

This work presents an oxidation-reduction model of the influence of bacterial activity on water composition, applied to the case of the Scheldt estuary. Basically the same phenomena occurs in natural water systems sustaining an intense heterotrophic activity, such as bottom water of stratified basins [Richards (1965)] or interstitial water of sediments [Thorstenson (1970)]. With a few modifications, the same model could be applied to these cases.

1.- Experimental results

Typical longitudinal profiles of concentration of several oxidation-reduction compounds are shown in fig. 1 for winter and summer situations. Note abrupt transitions between zones where a given substance is reduced or oxidized. According to these profiles, it is possible to define an upwards zone (whith chlorinities less than 2 g Cl/ℓ) where oxidants (O_2 , Mn^{4+}, NO_3^- , Fe^{+++}, SO_4^{--}) are successively reduced, and a downwards zone (with chlorinities higher than 2 g Cl/ℓ) where oxidants are regenerated in the opposite order. The reductive stage proceeds less far in the winter than in the summer : for instance, reduced iron does not appear in the winter.

Dark ^{14}C-bicarbonate incorporation, an index of heterotriphic bacterial activity has been determined along several longitudinal profiles of the Scheldt (fig. 2). Again, two zones can be distinguished : intense heterotrophic activity occurs upwards, approximately down to the point where 2 g/ℓ chlorinity is reached, and abruptly vanishes downwards. Bacterial activity is much less intense in the winter than in the summer; an empirical relation with water temperature T and river discharge d has been found : The mean upwards heterotrophic bicarbonate incorporation is proportional to $\frac{1}{d}\ 10^{T/d}$.

2.- General principles of the model

The above mentioned results are easily interpreted : The Scheldt Estuary is heavily polluted upwards Antwerp by important amounts of

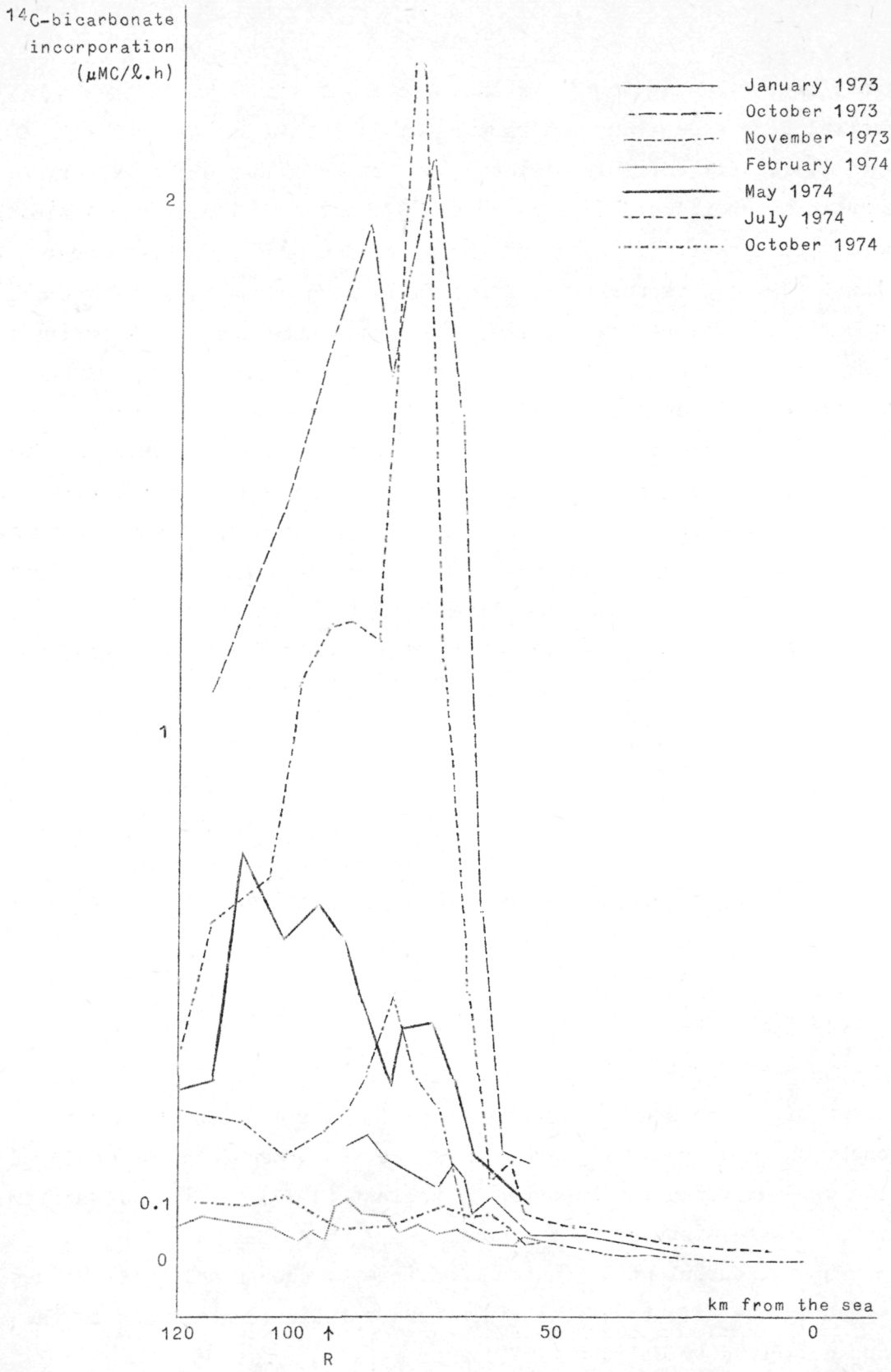


fig. 2.

Dark ^{14}C-bicarbonate incorporation along a profile of the Scheldt, at different seasons.

organic matter. Owing to the intense bacterial activity, the redox potential decreases from Dendermonde (km 120) to about Antwerp (km 80) . Oxygen is rapidly entirely depleted, and other oxidants are used by anaerobic metabolisms. Then, near km 70 , owing to increasing salinity, floculation and precipitation of the suspended organic matter occur [Wollast (1973)], bacterial activity falls down and a phase of recuperation begins, accelerated by mixing with unpolluted sea water. During this stage, reaeration not only restores the oxygen concentration but also regenerates the previously used oxidizing agents.

All these phenomena will be simulated by a model in which measured values of bacterial activity are introduced as a command parameter modifying the composition of the water without disturbing the thermodynamic internal equilibrium between all the involved oxidation-reduction couples.

The variations in the concentration of the considered chemical compounds are the result of advection, turbulent diffusion or consumption by oxidation reduction processes :

$$(1) \qquad \frac{\partial}{\partial t} x_i + u(s,t) \frac{\partial}{\partial s} x_i = D(s,t) \frac{\partial^2}{\partial s^2} x_i - C_i(s,t)$$

where t is the time, s is the longitudinal coordinate, x_i is the concentration of the i^{th} species, u is the residual velocity of the water, D is the turbulent diffusion coefficient, C_i is the rate of oxidation-reduction consumption.

2.1.- Hydrodynamical model

The residual velocity of the water has been calculated as the quotient of the residual outflow [the seasonal variation of which is given by the measurements published by the *Antwerpse Zeediensten* (1966)] to the wet section area [reported by Wollast (1973) to fit a logarithmic fonction of the distance to the mouth].

For the turbulent diffusion coefficient, phenomenological values, integrating the effects of the tides were calculated according to the method described by Wollast (1973).

This one dimensional hydrodynamic treatment is admittedly very simplistic. However, its ability to simulate the observed longitudinal profile of chlorinity for each cruise has been shown to be satisfactory.

2.2.- Microbiological model

The oxidation reduction processes, represented by the term C_i , are controlled by heterotrophic bacterial activity in the water. For oxygen, an additional aeration term occurs. It was taken as proportional to the oxygen saturation deficit, with a proportionality coefficient K about $6 \times 10^{-3}\ h^{-1}$, as estimated by Wollast (1973).

The bacterial activity can be viewed as an electron flux imposed to the water system, according to the reaction :

$$CH_2O + H_2O \xrightarrow{bact.} CO_2 + 4\ H^+ + 4\ e^- \ .$$

By writing this equation, we assumed that, from an overall point of view, fermentations play no important role, *i.e.* that no accumulation of uncompletely oxidized organic compounds (acids, cetones or alcohols) occurs. For organic acids, this has been experimentally confirmed.

This electron flux, $H(s,t)$, provocates one or several of the following reactions to go on :

a) $\quad 4\ e^- + O_2 + 4\ H^+ \rightleftharpoons 2\ H_2O$

b) $\quad 8\ e^- + NO_3^- + 10\ H^+ \rightleftharpoons NH_4^+ + 3\ H_2O$

c) $\quad 2\ e^- + MnO_2 + 4\ H^+ \rightleftharpoons Mn^{++} + 2\ H_2O$

d) $\quad 1\ e^- + Fe(OH)_3 + 3\ H^+ \rightleftharpoons Fe^{++} + 3\ H_2O$

d') $\quad Fe^{++} + HCO_3^- \rightleftharpoons FeCO_3 + H^+$

e) $\quad 14\ e^- + 2\ SO_4^{--} + Fe^{++} + 16\ H^+ \rightleftharpoons FeS_2 + 8\ H_2O$

so that $\quad H(s,t) = \sum_i \nu_i\ C_i(s,t)$.

Some of these reactions are biologically mediated and the presence of the responsible organisms has been demonstrated in the Scheldt (oxygen consumption, denitrification, nitrification, sulfato-reduction), others occur spontaneously although direct biological mediation can occur in certain

circumstances (iron oxidation and reduction, manganese oxidation and reduction). However this distinction in the reaction mechanisms is not essential for the overall balance we are doing.

To portion out the total electron flux $H(s,t)$ imposed to the system by heterotrophic activity between the different microbiological or chemical electron consuming pathways, the assumption is made that an internal thermodynamic equilibrium is achieved in the system for reactions a) to e). This imposes that five simultaneous equilibrium relations of the general form

$$Eh = E_i^0 + RT \log \frac{Ox_i}{Red_i}$$

hold. This is equivalent to saying that the bacteria only use thermodynamically favourable half reactions in their energy yielding metabolism.

Given a set of limit conditions (composition of the water at Rupelmonde and at the sea), the knowledge of the total bacterial activity $H(s,t)$ would allow to calculate the consumption term $C_i(s,t)$ for each oxidant considered, and hence the complete evolution of the water composition along a longitudinal profile of the estuary. Direct introduction of bacterial activity as a command parameter would allow to take implicitely into account a lot of phenomena that it would be difficult to consider explicitely, such as lateral import of organic matter, modification of the bacterial population with salinity, etc. According to Romanenko (1964), total carbon metabolism [and hence electron flux $H(s,t)$] can be evaluated from dark bicarbonate incorporation measurement by simply multiplying it by a constant factor α :

$$H(s,t) = 4 \times (\text{total C metabolism}) = 4\alpha \times (\text{bicarbonate incorporation}) .$$

However, critical examination of the literature [Romanenko (1964), Sorokin (1965), Overbeck (1974)] shows that this factor α can vary greatly with the bacterial species, the growth phase, the quality of the substrate, etc. Because of the lack of a precise value of α , and considering that α can vary because of changes in the bacterial community, we treated it as an ajustable parameter which can have different values from one season to the other.

3.- Mathematical resolution

To summarize preceeding discussion, the problem posed is to calculate the concentrations $X_i(s,t)$ of the considered oxidants and the concentrations $Y_i(s,t)$ of corresponding reduced form, by solving following system of equations :

i) 5 transport-diffusion equations

If $\mathbb{A}(s,t)$ represents the operator $\frac{\partial}{\partial t} + u(s,t)\frac{\partial}{\partial s} - D(s,t)\frac{\partial^2}{\partial s^2}$ the equations are :

$$\mathbb{A}X_i(X,t) = K(X_{1_{sat}} - X_1) - C_1(s,t) \tag{2}$$

where the subscript 1 refers to O_2 .

$$\mathbb{A}X_j = C_j(s,t) \tag{3}$$

$j = 2,5$ (*i.e.* NO_3^- , MnO_2 , $Fe(OH)_3$, SO_4^{--})

ii) one-relation on the C_i's

$$H(s,t) = \sum_{i=1}^{5} \nu_i C_i \ . \tag{4}$$

iii) 5 logarithmic relations between a sixth variable Eh and the X_i's and Y_i's

$$Eh(s,t) = \ell_1(X_1,Y_1) = \ell_2(X_2,Y_2) = \ell_3(X_3,Y_3) = \ell_4(X_4,Y_4) = \ell_5(X_5,Y_5) \tag{5}$$

These logarithmic relations enable to express the concentrations of oxidants as a function of the redox potential Eh . In the general case, the function ℓ_i has the form :

$$Eh = a_i + b_i \log \frac{X_i}{Y_i}$$

(see fig. 3) where Y_i refers to the concentration of the reduced form of the oxidant considered. (Note that if the oxidant or the reductor is a solid species, the corresponding value of X_i or Y_i to be used in the preceeding relation must be unity or zero.)

For the reduced form Y_j , we have

$$\mathbb{A}Y_j(s,t) = - C_j(s,t) \tag{6}$$

By summing this equation with the corresponding equation (3) for the X_j's , we have :

(7) $$\nabla\Delta Z_j(s,t) = 0$$

if $$Z_j \equiv X_j + Y_j \ .$$

i.e.

$$\nabla\Delta(NO_3^- + NH_4^+) = 0$$

$$\nabla\Delta(MnO_2 + Mn^{++}) = 0$$

$$\nabla\Delta[Fe(OH)_3 + Fe^{++} + FeCO_3 + FeS_2] = 0$$

$$\nabla\Delta(SO_4^{--} + 2\ FeS_2) = 0 \ .$$

The maximum possible value of $X_i(x,t)$ is of course $Z_i(s,t)$. The minimum considered is 10^{-6} moles/ℓ , which is approximated to zero. This divides the redox potential range into three domains for every oxidant :

$$Eh > L_A \ ,$$

$$X_i(x,t) = Z_i(s,t) \ ;$$

$$L_B > Eh > L_A \ ,$$

X_i given by the relation

$$Eh = a_i + b_i \log \frac{X_i}{Z_i - X_i} \ ;$$

$$Eh > L_B \ ,$$

$$X_i = 0 \ .$$

The numerical method used to solve the system utilizes time and space discretisation and, at each time step, the following sequential procedure is used :

i) solution of the four equations (7) for $Z_j(s,t)$;

ii) computation of the limits $L_A(s,t)$ and $L_B(s,t)$ for every oxidant in the Eh domain.

iii) computation of an associated variable

(8) $$F(s,t) = \sum_{i=1}^{5} \nu_i X_i$$

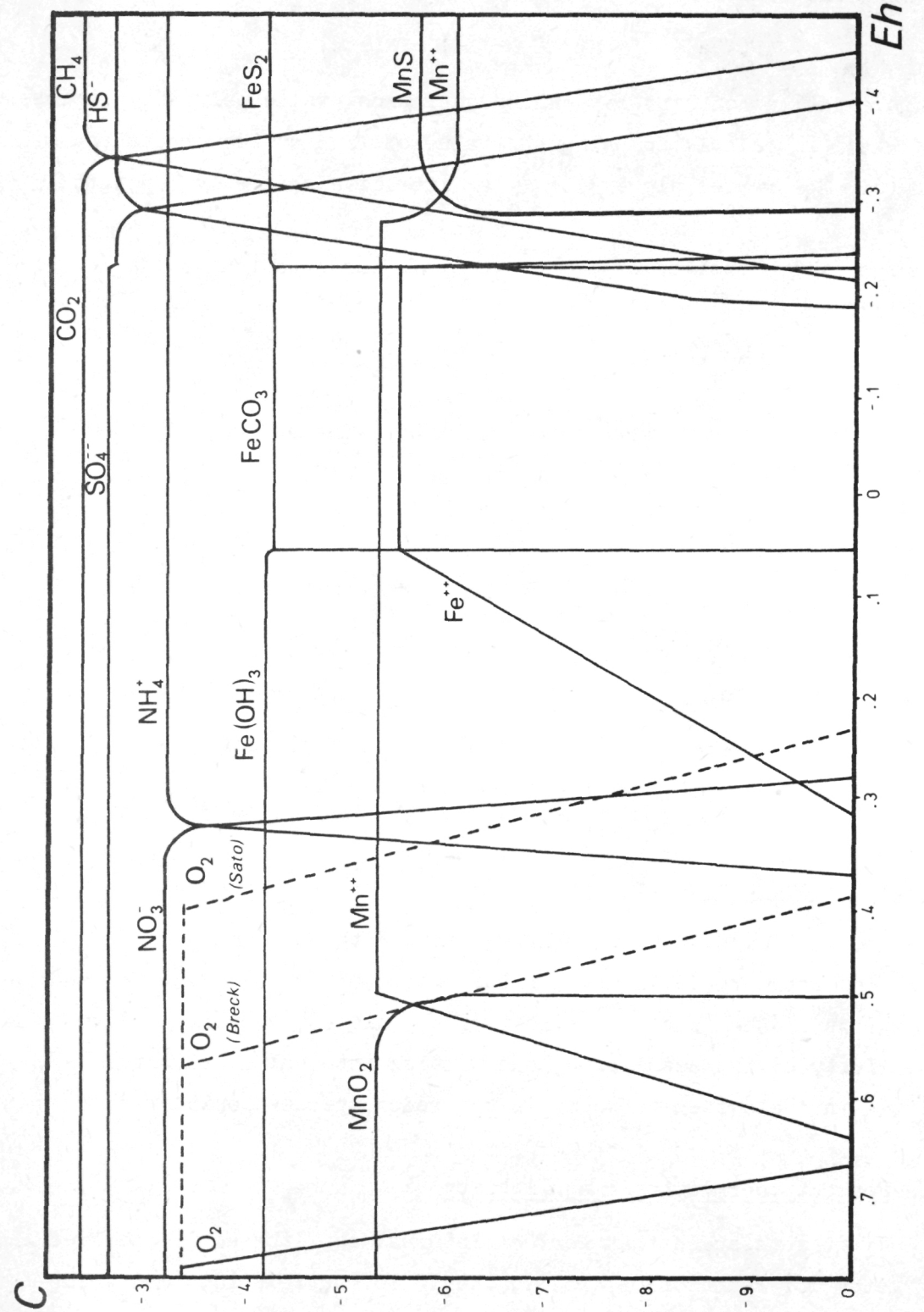


fig. 3.

Eh-concentration diagram for the water at Rupelmonde.

for which the following equation holds :

$$(9) \qquad \nabla\Delta F(s,t) = \nu_1 K(X_{1_{sat}} - X_1) - H(s,t)$$

As this equation contains oxygen concentration explicitely, the expression $(X_{1_{sat}} - X_1)$ is calculated using the value of X_1 at the preceeding time step (if X_1 varies slowly) or by an iterative scheme over points 3 and 4.

The discretization of transport-diffusion equations leads to tri-diagonal form :

$$- A_i F_{i+1} + B_i F_i - C_i F_{i-1} = D_i$$

which is then solved by recurrent algorithm [Adam and Runfola (1971), Adam (1975)].

iv) Solution of an implicit relation

$$F(s,t) = \Sigma \ \nu_i X_i = f(Eh , L_A , L_B) \ .$$

This relation allows to calculate the redox potential $Eh(s,t)$ and the concentration of the oxidants via the logarithmic relations

$$Eh = \ell_i(X_i) \ .$$

4.- Results and discussion

The present discussion will be limited to the simulation of the profile of February 1974, as an illustration of the capabilities and the limitations of the model used. Most of the discussion will be devoted to the validity of the assumption made that an internal equilibrium is achieved in the system between all the redox species considered.

4.1.- Perfect thermodynamic equilibrium

If it is assumed that perfect internal equilibrium is achieved in the system for reactions a) to e), the following relations must hold :

$$a) \qquad Eh = 1.26 - 0.059 \ pH + 0.015 \log O_2$$

b) $Eh = 0.882 - 0.074\ pH + 0.007 \log NO_3^-/NH_4^+$

c) $Eh = 1.229 - 0.118\ pH - 0.029 \log Mn^{++}$

d) $Eh = 1.057 - 0.177\ pH - 0.059 \log Fe^{++}$

d') $\log Fe^{++} - \log HCO_3^- + pH = - 0.286$

for $- 0.215 < Eh < 0.053$

e) $Eh = 0.354 + 0.008 \log SO_4^{--} - 0.067\ pH + 0.004 \log Fe^{++}$

These relations are diagramatically represented in figure 3 for the gross chemical composition of the water at Rupelmonde.

Figure 4 shows the calculated profile obtained with this assumption.

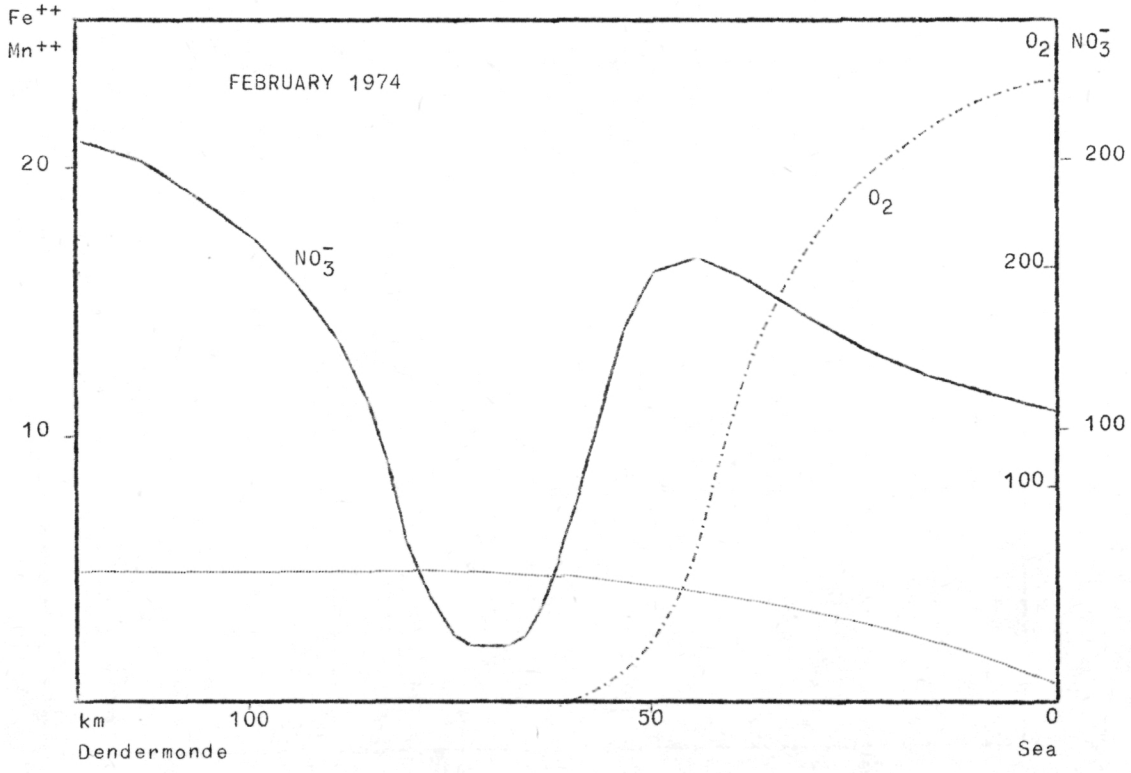


fig. 4.
Calculated profile for February 1974, obtained with a model assuming a perfect internal thermodynamic equilibrium.

Comparison with the experimental profile shows that the general trends of the evolution of the water composition are reproduced by the simulation.

However, oxygen concentration increases much later in the calculated profile. Clearly this is the consequence of our assumption of perfect internal equilibrium. With this assumption, oxygen can only begin to increase after all NH_4^+ and all Mn^{++} have been completely oxidized. To explain the observed profiles, kinetical limitations must be invocated : the rate of the chemical and microbiological reactions involved is not sufficient for an internal thermodynamic equilibrium between the NH_4^+/NO_3^- , Mn^{++}/MnO_2 , O_2/H_2O redox couples to be achieved.

4.2.- Empirical kinetic model for oxygen

It is possible to obtain a quite good simulation (see fig. 5) of the observed profile by expressing the oxygen consumption as a kinetical

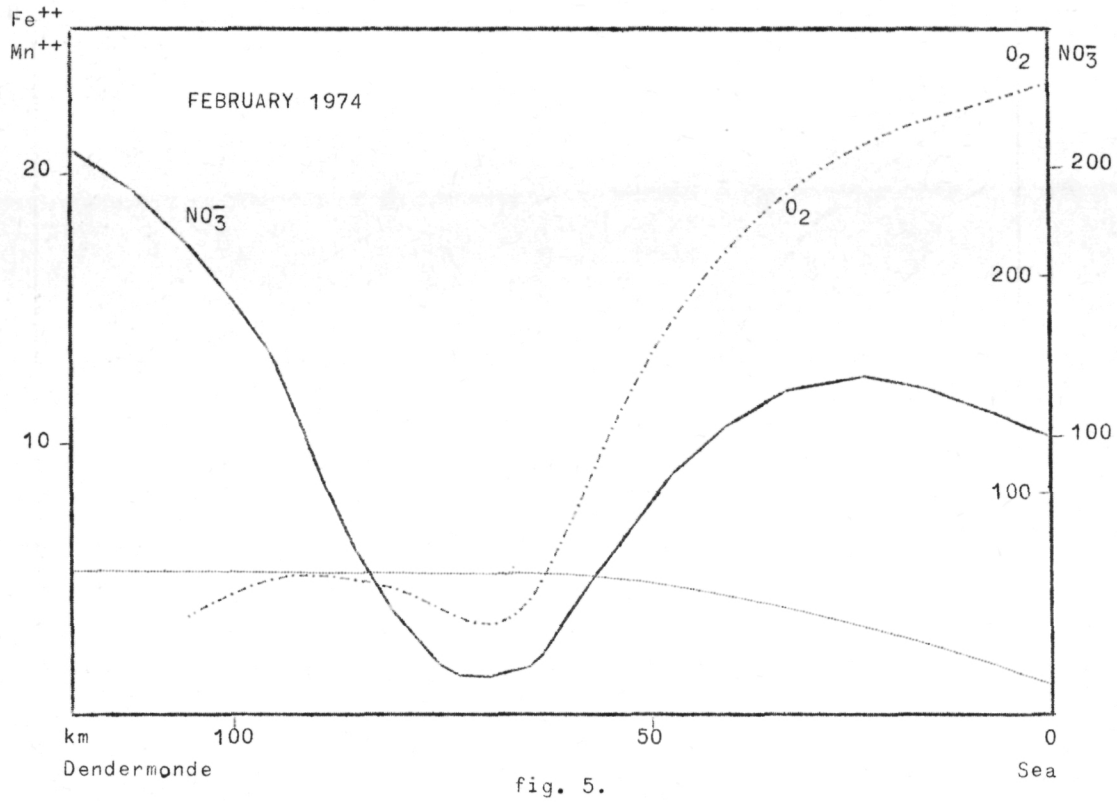


fig. 5.

Calculated profile for February 1974, obtained with a model using an empirical kinetic term for oxygen consumption.

term not immediately depending on Eh , but proportional to the concentration of reduced forms of the other redox couples :

$$\nabla x_i = K(x_{1_{sat}} - x_1) - k \left(\sum_{j=2}^{5} z_j - x_j \right) .$$

In this treatment, only equations b) to e) are considered for assessing Eh and the relation on the C_i's becomes :

$$H(s,t) = \sum_{j=1}^{5} C_j + k \sum_{j=1}^{5} (z_j - x_j) .$$

This treatment is not very satisfactory from the point of view of the microbiologist because it is only possible to justify the particular form given to the term representing oxygen consumtion by assuming that all heterotrophic activity is sustained by utilization of other oxidants than oxygen, the latter only reacting chemically to regenerate these oxidants. This is of course quite irrealistic, aerobic metabolisms constituting always an important part of heterotrophic activity. However the fact that this model does fit the experimental profiles, while the former does not, indicate that kinetical hindrances in the reactions of O_2 with NH_4^+ and Mn^{++} must be somehow taken into account.

4.3.- Kinetical hindrance to equilibrium

The first model, based on the assumption of thermodynamical equilibrium could not account for two observations :

i) Nitrate formation from ammonium is not completed before the beginning of oxygen concentration increase.

This can be explained by the physiology of nitrifying bacteria. The population of nitrifying bacteria of the Scheldt estuary are probably made of fresh water organisms of terrestrial origin, carried down by the river. As soon as the convenient Eh value is reached, their activity begins. However, because of increasing salinity, they cannot divide rapidly enough to counterbalance their dilution in sea water, so that nitrification cannot be completed [Billen (1975)]. A model of nitrification in the Scheldt estuary, taking into account the physiology of nitrifying bacteria is now in progress [Somville, Billen and Vanderborght (in preparation)].

ii) oxygen concentration increases before manganese oxidation begins

To explain this discrepancy, slowness of bacterial action cannot be invoked because manganese oxidation is a rapid spontaneous chemical process. In this case, the kinetical hindrance with respect to the equilibrium model probably originates from the mechanisms of Eh control by oxygen. This control has been discussed in detail by Sato (1960) and Breck (1972), (1974). Both authors stressed that the chemical reduction of oxygen is a multistep process in which oxygen peroxide is an intermediate : summarizing

a') $O_2 + 2\,H^+ + 2\,e^- \rightleftharpoons H_2O_2$

a") $H_2O_2 + 2\,H^+ + 2\,e^- \rightleftharpoons 2\,H_2O$.

The former of these processes is easy; the latter, involving rupture of an O-O bond, is very slow. A definite non neglectable H_2O_2 concentration can thus exist in natural oxygenated waters. A lot of chemical species (including oxidized forms of iron and manganese) readily react with H_2O_2 , decomposing it back to oxygen and preventing further oxidation of the solution by reaction a"). The steady state so established between O_2 and H_2O_2 is the effective way of control of the redox potential. This implies that relation a) must be replaced by the corresponding Nernst equation for reaction a'). The steady state concentration of H_2O_2 has been estimated by Sato and Breck respectively to 10^{-6} and 10^{-11} moles/ℓ . The two resulting Nernst relations are represented diagramatically in figure 3 (dotted lines).

Introduction of these relations in the model and comparison with preceeding data (experimental and calculated) will allow to estimate influence of oxygen peroxide process in the control of Eh potential in the Scheldt Estuary.

References

ADAM, Y., RUNFOLA, Y., (1971). *Numerical Resolution of diffusion equation*, Rapport N.9, Progr. Nat. Environnement Physique et Biologique, Projet Mer.

ADAM, Y., (1975). *A Hermitian finite difference method for the solution of parabolic equations*, to be published.

ANTWERPSE ZEEDIENSTEN, (1966). *Stormvloeden op de Schelde*, Ministerie van openbare werken; Bestuur der waterwegen.

BILLEN, G., (1975). Nitrification in the Scheldt Estuary (Belgium and the Netherlands), *Estuarine and Coastal Marine Science*, *3*, 79-89.

BRECK, W.G., (1972). Redox potentials by equilibration, *J. Mar. Res.*, *30*, 121-139.

BRECK, W.G., (1974). *Redox potentials in the sea*, in *The Sea*, Goldberg ed., vol. 5, Wiley, New York.

OVERBECK, J., DALEY, R.J., (1973). Some precautionary comments on the Romanenko technique for estimating heterotrophic bacterial production, *Bull. Ecol. Res. Comm.* (Stockholm) *17*, 342-344.

RICHARDS, F.A., (1965). *Anoxic basins and Fjords*, in *Chemical oceanography*, Vol. 1, 611-645, Eds. Riley, S.P. and Skirrow, G., Academic Press, New York.

ROMANENKO, V.I., (1964). Heterotrophic CO_2 assimilation by bacterial flora of water, *Mikrobiol.*, *33*, 779-683.

SATO, M., (1960). Oxidation of sulfide ore bodies, 1. Geochemical environments in terms of Eh and pH, *Econ. Geol.*, *55*, 928-961.

SOROKIN, Y.I., (1965). On the trophic role of chemosynthesis and bacterial synthesis in water bodies, *Mem. Ist. Ital. Idrobiol.*, *18 Suppl.*, 187-205.

THORSTENSON, D.C., (1970). Equilibrium distribution of small organic molecules in natural waters, *Geochim. Cosmochim. Acta*, *34*, 745-770.

WOLLAST, R., (1973). *Origine et mécanismes de l'envasement de l'estuaire de l'Escaut, Rapport de Synthèse*, Recherche effectuée dans le cadre de l'étude de l'envasement de l'Escaut dirigée par le Laboratoire de Recherches Hydrauliques, Borgerhout, Ministère des Travaux Publics.

WOLLAST, R., (1973). *Circulation, accumulation et bilan de masse dans l'estuaire de l'Escaut*, in *Modèle mathématique de la pollution en mer du Nord, Rapport de synthèse 1972*, Commission interministérielle de la politique scientifique (Belgium).

II

Determination of Cu, Pb, Cd, Zn in sea water by anodic stripping voltammetry. A first approach to the problem of the speciation of heavy metals in sea water.

by

G. DUYCKAERTS and G. GILLAIN

Based on work by G. DUYCKAERTS, G. GILLAIN, L. MACHIROUX (Laboratoire de Chimie analytique, Université de Liège) and I. ELSKENS (Analytische Scheikunde, Vrije Universiteit Brussel).

Introduction

Many publications in recent years are dealing with different methods proposed for the determination of heavy metals in sea water [Dyrssen *et al.* (1972)] : as the concentrations are normally very low, in the µg/ℓ range, a preconcentration step is often necessary (coprecipitation, solvent extraction, anion exchange, chelating ion exchange) and because of the presence of high concentration of salts, some methods like activation analysis require removal of the main constituents. In our case, we shall limit our interest only in the four heavy metals : copper, lead, cadmium and zinc. Beyond the fact that the concentrations of these heavy metals are very low (µg/ℓ or sub-µg/ℓ level) which means that contamination during collection and analysis (filters, glassware, chemicals, air-borne

dust, a.s.o. or loss during preservation and shipping of the sample) may easily lead to meaningless values, especially if preconcentration steps are necessary, this analytical problem is still more complicated by the fact that these metals are present in the Sea Liquid Medium in different forms : soluble species like Cu^{++} , $CuOH^{+}$, CuOHCl , $CuCO_3$, $CuCl^{+}$, complexed amino acids and those associated with suspended particulate organic and inorganic matter [Dyrssen *et al.* (1974)].

It is therefore not surprising that the results found in the literature differ so greatly from one method to an other, even when they are obtained in the same laboratory on the same sample, mainly because each method gives the results for different species. The situation is still worse if the results concern samples resulting from different sampling or storing techniques. Nevertheless, as it is pointed out in many recent publications [Laitinen (1974)], the understanding and the evaluation of pollution by metals require from the analytical chemist not only the determination of their bulk concentration in the water phase, the planktons, the organisms, the sediments but, in each compartment the discrimination among various species in which the metal is present. Evidently, this represents an enormous task for the analytical chemists [Dyrssen (1972, 1974), Laitinen (1974)].

Amont the multi-element methods of analysis that may be considered for the heavy metals or some of those we are considering, one finds, neutron activation analysis, mass spectrometry, arc, spark or flame emission spectrometry or anodic stripping voltammetry. We adopted like several others [Whitnack (1961, 1964), Sinko and Dolezal (1970), Macchi (1965), Ariel *et al.* (1964), Naumann and Schmidt (1971), Baric and Branica (1967), Whitnack and Sasselli (1969), Ariel and Eisner (1963), Odier and Pichon (1963), Florence (1972), Nikelly and Cooke (1957), Le Meur and Courtot-Coupez (1973)] the last technique for different reasons : the equipment is rather simple and inexpensive, the method does not require preliminary concentration or separation of the main salts which means a minimum contamination risk during analysis. On the other hand, as we shall see later, this method seemed to offer a rather simple, although crude, approach to the problem of the speciation of those heavy metals in sea water.

In the second part, some preliminary results concerning comparison between atomic absorption and anodic stripping will be mentioned in order to find out if the results obtained by both methods are reliable; a systematic difference between the results of both methods would perhaps allow us to find more informations about the species given by each method.

1.- Determination of Cu , Cd , Pb , Zn in sea water

1.1.- Sampling, storage and filtration of the samples

The sea water samples were collected by a centrifugal pump made of teflon, stored in polythene bottles, rapidly frozen at - 40 °C and maintained at - 20 °C , prior to analysis.

We have observed, as many others did before [Robertson (1968a,b)] that sea water samples stored in a polythene bottle at room temperature and sea pH undergo after three days a noticeable loss probably by adsorption on the vessel walls (table 1).

Table 1

Dates	Cu (µg/ℓ)	Pb (µg/ℓ)	Cd (µg/ℓ)	Zn (µg/ℓ)	Conditions
19- 1 -72	30.2	5.5	1.7	76	Room temperature pH = 8
21- 1 -72	13,2	2.6	1.0	39	
1-7-71	17.6	7,0	0.20	84.5	Stored at - 20°C pH = 8
8-9-71	18,2	6.4	0.19	91	
21- 1 -72	19.5	6.6	0,22	80	
18- 1 -72	30	5.5	1.0	66	Room temperature pH = 1
20- 3 -72	29	5,3	1,0	68	
26- 6 -72	30	5.8	1.2	65	

Storage at room temperature after acidifying at pH = 1 with HCl or at a temperature of - 20 °C does not indicate (in that concentration range) any noticeable loss even after several months.

All our samples have been stored at - 20 °C ; they are quickly thawed immediately before they are required for analysis and filtered through a 0,22 µm pore size Millipore filter. Here again, it is

important to wash the filters [Tolg (1972), Burrel (1972)] with 100 mℓ of a 10^{-2} M DTPA solution before filtering the sea water (table 2). The results on the heavy metal content of these Millipore filters were obtained by anodic stripping after dry ashing with microwave-activated oxygen and dissolving the residue with 2 mℓ of suprapur HCl .

Table 2

	µg Cu	µg Pb	µg Cd	µg Zn	Weight of Millipore filters in mg
Analysis of unwashed Millipore filters	1.15	0.01	0.01	0.52	82
	1.25	0.50	0.05	0.91	83
	3.0	0.06	0.32	19.7	83.4
	1.25	0.01	0.22	0.30	83
	2.3	0.07	0.23	0.27	83.4
Millipore filter washed with DTPA	0.01	0.005	0.02	0.01	83

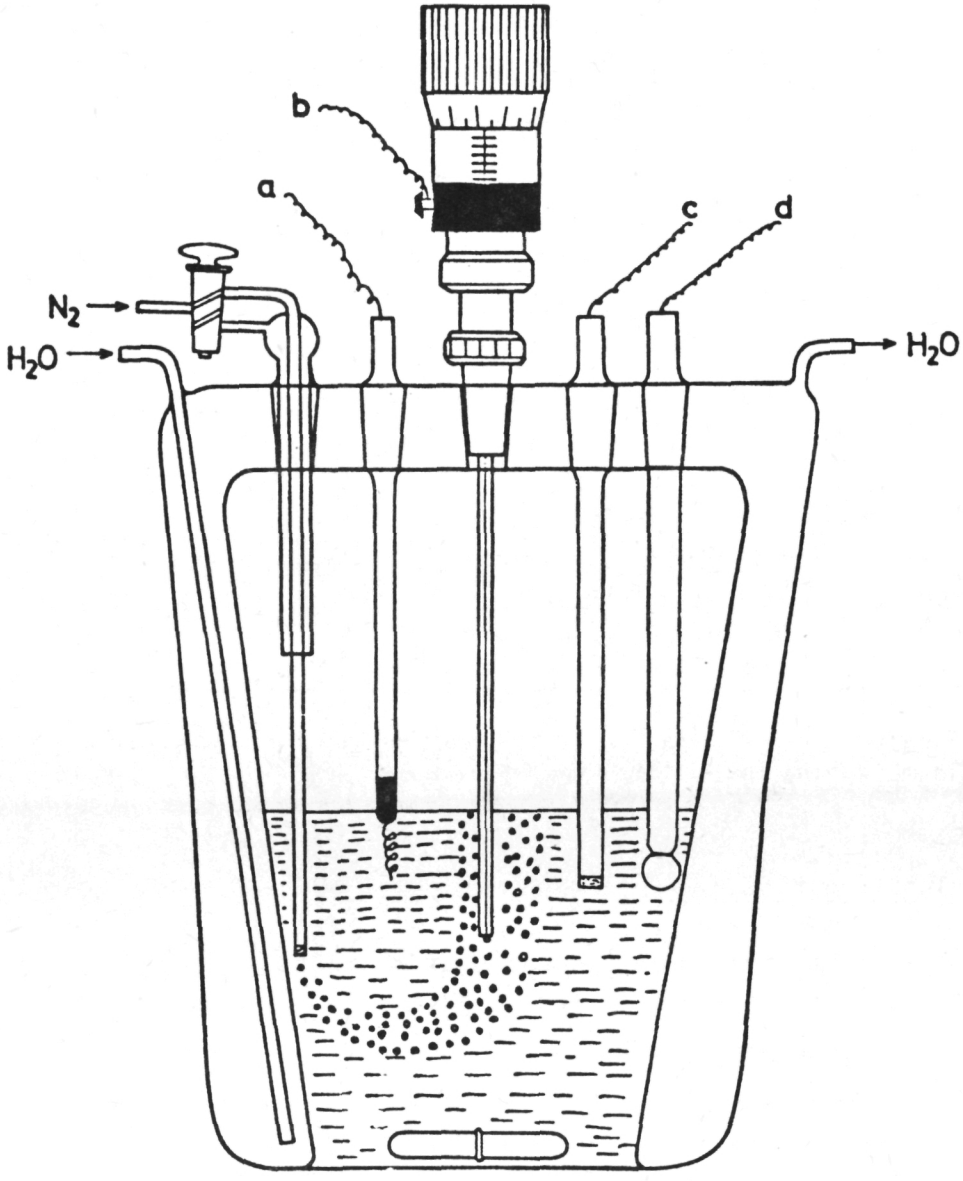
N.B. *These values are corrected for the blank coming from the 2 mℓ of HCl used in dissolving the residue from dry ashing.*

1.2.- Instrumentation

The determination of the four heavy metals is carried out on the freshly obtained filtrate by anodic stripping voltammetry with a hanging mercury drop electrode (HMDE).

The experiments were performed with the electronic unit (E.S.A. Multiple Anodic Stripping Analyzer Model 2014 - ESA Inc. Mass. U.S.A.) allowing the use of four cells simultaneously : it contains four units for electrolysis and one unit for the redissolution step. Instead of using the original cell of the manufacturer containing a mercury coated graphite cathode of large area, we prefered to adapt a more elaborate cell with a mercury drop cathode (HMDE).

Fig. 1 shows a drawing of our cell consisting of a Metrohm hanging mercury drop electrode, a platinum working electrode and a silver-silver chloride reference electrode. The glass electrode proved to be usefull for our experiments at different pH. The cell temperature was adjusted



a : counter electrode
b : hanging mercury drop electrode
c : reference electrode : silver-silver chloride
d : glass electrode

fig. 1.

at 25 °C by a thermostat. The details of the procedure we have finally adopted are best illustrated by referring to fig. 2.

The cell contains 30 mℓ of solution; the distance between the mercury drop electrode and the magnetic stirrer is 25 mm . The diameter

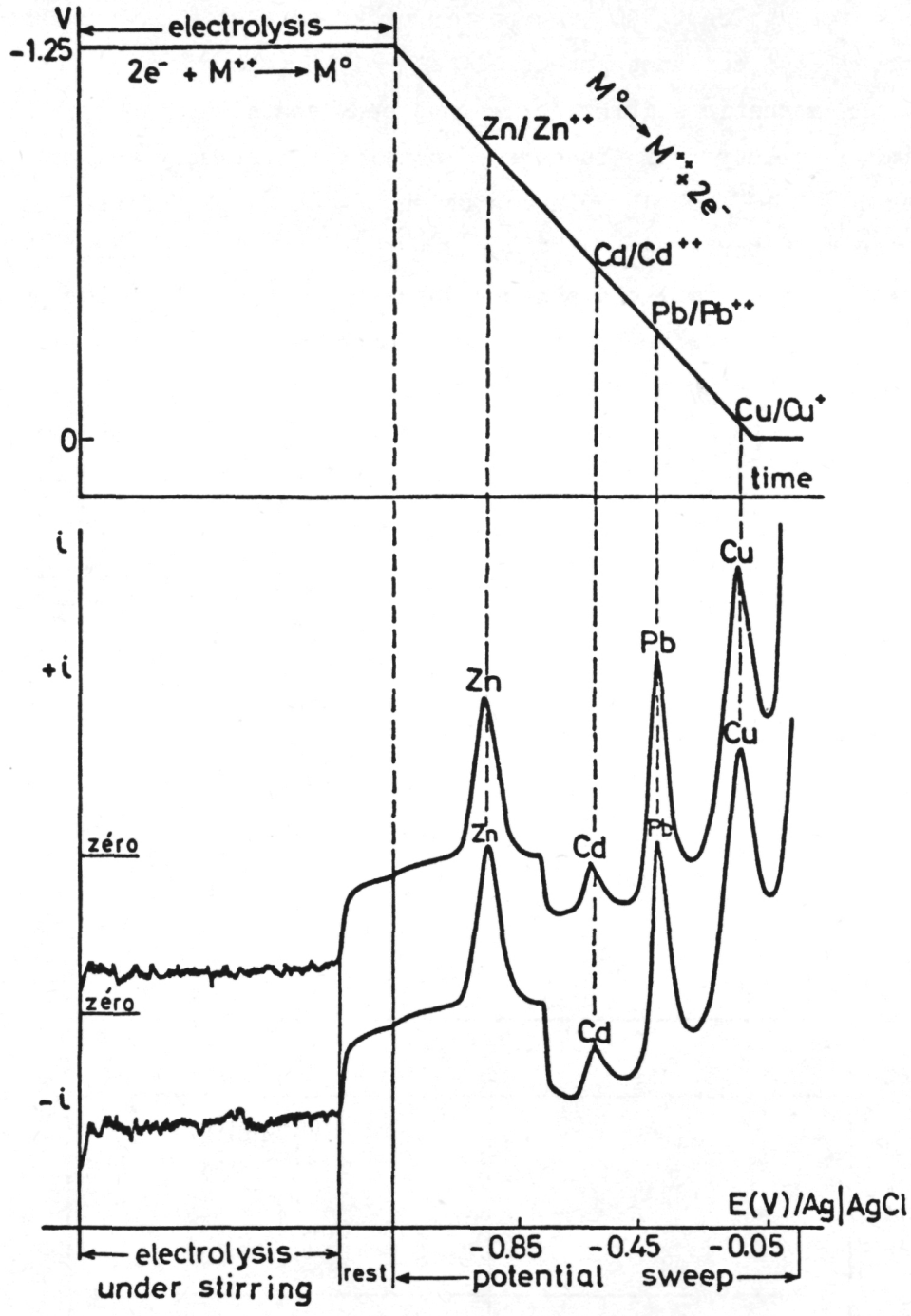

V
electrolysis
-1.25
2e⁻ + M⁺⁺ → M°
M° → M⁺⁺ + 2e⁻
Zn/Zn⁺⁺
Cd/Cd⁺⁺
Pb/Pb⁺⁺
Cu/Cu⁺
0
time
i
+i
zéro
zéro
-i
Zn
Cd
Pb
Cu
Zn
Cd
Pb
Cu
Cd
E(V)/Ag|AgCl
-0.85
-0.45
-0.05
electrolysis
under stirring
rest
potential sweep

fig. 2.

of the drop is 0.76 mm . After bubbling very pure nitrogen through the solution for at least 30 minutes in order to remove oxygen, electrolysis is started at a constant potential of - 1.25 volt versus reference electrode, the magnetic stirrer being in steady state at 550 revolutions per minute; electrolysis is carried out for a precisely measured time ranging from 10 to 15 minutes depending on the concentrations of the metals to be determined.

After that time, the stirrer motor is stopped and after one more minute, the metals concentrated in the mercury drop are dissolved by linear sweep voltammetry at a rate of 200 mV/min .

In order to obtain the concentration of the four elements in the solution, we adopted the standard addition method, the volume of the injected standard solutions being adapted to the concentrations to be evaluated. This equipment allowed us to carry out the analysis of twelve samples per day with one operator.

1.3.- Reproducibility of the method

The reproducibility of the method has been tested on a sea water sample by carrying out five experiments and two recordings on each solution. The results are given in table 3.

Table 3

Number	Cu (μg/ℓ)	Pb (μg/ℓ)	Cd (μg/ℓ)	Zn (μg/ℓ)
1	3.0	5.1	1.2_5	5.2
2	2.8	5.7	1.3_5	4.5
3	3.0	5.6	1.5_5	4.8
4	2.9	6.1	1.5	4.4
5	2.6	6.1	1.4_5	5.0
Standard deviation (%) for 95 % confidence limits	7.0	8.5	13	6.5

1.4.- Influence of the pH on the results [Duursna and Seven Huysen (1966); Mancy]

As we have mentioned previously, the heavy metal content in the filtered sea water sample is distributed among different soluble species and perhaps some inorganic and organic particulate matter which passed through the filter.

The distribution between these species depending on the solution pH and the reduction rate on the mercury drop being different from one to another, one would expect an influence of the pH on the analytical result. This influence is illustrated in figure 3.

These results were obtained by starting with an acidified sea water sample and by increasing progressively the pH by NaOH addition. As pointed out by Dyrssen and Wedborg (1974), most complexation of heavy metal ions with organic ligands probably occurs within particulate matter of biological origin even if the amount of dissolved organic matter may be considerably larger. A part of this is certainly collected on the Millipore filter but as we shall see later, a not negligeable amount remains in the filtered sample. Concerning the rest of the soluble species, we must consider, beside the free ions, those complexed by inorganic and organic ligands. The autors just mentioned above have evaluated the percentage speciation for those inorganic complexes (table 4).

Table 4

Percentage speciation in sea water at natural pH

Complex	Cu	Pb	Cd	Zn
M^{++}	0.7	4.5	1.8	16.1
MOH^{+}	3.7	10.2	-	2.3
$MHCO_3^{+}$	-	1.4	-	0.3
MCO_3	21.6	0.4	0.2	3.3
MSO_4	-	0.5	0.2	1.9
MF^{+}	-	-	-	-
MCl^{+}	5.8	18.9	29.2	44.3
MCl_2	1.6	42.3	37.5	15.4

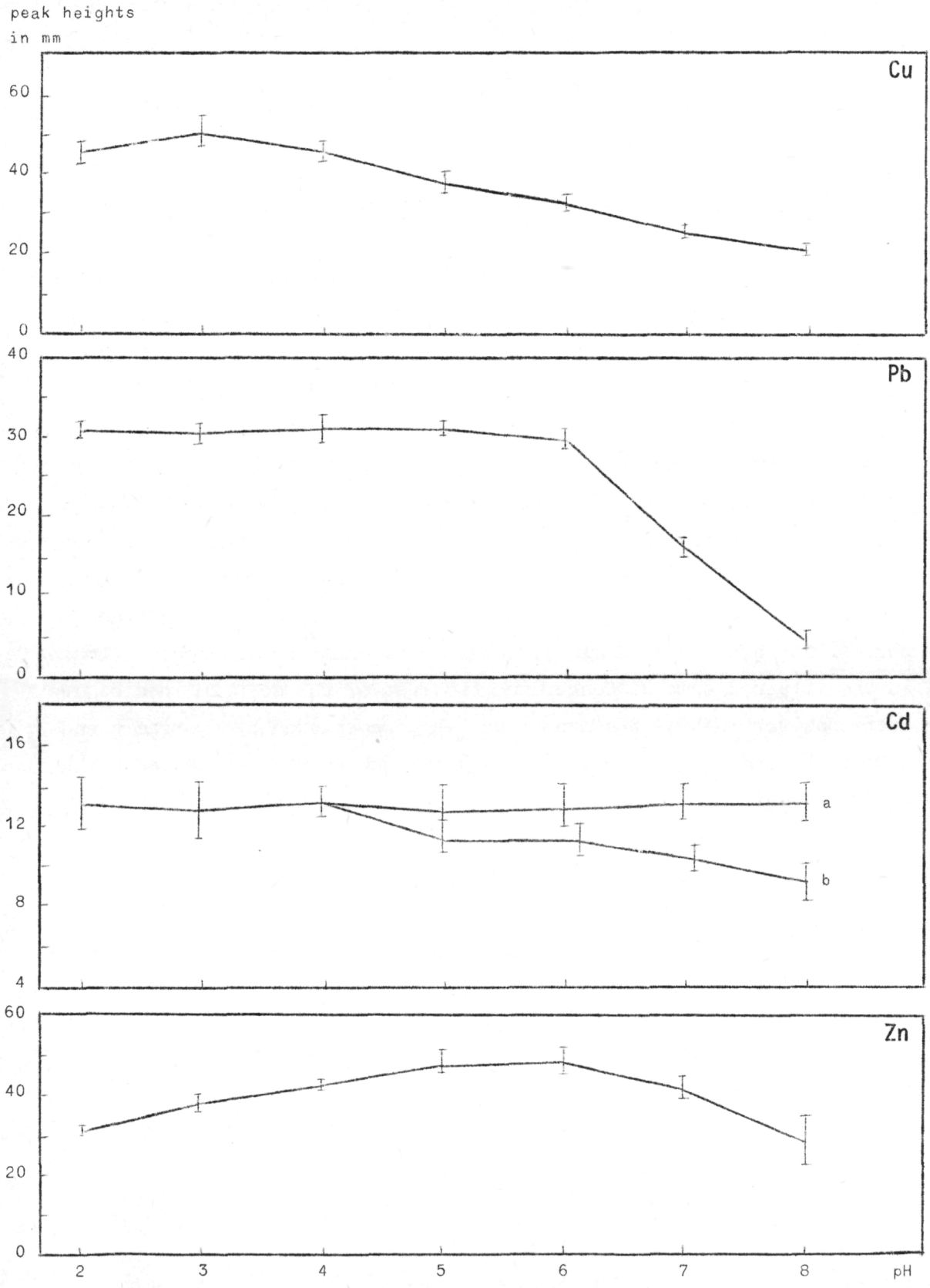

peak heights
in mm
Cu
60
40
20
0
Pb
40
30
20
10
0
Cd
16
12
8
4
a
b
Zn
60
40
20
0
2
3
4
5
6
7
8
pH

fig. 3.

Table 4

(continuation)

Complex	Cu	Pb	Cd	Zn
MCl_3	0.7	9.2	27.9	1.7
MCl_4^{--}	0.5	3.6	-	2.3
MOHCl	65.2	8.8	2.9	12.5
MBr^+	-	0.15	0.2	-

(Taken from The Sea, vol. 5, Marine Chemistry, Dyrssen and Wedborg).

It should be noticed from fig. 3 that the behaviour differs for the four cations : between the limits of errors, the concentration of cadmium given by this method is more or less independent of the pH between 2 and 8 , a result which is not too surprising since the chlorocomplexes are the main constituents (in some samples, a decrease with pH is observed nevertheless).

For lead and copper, we observe a progressive decrease of the measured content with increasing pH ; this could perhaps be more or less related with the percentage of hydroxychlorocomplexes.

The curve for zinc looks, at first sight, more surprising, but the decrease with decreasing pH is probably partly due to the interference of proton reduction at - 1.25 volt .

Beside these mentioned effects, it is quite reasonable to assume that this increase in heavy metal content observed for copper, lead and zinc by acidifying the sea water may be partly due to the dissociation of some organic complexes.

In order to give some very crude evaluation of the relative importance of the labile complexes with respect to the soluble species which are reducible at the pH of sea water, we decided to carry out, for each sample, an evaluation of the four cations respectively at pH = 3 and pH = 8 .

1.5.- Effect of irradiation by ultraviolet light

Armstrong has shown that irradiation of the sea water by ultraviolet light gives rise to some decomposition of the organic material [Johnston (1964), Pocklington (1971)] with liberation of complexed metallic ions [Armstrong *et al.* (1966)]. We therefore decided to analyze again the sample after irradiation for 12 hours under the light of germicide tubes TUV of 30 watts; the 30 mℓ sample is contained in a slowly rotating quartz tube of 15 mm diameter (fig. 4). pH of sample = 1 .

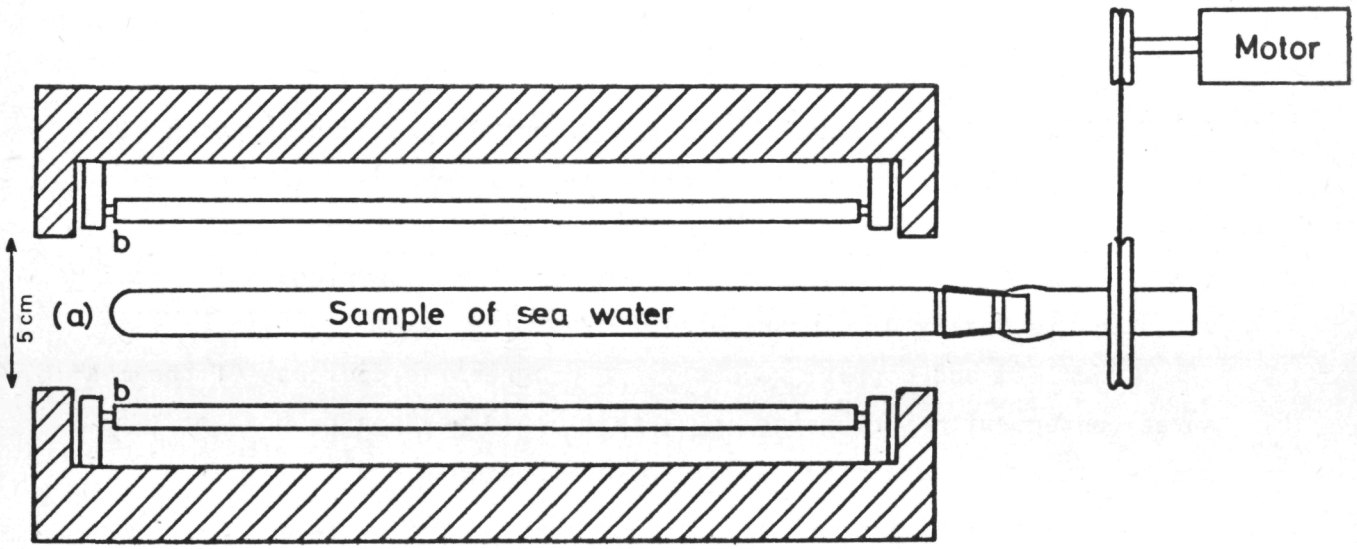


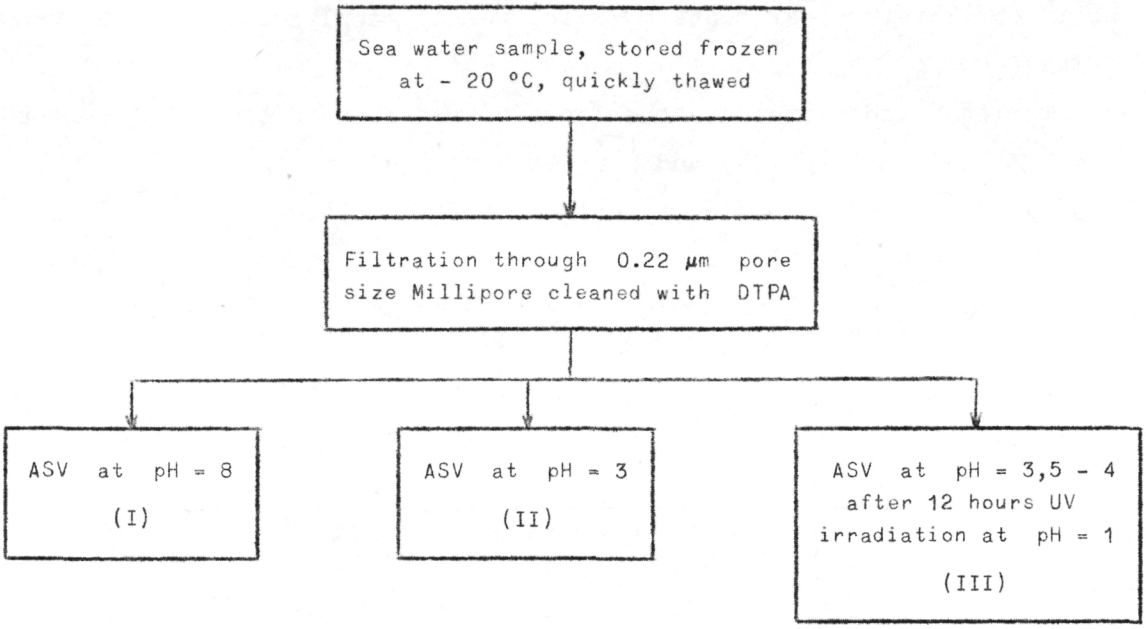
fig. 4.
UV Irradiation system.
a : quartz tube containing the sea water sample pH = 1 b : germicide-TUV lamps

As we shall see later, the heavy metal content observed by anodic stripping voltammetry (ASV) in acid medium has increased systematically after irradiation[1].

1. Some authors propose the destruction with persulfuric acid of the organic ligands causing the masking of a more or less important fraction of the heavy metal content [Noakes and Wood (1961); Slowey, Jeffery and Wood (1967)].

1.6.- Analysis schema

These considerations led us to the following scheme of analysis :



Those three results (I), (II) and (III) expressed in µg/ℓ allowed us to make a rough estimate of a certain speciation of those metals in the filtered sea water [Rozhanskaya (1970), William (1969), Barker and Ryther (1969)]; the fraction corresponding to the result (I) will be called arbitrarely "ionic species"; the difference between the concentrations of (II) and (I) represents the fraction corresponding to the metals bonded in weak complexes at the pH of sea water : we indicate this by "weakly-complexed cations" and finally the fraction given by the difference (III) - (II) is called " strongly-complexed cations". The figure given by (III) represents of course the maximum concentration of dissolved metals we could detect by our method of analysis.

1.7.- Results

More than one thousand sea water samples were analyzed by this method during the last three years; these samples were collected in the North Sea at different locations, periods of the year and depths.

As a matter of illustration of the method we have just described, we represent in tables 5 and 6 and in figures 5 to 8, the analytical results obtained for "solution species" of copper, lead, cadmium and zinc in the three compartments — ionic, weakly-complexed and strongly-complexed.

Tables 5 and 6 indicate the location reported on the map (figures 5 to 8) as well as the date and hour of sampling.

It is not our intention to discuss in this place the results in connexion with the problem of pollution or with the question of retention of heavy metals by microorganisms or inorganic particulates.

Table 5

Cruise of May 27th, 1974

Identification	Cu (µg/ℓ)			Pb (µg/ℓ)		
	I pH in situ	II pH = 3	III U.V.	I pH in situ	II pH = 3	III U.V.
M01.270574.1300.05	1.9	7.9	12.2	2.3	5.3	9.3
M02.270574.1530.05	1.4	7.3	17.6	2.9	5.1	4.9
M04.270574.1900.05	1.0	7.9	11.6	3.0	4.3	21.8
M20.280574.0830.05	1.8	5.5	5.2	3.8	5.0	10.7
M25.280574.1200.05	2.9	5.8	6.1	2.6	4.0	8.3
M22.280574.1600.05	2.9	5.8	8.4	3.0	4.4	7.8
M05.290574.0700.05	2.7	6.6	6.4	2.2	17.7	25.8
M55.290574.1030.05	2.5	9.3	12.5	5.0	5.1	13.0
M09.290574.1400.05	1.5	5.5	8.6	2.0	3.5	13.0
M15.290574.1700.05	2.1	3.0	3.1	3.1	7.9	8.1
M21.300574.0700.05	4.0	6.0	11.0	9.0	13.0	15.0
M16.300574.1030.05	2.9	5.2	4.8	2.4	4.0	7.1
M11.300574.1600.05	1.3	6.5	6.7	3.7	5.5	6.0
M12.300574.1800.05	2.8	5.5	8.7	3.5	4.7	5.1

M05.290574.0700.05 means a sample taken by the Mechelenship at point 05, the 29th May 1974, at 7.00 a.m. and at five meter depth.

Table 5 (continuation)

Identification	Cd (µg/ℓ)			Zn (µg/ℓ)		
	I pH in situ	II pH = 3	III U.V.	I pH in situ	II pH = 3	III U.V.
M01.270574.1300.05	0.08	0.22	0.45	0.5	3.5	3.8
M02.270574.1530.05	0.26	0.31	1.39	1.0	2.6	16.6
M04.270574.1900.05	0.07	0.23	0.66	0.9	1.3	2.6
M20.280574.0830.05	0.11	0.53	0.77	1.4	4.0	13.3
M25.280574.1200.05	0.15	0.46	0.40	0.6	2.7	4.7
M22.280574.1600.05	0.38	0.38	0.38	5.8	7.2	10.0
M05.290574.0700.05	0.08	0.21	1.00	0.5	2.3	5.0
M55.290574.1030.05	0.07	0.64	1.00	0.8	4.4	6.0
M09.290574.1400.05	0.17	0.29	0.81	2.5	3.5	18.3
M15.290574.1700.05	0.10	0.35	0.30	0.8	1.5	4.2
M21.300574.0700.05	0.20	0.22	1.30	1.5	2.4	9.6
M16.300574.1030.05	0.18	0.18	0.30	3.0	4.6	5.5
M11.300574.1600.05	0.10	0.75	0.68	2.3	5.0	11.1
M12.300574.1800.05	0.13	0.72	0.68	1.6	7.2	8.5

Table 6

	Cu (µg/ℓ)				Pb (µg/ℓ)				Cd (µg/ℓ)				Zn (µg/ℓ)			
	a	b	c	III	a	b	c	III	a	b	c	III	a	b	c	III
M01	1.9	6.0	4.3	12.2	2.3	3.0	4.0	9.3	0.08	0.14	0.23	0.45	0.5	3.0	0.0	3.8
M02	1.4	5.9	10.3	17.6	2.9	2.2	0.0	5.1	0.26	0.05	1.08	1.39	1.0	1.6	14.0	16.6
M04	1.0	6.9	3.7	11.6	3.0	1.3	17.5	21.8	0.07	0.16	0.43	0.66	0.9	0.4	1.3	2.6
M20	1.8	3.7	0.0	5.5	3.8	1.2	5.7	10.7	0.11	0.42	0.24	0.77	1.4	2.6	8.7	13.3
M25	2.9	2.9	0.0	5.8	2.6	1.4	4.3	8.3	0.15	0.31	0.00	0.46	0.6	2.1	2.0	4.7
M22	2.9	2.9	2.6	8.4	3.0	1.4	3.4	7.8	0.38	0.00	0.00	0.38	5.8	1.4	2.8	10.0
M05	2.7	3.9	0.0	6.6	2.2	15.5	8.1	25.8	0.08	0.13	0.79	1.00	0.5	1.8	2.7	5.0
M55	2.5	6.8	3.2	12.5	5.0	0.0	8.0	13.0	0.07	0.57	0.36	1.00	0.8	3.6	1.6	6.0
M09	1.5	4.0	3.1	8.6	2.0	1.5	9.5	13.0	0.17	0.12	0.52	0.81	2.5	1.0	14.8	18.3
M15	2.1	1.0	0.0	3.1	3.1	4.8	0.0	7.9	0.10	0.25	0.00	0.35	0.8	0.7	2.7	4.2
M21	4.0	2.0	5.0	11.0	9.0	4.0	2.0	15.0	0.20	0.00	1.10	1.30	1.5	1.0	7.2	9.7
M16	2.9	2.3	0.0	5.2	2.4	1.6	3.1	7.1	0.18	0.00	0.12	0.30	3.0	1.6	1.0	5.5
M11	1.3	5.2	0.0	6.5	3.7	1.8	0.0	6.0	0.10	0.65	0.00	0.75	2.3	2.7	6.1	11.1
M12	2.8	2.7	3.2	8.7	3.5	1.2	0.0	4.7	0.13	0.59	0.00	0.72	1.6	5.6	1.3	8.5

Column a : concentration of ionic species; column b : concentration of "weakly-complexed cations"; column c : concentration of "strongly complexed cations"; column III : maximum concentration observed. The samples correspond to those of table 5.

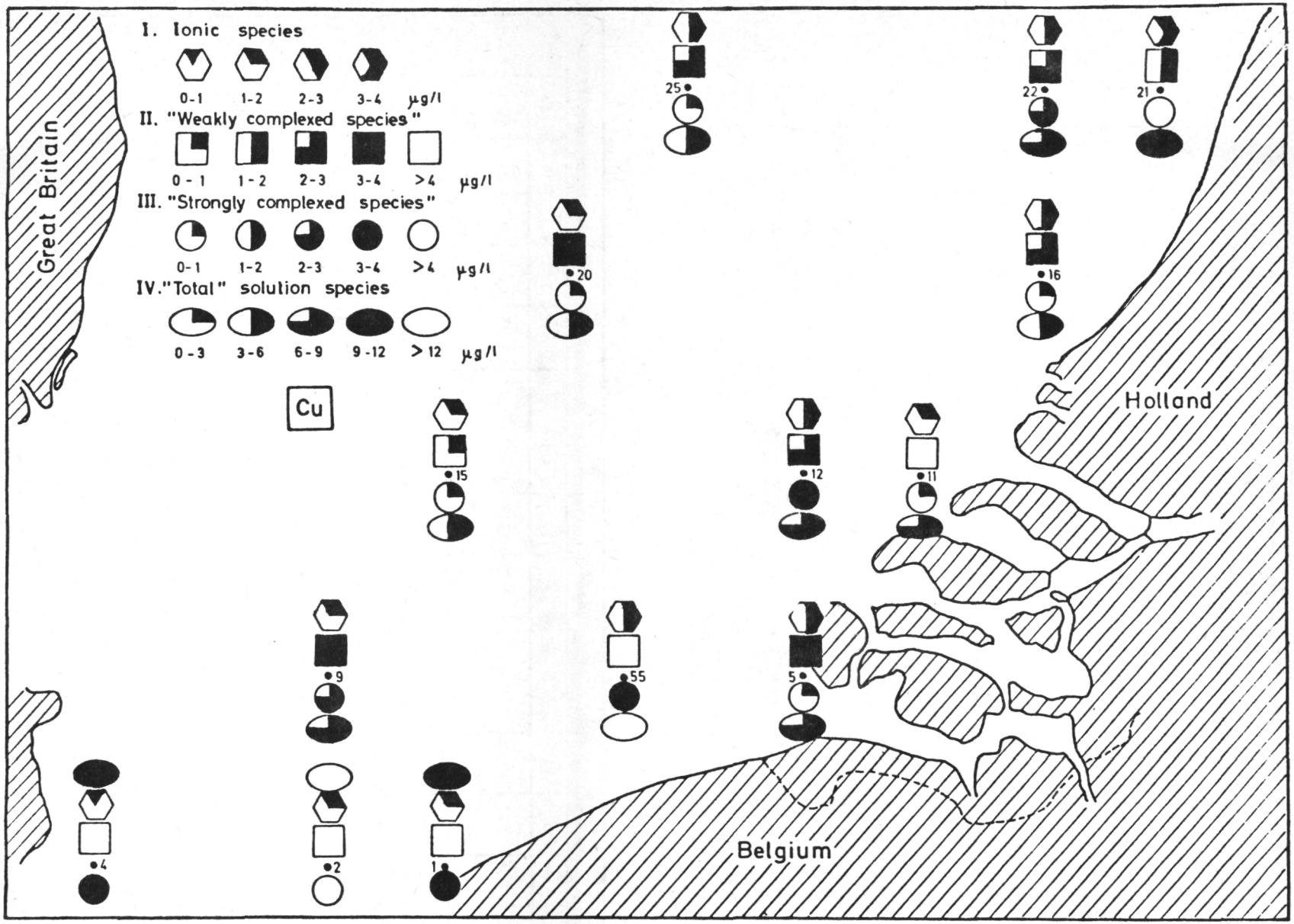

I. Ionic species
0-1 1-2 2-3 3-4 µg/l
II. "Weakly complexed species"
0-1 1-2 2-3 3-4 >4 µg/l
III. "Strongly complexed species"
0-1 1-2 2-3 3-4 >4 µg/l
IV. "Total" solution species
0-3 3-6 6-9 9-12 >12 µg/l
Cu
Great Britain
Holland
Belgium
25
22
21
20
16
15
12
11
9
55
5
4
2
1

fig. 5.

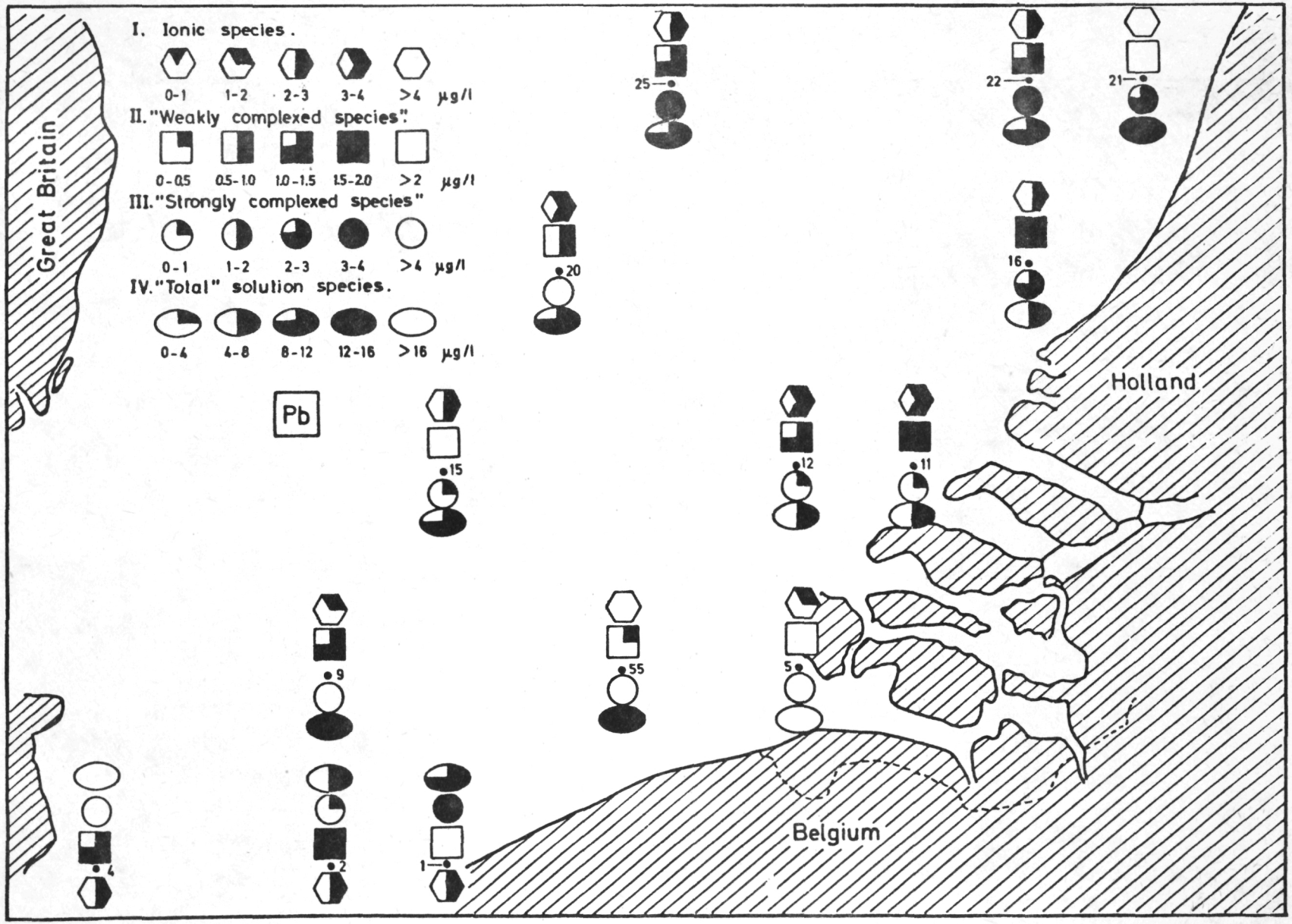

I. Ionic species.
0-1 1-2 2-3 3-4 >4 µg/l
II. "Weakly complexed species".
0-0.5 0.5-1.0 1.0-1.5 1.5-2.0 >2 µg/l
III. "Strongly complexed species"
0-1 1-2 2-3 3-4 >4 µg/l
IV. "Total" solution species.
0-4 4-8 8-12 12-16 >16 µg/l
Pb
Great Britain
Holland
Belgium
25
22
21
20
16
15
12
11
9
55
5
4
2
1

fig. 6.

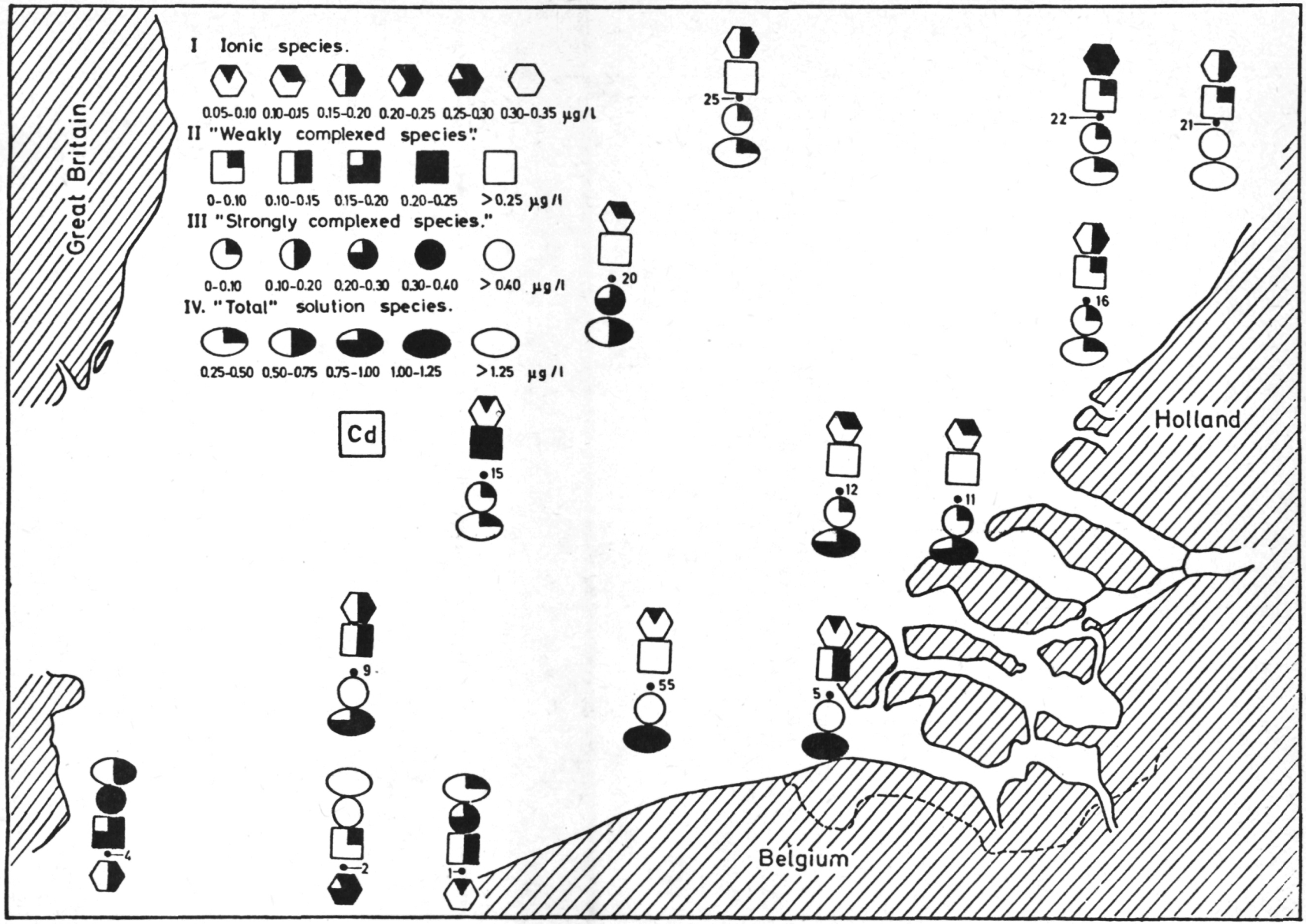

I Ionic species.
0.05-0.10 0.10-0.15 0.15-0.20 0.20-0.25 0.25-0.30 0.30-0.35 µg/l
II "Weakly complexed species".
0-0.10 0.10-0.15 0.15-0.20 0.20-0.25 >0.25 µg/l
III "Strongly complexed species."
0-0.10 0.10-0.20 0.20-0.30 0.30-0.40 >0.40 µg/l
IV. "Total" solution species.
0.25-0.50 0.50-0.75 0.75-1.00 1.00-1.25 >1.25 µg/l
Great Britain
Cd
Holland
Belgium
25
22
21
20
16
15
12
11
9
55
5
4
2
1

fig. 7.

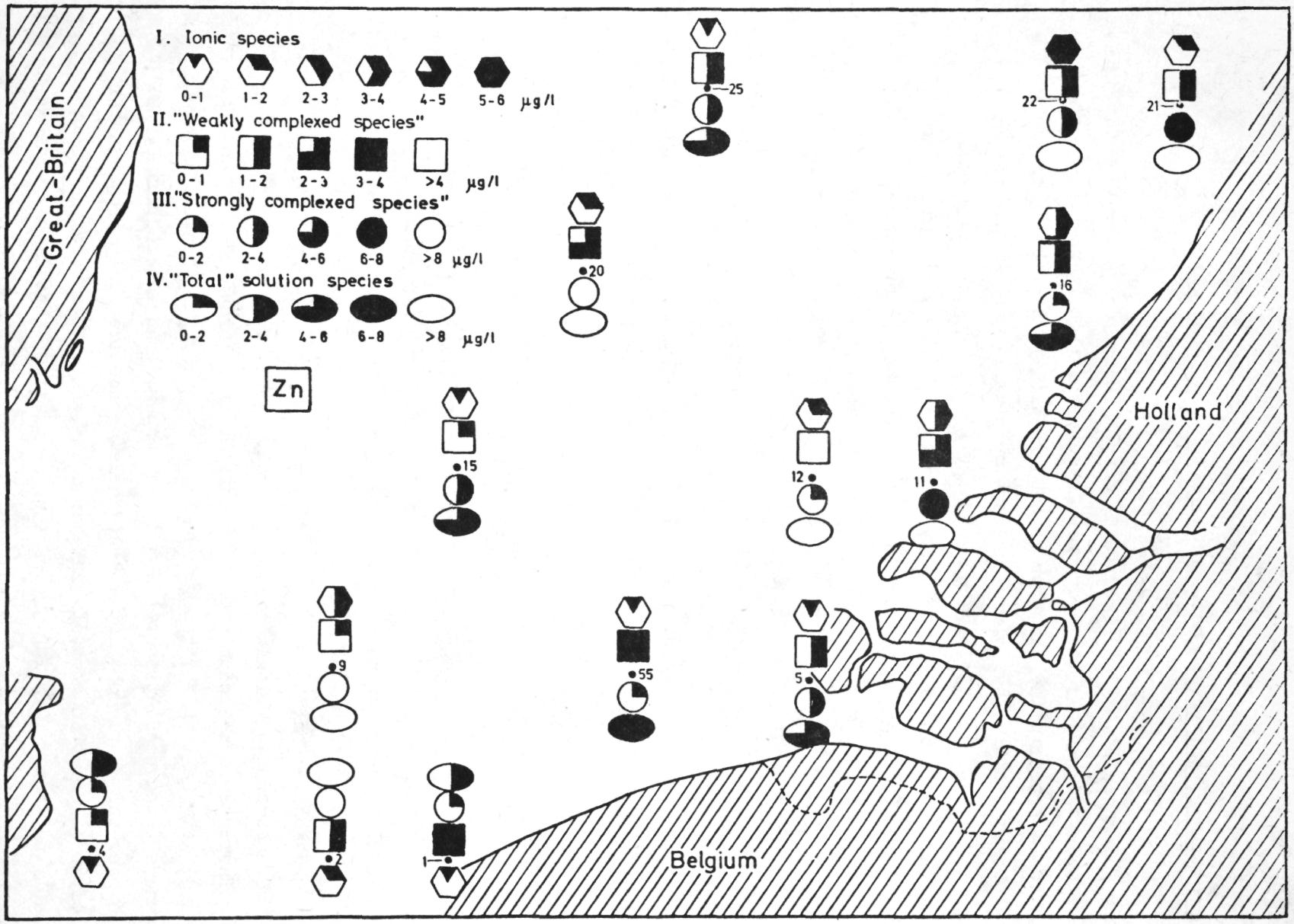

I. Ionic species
0-1 1-2 2-3 3-4 4-5 5-6 µg/l
II."Weakly complexed species"
0-1 1-2 2-3 3-4 >4 µg/l
III."Strongly complexed species"
0-2 2-4 4-6 6-8 >8 µg/l
IV."Total" solution species
0-2 2-4 4-6 6-8 >8 µg/l
Zn
Great-Britain
Holland
Belgium
25
22
21
20
16
15
12
11
9
55
5
4
2
1

fig. 8.

2.- Preliminary comparison between ASV and atomic absorption

Atomic absorption spectrometry is used by many laboratories [Segar and Gonzales (1972), Fabricand, Sawger, Ungar and Adler (1962), Burrel and Wood (1969)] for heavy metals determination in sea water, the solution injected in the flame or in the graphite furnace being an extract obtained either by solvent extraction usually with APDC-MIBK [Paus (1973), Burrel (1967), Kuwata *et al.* (1971), Magnee and Rahman (1965), Armittage and Zeitlin (1971), Brooks *et al.* (1967)] (ammonium pyrrolidine dithiocarbamate — methylisobutylketone) or by chromatography on a chelating ion-exchange resin [Riley and Taylor (1968), Le Meur et Courtot-Coupez (1973)] (chelex-100 or Dowex A1). This preliminary extraction step is required by the necessity to remove the salt matrix for atomic absorption and to concentrate the solution in heavy metals. A great deal of literature exists on this subject. Intercalibration of different methods between different laboratories has been carried out in the USA recently for lead in ocean water [Patterson (1974)] and a project between several laboratories in Great Britain, Holland and Belgium is considering this problem; from the results already obtained, it seems that some very general conclusions can be drawn. One should mention first of all that three methods were used on the same samples :

1) Heavy metal extraction by APDC-MIBK or APDC-$CHCl_3$ *at the pH of sea* water followed by atomic absorption with the graphite furnace;
2) Heavy metal extraction by Chelex 100 (50-100 mesh Bio-Rad Lab) *at pH = 7.6* eluted with HNO_3.2N and analysis by flame or graphite furnace atomic absorption;
3) Anodic stripping voltammetry on the sample acidified until pH = 3 .

These three methods, applied in different laboratories on the same samples, gave, except for zinc, results which are significantly different. In general, the concentrations found for copper, lead and cadmium by ASV are higher than those obtained by AA-Chelex concentration and the latter are often higher than those by AA-extraction APDC. This observation is probably not too surprising by considering the fact that on one side AA gives the concentration of those species which are extracted at pH = 8

by APDC or by Chelex and on the other side, ASV gives the concentration of those species which are reduced to metal at - 1,25 volts and at pH = 3 .

As we know that the pH influences considerably the distribution of the heavy metal ions between different species, it seemed worth comparing these three methods on the same sea water solution at the same moment in the same laboratory.

The results presented in table 7 were carried out by Machiroux *et al.* (1973) for APDC-MIBK extraction and AA and by Machiroux et Dupont (1974) for Dowex A1 extraction and AA.

Table 7

Comparison of the results obtained by the three methods

N°	Cu (µg/ℓ)			Pb (µg/ℓ)		Cd (µg/ℓ)		Zn (µg/ℓ)	
	ASV	AAS	AAR	ASV	AAS	ASV	AAS	ASV	AAS
427	5.2	4.8		6.3	2.7	0.91	0.86	6.2	5.9
428	4.2	4.0		1.4	1.5	0.45	0.43	1.2	1.1
429	1.5	1.3		4.3	4.9	2.4	2.1	41.2	29.2
430	4.7	4.5		1.5	1.7	0.28	0.20	3.5	3.3
432	3.8	1.1		1.2	1.4	0.33	0.14	1.9	
433	4.1	1.6		2.6	0.4	0.14	0.16	2.2	
1	6.5		7.1						
2	15.2		13.8						
3	6.9		7.2						
4	14.8		11.6						
5	3.5		3.3						

ASV : anodic stripping voltammetry
AAS : atomic absorption after solvent extraction with APDC-MIBK
AAR : atomic absorption after Dowex A1 separation

The experimental conditions adopted are briefly the following : the sea water samples are quickly thawed, immediately filtered through a 0.22 µm pore size Millipore and divided in three parts for analysis :
1) Anodic stripping voltammetry at pH = 3.5 - 4 (ASV);

2) Atomic absorption with the graphite furnace on the organic phase obtained by extracting three times by 5 mℓ MIBK 20 mℓ of sea water at pH = 4 containing 2 mℓ of APDC 1 % (AAS);
3) Atomic absorption with the graphite furnace on the following eluted solution : 100 mℓ of sea water pH = 8 passed through a column of Dowex A1 50-100 mesh with a flow rate of 0,5 mℓ/min × cm^2 ; the elution is performed with 100 mℓ of HNO_3.2N at the same flow rate (AAR).

Considering the fact that the greatest discrepancies between different methods occur generally for copper, we carried out the comparison between ASV and AAR only on that element.

The results are presented in table 7.

Keeping in mind the low concentrations we are dealing with and the fact that atomic absorption requires a series of operations subject to contaminations and considering the errors inherent to each method, it seems reasonable to conclude that all three methods are capable to give, *under the described conditions*, the same result.

References

ARIEL, M. and EISNER, U., (1963). *J. Electroanal. Chem.*, *5*, 362-374.

ARIEL, M., EISNER, U. and GOTTESFELDS, S., (1964). *J. Electroanal. Chem.*, *7*, 307-314.

ARMITTAGE, B. and ZEITLIN, H., (1971). *Anal. Chim. Acta*, *53*, 47-53.

ARMSTRONG, F.A.J., WILLIAM, P.M. and STRIEKLAND, J.B.H., (1966). *Nature*, *211*, 481-483.

BARIC, A. and BRANICA, M., (1967). *Limnol. Oceanog.*, *1*, 4-8.

BARKER, R.T. and RYTHER, J.H., (1969). *J. Exp. Mar. Biol.*, *3*, 191-199.

BROOKS, R.R., PRESLEY, B.J. and KAPLAN, I.R., (1967). *Talanta*, *14*, 809-816.

BURREL, D.C. and WOOD, G.G., (1969). *Anal. Chim. Acta*, *48*, 45-49.

BURREL, D.C., (1967). *Anal. Chim. Acta*, *38*, 447-455.

BURREL, D.C., (1972). *Proc. third Intern. Atom. Spectr. Cong.*, Paris, 409-428.

DUPONT, J.C., (1974). mémoire de licence (Université de Liège).

DUURSNA, E.K. and SEVEN HUYSEN, W., (1966). *Netherlands of Sea. Res., 31*, 95-106.

DYRSSEN, D., PATTERSON, C., UI, J., WEICHART, G.F., (1972). *A guide to Marine Pollution*, compiled by E.D. Goldberg, Chapter 3, *Inorganic Chemicals*, 41-48, Gordon and Breach Science Publishers, New York.

DRYSSEN, D. and WEDBORG, M., (1974). *Equilibrium Calculations of the Speciation of Elements in Sea Water*, in *The Sea*, vol. 5, 181-195, edited by E.D. Goldberg, A. Wiley Interscience, New York.

FABRICAND, B.P., SAWGER, R.R., UNGAR, S.G. and ADLER, S., (1962). *Geochim. and Cosmochim. Acta, 26*, 1023-1027.

FLORENCE, J., (1972). *J. Electroanal. Chem., 35*, 237-245.

JOHNSTON, R., (1964). *J. Mar. Biol. Ass. U.K., 44*, 87-109.

KUWATA, K., HISATOMI, K. and HASEGAWA, T., (1971). *Atom. Absorp. Newslett., 10*, 111-115.

LAITINEN, H.A., (1974). *Analyst, 99*, 1011-1018.

LE MEUR, J.F. et COURTOT-COUPEZ, J., (1973). *Bull. Soc. Chim. France*, 929-935.

MACCHI, G., (1965). *J. Electroanal. Chem., 9*, 299-304.

MACHIROUX, R., BRIHAYE, C. and BUI KIM HANH, (1973). Technical Report Chim., Synthèse 2, Centre Interministériel de la Politique Scientifique, Bruxelles.

MAGNEE, R.J. and RAHMAN, A.K.M., (1965). *Talanta, 12*, 403-416.

MANCY, K.H., (Editor), (1971). *Instrumental Analysis for Water Pollution Control*, Ann. Arbor, Science Publishers, Mich.

NAUMANN, R., SCHMIDT, W., (1971). Z. *Anal. Chem., 257*, 337-340.

NIKELLY, J.G. and COOKE, W.D., (1957). *Anal. Chem., 29*, 933-939.

NOAKES, J.E. and WOOD, D.W., (1961). *Deep Sea Res., 8*, 121-130.

ODIER, M. and PICHON, V., (1963). *Anal. Chim. Acta, 55*, 209-220.

PATTERSON, C.C., (1974). *Science, 183*, 553-554, N.Y.

PAUS, P.E., (1973). *Z. Anal. Chem., 264,* 118-122.

POCKLINGTON, R., (1971). *Nature, 230,* 374-375.

RILEY, J.R. and TAYLOR, D., *Anal. Chim. Acta, 40,* 479-485.

ROBERTSON, D.E., (1968a). *Anal. Chem., 40,* 1067-1072.

ROBERTSON, D.E., (1968b). *Anal. Chim. Acta, 42,* 533-536.

ROZHANSKAYA, L.I., (1970). *References Methods for Marine Radioactivity Studies,* I.A.E.A., Technical Report Series N° 118, Vienna.

SEGAR, B.A. and GONZALEZ, J.G., (1972). *Anal. Chim. Acta, 58,* 7-14.

SINKO, I. and DOLEZAL, J., (1970). *J. Electroanal. Chem., 25,* 299-306.

SLOWEY, J.F., JEFFERY, L.M., WOOD, D.W., (1967). *Nature, 214,* 377-378.

TOLG, G., (1972). *Talanta, 19,* 1489-1521.

WHITNACK, G.C., (1961). *J. Electroanal. Chem., 2,* 110-115.

WHITNACK, G.C., (1964). Polarography 1964, *Proceeding of the third international conference Southampton,* vol. 1, edited by G.J. Hills.

WHITNACK, G.C. and SASSELLI, R., (1969). *Anal. Chim. Acta, 47,* 267-274.

WILLIAM, F.F., (1969). Thesis, Massachusetts Institute of Technology.

III

Mass transfer in disturbed sediments

by

J.-P. VANDERBORGHT, R. WOLLAST and G. BILLEN

(Laboratoire d'Environnement, Institut de Chimie Industrielle, U.L.B. and Laboratorium voor Ekologie en Systematiek, V.U.B.)

Introduction

The knowledge of the properties of the water-sediment interface, as well as the kinetics of the chemical reactions taking place in the sediments, are essential for the description and understanding of the mass transfer processes between sea-water and marine deposits.

It must be recognized that the boundary conditions at this interface are often poorly known; in some cases, its exact position is not even well defined.

One of the most important reasons for this situation is the difficulty of collecting cores without disturbing the water-sediment interface.

With the classical gravity or piston corer, and to a lesser extent the box corer, the turbulence caused by the instrument itself is able to resuspend the poorly compacted top sediments.

The removal of the supernatant water of the core may possibly carry away another fraction of the surface layer of the sediments.

It is thus necessary to use an adequate coring technique and to perform a careful treatment of the core in order to avoid any loss of information.

The properties of the surface layer of the sediments generally differ very much from those of the deeper layers, and may considerably affect the mass transport across the water-sediment interface.

The degree of compaction in the surface layer is low, especially in the case of muds.

The shear stresses produced by the overflowing water induce perturbations of this uncompacted layer, and increase the mass transfer coefficient of dissolved species within the layer.

Also, the high porosity favours the diffusion process in the interstitial waters.

Furthermore, the biological activity of various benthic organisms is generally more intense in the surface layer.

This activity affects not only the chemistry of the whole environment, but produces mechanical transports known as bioturbation.

This paper is an attempt to describe the properties of the upper sediments of the North Sea along the Belgian coast.

These sediments are essentially constituted by organic rich muds (up to 5 % of organic C) deposited in shallow waters, at a mean depth of about 20 meters. The surface currents are high and the storms frequent, inducing important shear stresses on the water-sediment interface and favouring the existence of a disturbed boundary layer.

At the opposite, the activity of the benthic macro- and meio-fauna is extremely low in these sediments [De Coninck (1972)]. The existence of this layer has been demonstrated by careful coring techniques and chemical analysis performed on very closed vertical spacings. The analytical results were interpreted by kinetic models describing the vertical concentration profiles of various dissolved species in the porewater.

In a first part, special attention has been given to the influence of the disturbed layer on the vertical profiles and mass transfer coefficients have been computed through a kinetic model for dissolved silica.

A comprehensive model for sulfate, nitrate and ammonia will be presented in a second part.

We will present here as an example the results obtained on two cores taken in the North Sea at the position 51°19'45" N ; 3°04'44" E . These cores are representative of a large muddy zone along the Belgian and Dutch coast and display the typical pattern of the disturbed upper layer. It must be pointed out, however, that sandy sediments, which can also be found in the same region, do not show this pattern.

The results reported here may only be considered as representative of the behaviour of poorly consolidated sediments in shallow waters.

1.- Experimental

The cores were collected by divers of the Belgian Navy in 6.35 cm PVC core-liner tubes. The inner part of the tubes was covered with a thin polyethylene shield which allowed an easy removal of the sediments from the core barrel. The penetration of the core-liner tube was restricted to the first 25 cm . The tube was then sealed *in situ* with two rubber corks and brought aboard the ship in a vertical position. Two cores were collected at each site. The first one was immediately treated by discarding the supernatant water and cutting the sediment in short segments 1 to 4 cm long. These samples were then immediately centrifugated and the Eh , pH and alcalinity were measured on the interstitial water. The remaining part of the sample was deep frozen for subsequent chemical analysis.

The second core was immediately deep frozen. Segmentation was performed in the laboratory where the fractions were centrifugated. The chemical analysis included the determination of ammonia, nitrate, nitrite, silica and sulfate. It became apparent by comparison of the results of the chemical analysis performed on the interstitial water of the two cores that the 3 upper centimeters of the first core were lost when discarding the supernatant water. Only the second procedure did not disturb the structure of the water-sediment interface.

2.- Results

2.1.- Porosity

The vertical profile of porosity is given in figure 1. The porosity decreases rapidly from 100 % to about 65 % in the first 4 cm and remains practically constant at a greater depth.

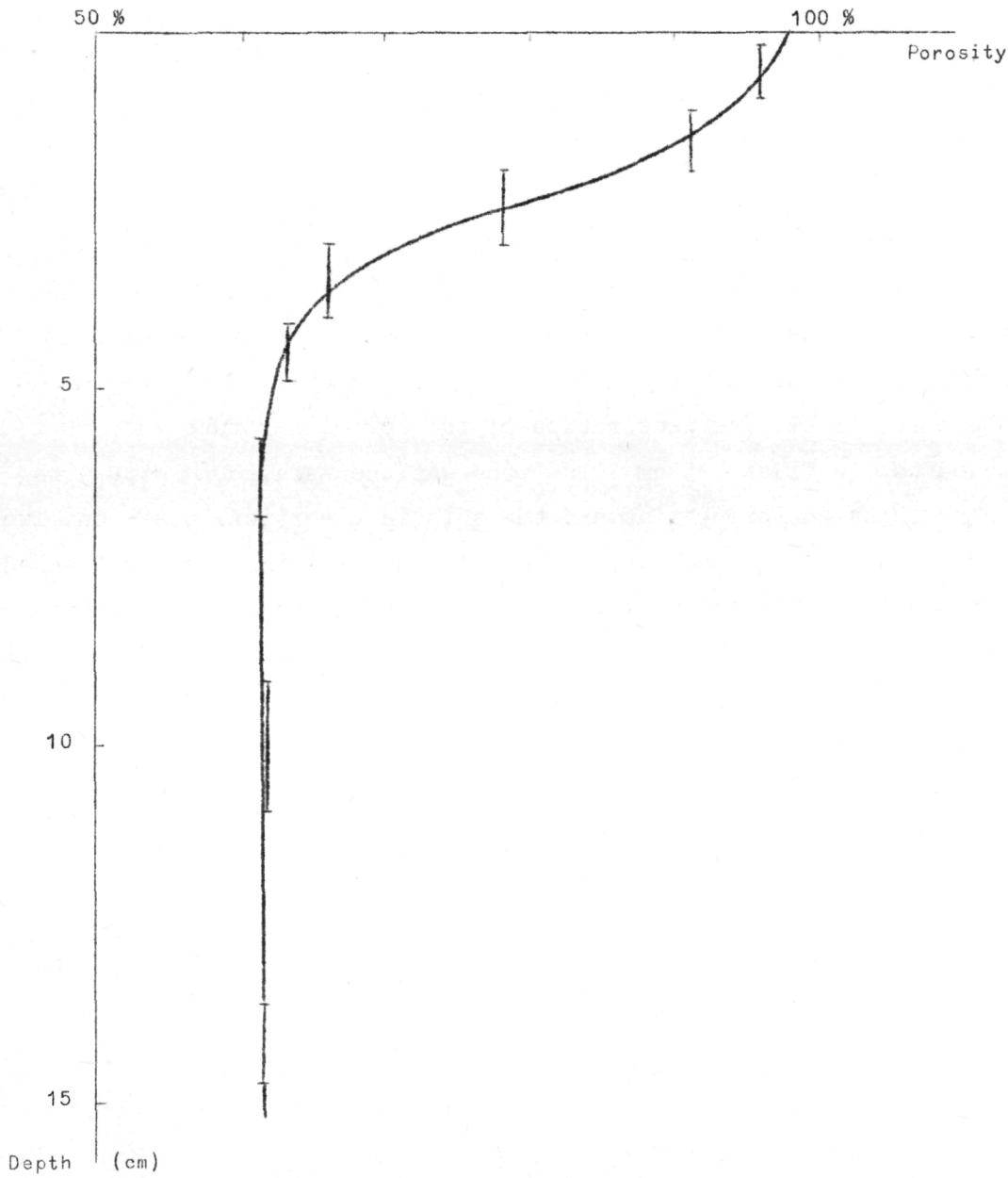


fig. 1.

2.2.- Redox potential

The existence of a sharp transition at a depth of 3.5 cm between a brown colored oxidized layer and a black reduced layer indicates that, in spite of the high amount of organic matter present, oxidizing conditions prevail in the upper part of the sediments. On the other hand, redox potentials as low as - 150 mV were measured in the lower part. This situation is in contrast with the Eh profiles of cores taken in a small lagoon near the Belgian coast [Vanderborght and Billen (1975)] where similar sediments are deposited but are not submitted to high shear stresses as in the open sea. In this case, reducing conditions are encountered at less than a few millimeters from the water-sediment interface.

2.3.- Dissolved silica

Figure 2 shows the vertical profile of dissolved silica obtained on the core. A sharp gradient discontinuity is observed at a depth of about 4 cm , with a very low gradient of concentration in the upper part of the sediment. This profile differs from those usually described [Anikouchine (1967), Hurd (1973), Fanning (1974)], where high gradients of dissolved silica are observed at the interface.

2.4.- Sulfate

The classically described anaerobic reduction of sulfate can be observed in the deeper part of the North Sea sediments (fig. 3), where sulfate is completely depleted at a 25 cm depth. As may be expected, the reduction of sulfate does not occur in the upper oxidizing layer.

2.5.- Nitrate

Nitrate profiles in the North Sea cores display a maximum value in the upper layer at a depth of about 2 cm (fig. 4). It is interesting to compare these results with those obtained for muddy and sandy deposits taken from a lagoon near the Belgian coast. It has been shown [Vanderborght and Billen (1975)] that in the muddy organic rich sediments, the nitrate concentration is always lower in the interstitial water than in

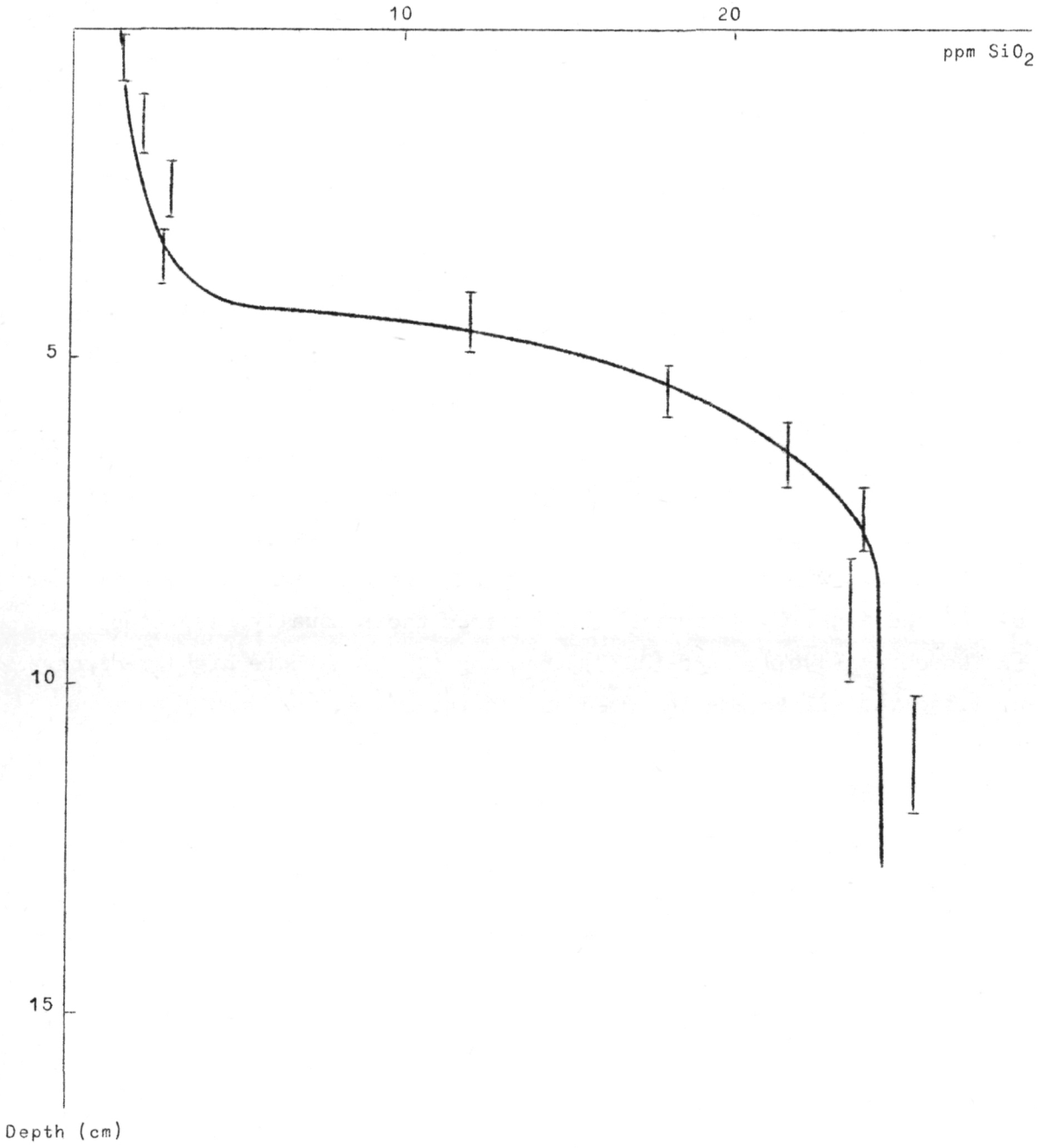


fig. 2.

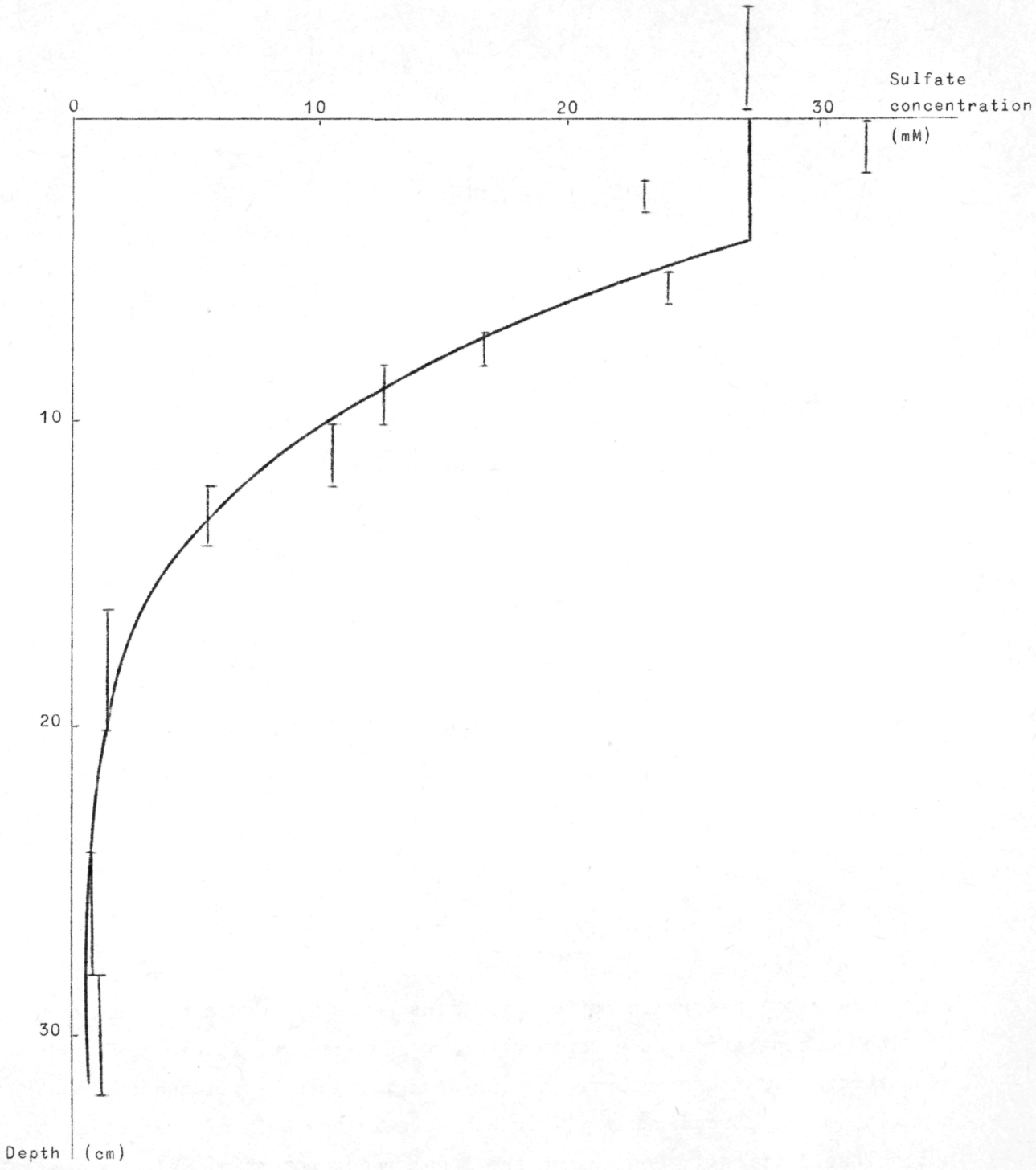


fig. 3.

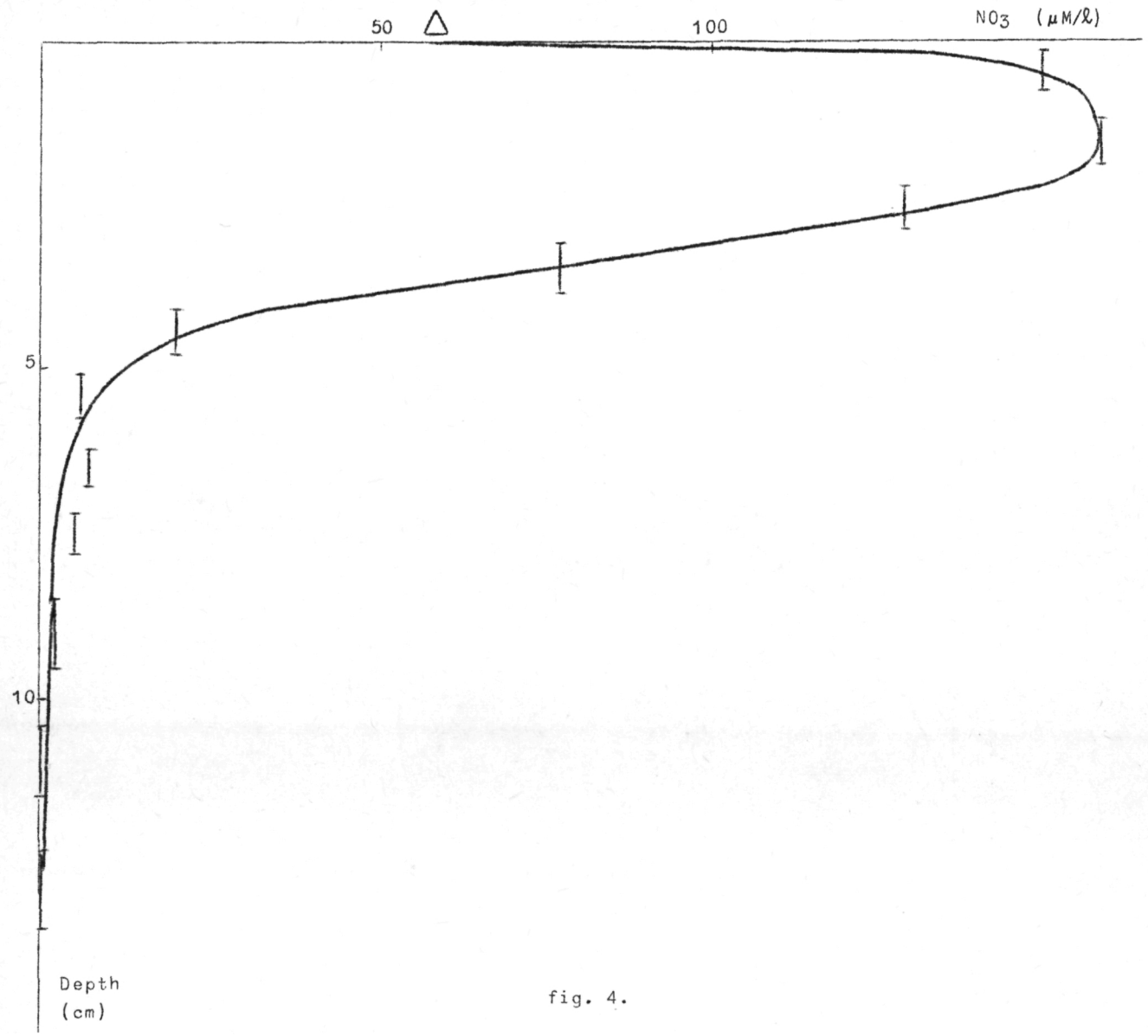


fig. 4.

overlying water, and decreases rapidly with depth. In sandy sediments, which are poor in organic matter, profiles commonly show a maximum in nitrate concentration at a depth of a few centimeters. It has also been demonstrated by these authors that this maximum can be related to the activity of autotrophic nitrifying bacteria in the bulk of the sediments, which itself strongly depends on the local redox potential value. This nitrification may also occur in the disturbed layer of muddy sediments because of the oxidizing conditions prevailing there.

2.6.- Ammonia

The increase of the ammonia concentration in pore water due to decomposition of organic material is also observed in the North Sea cores (fig. 5). However, in contrast with the usual profiles obtained in deep-sea cores, a sharp discontinuity of the concentration gradient occurs at a depth of about 4 cm .

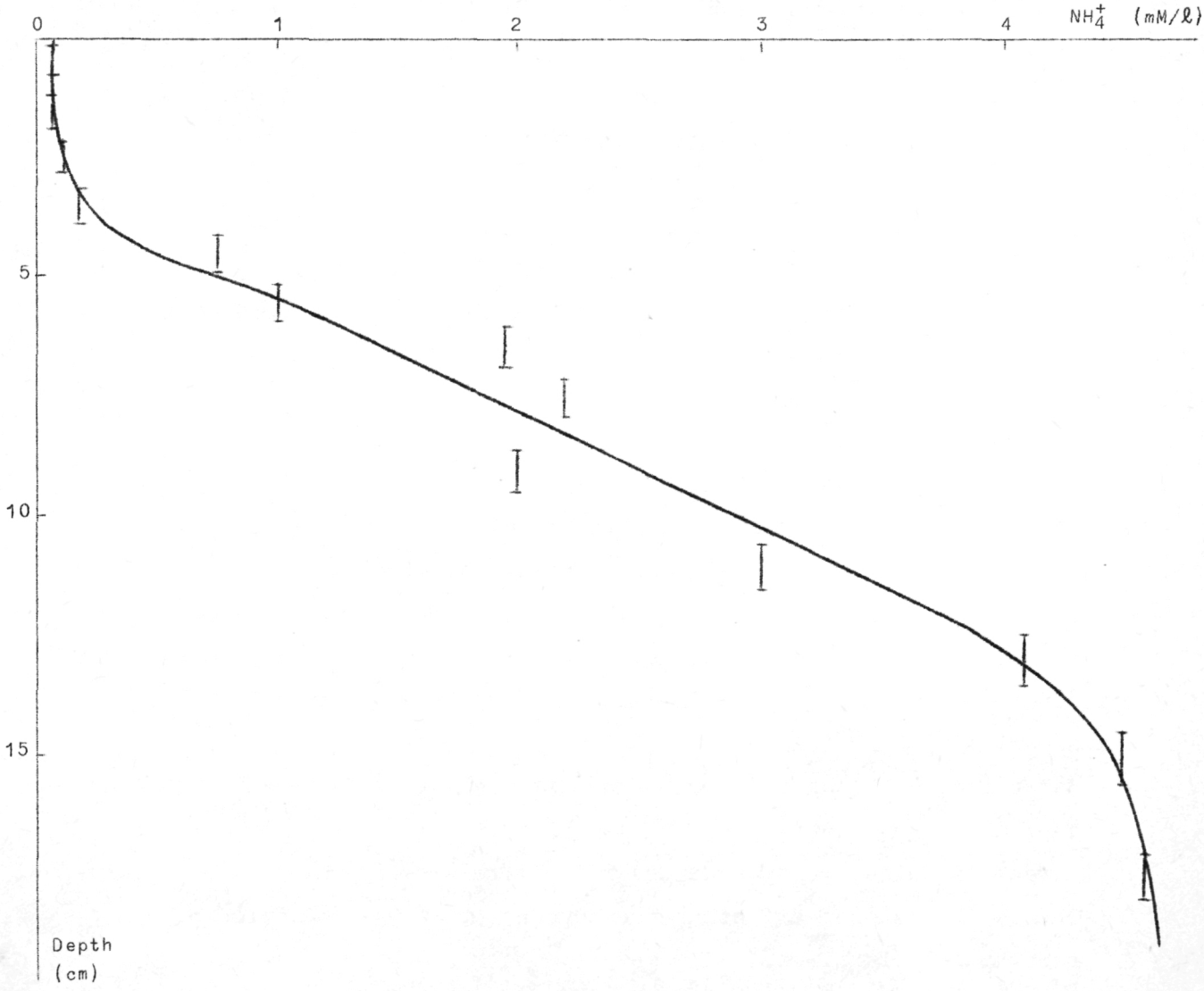


fig. 5.

3.- Kinetic model for dissolved silica

To analyse more quantitatively the importance of the upper layer of the sediments in the exchange with surface waters, we have tried to describe the vertical concentration profile of the dissolved silica in pore water by considering the various physical and chemical processes taking place in the sediments. The general approach of the proposed kinetic model has been extensively described by Berner (1971), (1974) for homogeneous sediments. However, simple models for homogeneous deposits are not able to describe the existence of discontinuities in the concentration gradient, as observed in the profiles of the North Sea cores. These profiles strongly suggest that one distinguishes a thin disturbed layer near the water-sediment interface from a rather consolidated underlying sediment.

The continuous decrease of porosity and of mechanical perturbations with depth imply that the mass transfer coefficient be a continuous function of depth. However, a simplification of the mathematical treatment has been made by considering a two-layer sediment system, where each layer is characterized by a constant mass transfer coefficient. Furthermore only a steady-state model will be considered here, implying that all the parameters appearing in the kinetic equation are time independant. This hypothesis has been mathematically justified for a similar case [Vanderborght and Billen (1975)].

In the kinetic equation describing the vertical concentration profile of silica, we will consider the contribution of the following processes :

- diffusion in the pore water of the dissolved substance under its concentration gradient;
- advection related to the deposition of fresh sediments;
- chemical reactions affecting the concentration by production or consumption of silica.

The net rate of dissolved silica production results from a competition between dissolution of highly reactive opal and reprecipitation processes. These are not well understood, but it is generally admitted that, in the presence of clay minerals, reprecipitation of dissolved silica due

to reactions with solids in the sedimentary column must be considered. It can be shown [Hurd (1973), Berner (1974), Fanning and Pilson (1974), Wollast (1974)] that the net rate of reaction may be simply described by the kinetic relation :

$$r_{Si} = k_{Si} \left([Si]_\infty - [Si]\right)$$

where k_{Si} is an apparent kinetic constant, $[Si]$ is the concentration of dissolved silica and $[Si]_\infty$ is either an equilibrium concentration of dissolved silica or a steady state value of this concentration which is reached at high depth.

The equation describing the behaviour of dissolved silica in the upper and lower layers can be written :

$$(1) \qquad D_i \frac{d^2[Si]}{dz^2} - \omega \frac{d[Si]}{dz} + k_{Si} \left([Si]_\infty - [Si]\right) = 0$$

where D_i represents the global mass transfer coefficient in the considered layer.

The following boundary conditions are imposed to solve the system :

- at $z = 0$, the concentration is equal to the concentration $[Si]_0$ in the overlying sea-water;
- at large z-values, the concentration tends towards a finite value;
- at the interface between the upper and lower layer $(z = z_n)$, there is no discontinuity in the concentration profile, on the other hand, the fluxes across this interface are conservative :

$$(2) \qquad \Phi_n = - D_1 \frac{d[Si]}{dz}\Big|_1 = - D_2 \frac{d[Si]}{dz}\Big|_2 \qquad \text{at} \qquad z = z_n \ .$$

The solution to equation (1) is, for the upper layer :

$$(3) \quad [Si]_1 = [Si]_\infty - \left([Si]_\infty - [Si]_0\right) \left\{\frac{ch[\alpha_1(z_n - z)] - \beta\ sh[\alpha_1(z_n - z)]}{ch(\alpha_1 z_n) + \beta\ sh(\alpha_1 z_n)}\right\} e^{\frac{\omega}{2D_1} z}$$

for the lower layer :

$$(4) \quad [Si]_2 = [Si]_\infty - \left([Si]_\infty - [Si]_0\right) \left[\frac{e^{\frac{\omega}{2D_1} z_n}}{ch(\alpha_1 z_n) + \beta\ sh(\alpha_1 z_n)}\right] e^{\left(\frac{\omega}{2D_2} - \alpha_2\right)(z - z_n)}$$

with $$\alpha_1 = \left(\frac{\omega^2}{4 D_1^2} + \frac{k_{Si}}{D_1}\right)^{\frac{1}{2}} ,$$

$$\alpha_2 = \left(\frac{\omega^2}{4\, D_2^2} + \frac{k_{Si}}{D_2}\right)^{\frac{1}{2}} ,$$

$$\beta = \frac{D_2\ \alpha_2}{D_1\ \alpha_1} .$$

The depth z_n is estimated from the porosity profiles. A value of 3.5 cm , which also corresponds to the color transition in the cores, was used throughout the calculations. Many estimations have been made on the deposition rate ω for the southern part of the North Sea and a mean

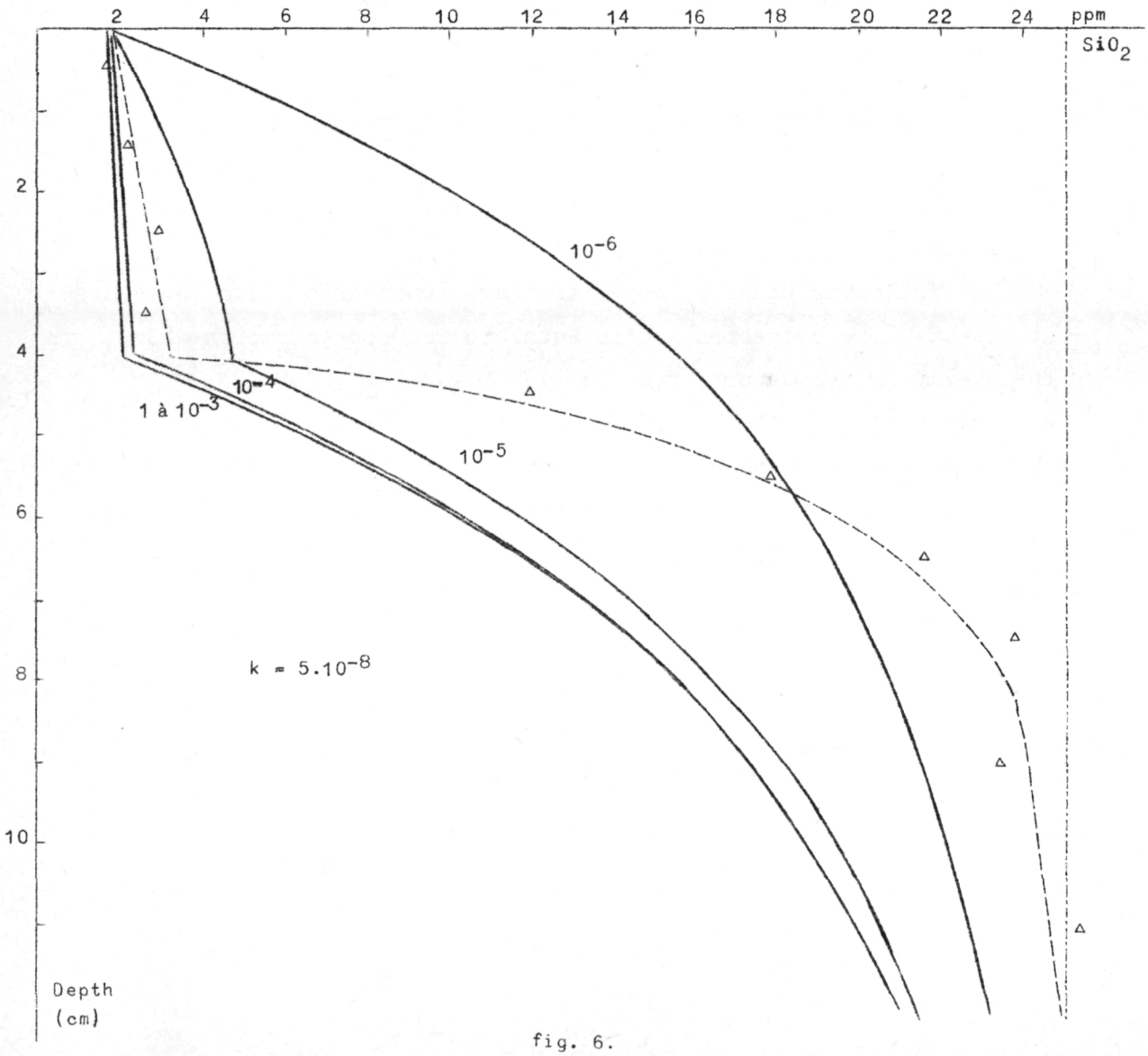


fig. 6.

value of 3 cm per 100 years seems to be the best approximation [MacCave (1971)]. Deposition rates one or two orders of magnitude higher can be locally observed. The mass transfer for the lower part may be considered as only due to molecular diffusion. At the mean temperature of the system 11 °C and taking into consideration the porosity and an estimation of the tortuosity of this layer, the diffusion coefficient for the lower layer approximately equals 10^{-6} $cm^2.s^{-1}$ [Anikouchine (1967), Wollast, Garrels (1971), Hurd (1973), Berner (1974), Fanning (1974)]. The asymptotic value of the dissolved silica concentration $[Si]_\infty$ can be deduced from the experimental profiles (fig. 2) : a value of 400 µmoles.

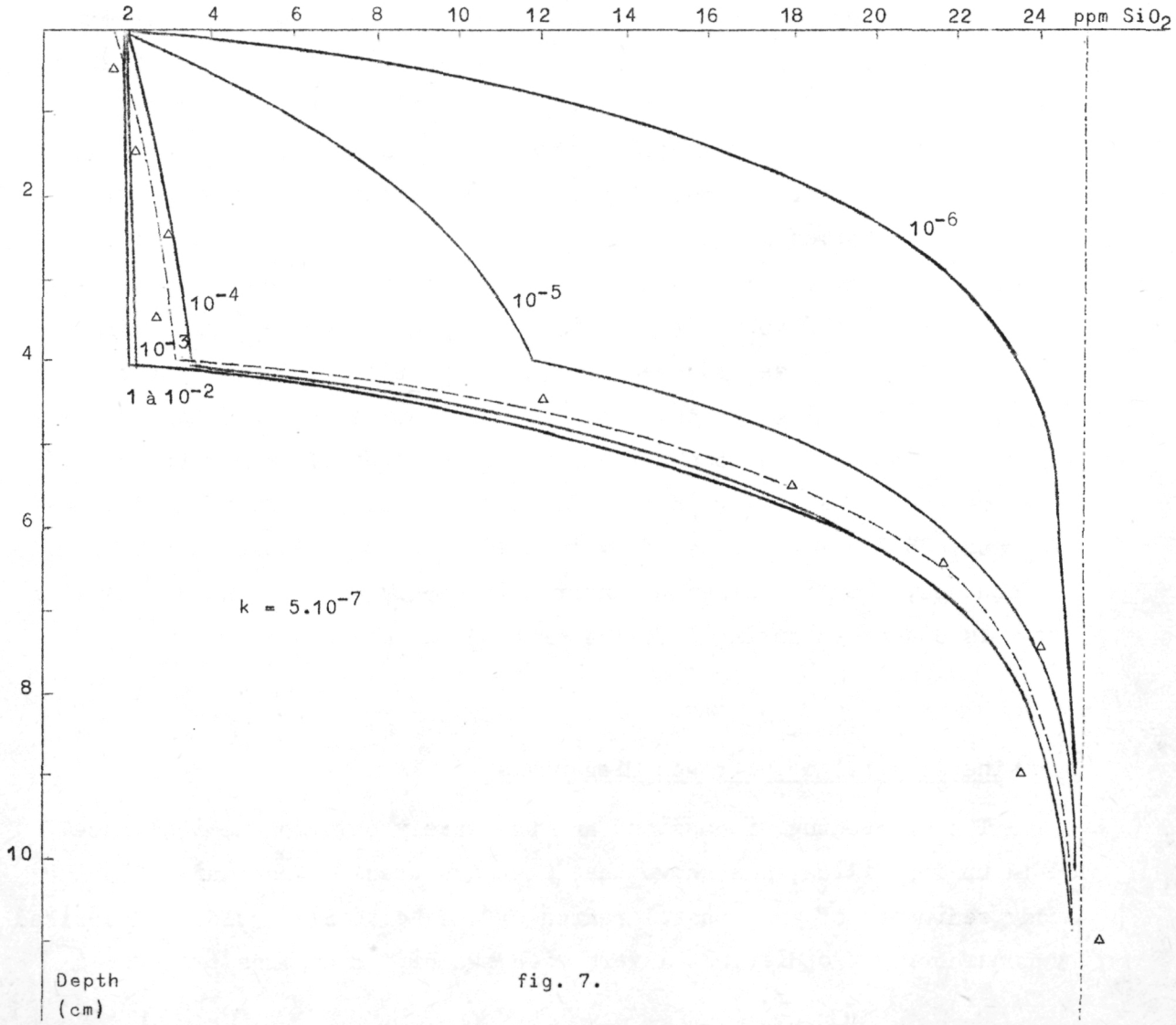


fig. 7.

ℓ^{-1} has been selected. The only unknown parameters are D_1 and k_{Si}. A set of curves has been drawn for various values of k_{Si} and D_1 (fig. 6 and 7). The distribution of dissolved silica in the lower part of the sediments is very sensitive to the values of k_{Si} which allows one to select the value

$$k_{Si} = 5 \times 10^{-7}\ s^{-1} .$$

The best fit for the surface layer is then obtained for

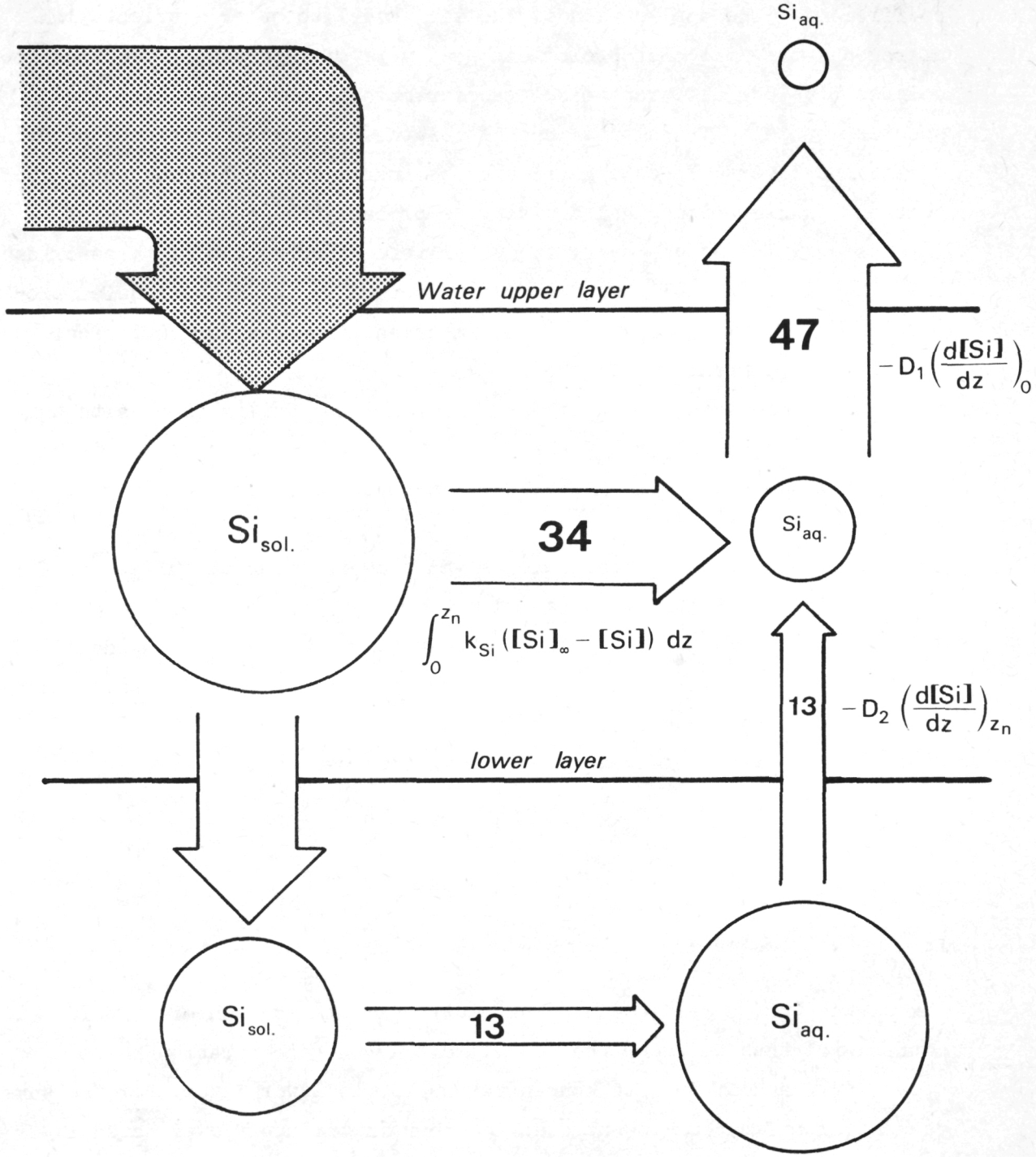
$$D_1 = 10^{-4}\ m^2.s^{-1} .$$

Our value for k_{Si} is in agreement with the value calculated from the laboratory experiments of Grill and Richards (1964) on diatoms, and Hurd (1972) on radiotarians. The rate constant deduced from these experiments are respectively equal to 2×10^{-7} and $7 \times 10^{-7}\ s^{-1}$. It should be noticed that the sedimentation rate ω can be neglected as long as it is less than 10 cm/year and has not to be known with a great precision. The value of the mass transfer coefficient D_1 for the upper layer is 100 times greater than the apparent diffusion coefficient in the compacted layer. This large increase is partially due to the change of porosity and tortuosity (approximately a factor of 2), but mainly to the advective processes induced by the movement of overlying water.

The model allows to calculate the flux across the boundary between layer 1 and layer 2, across the water-sediment interface and the net dissolution rate of silica (fig. 8). The contribution of the upper layer represents 75 % of the total flux of silica out of the sediments. As a consequence, the fluxes may be underestimated by a factor of 4 if this layer is discarded during sampling or handling of the core.

4.- Kinetic model of nitrogen diagenesis

The preceeding discussion, and the purely physico-chemical model build up for silica, has shown that the mass transfer mechanisms in the muddy sediments of the coastal region of the North Sea could be described by considering two distinct layers with two different mass transfer



mg Si/m^2.day

fig. 8.

coefficients. The application of the same model to other nutrients like nitrogen, for which microbiological action is of importance, requires not only to consider different mass transfer mechanisms for the dissolved species, but also fundamental changes of the biological processes occuring in the two layers. In an organic rich sediment, the most important factor controlling microbiological activity is probably the availability of oxidants. As far as the overlying water is a major source of these oxidants their availability will be strongly influenced by the mass transfer properties of the two layers. The most important oxidants for biological activity are oxygen and sulfate.

Manganese oxide, nitrate and iron hydroxide utilization, although it can account for a part of the oxidation of the organic matter in sediments, will not be taken explicitely into account in the present simplified model.

The results of Eh measurements and the experimental sulfate profile (fig. 3) suggest that oxygen is available in the upper layer and prevents sulfate utilization, while sulfate is extensively used as an oxidant in the lower layer. The microbiological decomposition of organic matter can thus be represented by coupling equation (a) with equation (b) in the disturbed layer and with equation (c) in the lower compacted layer :

(a) $$CH_2O + 2H_2O \rightarrow HCO_3^- + 5H^+ + 4e^-$$

(b) $$4e^- + O_2 + 4H^+ \rightarrow 2H_2O$$

(c) $$4e^- + \frac{1}{2} SO_4^{--} + \frac{9}{2} H^+ \rightarrow \frac{1}{2} HS^- + 2H_2O \ .$$

Ammonification, a result of the heterotrophic utilization of organic matter will thus be under the control of oxygen concentration in the upper layer and of sulfate concentration in the lower layer. For the same reason, nitrification is supposed to occur in the upper oxygenated layer while denitrification is only possible in the lower layer.

The behaviour of O_2 , SO_4^{--}, NH_4^+ and NO_3^- in the pore water of the sediment can be described by the following general equation :

(5) $$\frac{\partial C}{\partial t} = D \frac{\partial^2 C}{\partial z^2} - \omega \frac{\partial C}{\partial z} + r$$

where C is the concentration of the dissolved substance (mole.ℓ^{-1}) and r the rate of production (r > 0) or consumption (r < 0) (mole.ℓ^{-1}.s^{-1}), z, D and ω as above. Under the assumption of steady state

$$\frac{\partial C}{\partial t} = 0 \ .$$

The expression of the rates of reaction will now be discussed briefly for each constituent.

4.1.- Oxygen

A Michaelis-Menten function would be the best way of expressing the oxygen consumption rate. However, for reasons of mathematical simplification, this Michaelis-Menten kinetics has been approximated by a zero order kinetics at oxygen concentration higher than some critical value (around 1 % saturation) and a first order kinetics at lower concentration. It is also assumed that this critical oxygen concentration is reached at the boundary between the upper and the lower layer, so that

$$r_{O_2} = \begin{cases} - k_{O_2} & \text{for} \quad z < z_n \\ - k'_{O_2} \, [O_2] & \text{for} \quad z > z_n \ . \end{cases}$$

4.2.- Sulfate

As stated above, sulfate reduction does not occur in the well aerated part of the sediment, but only in the lower layer. In his kinetic model of sulfate distribution in sediments, Berner (1964), (1974), postulated that the rate of bacterial sulfate reduction was first order with respect to the concentration of a particular fraction of organic material used by sulfate reducing bacteria. In the case of these organic rich sediments, however, the organic content (measured both as total organic carbon and as aminoacids) was found to be degraded only to a small extent (15 to 20 %) at a depth of 25 cm whereas sulfate is completely depleted. This suggests that the rate of organic decomposition is limited by the availability of oxidants rather than by

the concentration of organic matter. Sulfate reduction rate will then be first order with respect to sulfate concentration :

$$r_{SO_4} = \begin{cases} 0 & \text{for} \quad z < z_n \\ - k_{SO_4} [SO_4] & \text{for} \quad z > z_n \end{cases}$$

4.3.- Nitrate

The modelling of nitrification and denitrification in sediments has been extensively discussed in a previous paper [Vanderborght and Billen (1975)]. The same model will be used here : a constant nitrification term will be assumed in the upper layer :

(d) $$NH_4^+ + 2\,O_2 + 2\,H^+ \rightarrow NO_3^- + H_2O \ .$$

A first order denitrification rate will be postulated in the lower one :

$$r_{NO_3} = \begin{cases} + k_{NO_3} & \text{for} \quad z < z_n \\ - k'_{NO_3} [NO_3] & \text{for} \quad z > z_n \ . \end{cases}$$

4.4.- Ammonium

As ammonium production is related to heterotrophic activity, its rate is proportional to the rate of oxygen consumption in the upper layer and to the rate of sulfate reduction in the lower layer. A consumption term due to nitrification must further be taken into account in the upper layer. Several works show that denitrification in natural water and sediments produces essentially nitrogen and no ammonium [Chen *et al.* (1972), Wheatland *et al.* (1959), Chan and Campbell (1973)]. There is thus no additional production term in the lower layer :

$$r_{NH_4} = \begin{cases} - k_{NO_3} + k_{NH_4} & \text{for} \quad z < z_n \\ + \alpha\, k_{SO_4} & \text{for} \quad z > z_n \ . \end{cases}$$

The equations of table 1 can then be solved analytically; the solutions are summarized.

Table 1

	Upper layer ($z < z_n$)	Lower layer ($z > z_n$)
Oxygen	$D_1 \frac{d^2[O_2]}{dz^2} - \omega \frac{d[O_2]}{dz} - k_{O_2} = 0$	$D_2 \frac{d^2[O_2]}{dz^2} - \omega \frac{d[O_2]}{dz} - k'_{O_2} [O_2] = 0$
Sulfate	$D_1 \frac{d^2[SO_4]}{dz^2} - \omega \frac{d[SO_4]}{dz} = 0$	$D_2 \frac{d^2[SO_4]}{dz^2} - \omega \frac{d[SO_4]}{dz} - k_{SO_4} [SO_4] = 0$
Nitrate	$D_1 \frac{d^2[NO_3]}{dz^2} - \omega \frac{d[NO_3]}{dz} + k_{NO_3} = 0$	$D_2 \frac{d^2[NO_3]}{dz^2} - \omega \frac{d[NO_3]}{dz} - k'_{NO_3} [NO_3] = 0$
Ammonium	$D_1 \frac{d^2[NH_4]}{dz^2} - \omega \frac{d[NH_4]}{dz} - k_{NO_3} + k_{NH_4} = 0$	$D_2 \frac{d^2[NH_4]}{dz^2} - \omega \frac{d[NH_4]}{dz} + a\, k_{SO_4} [SO_4] = 0$

Solution of the differential equations of table 1

Oxygen Upper layer

$$[O_2]_1 = \frac{k_{O_2}}{2 D_1} z^2 + Az + [O_2]_0$$

Lower layer

$$[O_2]_2 = B \; e^{-(\frac{k'_{O_2}}{D_2})^{\frac{1}{2}} (z - z_n)}$$

with

$$A = \frac{-\frac{k_{O_2}}{D_1} \{\frac{z_n^2}{2} + z_n(\frac{D_2}{k'_{O_2}}) \} - [O_2]_0}{(\frac{D_2}{k'_{O_2}})^{\frac{1}{2}} + z_n}$$

$$B = \frac{k_{O_2}}{2 D_1} z_n^2 + Az_n + [O_2]_0$$

Sulfate Upper layer

$$[SO_4]_1 = [SO_4]_0 \; e^{\frac{\omega}{2D_1} z} \; \frac{\omega \; ch \{\frac{\omega}{2D_1} (z - z_n)\} - \beta \; sh \{\frac{\omega}{2D_1} (z - z_n)\}}{\omega \; ch (\frac{\omega}{2D_1} z_n) + \beta \; sh (\frac{\omega}{2D_1} z_n)}$$

Lower layer

$$[SO_4]_2 = [SO_4]_0 \; e^{\frac{\omega}{2D_1} z_n} \; \frac{\omega \, e^{\frac{\gamma}{2D_2}(z - z_n)}}{\omega \, ch\left(\frac{\omega}{2D_1} z_n\right) + \beta \, sh\left(\frac{\omega}{2D_1} z_n\right)}$$

with

$$\beta = (\omega^2 + 4 \, k_{SO_4} \, D_2)^{\frac{1}{2}}$$

$$\gamma = \omega - \beta$$

Nitrate Upper layer

$$[NO_3]_1 = - \frac{k_{NO_3}}{2 \, D_1} z^2 + Az + [NO_3]_0$$

Lower layer

$$[NO_3]_2 = B \; e^{- \left(\frac{k'_{NO_3}}{D_2}\right)^{\frac{1}{2}} (z - z_n)}$$

with

$$A = \frac{\frac{k_{NO_3}}{D_1} \left\{\frac{z_n^2}{2} + z_n \left(\frac{D_2}{k'_{NO_3}}\right)^{\frac{1}{2}}\right\} - [NO_3]_0}{\left(\frac{D_2}{k'_{NO_3}}\right)^{\frac{1}{2}} + z_n}$$

$$B = - \frac{k_{NO_3}}{2 \, D_1} z_n^2 + Az_n + [NO_3]_0$$

Ammonium Upper layer

$$[NH_4]_1 = [NH_4]_0 - \alpha \, [SO_4]_0 \left[e^{\frac{\omega}{2D_1} z} \; \frac{\omega \, ch\{\frac{\omega}{2D_1}(z - z_n)\} - \beta \, sh\{\frac{\omega}{2D_1}(z - z_n)\}}{\omega \, ch\left(\frac{\omega}{2D_1} z_n\right) + \beta \, sh\left(\frac{\omega}{2D_1} z_n\right)} - 1 \right]$$

$$+ \frac{h}{\omega^2} \; e^{- \frac{\omega}{D_1} z} \left(1 - e^{\frac{\omega}{D_1} z}\right) + \frac{h}{\omega} z$$

Lower layer

$$[NH_4]_2 = [NH_4]_0 - \alpha \, [SO_4]_0 \left[e^{\frac{\omega}{2D_1} z_n} \; \frac{\omega \, e^{\frac{\gamma}{2D_2}(z - z_n)}}{\omega \, ch\left(\frac{\omega}{2D_1} z_n\right) + \beta \, sh\left(\frac{\omega}{2D_1} z_n\right)} - 1 \right]$$

$$+ \frac{h}{\omega^2} \; e^{- \frac{\omega}{D_1} z_n} \left(1 - e^{\frac{\omega}{D_1} z_n}\right) + \frac{h}{\omega} z_n$$

with

$h = k_{NH_4} - k_{NO_3}$

β , γ as above

Eleven parameters (z_n , ω , D_1 , D_2 , k_{O_2} , k'_{O_2} , k_{SO_4} , k_{NO_3} , k'_{NO_3} , k_{NH_4} , α) have to be fixed for the calculation of the concentration profiles from these theoretical solutions. Of these, four (z_n , ω , D_1 , D_2) have been determined by the aid of the silica model discussed above. A further parameter, α , can be easily estimated. The results of the determination of alcalinity and ammonium in the pore water of the lower layer (fig. 9) show that one mole of ammonium is produced for each 11 moles of organic carbon oxidized. Considering the stoechiometry of reaction (a) and (c), the value of α is then

$$\frac{2}{11} \simeq 0.18 \ .$$

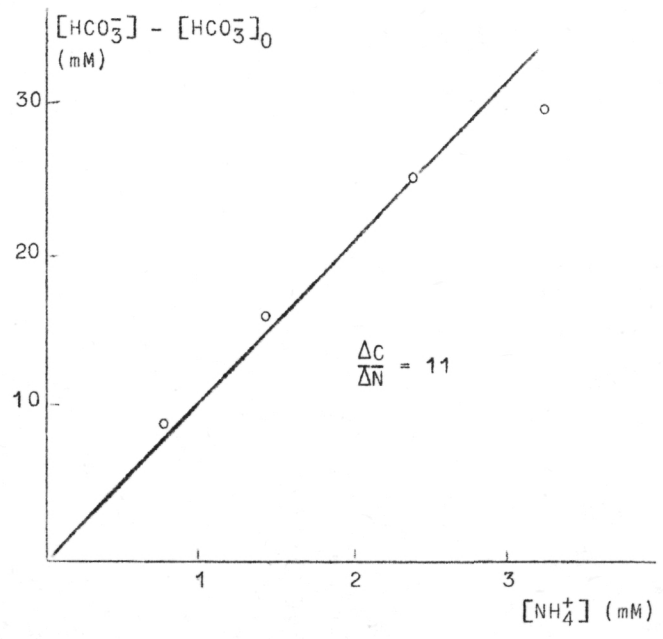


fig. 9.

Furthermore, a relation must exist between three other parameters, k_{O_2} , k_{NO_3} and k_{NH_4} : the oxygen consumption is indeed the result of both aerobic heterotrophic activity and nitrification. Considering a $\frac{\Delta C}{\Delta N}$ ratio equal to 8 for this upper layer, the stoechiometry of reactions (a) and (b), and of reaction (d), the value of k_{O_2} can be expressed by

(6) $$k_{O_2} = 8\, k_{NH_4} + 2\, k_{NO_3} \ .$$

The remaining parameters must now be chosen in order to fit simultaneously

the three experimental profiles SO_4^{--}, NO_3^-, NH_4^+. As far as oxygen is concerned, no experimental profile is available. However, some constraints can be formulated : oxygen concentration at the water-sediment interface is supposed to be 100 % saturation, *i.e.* 340 µM . Oxygen concentration must be higher than about 1 % saturation (3.4 µM) all over the upper layer and lower than this value in the lower layer, for the upper layer has been assumed aerobic and the lower layer anaerobic.

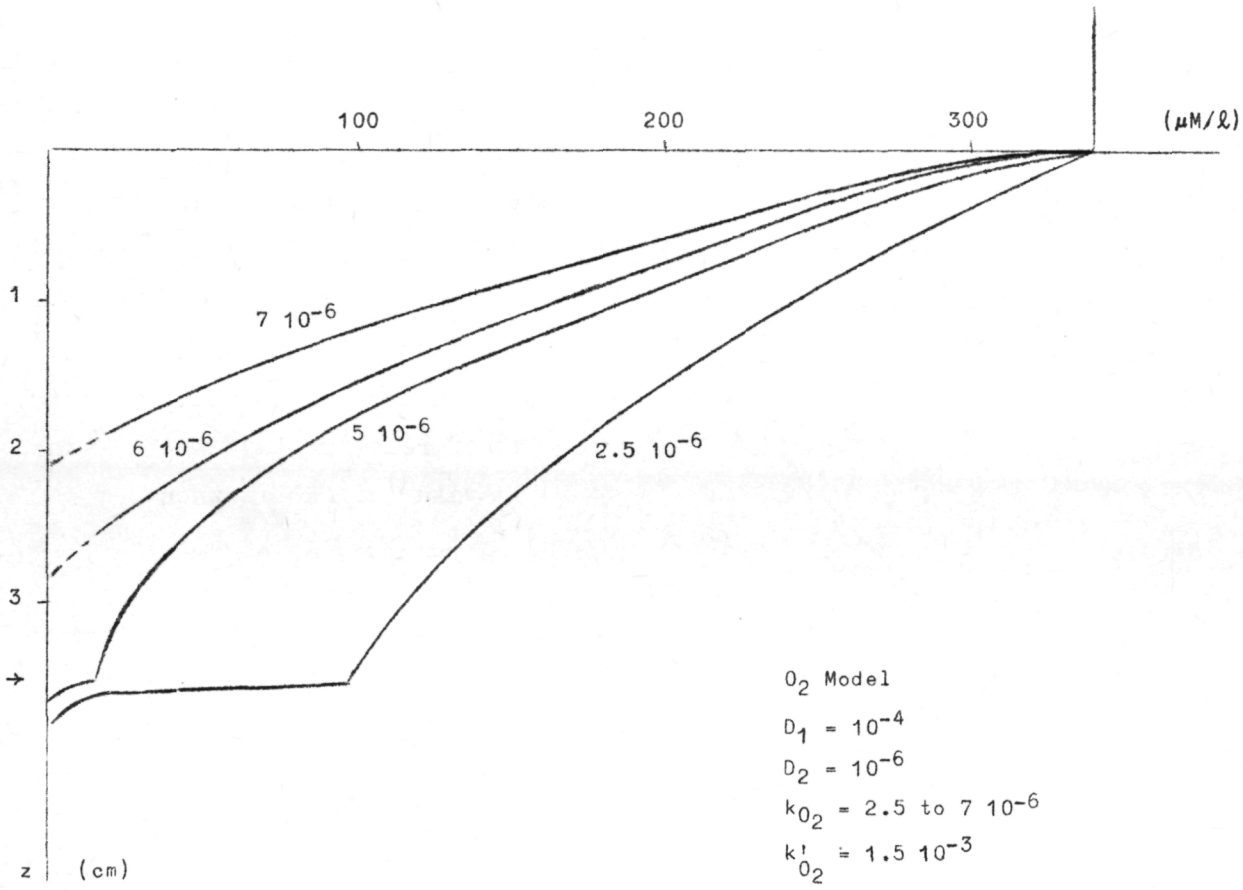


fig. 10.

Figures 10, 11, 12 and 13 show the solution of the equations of table 1 for selected values of the parameters. It can be seen that the theoretical curves are very sensitive to small variations of the parameters. The permitted range of values for the parameters is thus very narrow. The best fit is obtained for the following values :

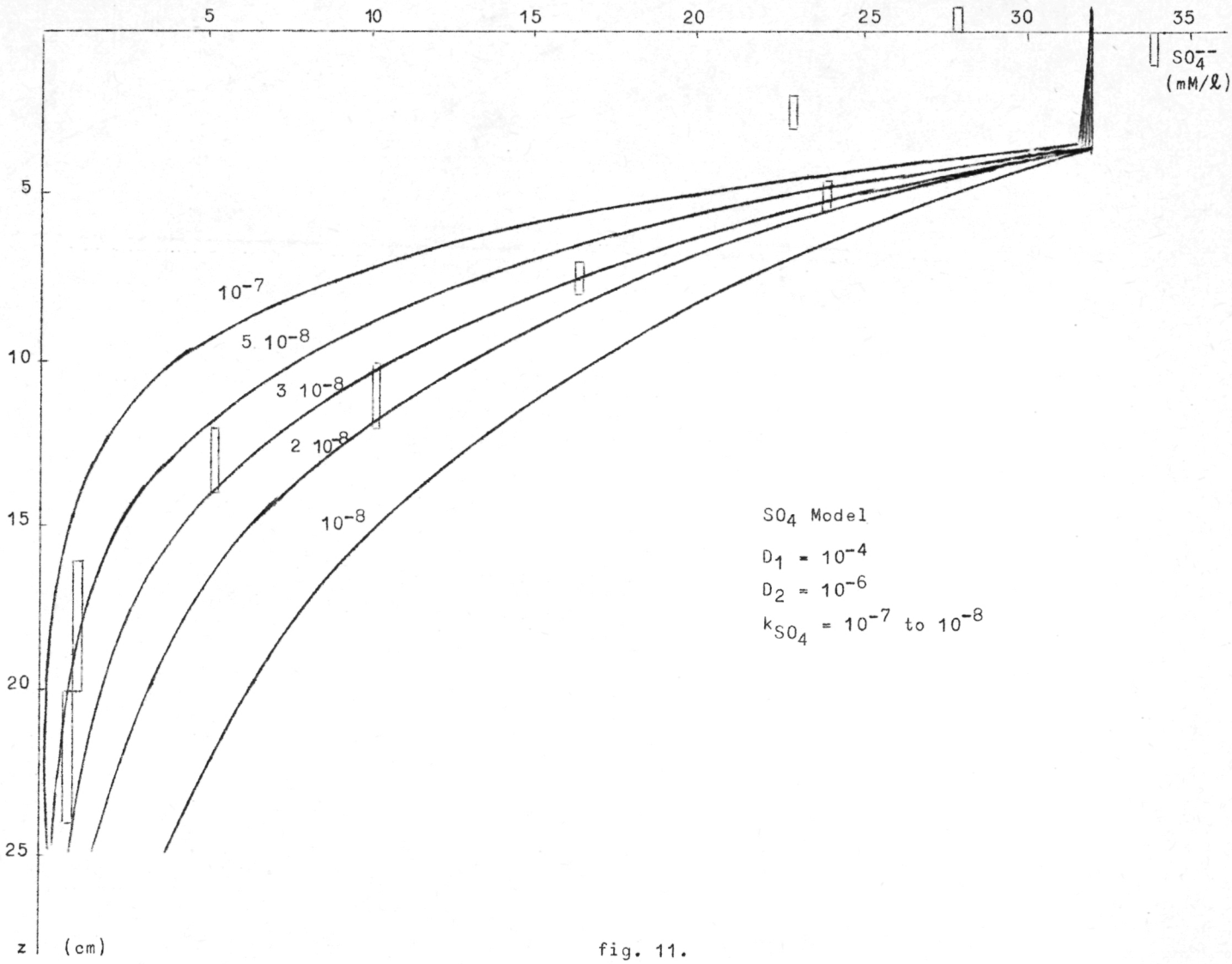


fig. 11.

$k_{O_2} = 5 \times 10^{-6}$ µmoles cm^{-3} s^{-1}

$k'_{O_2} = 1.5 \times 10^{-3}$ s^{-1}

$k_{SO_4} = 2.5 \times 10^{-8}$ s^{-1}

$k_{NO_3} = 1.5 \times 10^{-6}$ µmoles cm^{-3} s^{-1}

$k'_{NO_3} = 5 \times 10^{-6}$ s^{-1}

$k_{NH_4} = 2 \times 10^{-6}$ µmoles cm^{-3} s^{-1}

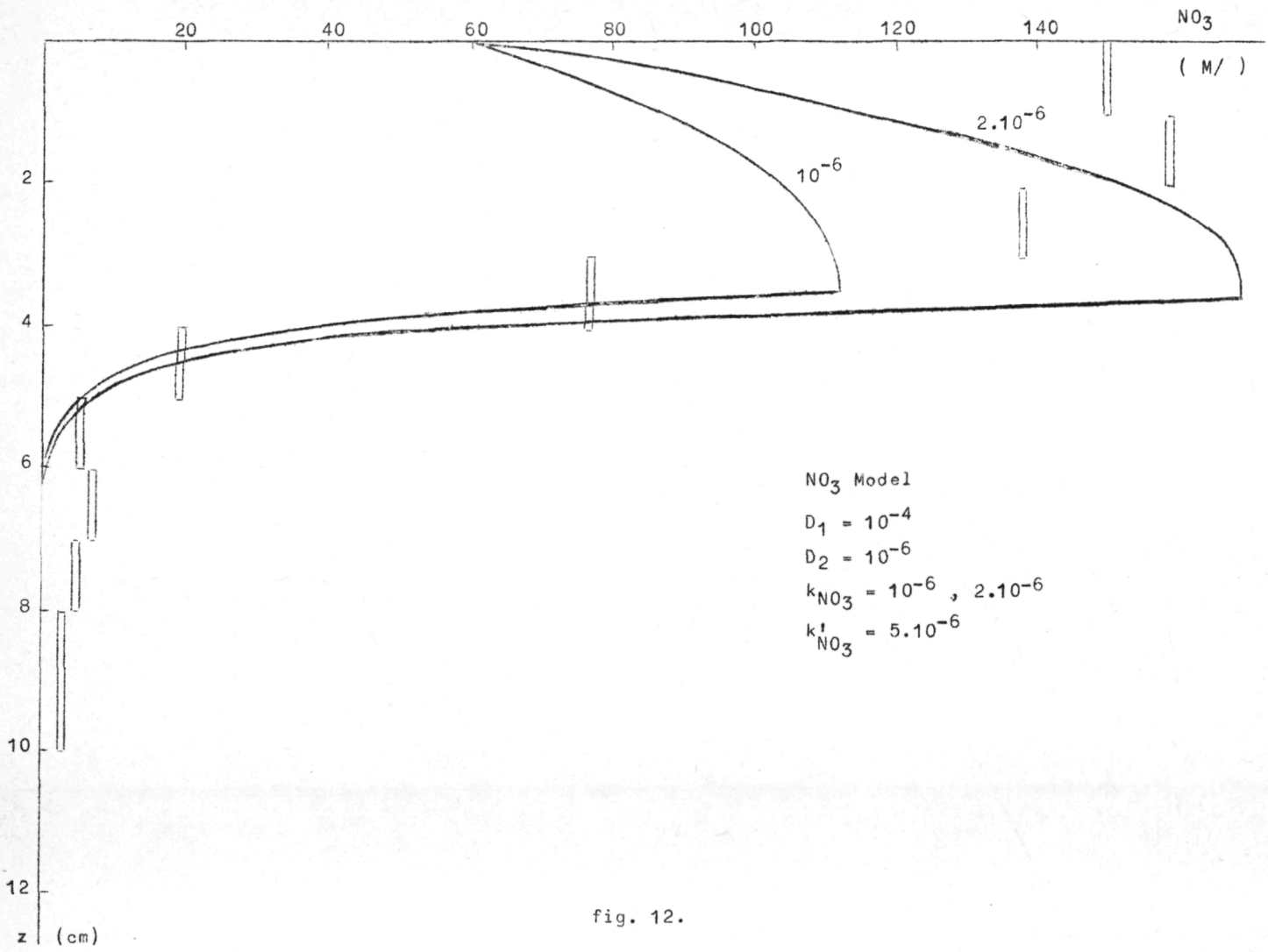


fig. 12.

$\alpha = 0.18$.

All these values appear realistic when compared with direct measurements of microbiological activities in sediments published in the literature [Sorokin (1962), Billen (1975)].

It should be noticed that the value of k_{O_2} is too low by a factor of 3.5 to satisfy relation (6). This is probably due to the fact that other oxidants can be used in the upper layer, [MnO_2 , NO_3^- , $Fe(OH)_3$], and have not been taken into account by the model. If these oxidants are used successively as in the Scheldt estuary [Billen and Smitz (1975)], a multilayer model would be necessary to describe the phenomena. However, experimental results are not yet sufficient to allow such a model to be elaborated.

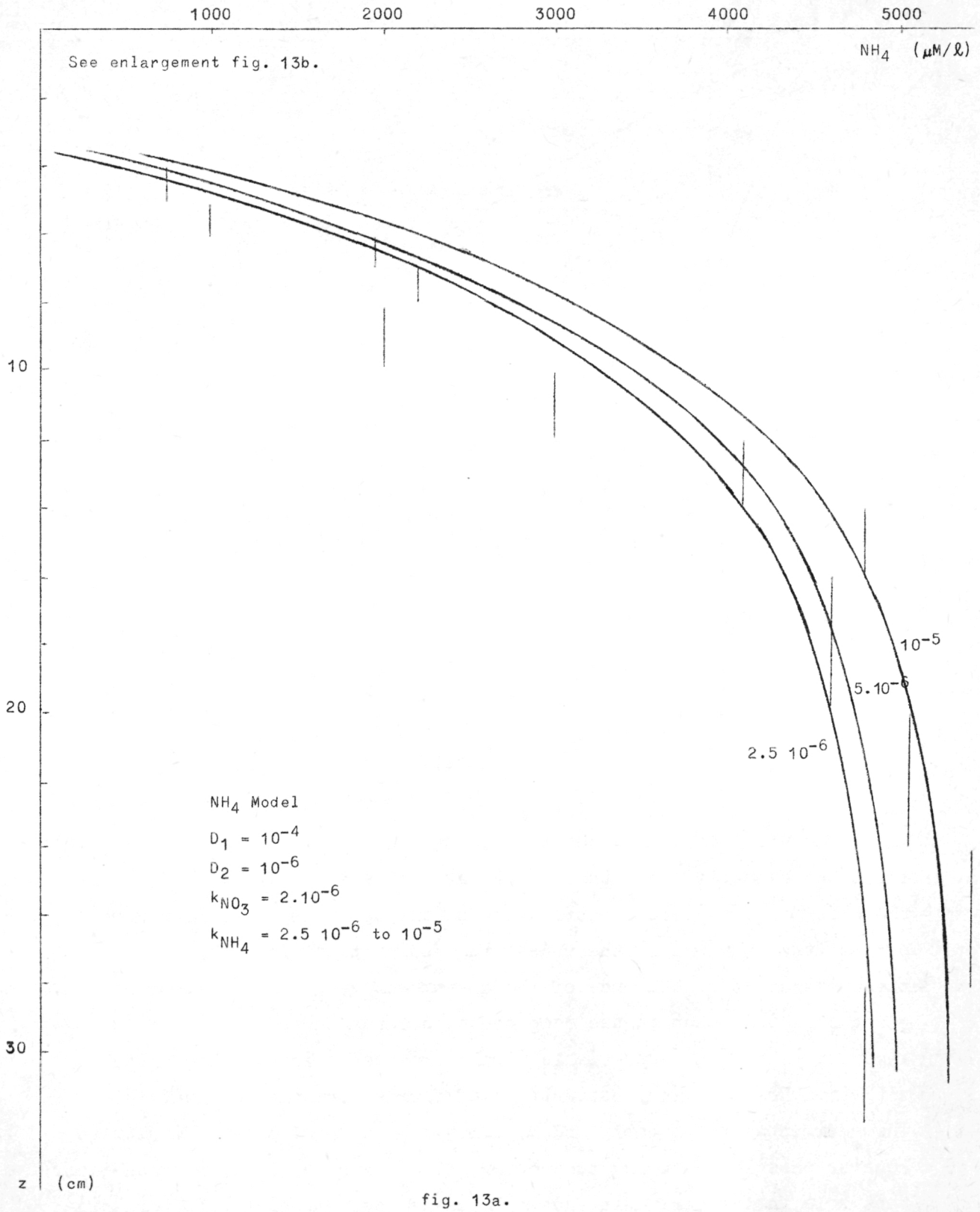

1000
2000
3000
4000
5000
NH4 (µM/ℓ)
See enlargement fig. 13b.
10
20
30
z (cm)
10-5
5.10-6
2.5 10-6
NH4 Model
D1 = 10-4
D2 = 10-6
kNO3 = 2.10-6
kNH4 = 2.5 10-6 to 10-5

fig. 13a.

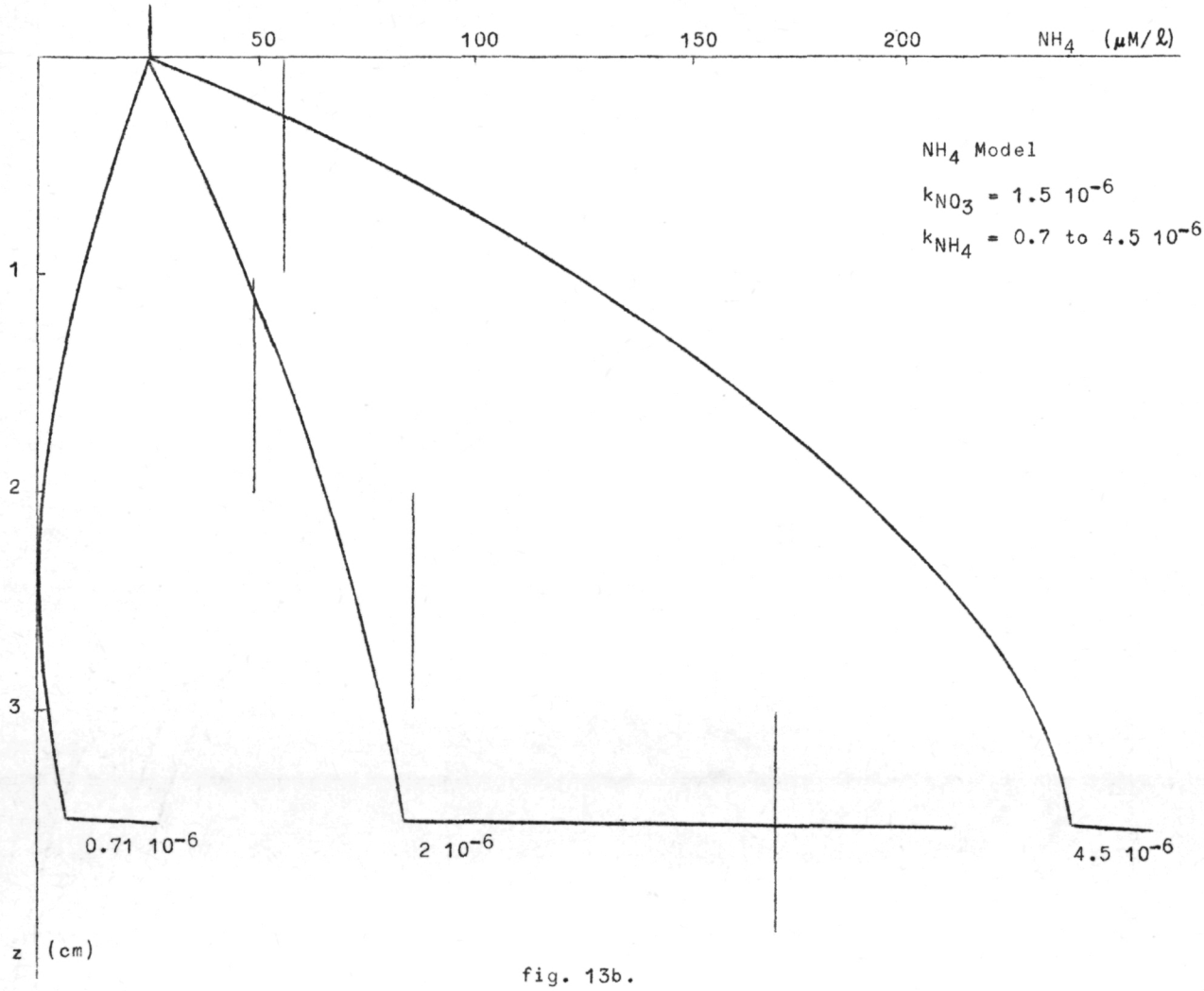


fig. 13b.

The value of the different mass transfers were calculated from the equations of table 1 and the results are represented in fig. 14. As in the case of silica, the contribution of the upper layer is much more important than the one of the underlying sediment. It is probable that the thickness and the influence of the disturbed layer is more important in coastal regions than in the deep ocean, because the existence of this layer is related to appreciable shear stresses or intense biological activity. However, many estimations of fluxes from the pore waters of the sediments are probably underestimated because of the difficulty to recover this layer during the coring. Also, this layer may play an important role in the early diagenetic processes and especially for organic

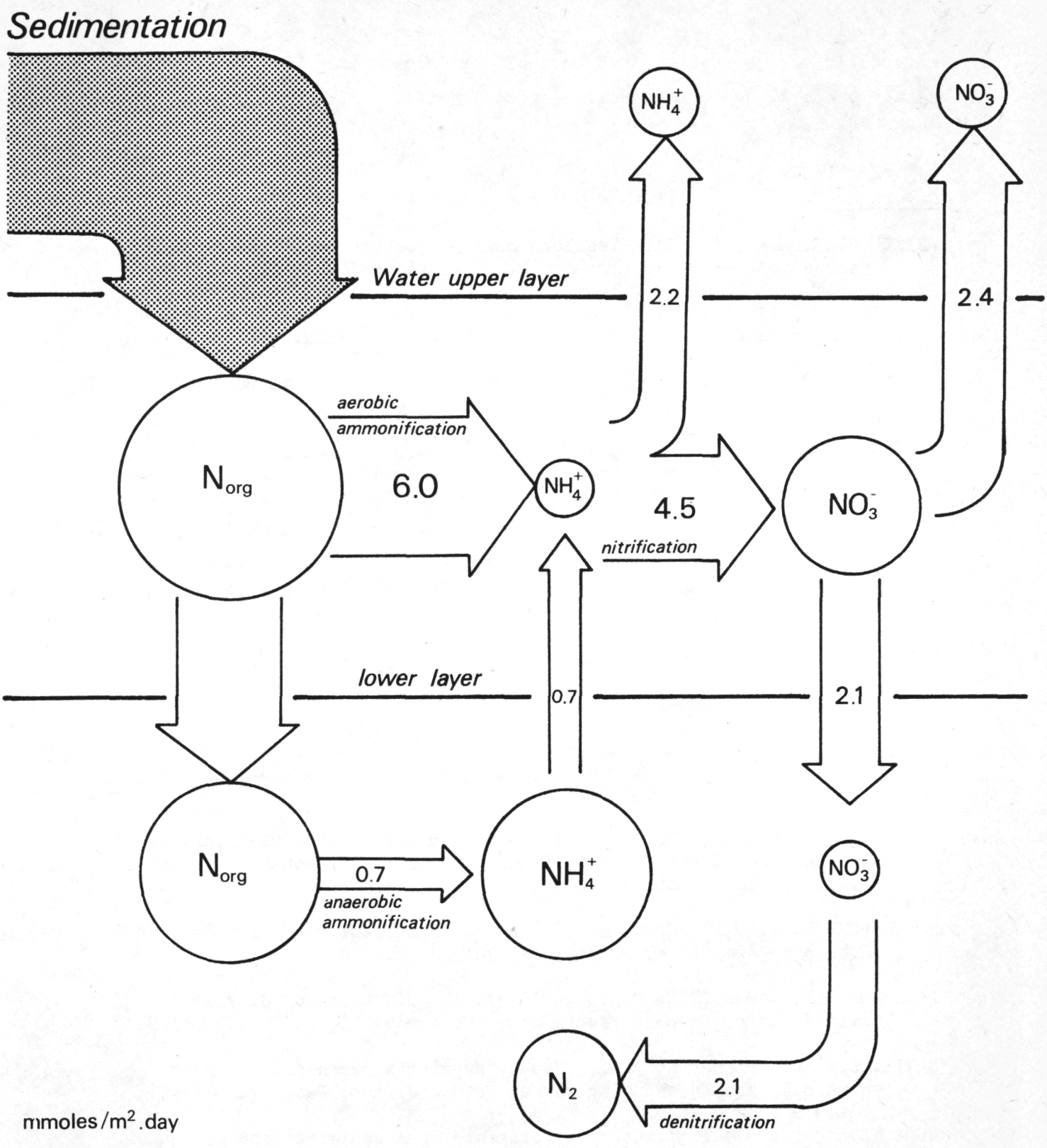

Sedimentation
NH_4^+
NO_3^-
Water upper layer
2.2
2.4
aerobic
ammonification
N_{org}
6.0
NH_4^+
4.5
nitrification
NO_3^-
lower layer
0.7
2.1
N_{org}
0.7
anaerobic
ammonification
NH_4^+
NO_3^-
N_2
2.1
denitrification
mmoles/m^2.day

fig. 14.

matter. It may be assumed that most of the decomposition of the organic matter takes place in this well aerated layer.

References

ANIKOUCHINE, W.A., (1967). Dissolved chemical substances in compacting marine sediments, *J. Geophys. Res.*, *72*, 505-509.

BERNER, R.A., (1964). An idealized model of dissolved sulfate distribution in recent sediments, *Geochim. Cosmochim. Acta*, *28*, 1497-1503.

BERNER, R.A., (1971). *Principles of chemical sedimentology*, McGraw Hill, N.Y., 240 pp.

BERNER, R.A., (1974). *Kinetic model for the early diagenesis of nitrogen, sulfur, phosphorus and silicon in anoxic marine sediments*, in *The Sea*, Vol. 5, *Marine Chemistry*, Ed. E.D. Goldberg, J. Wiley and Son Inc.

BILLEN, G., (1975). Evaluation of nitrifying activity in sediments by dark ^{14}C-bicarbonate incorporation, Submitted for publication to *Water Research*.

BILLEN, G. and SMITZ, J., (1975). *A mathematical model of microbial and chemical oxidation-reduction processes in the Scheldt estuary*, in *Mathematical model, Annual Report, IV*.

CHEN, R.L., KEENEY, D.R., KONRAD, J.C., HOLDING, A.J., GRAETZ, D.A., (1972). Gas production in sediments of Lake Mendota, Wisconsin, *J. Env. Qual.*, *1*, 155-157.

CHAN, Y.K., CAMPBELL, N.E.R., (1973). A rapid gas extraction technique for the quantitative study of denitrification in aquatic systems by N isotope ratio analysis, *Can. J. Microbiol.*, *20*, 275-281.

DE CONINCK, L., (1972). *Etude qualitative et quantitative du benthos*, in *Modèle mathématique, Rapport de synthèse, I.*

FANNING, K.A. and PILSON, M.E.Q., (1973). The diffusion of dissolved silica out of deep-sea sediments, *J. Geophys. Res.*, *79*, 1293-1297.

GRILL, E.V. and RICHARDS, F.A., (1964). Nutrients regeneration from phytoplancton decomposing in sea water, *J. Mar. Res.*, *22*, 51-69.

HURD, D.C., (1973). Interaction of biogenic opal sediments and sea water in the central equatorial Pacific, *Geochim. Cosmochim. Acta*, *37*, 2257-2282.

MacCAVE, I.N., (1973). *Mud in the North Sea*, in *North Sea Science*, Ed. Goldberg, MIT Press, Cambridge, USA, 75-100.

SOROKIN, Y.I., (1962). Experimental investigation of bacterial sulfate reduction in the Black Sea using ^{35}S, *Mikrobiol., 31*, 402-410.

VANDERBORGHT, J.P. and BILLEN, G., (1975). Vertical distribution of nitrate concentration in interstitial water of marine sediments with nitrification and denitrification, *Limnol. Oceanogr.*, in press.

WHEATLAND, A.B., BARRETT, M.S. and BRUCE, A.M., (1959). Some observations on denitrification in rivers and estuaries, *J. Inst. Sew. Purif. 1959*, Pt 2, 149-159.

WOLLAST, R., (1974). *The silica problem*, in *The Sea*, Vol. 5, *Marine Chemistry*, Ed. Goldberg, Wiley, N.Y., 359-392.

IV

Sorption by some North Sea sediments

by

A. BASTIN and M. MEEUSSEN

(Laboratory of Marine Geology and Recent Sediments, Institut Royal des Sciences Naturelles de Belgique)

The sorption properties of about seventy soil samples of the thousand points system were investigated up to now by means of four radioisotopes, namely Cs^{137}, (Cs^{134}), Co^{60}, Mn^{54} and Cd^{109}. Similar tests with Zn^{65} are now being conducted actively. The methods and measuring systems used have been described in previous reports. Special attention was devoted to non-sandy samples which explains why most of the samples investigated derive from the South of the survey network and toward to coast. Figure 1 shows the specimens examined and their place within the thousand points system. About thirty new samples are being investigated in order to obtain a better spread over the entire area under survey. To note that further toward the sea, the samples become increasingly sandy and the values for capacities and coefficients of distribution decrease significantly. As already premised in previous reports, the sediments rich in clay and silt are actually the only ones featuring high values for sorption. However, the contribution of sandy samples to sorption may not be neglected considering that these soils cover much larger surfaces.

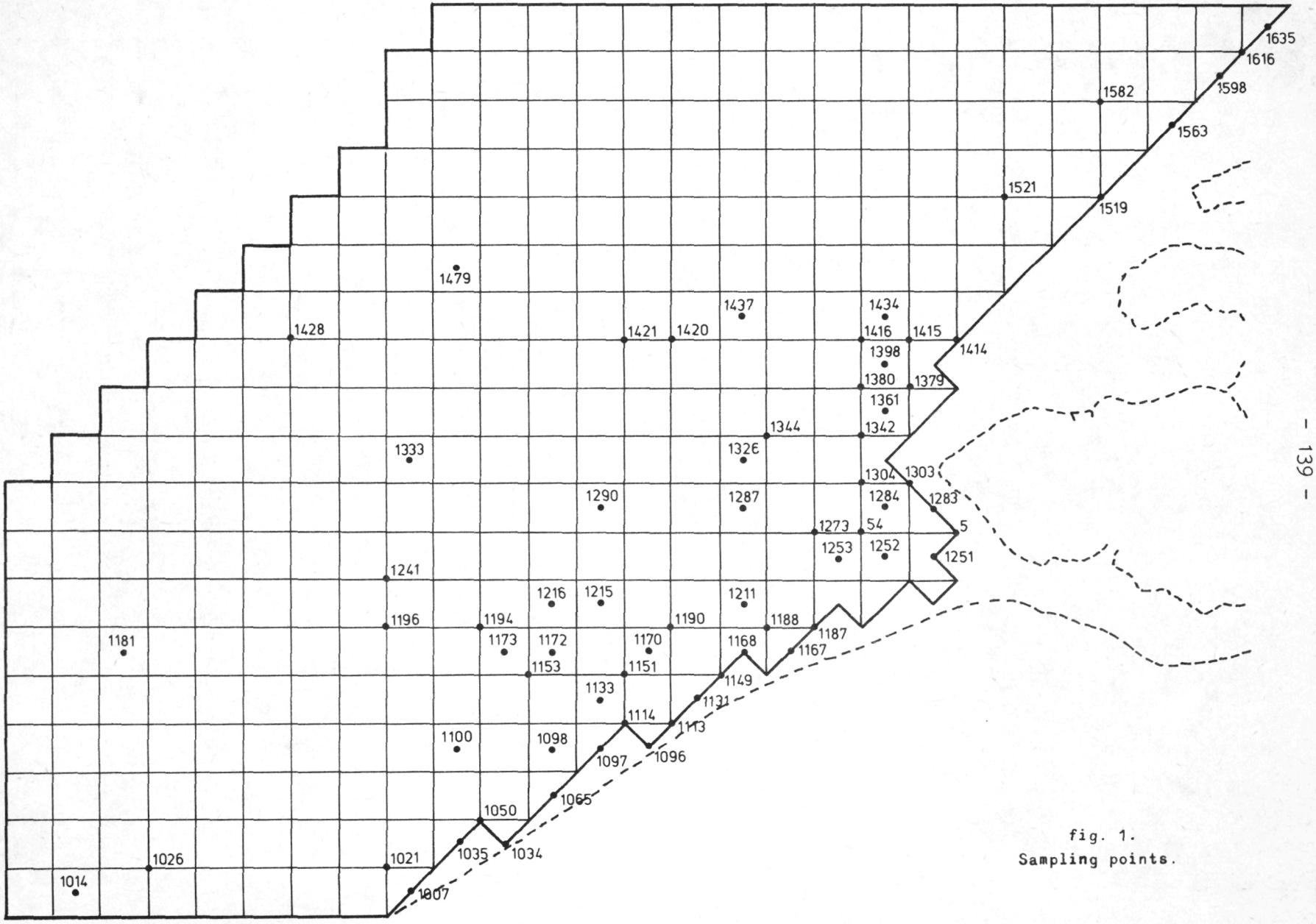


fig. 1.
Sampling points.

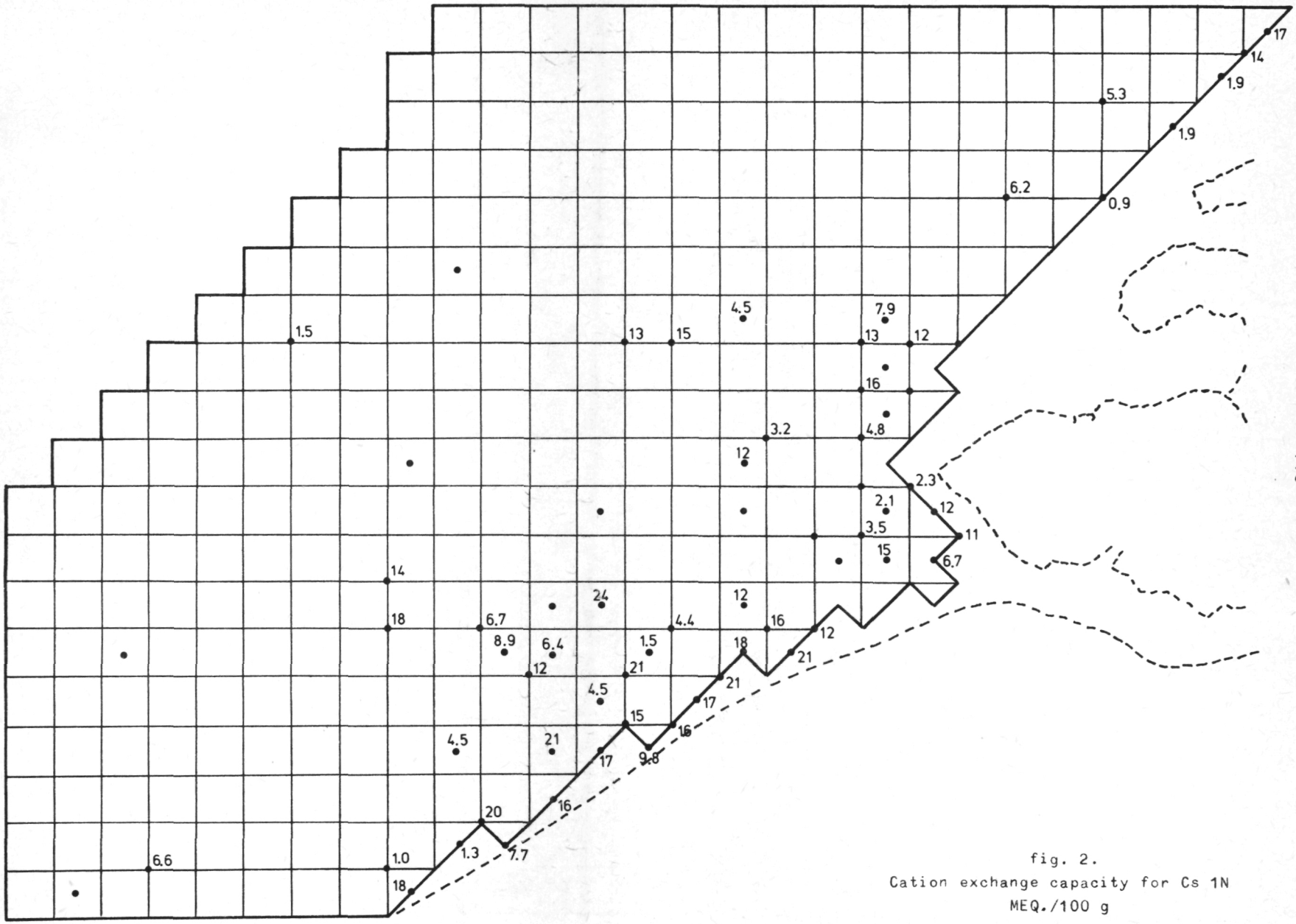


fig. 2.
Cation exchange capacity for Cs 1N
MEQ./100 g

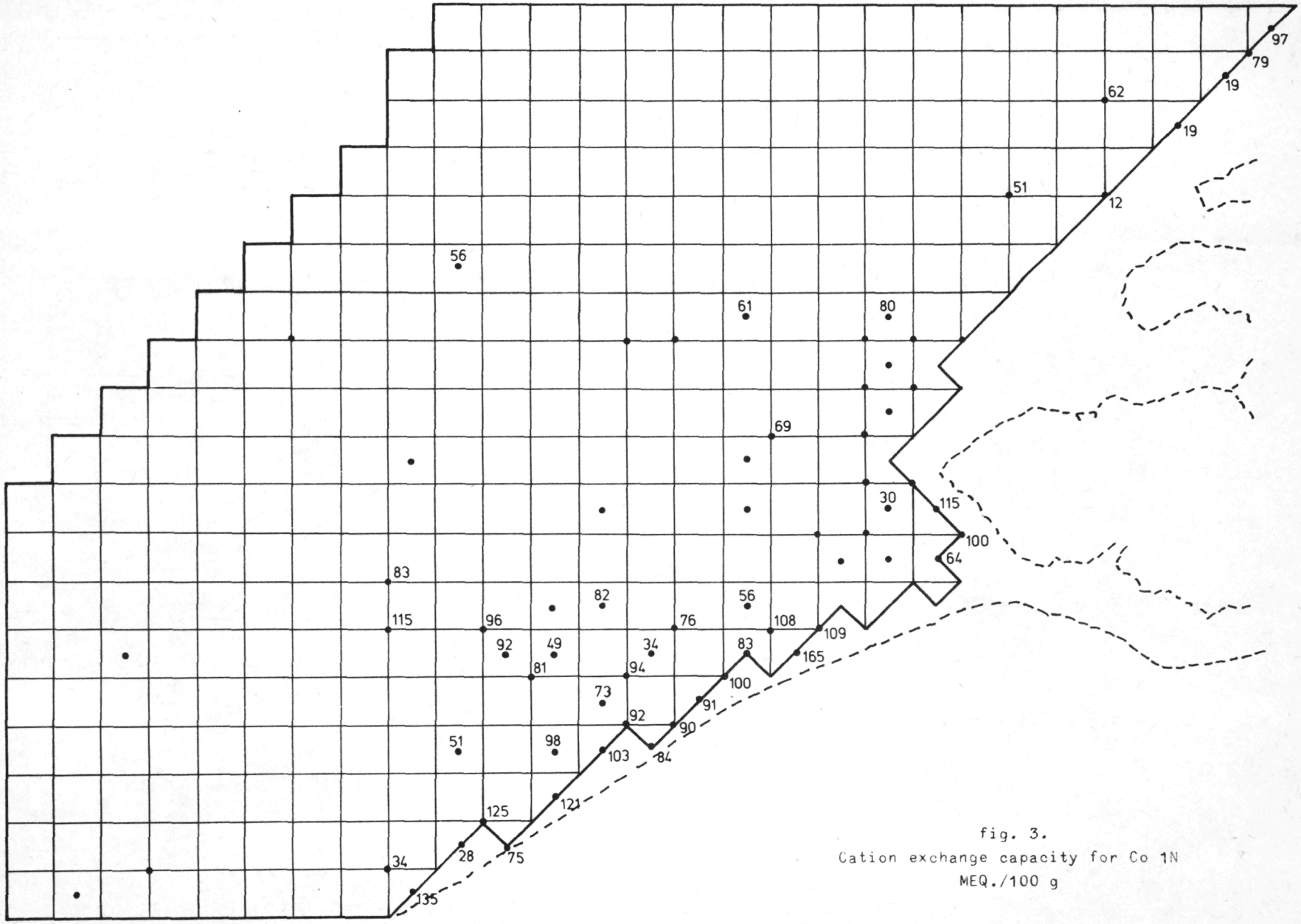


fig. 3.
Cation exchange capacity for Co 1N
MEQ./100 g

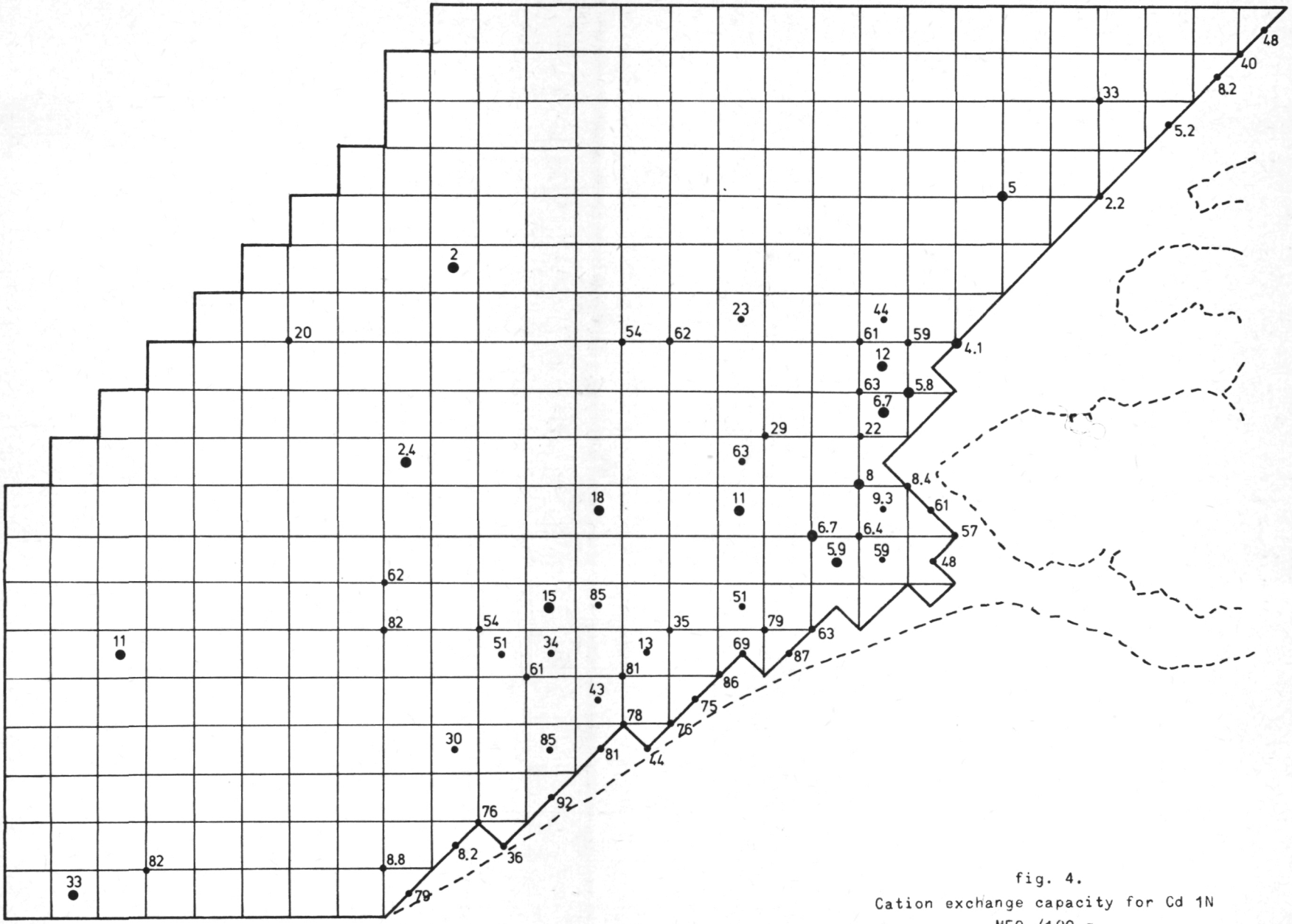


fig. 4.
Cation exchange capacity for Cd 1N
MEQ./100 g

Figures 2, 3 and 4 show the capacity Q of the specimens with respect to the various elements. The capacity of most specimens has been determined by means of the fraction < 150 μ . For some sand-containing specimens we were forced to apply fraction < 300 μ because, otherwise, we would have had no material left. These latter mostly present much lower capacity values.

A comparison of the capacity between the various elements has taught us that we may classify the elements in the following order of decreasing capacity with respect to soil specimens :

$$Mn \gg Co > Cd \gg Cs \ .$$

There is a definite difference between monovalent and bivalent radio-isotopes where their capacities are concerned. While with Cs , Co and Cd the capacities of sandy samples are small (< 0.1 meq/g) , they remain for all samples with Mn > 0.6 meq/g . This shows that with Mn there is surely another phenomenon than the exchange of ions. With Co we determine the largest relative dispersion of the capacity values and with Cs we find the smallest differences.

These capacity values do not offer an accurate picture of what may actually take place on the ocean bottom. They only offer the possibility to fix specific elements under extreme conditions (1 N solution!) from the sediment.

Figures 5, 6, 7 and 8 show distribution constants K_d . The following indications have been used : (∘) fraction < 150 μ and (o) fraction < 300 μ of the specimen.

These distribution constants offer a truer picture of what may occur in seawater upon contact with sediments. They have been determined in seawater and with respect to the element in tracer quantities. They show the distribution of the element concerned between the solid and the fluid phase.

The coefficients of distribution determined in sea-water show the following picture for the various radio-isotopes :

$$Co \geq Cs \gg Cd \geq Mn \ .$$

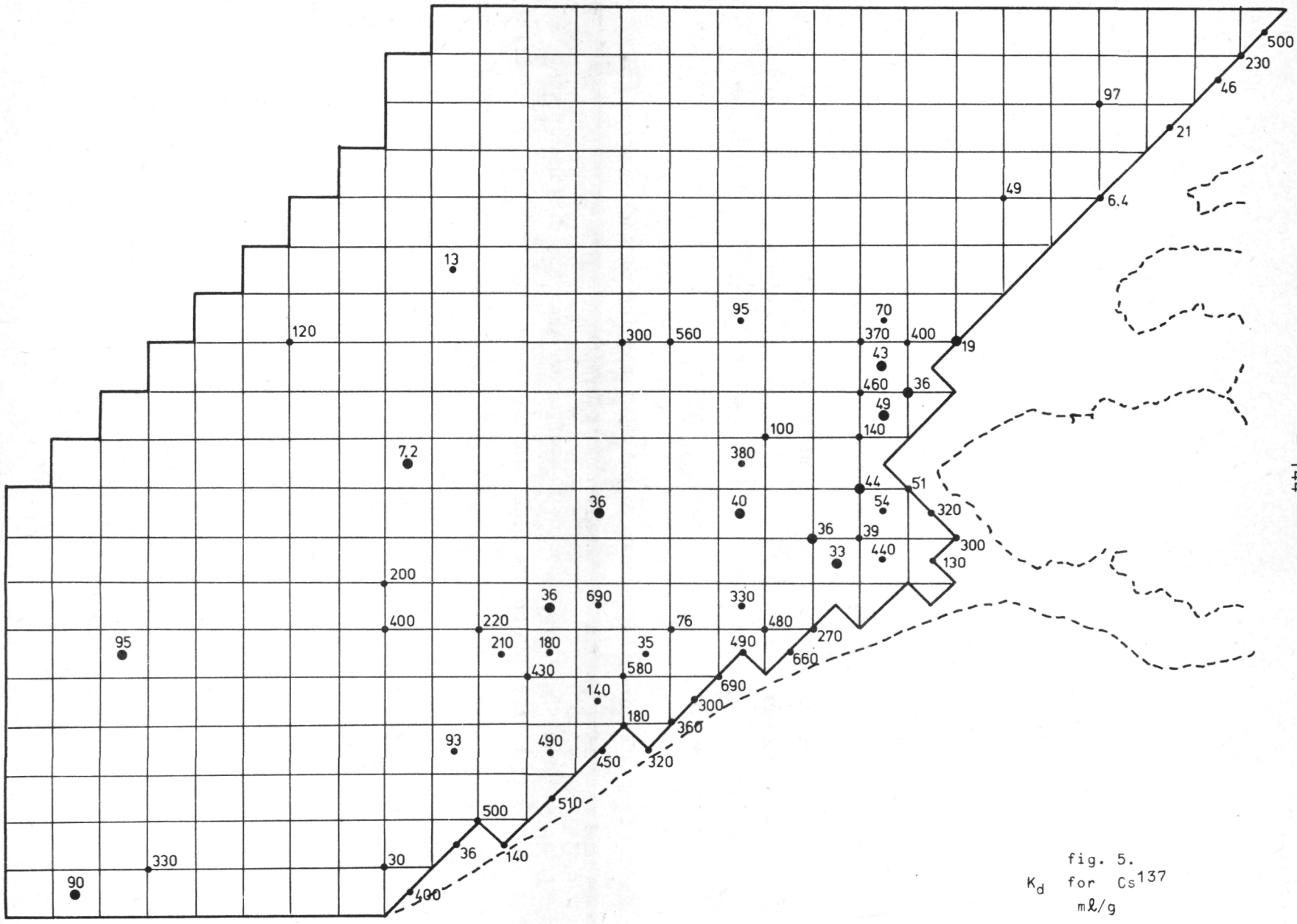


fig. 5.
K_d for Cs^{137}
mℓ/g

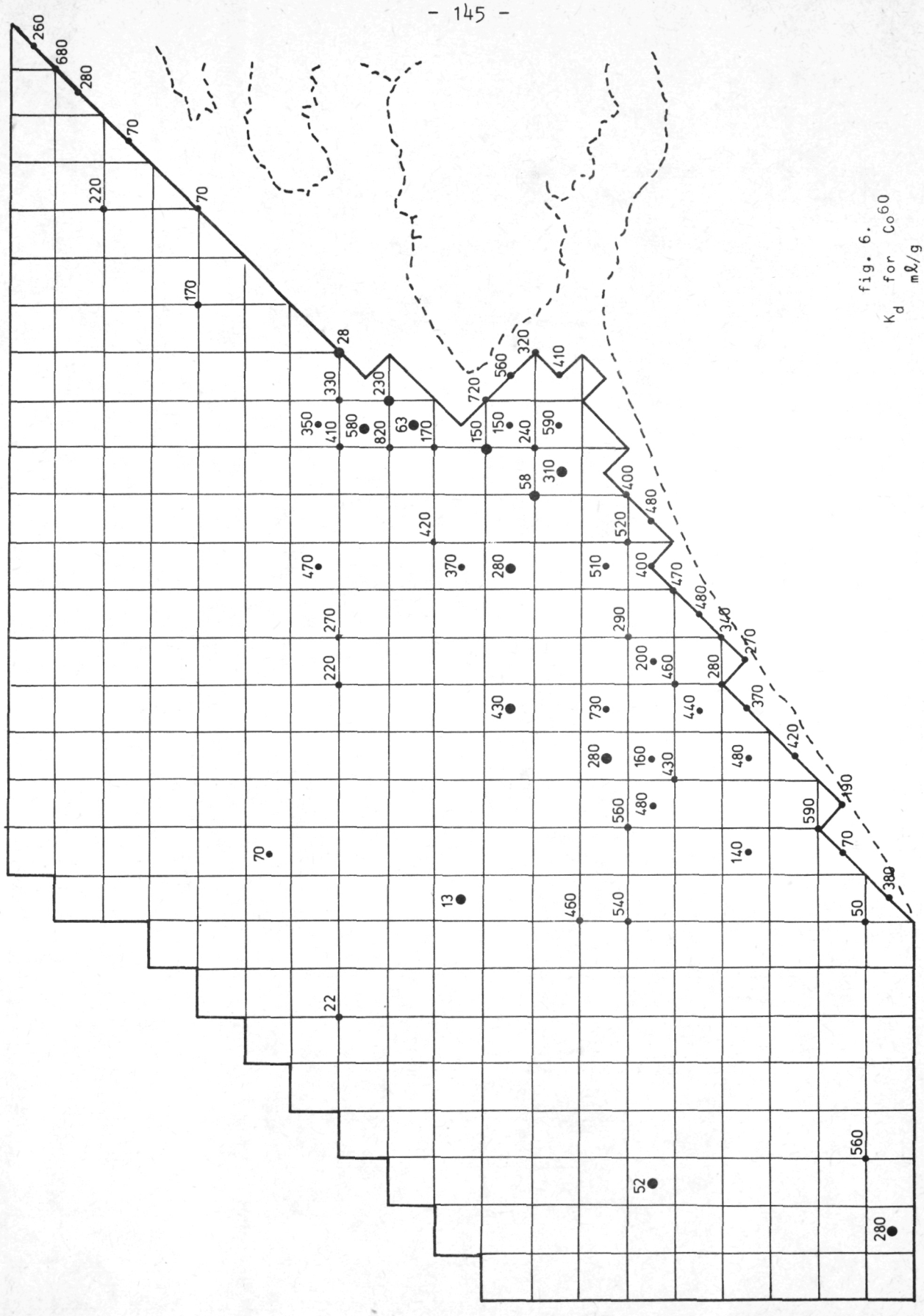


fig. 6.
K_d for Co^{60}
ml/g

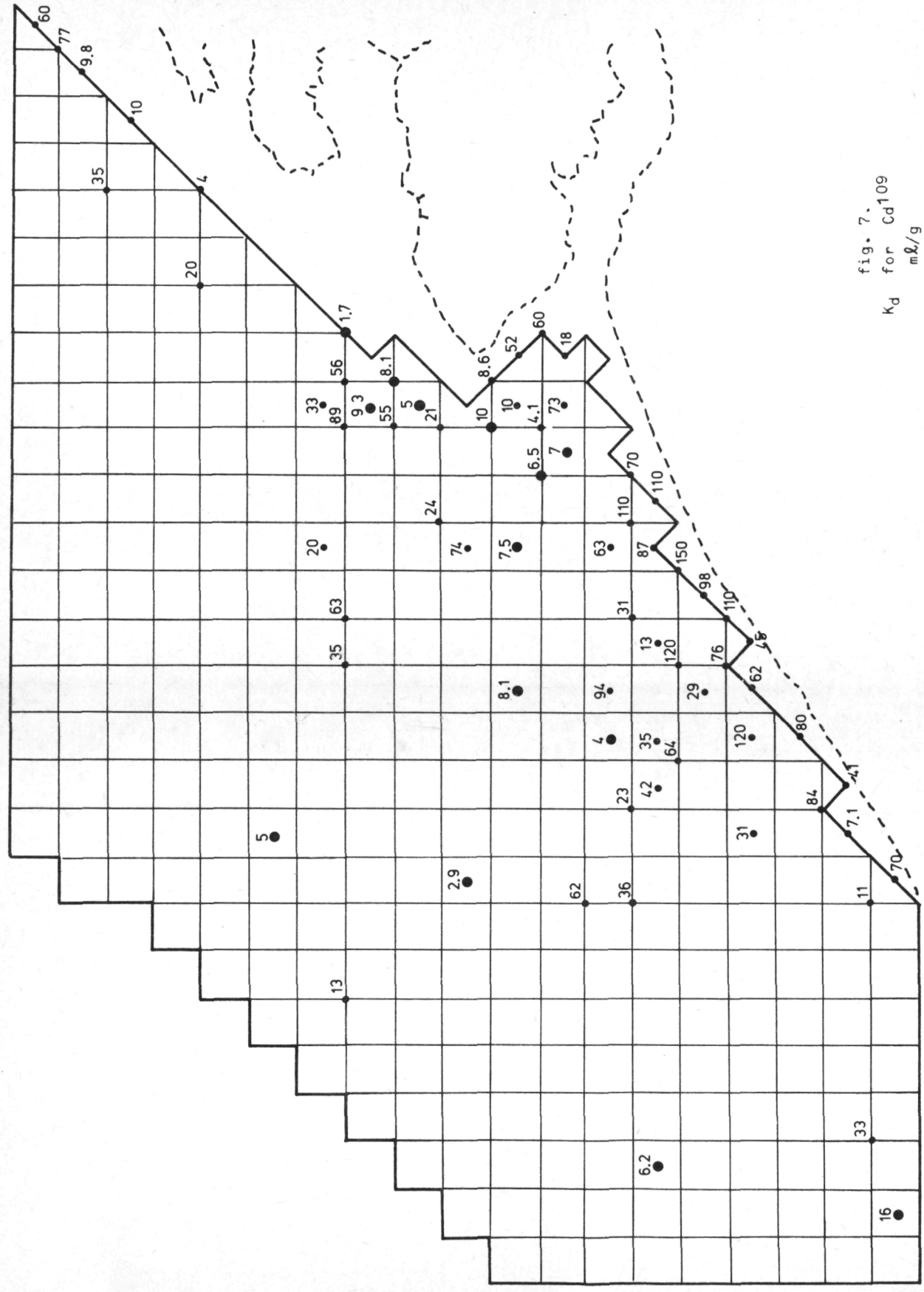


fig. 7.
K_d for Cd^{109}
mℓ/g

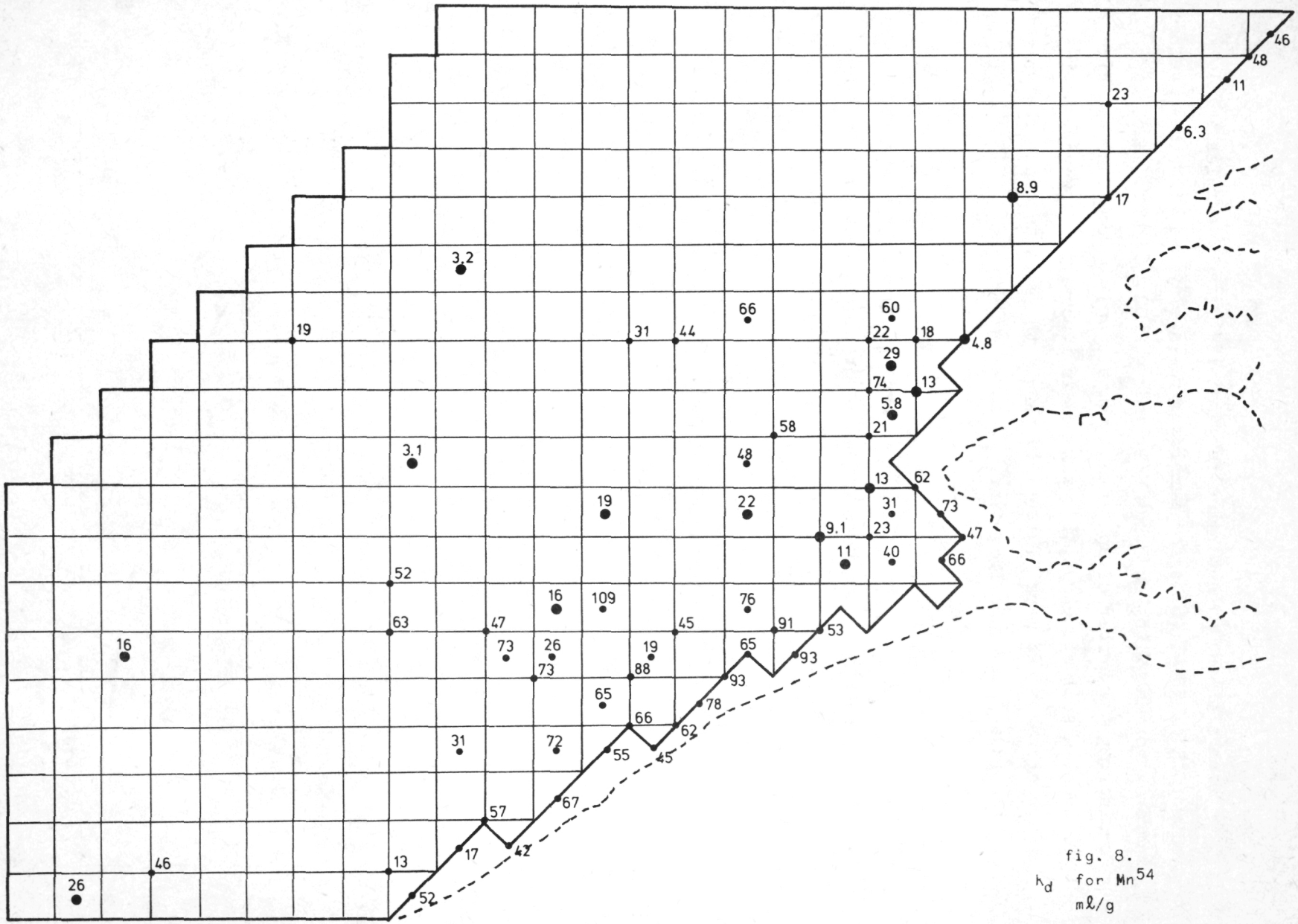


fig. 8.
k_d for Mn^{54}
mℓ/g

With all ions we determine for definitely sandy samples small K_d values ($K_d < 50$), while for samples rich in clay and silt these values increase to 100 with Mn and Cd, and to 600 with Co and Cs. Considering the number of specimens examined and the considerable differences in soil structure, it will remain impossible, however, to indicate areas on the maps. This explains why the maps show but the value determined at that specific point.

When we compare the values measured with regard to capacity and K_d for one and the same ion, we note a certain connection determined

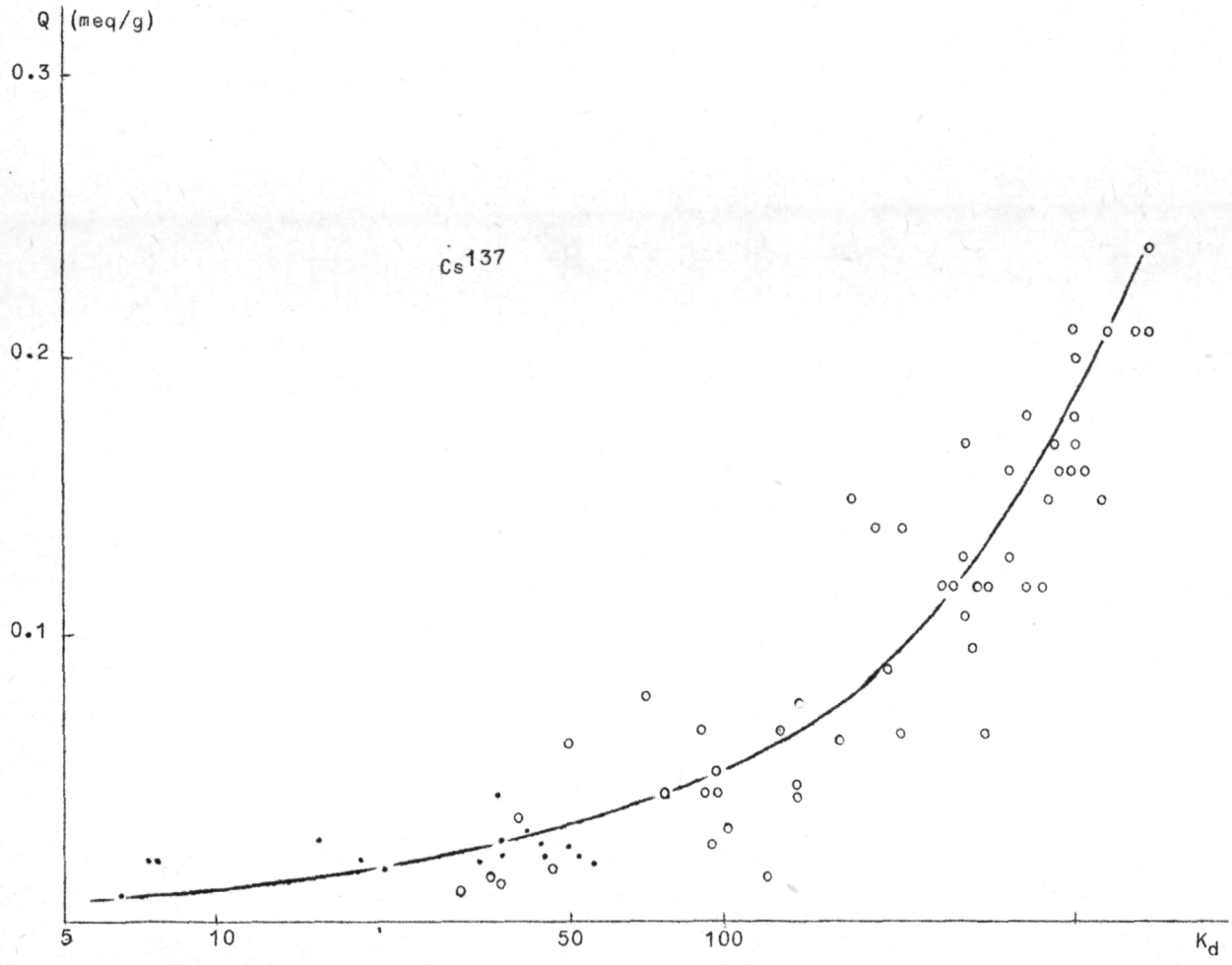


fig. 9.

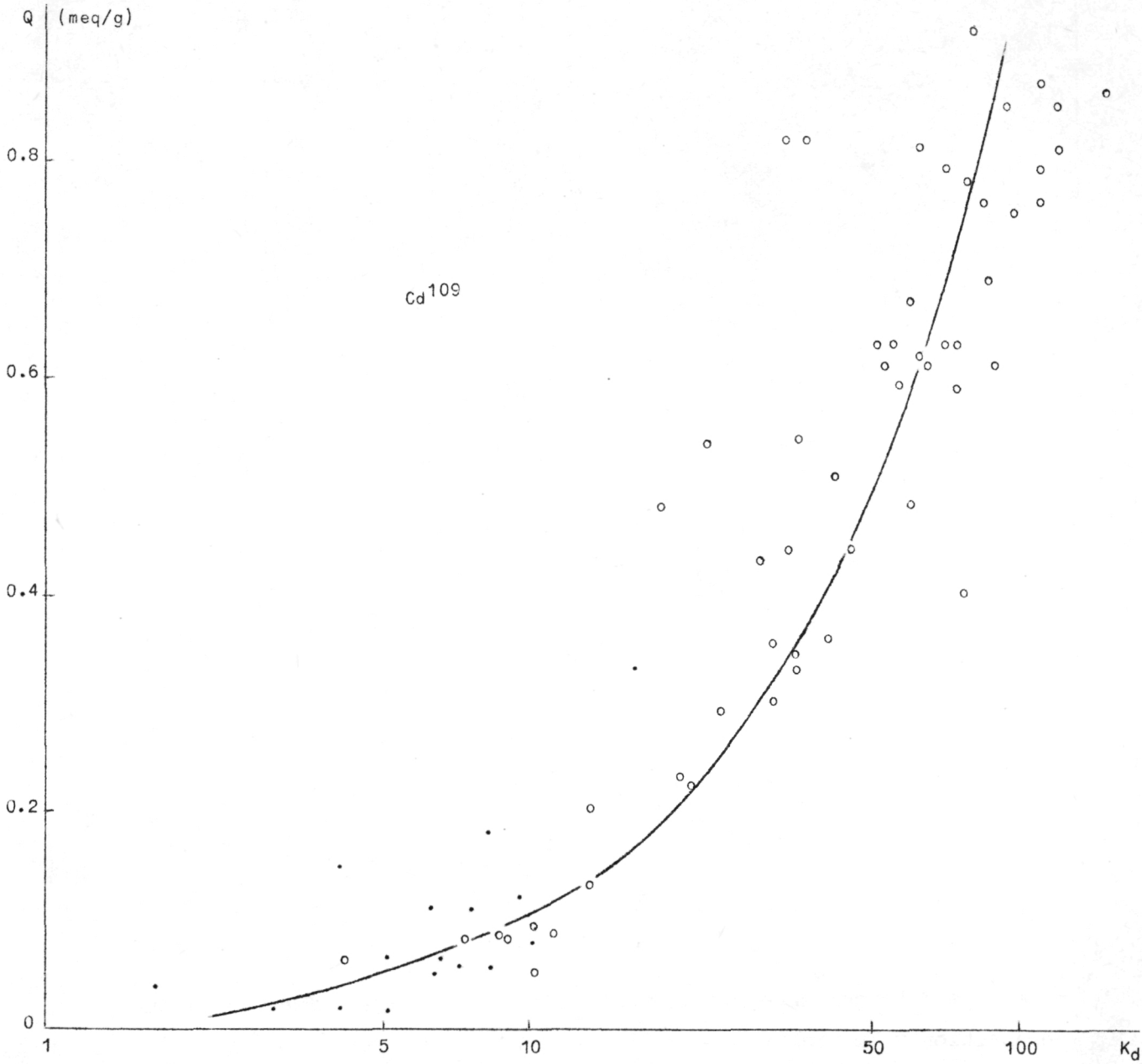


fig. 10.

between both quantities only with Cs and Cd (fig. 9, 10). With Co and Mn there actually seems to be no connection (fig. 11, 12). Investigations conducted by Duursma (1973) on soil samples from all over the

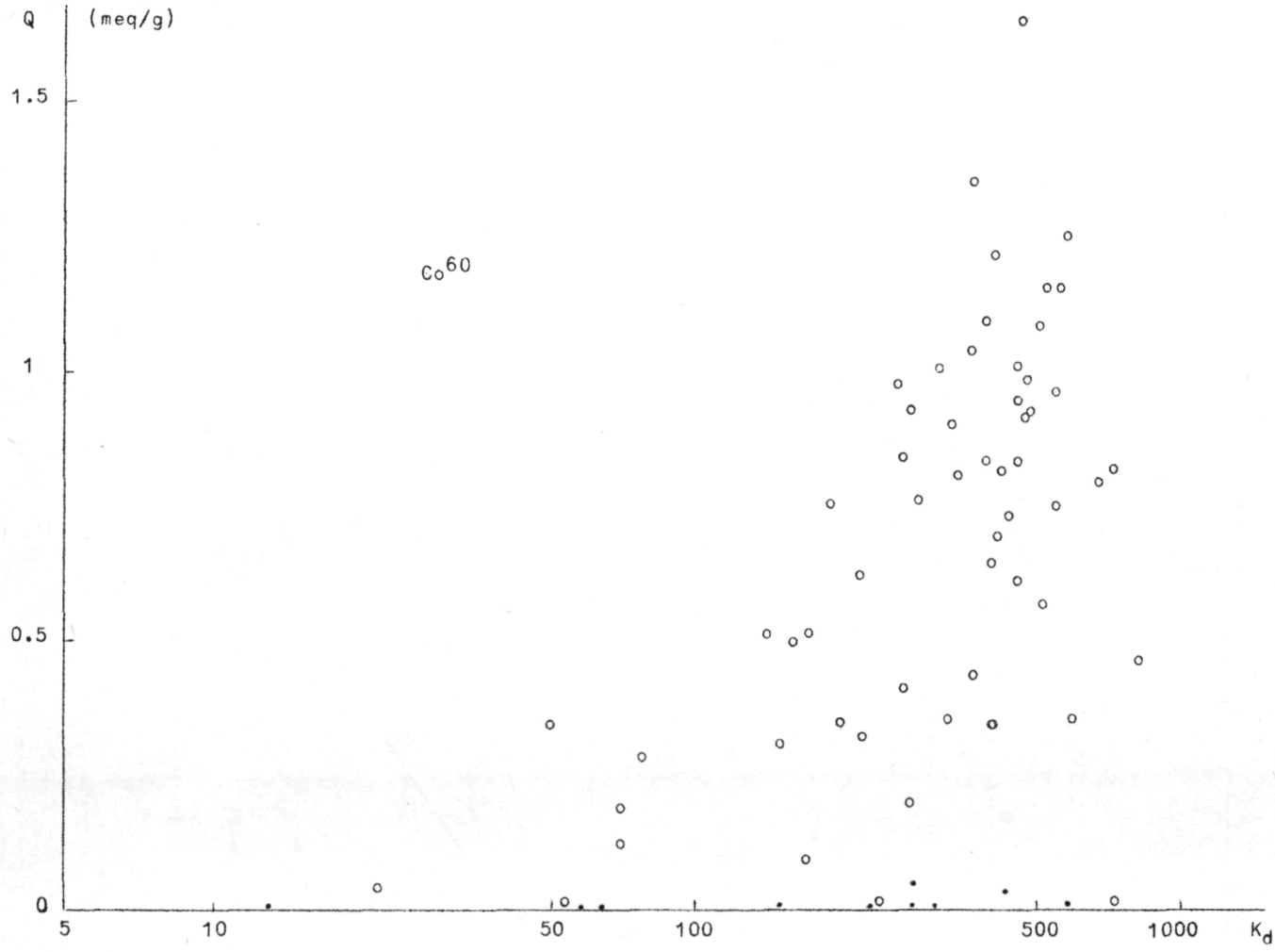


fig. 11.

world lead to the same result where Cs is concerned. They determine a connection with Zn too.

Our determinations with Zn^{65} are still being conducted but already they point in this direction too. He did not investigate Cd^{109}. We also find a certain correlation to exist between the capacity and the K_d determined with Cd and Cs for one and the same sample. Duursma, too, determines no connection between K_d and Q with Co and Mn. For this reason and based on sorption reaction speed determinations he concludes that there can be an exchange of ions only with Cs

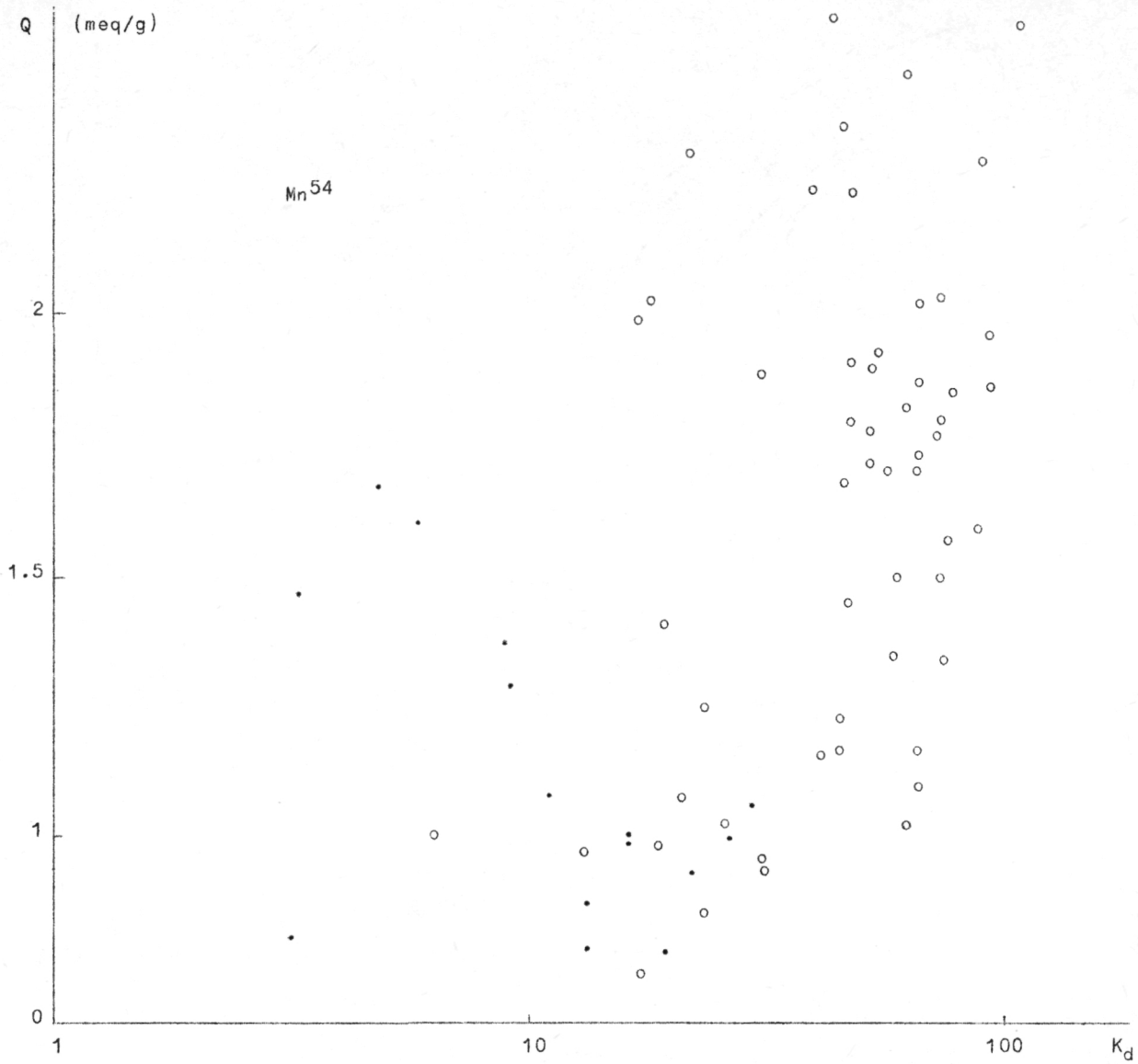


fig. 12.

and Zn while different mechanisms play a more important part for the other radio-isotopes (precipitation, isotopic exchange, complex formation, ...). The speed of the sorption reaction which supplies an indication for the sorption mechanism will be further investigated in order to check the possibilities proposed by Duursma.

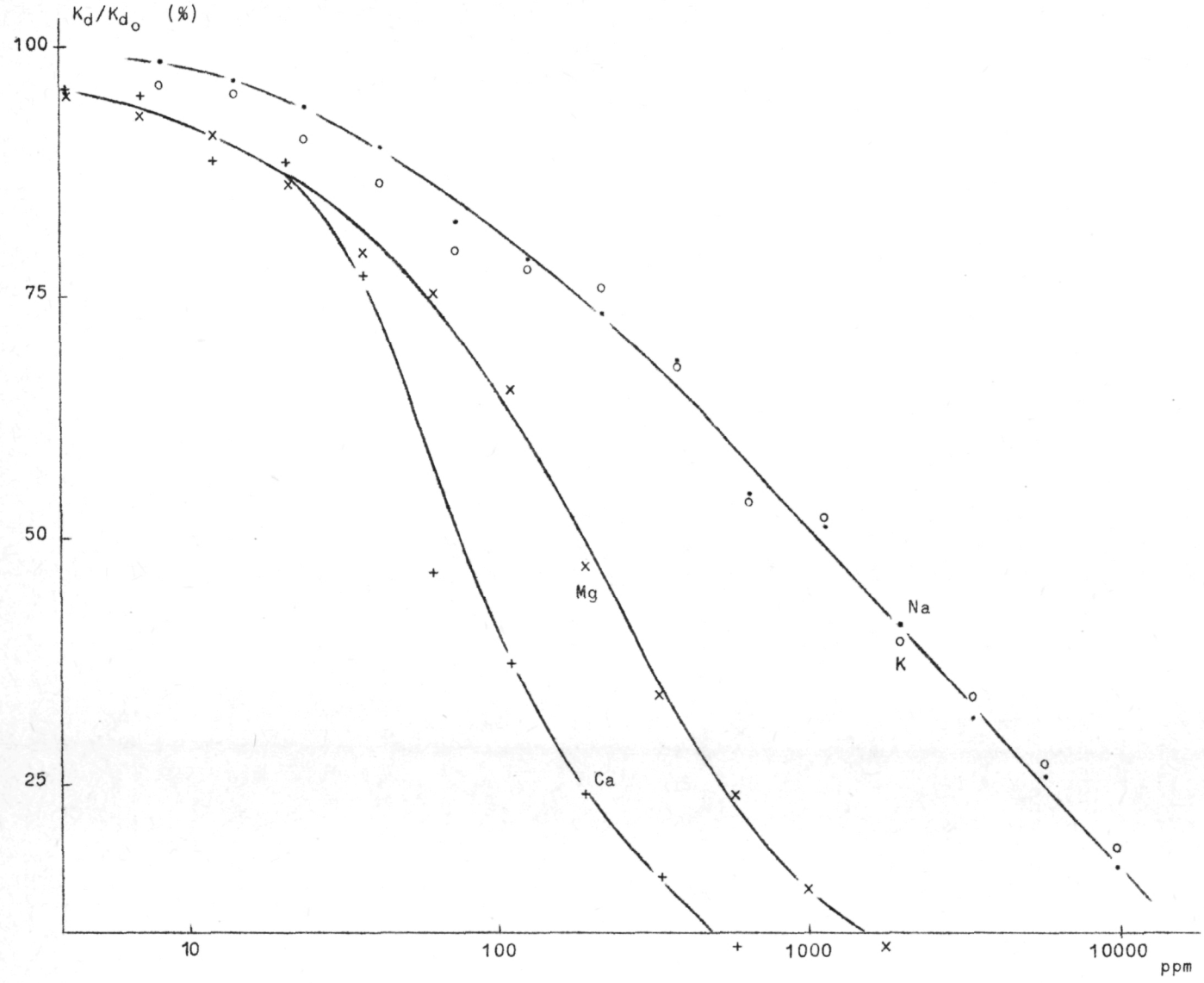


fig. 13.
Cd^{109} Sorption versus competing cation concentration.

The influence of other ions (Na , K , Ca and Mg) on the sorption of Cd , Co and Mn was investigated. While with Cs (*cf.* 1973/Sed.-Synthesis 01) it was mostly Na and K that caused a significant decrease of K_d whereas Ca and Mg had lesser influence, conditions are different where bivalent radio-isotopes are concerned. With Cd^{109} the differences between monovalent and bivalent ions are much less pronounced. Ca and Mg have a greater influence here as

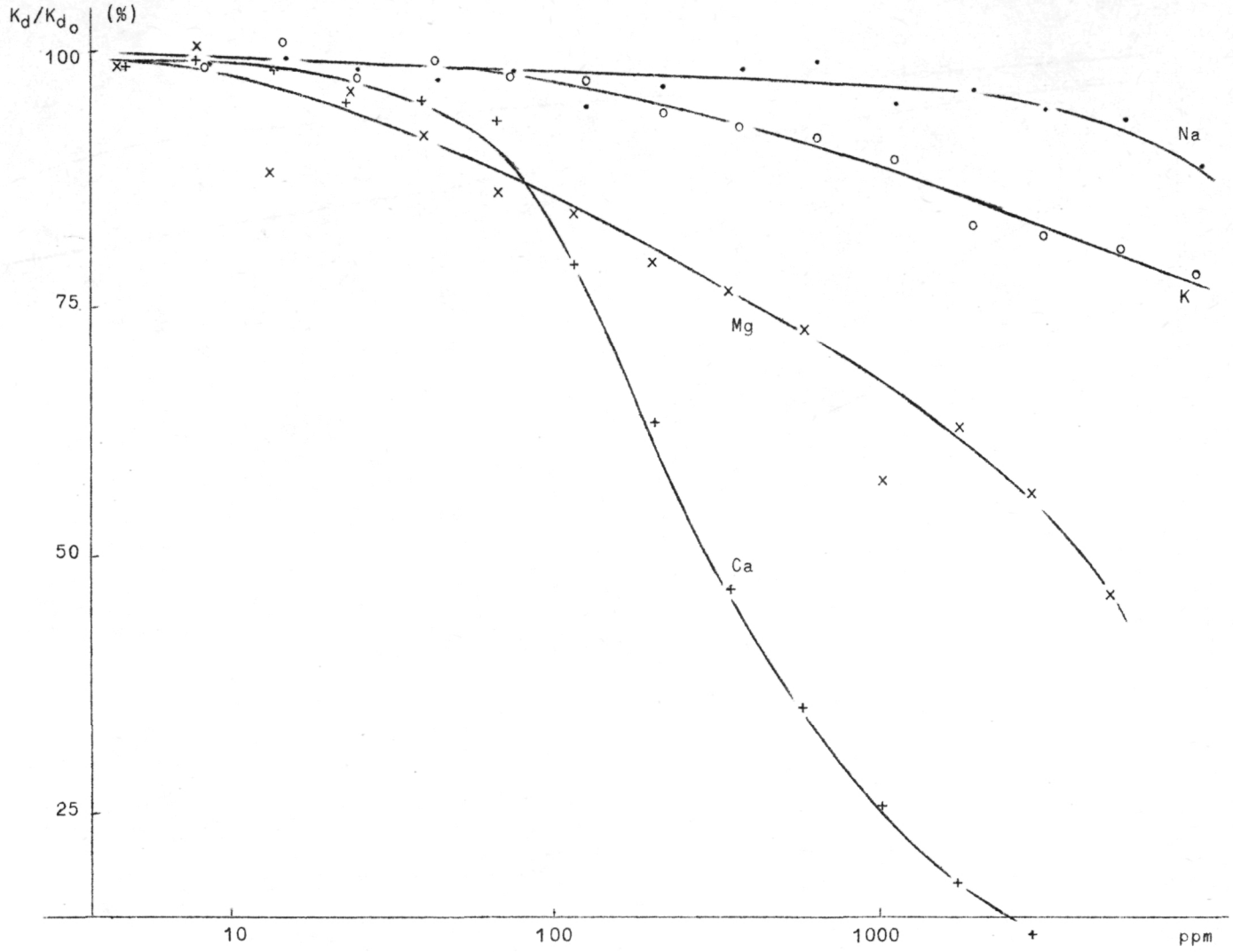


fig. 14.
Co^{60} Sorption versus competing cation concentration.

compared to Na and K . We have the same picture again with the sorption of Mn^{54} and Co^{60} where the influence of Na and K is considerably decreased (fig. 13, 14, 15).

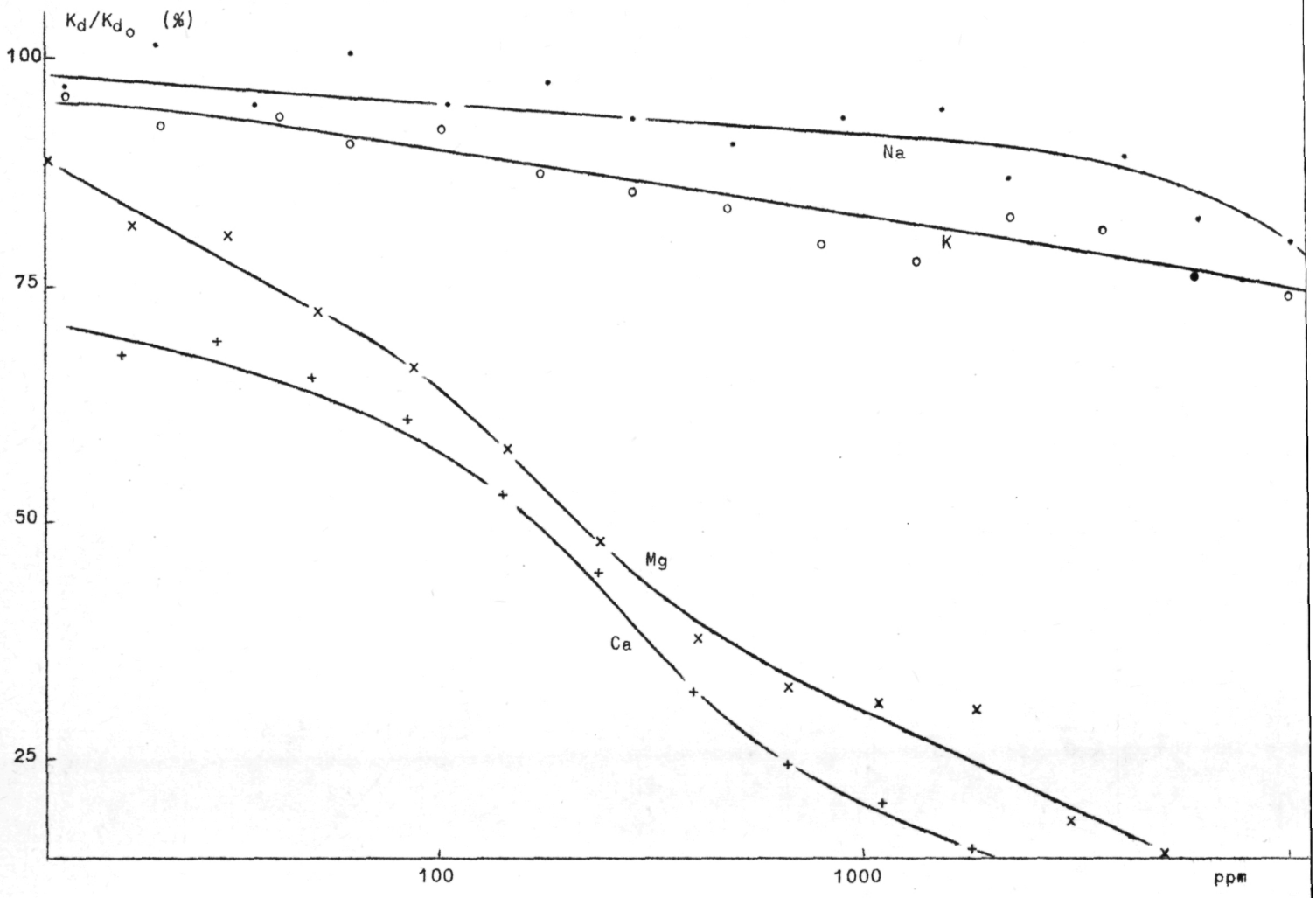


fig. 15.
Mn^{54} sorption versus competing cation concentration.

In order to bridge the gap existing between capacities determined by 1N solution and distribution constants determined by tracer quantities, we determined in seawater the K_d for five specimens with an increasing concentration of the same ion. With Mn^{54}, Co^{60} and Cd^{109} this influence is much smaller than with Cs^{137} which also points to other reaction mechanism than a pure exchange of ions (fig. 16, 17, 18, 19).

There will be further investigation to determine a possible connection with the granulometric data of the soil samples as collected by

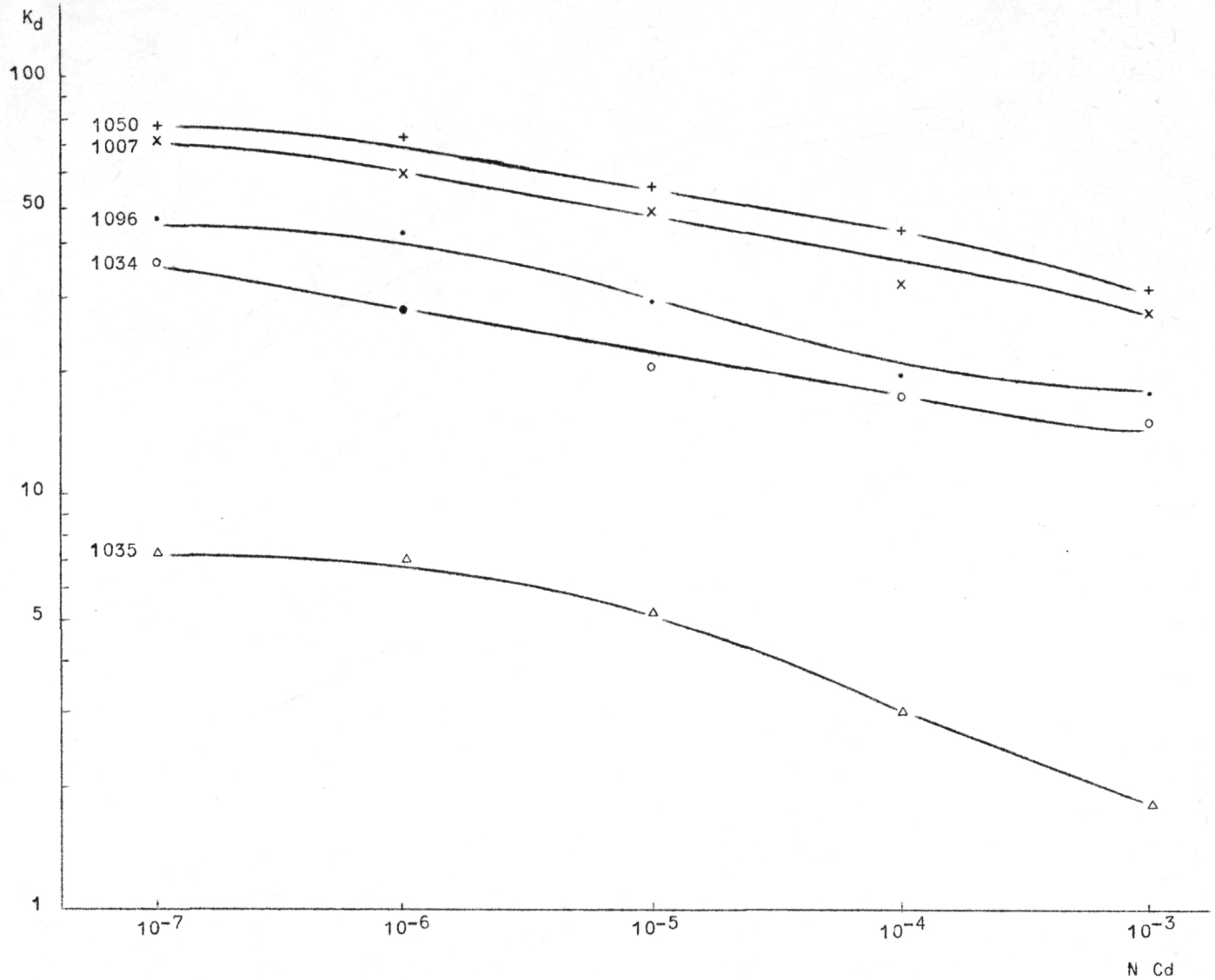


fig. 16.
Cd^{109} sorption versus Cd concentration.

Prof. Gullentops' research team. The average diameter as well as the quantity of clay and silt in the samples appear to be the most appropriate parameters for this purpose. Other investigations will determine possible influence by the lime contents and by the organic material.

The tests proposed and worked out by Duursma for the purpose of determining the cleaning effect produced by suspensions on the radioactive solutions and the pertaining values of Kd will also be conducted

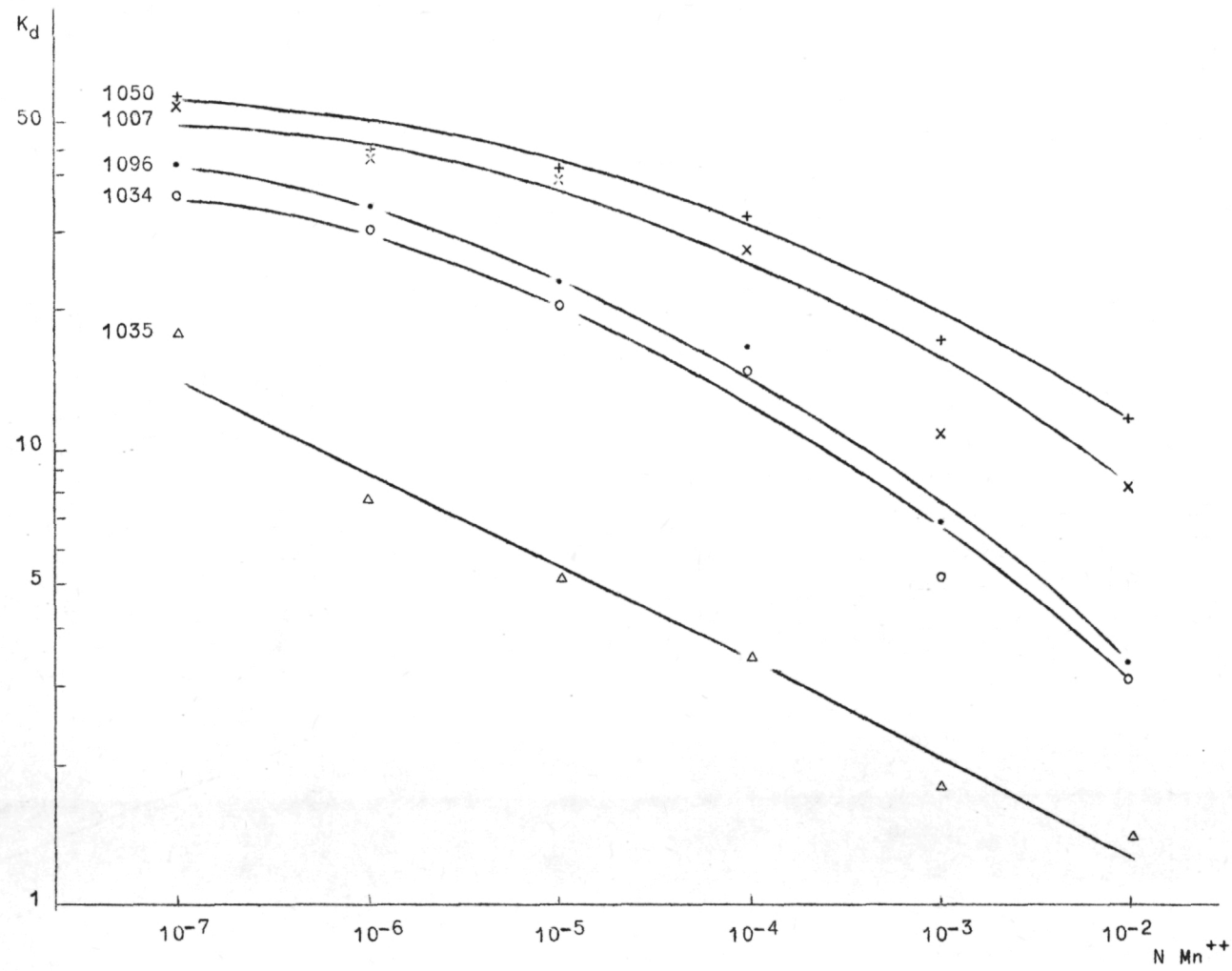


fig. 17.
Mn^{54} sorption versus Mn concentration.

in the future where samples rich in clay and silt are concerned. He draws, however, attention to the fact that K_d values obtained by means of different methods may mutually vary to a greater extent as compared to those obtained with one and the same method applied to different samples. He suggests, consequently, to use K_d values of these tests that best agree with what occurs in nature. Thus the results obtained with the precipitation will be more appropriate for describing the absorption of ions by soil material which has been brought again into

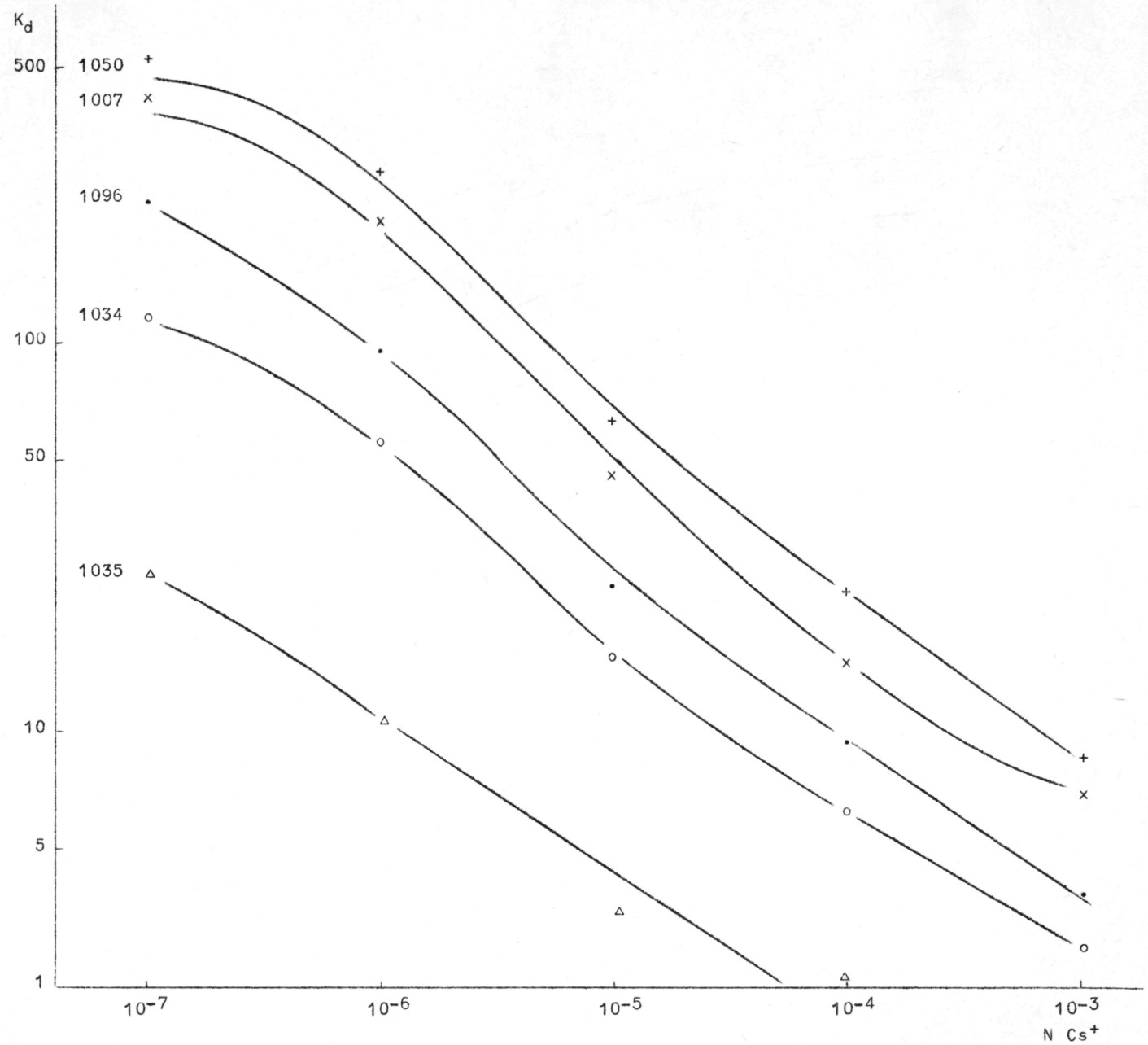


fig. 18.
Cs^{137} sorption versus Cs concentration.

a state of suspension and subsequently precipitates. Also, the thin layer method will be more appropriate in conditions where a simple contact exists between the water and the sediments without having these latter return to a state of suspension.

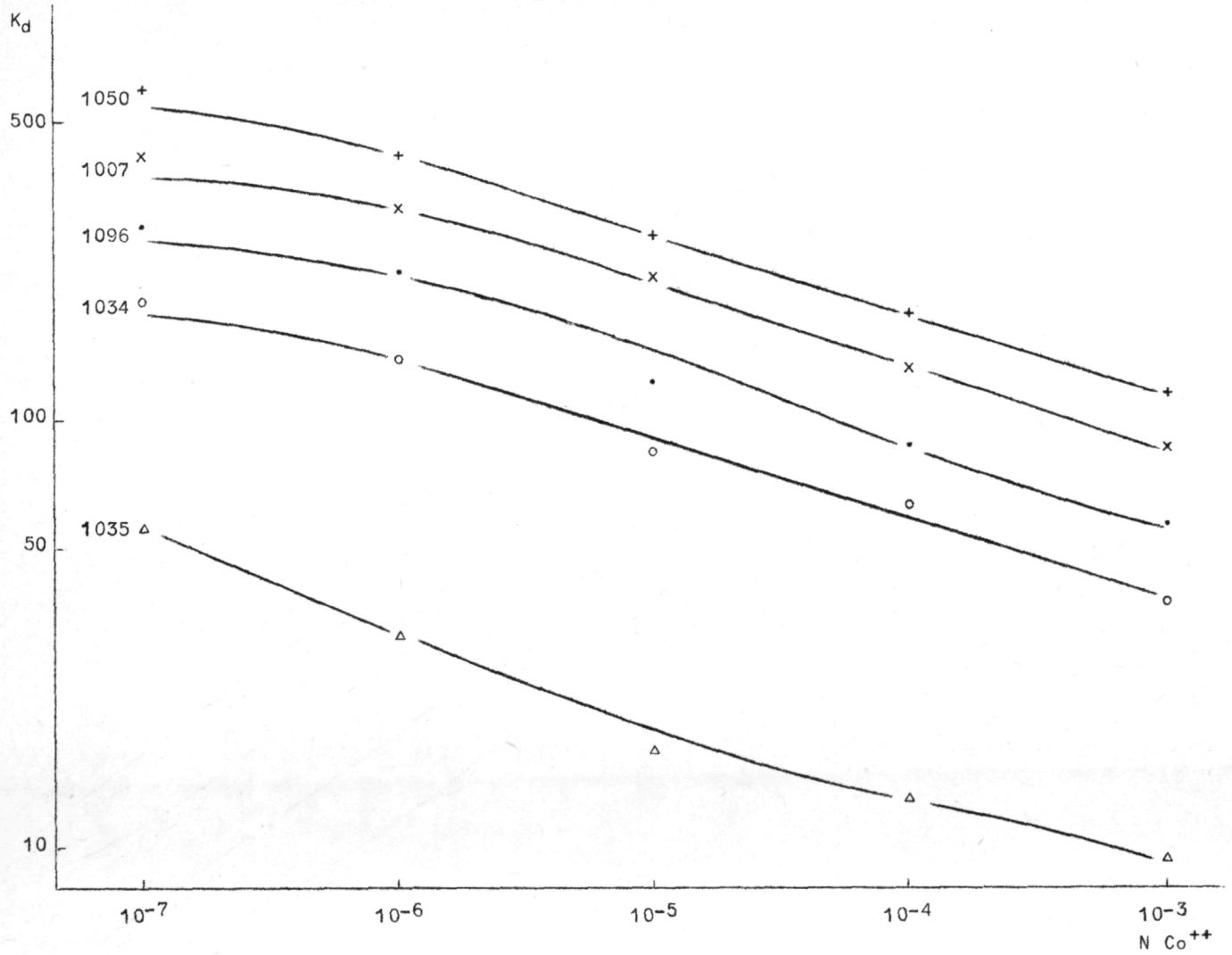


fig. 19.
Co^{60} sorption versus Co concentration.

Reference

DUURSMA, E.K. and EISMA, D., (1973). Studies concerning reactions of radio-isotopes with sediments and suspended particles of the sea, *Netherlands Journal of Sea Research, 6,* (3), 265-324.

Chapter III

Data acquisition and processing

I

Automatic acquisition of meteorological and oceanographic data : further developments and first results

by

G. PICHOT

(Based on work by A. DE HAEN, H. PICARD, G. PICHOT, A. POLLENTIER, F. RIGOLE and M. VANDENBOSSCHE)

Introduction

Mathematical models describing and predicting the state of ecosystems such as the North Sea require many long time series of data which allow to effect good numerical values to the interactions parameters and to check their accuracy in the preparatory phase and which

The author is endebted to Lt. J.P. BARBIEUX and the Section Studies and Research of the Belgian Navy for the help he received in this field.

give the precise boundary conditions in the operational one. These can only be furnished by automatic data stations. It is the reason why a network of meteorological and oceanographic buoys has been planned in the frame of our research programme. These were widely described by Pichot *et al.* (1974).

Nevertheless, it seems worth while to present more clearly the data acquisition system, to give more details about the sensors which are used now and to comment the first results obtained during spring 1974.

1.- The data acquisition system

The major functions of the data acquisition system are shown in the block diagram (fig. 1).

The various meteorological and oceanographic sensors, together with a number of housekeeping data, are interrogated under control of the general timing unit. This general timing unit, which is programmed to give the required frequency of sampling and data collection, controls in fact the extendable 32 channel data multiplexer and the power scanner.

The power scanner, consisting of a number of relays, provides the appropriate power supply to the different sensors in a programmable sequence. This sequence depends upon the actual needed warming up time and the period a particular parameter needs to be interrogated.

The data multiplexer itself is divided into two distinct parts which consist in their standard version of a 16 channel analog (f.m.) signal scanner and of a 16 channel digital information multiplexer. Depending upon the nature of a certain sensor the output signal is an analog signal or is already present under digital form.

If a parameter is available in digital form the information is stored in a small buffer memory in BCD form, eventually after level adaptation and code conversion. This storage can happen during the actual measurement cycle or before, in this manner providing instantaneous or integrated measurements.

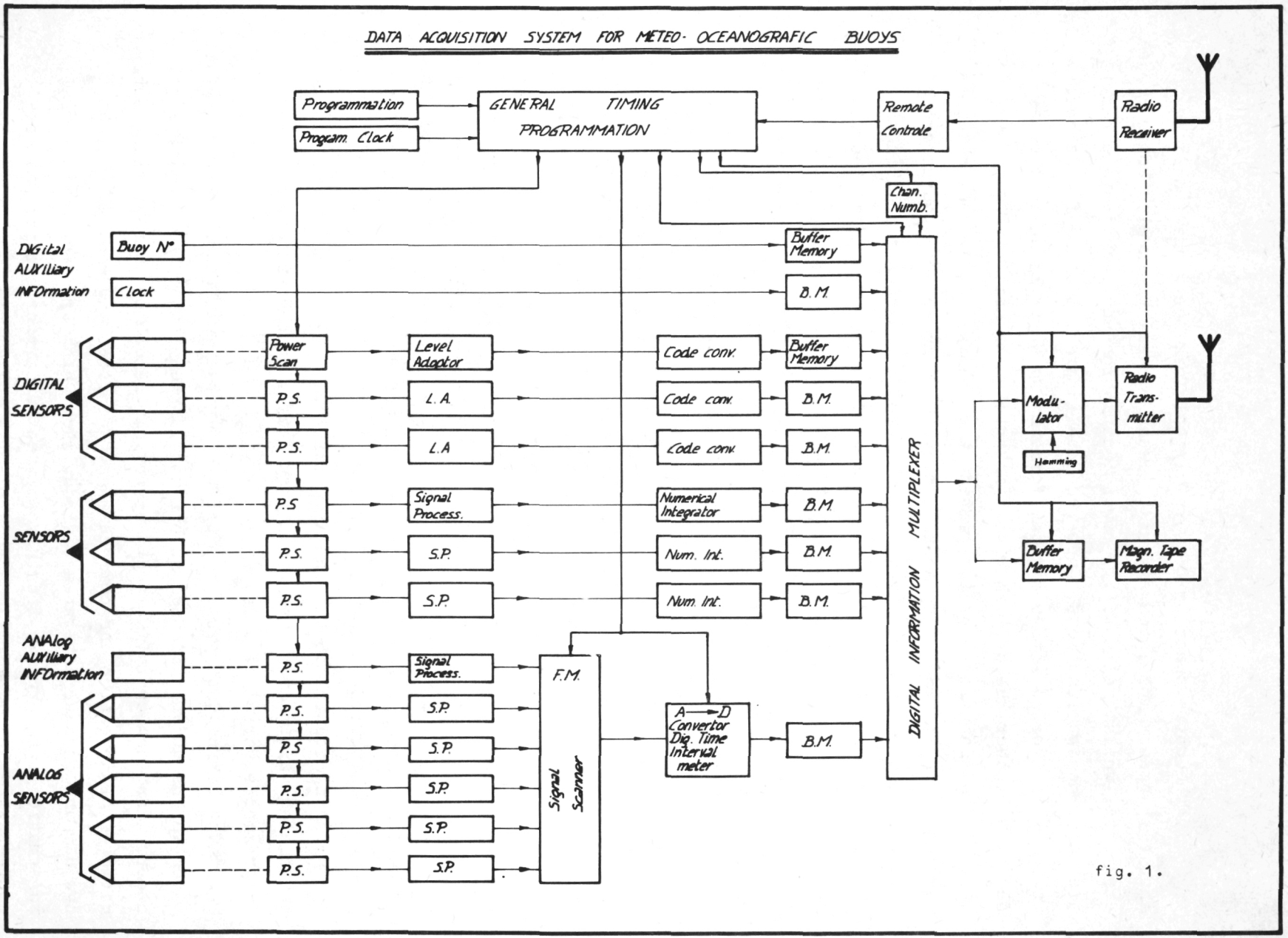

DATA ACQUISITION SYSTEM FOR METEO-OCEANOGRAFIC BUOYS
Programmation
Program. Clock
GENERAL TIMING PROGRAMMATION
Remote Controle
Radio Receiver
Chan. Numb.
DIGital AUXiliary INFOrmation
Buoy N°
Clock
Buffer Memory
B.M.
DIGITAL SENSORS
SENSORS
Power Scan
Level Adaptor
Code conv.
Buffer Memory
P.S.
L.A.
Code conv.
B.M.
Signal Process.
Numerical Integrator
S.P.
Num. Int.
ANAlog AUXiliary INFOrmation
ANALOG SENSORS
F.M.
Signal Scanner
A→D Convertor Dig. Time Interval meter
DIGITAL INFORMATION MULTIPLEXER
Modu-lator
Hamming
Radio Trans-mitter
Magn. Tape Recorder

fig. 1.

If the data is not present in digital form the signal is processed into a frequency modulated signal by means of well known electronic circuitry, whilst reliability, power consumption and required accuracy are major design functions. Once the data is present as an f.m. signal it can be converted into a digital form in two ways taking into consideration whether the data should be integrated or not.

If the data is to be integrated, the analog-digital conversion is carried out by a frequency measurement with a time resolution according to authoritative data requirements. Each result is then stored in an identical buffer memory as normal digital data. Nevertheless, the flexibility of the system allows that this data is still available for instantaneous interrogation, *e.g.* for time series or in the event of a considerable difference between research and observational requirements.

If the data is not to be integrated the signal passes through the 16 channel analog multiplexer which is immediately followed by a time interval meter and the result is momentarily stored in a buffer memory. The sampling rate of the time interval meter is synchronous with the scanning frequency and the information of each analog channel is in turn available in the buffer memory.

Once the general timing clock starts a measurement cycle the contents of the buffer memories are, under control of the digital multiplexer, serially shifted towards the Hamming encoder and to the modulator. If analog channels are to be interrogated the digital multiplexer stays locked on the buffer memory related to the time interval meter and passes the scanning control to the analog multiplexer. As an additional feature the analog multiplexer itself can stay locked on certain channels for a programmable period of time.

The serial data present after the digital multiplexer receives also a continuous updated channel number and is then fed to the Hamming encoder. This encoder is in fact a parity bit generator that provides automatic error detection and correction at the receiving end. The output of the Hamming encoder activates the modulator which transforms the serial information into a pulse length modulated subcarrier applied directly to the transmitter input.

At the receiving station situated on shore or on an oceanographic vessel the data is available in real time. For certain applications, as in the case of too great distance, it can be more convenient to store the data *in situ* on a magnetic tape recorder. For this reason a serial data output is available before the Hamming encoder.

At last, the receiving station can also transmit a remote control signal which activates a sensing circuit. If at that moment the general timing unit has not prepared a measurement cycle it can be triggered off to start by the remote sensing circuit.

2.- The sensors

A "clever" sensor is a device sensitive to a given stimulus and able to transmit it under the form of an electrical signal such as a frequency, an AC or DC voltage, a binary coded decimal imput, etc.

For now the buoy is only equipped with such clever sensors measuring air and water temperatures, incident radiation, barometric pressure, salinity, heave, wind speed and direction for which a rather good mean term fiability can be hoped.

Table 1 gives details on these sensors concerning the working principle, the output signal, the measurement range and the accuracy.

Figure 2 shows one of the temperature sensors we have developed. It has been noticed that these can give, in the air, a little variable results probably when differently shielded from the solar radiation. To check this hypothesis, a simple sensor for the incident light we built has been added on the buoy. As it very quickly reaches its saturation level, it only shows if there is a high amount of incident radiation but it cannot be useful for scientific needs such as the measure of the light available for the photosynthesis. It is why it must be replaced by a KIPP albedometer for which the sensitive device is a photoelectric cellule measuring incident and reflected light within a wave length range from 3×10^{-7} to 2.5×10^{-6} m .

Table 1

Sensors now working on our buoy .

Parameter	Principle	Manufactured by	Output	Range	Accuracy	Remarks
Air and water temperature	R.C. oscillating circuit of which the frequency is controlled by a thermistor	us	F.M. pulses 16 - 100 Hz	3-30 °C	± 0.05 °C	Time constant : 1 s
Incident radiation	R.C. oscillating circuit of which the frequency is controlled by a photoresisting cellule	us	F.M. pulses 400-750 Hz	50-1300 mW / cm^2		intercalibrated with a KIPP albedometer
Barometric pressure	Straingage connected to a Wheatstone bridge	M.B.	A.C. Voltage 0 - 10 mV	900-1100 mbars	± 0.5 mbars	calibrated at the pressure room of the Royal Meteorological Institute, Brussels
Salinity	Measure of sea water conductivity by induction	PLESSEY	F.M. pulses 4995-7901 Hz	10-40 ‰	± 0.03 ‰	intercalibrated with a Beckman lab salinometer
Heave	Twice integrated accelerometer	DATAWELL	D.C. Voltage ± 10 V	± 10 m	± 3 %	
Wind speed	Three-cups assembly directly coupled to an optical interrupter device	NBA	F.M. pulses 10-50 Hz	3-150 knots	± 0.3 knots	
	Three-cups assembly directly coupled to a disc moving in a magnetic field	FRIEDRICHS	F.M. pulses 0.2 - 40 Hz	0.6-120 knots	± 0.3 knots	
Wind direction	Vane coupled to a disc optically coded in a 7 bits Gray code	NBA	B.C.D. parallel	0 - 360°	± 2.8°	

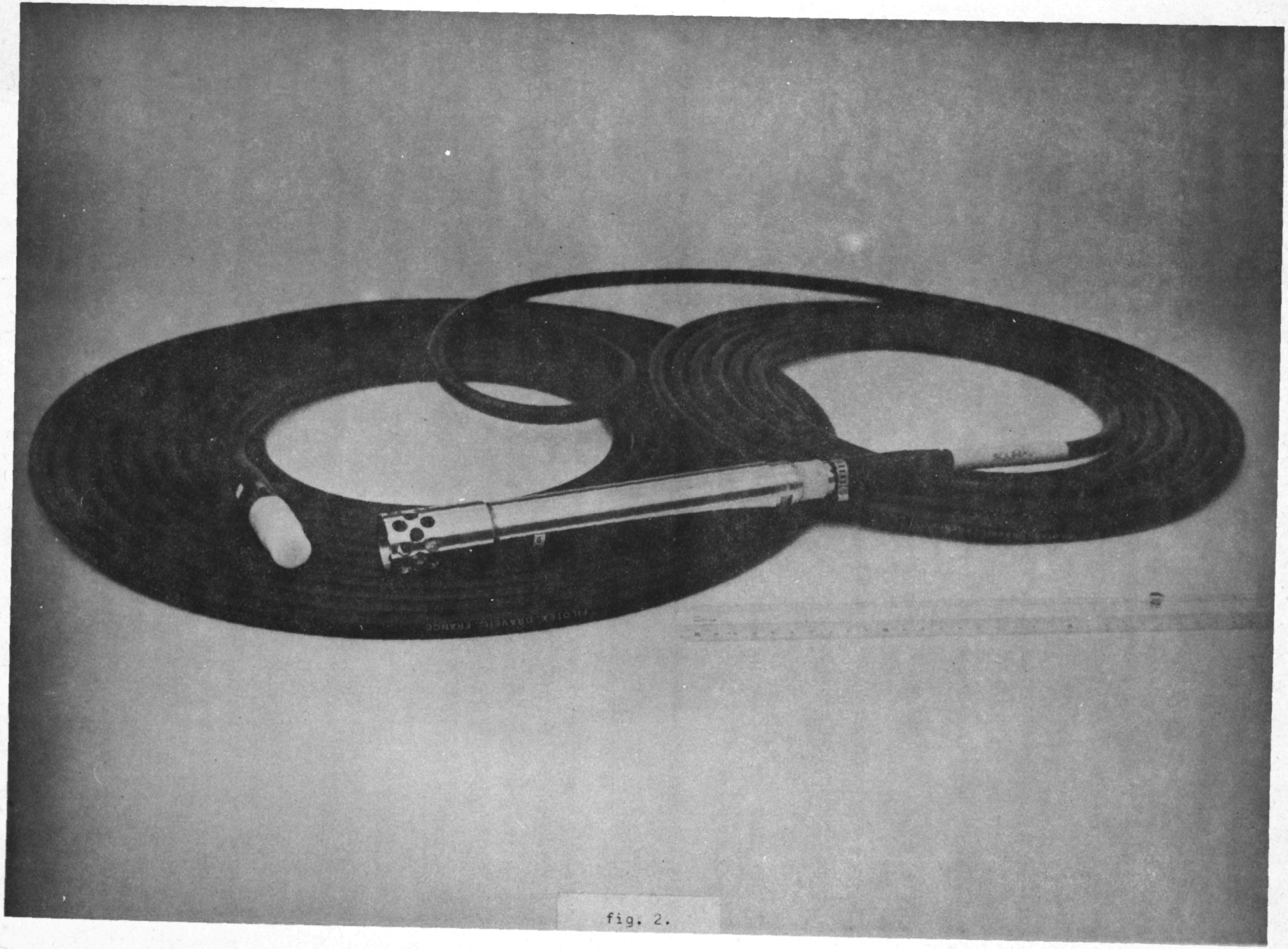


fig. 2.

As far as the wind speed and direction are concerned, the instantaneous values which are measured do not have many meanings because of the movement of the buoy itself. So, it seemed necessary for our purposes to take not only the average speed and direction values over a given time but also their vector averaging ones. All the details on these technics are given by Pollentier *et al.* (1974). To summarize them, let us remember that during the integration time, the wind direction is sampled every time that the anemometer has counted 20 pulses which correspond to an air displacement of 3.08 m . At each sampling, this unit vector is projected on the north and east axis. At the end of the integration, it is easy to express the air displacement and direction in function of sums of north and east components of all these unit vectors.

3.- First results

A first experimental mooring occured from March 19th to April 15th 1974 at the station 51° 20' 45" N 2° 53' 40" E , 13 km from the Ostend receiving station (fig. 3).

There were two sensors for the air temperature, two for the subsurface water temperature, two for the wind speed and one for the heave. House keeping sensors continuously watched over the current supplied by the wind generators, the voltage of the batteries and the humidity inside the electronics compartment.

All the sensors except the heave one were sampled every hour. Each hourly interrogation cycle has immediately been repeated three times in order to check the errors which could occur during the transmission. The heave has been sampled once per second during ten minutes every two hours. Each interrogation gave thus a record of 600 measurements which becomes sufficient for spectral analysis purposes. Figure 4 is an example of a one day heave record.

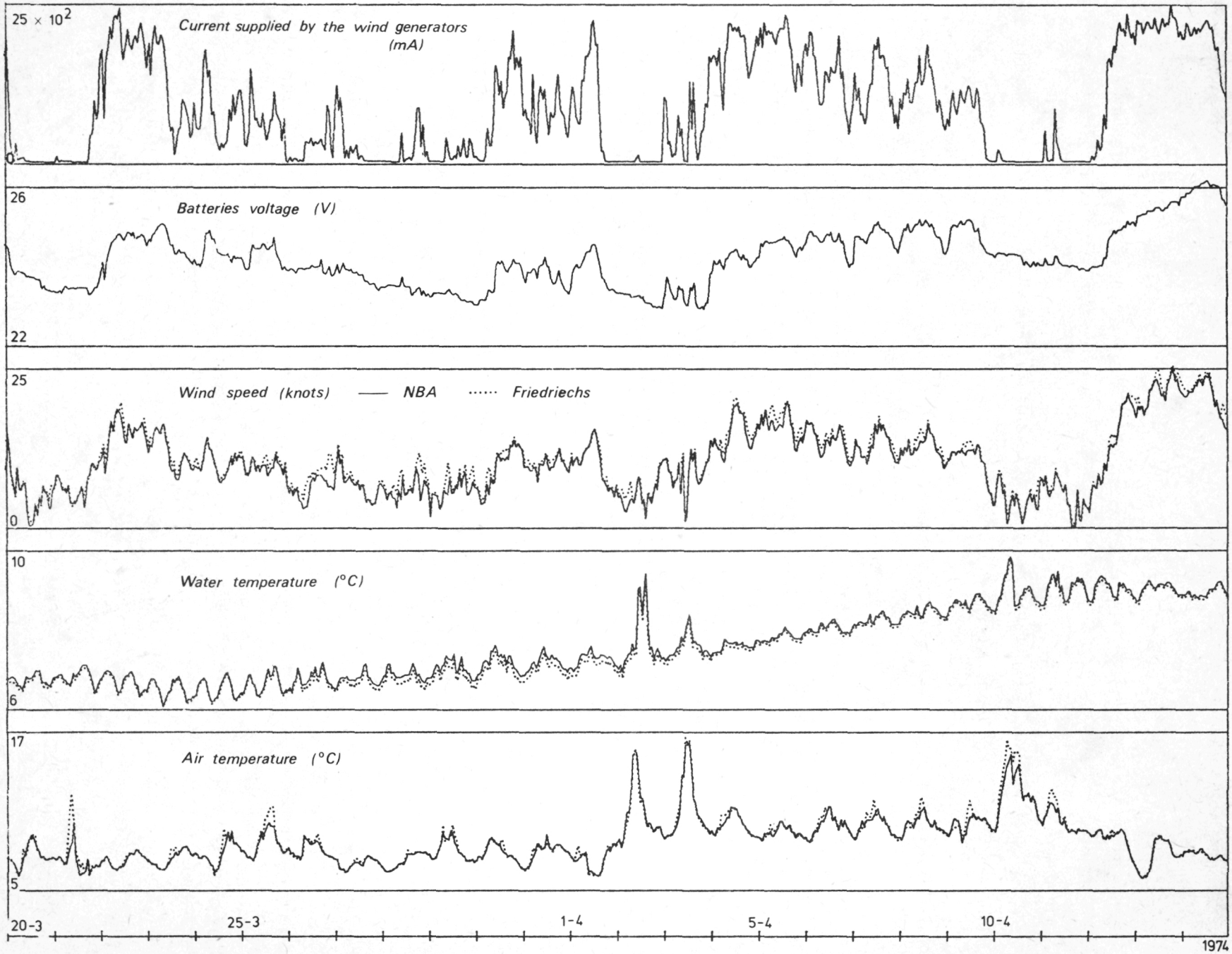

25 × 10²
Current supplied by the wind generators (mA)
0
26
Batteries voltage (V)
22
25
Wind speed (knots) —— NBA ····· Friedriechs
0
10
Water temperature (°C)
6
17
Air temperature (°C)
5
20-3
25-3
1-4
5-4
10-4
1974

fig. 3.

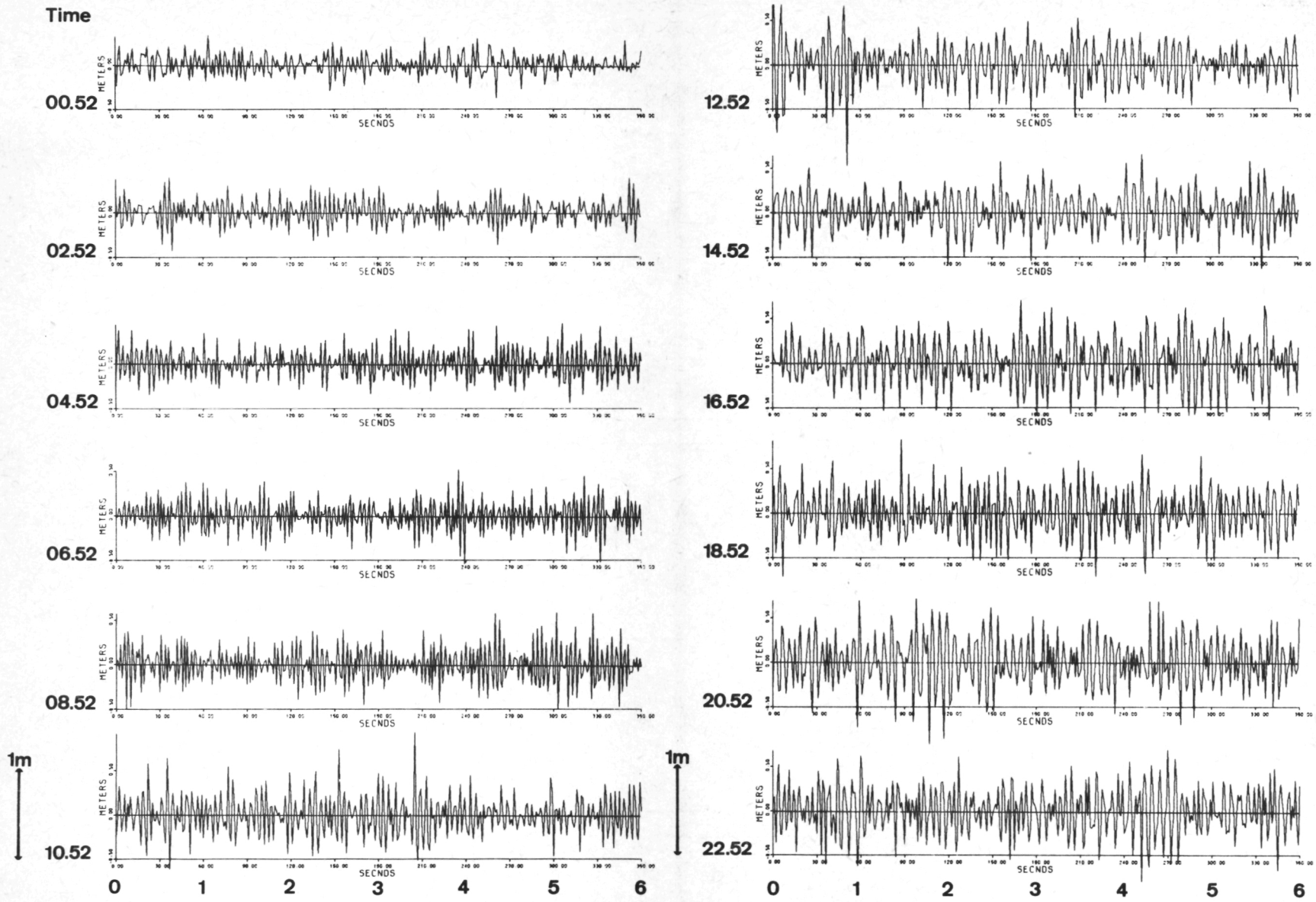

Time
00.52
02.52
04.52
06.52
08.52
10.52
12.52
14.52
16.52
18.52
20.52
22.52
METERS
SECNDS
1m
0
1
2
3
4
5
6

fig. 4.

3.1.- House keeping sensors

The current supplied by the wind generators roughly follows the profile of the wind speed. But it vanishes for wind speeds equal to 7 knots which is the starting velocity of the generators. It occured during 25 % of the mooring period and corresponds to a decrease of the batteries voltage of about 0.5 volt per day. This confirms that the buoy can properly work during at least seven days without any external energy supply.

3.2.- Air temperature

The air temperature profiles have classical diurnal oscillations. The two sensors give slightly different results mainly when the air temperature increases or reaches its maximum at midday. This error which has a maximum of 1 °C probably occurs because of thermistors differently shielded from the solar radiation, as explained above.

3.3.- Water temperature

The two sensors give almost the same results. The curves of the subsurface water temperature shows up a little increasing trend without any clear cross correlation with the air temperature.

It has to be noticed that from March 20th to March 26th, the water temperature semi-diurnally oscillates with a mean amplitude of 0.56 °C . This could reveal an input of cold fresh water from the Schelde estuary reaching at least the area in front of Ostende. If it is true, this confirms the water gyres predicted by the hydrodynamical models of Nihoul and Ronday (1975).

3.4.- Wind speed

The two sensors are manufactured by two different firms and work differently. For the first one (NBA), the measure consists in reading an optical disc and for the second one (Friedrichs), in recording an induction variation.

Nevertheless the results which are the mean values over ten minutes are very similar and have a maximum error of 1.5 knots . They have been compared with the data taken every day at 6 , 9 , 12 , 15 and 18 hours by the light-vessel West Hinder which stays 32 km west from the mooring station. These are received at Liège University by telex via the *Régie des Voies Aériennes*.

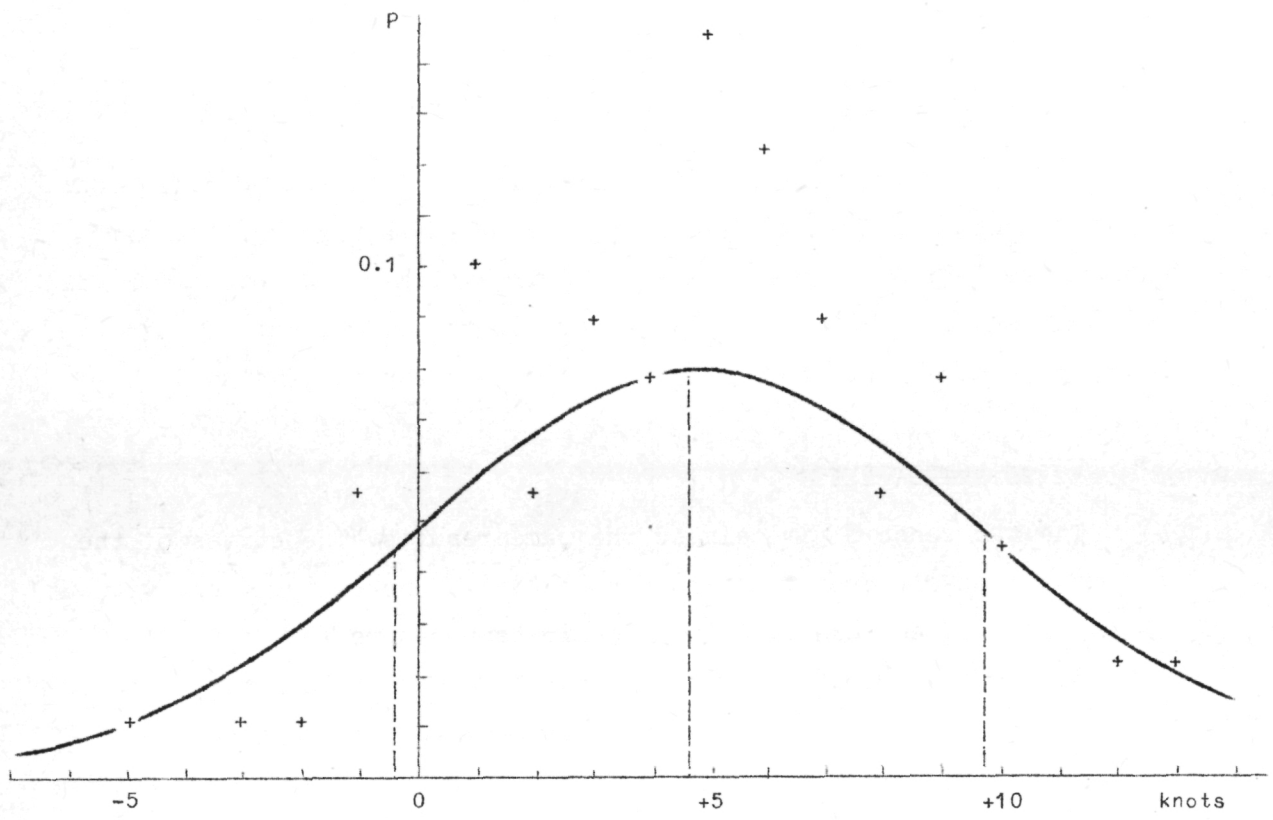
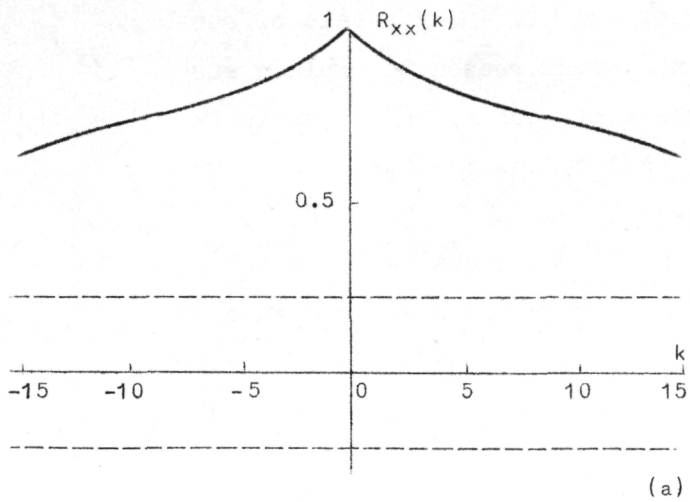
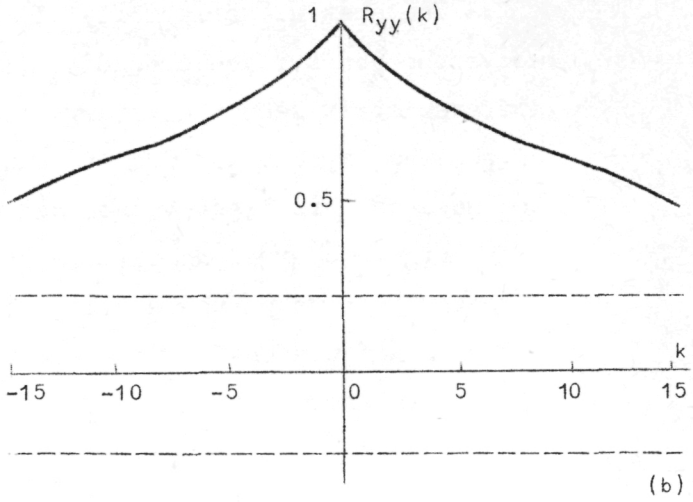


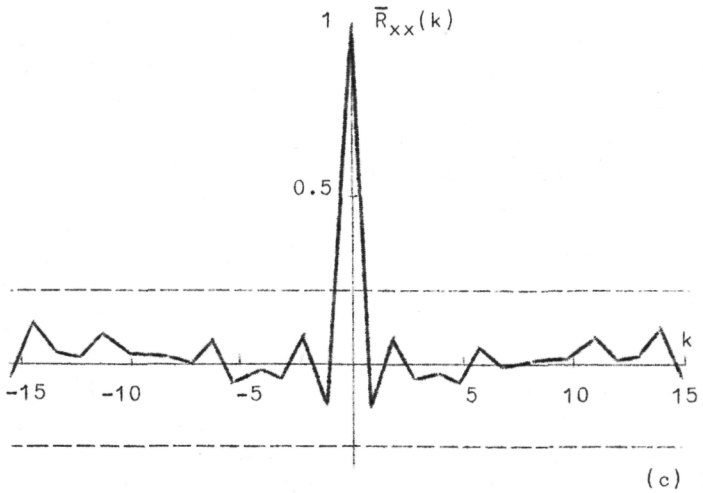
fig. 5.

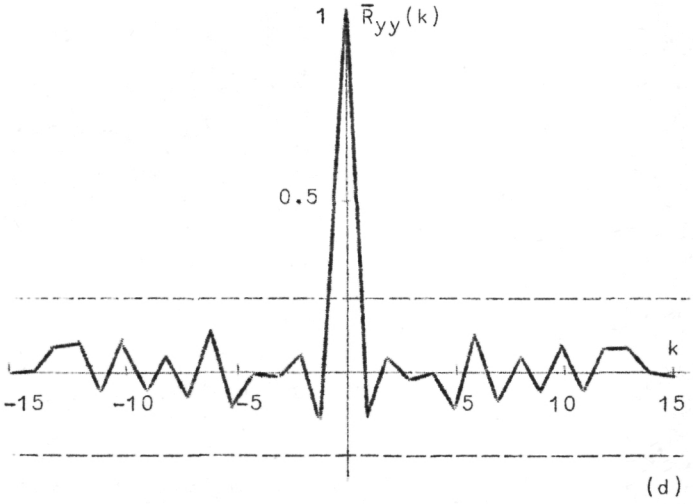
Frequency distribution of the difference between the wind speed data of the West-Hinder and of our buoy. Mean : + 4.86 knots ; standard deviation : 4.96 knots ; number of observations : 90 .

Figure 5 shows the frequency distribution of the difference between the wind speed measurements of the West Hinder and of our buoy. This difference is equal to + 4.86 ± 4.96 knots . So, the West Hinder systematically gives higher values than our station and this is observed for any wind direction.









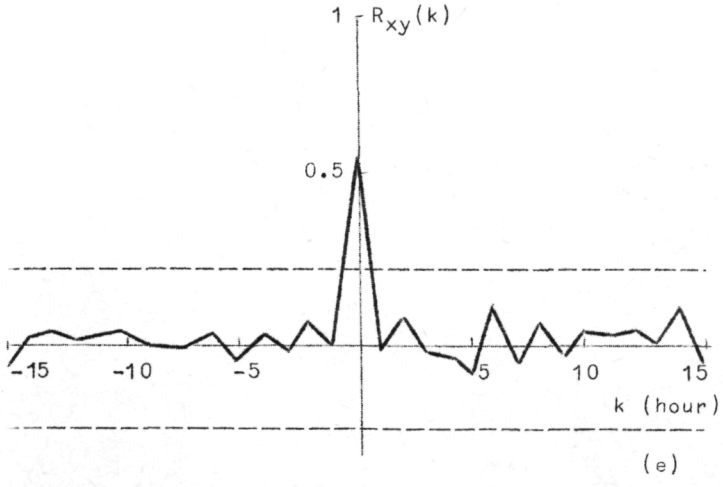


fig. 6.

(a) : autocorrelogram of the wind speed data.

(b) : autocorrelogram of the current supplied by the wind generators data.

(c) : autocorrelogram of the wind speed data, after filter of first order desautocorrelation.

(d) : autocorrelogram of the current supplied by the wind generators data after filter of first order desautocorrelation.

(e) : crosscorrelogram between the wind speed and the current from the wind generators.

The spatial variability of the wind and different levels of sensors above the sea surface are not sufficient enough reason to explain such a difference. It seems necessary to plan a next mooring in the vicinity of the West Hinder in order to make an *in situ* intercalibration between the data of this light vessel and ours.

Figure 6 gives an example of the kind of processing which can directly be made on these time series. Figures 6a and b are the autocorrelograms of the data of the NBA wind speed and of the current supplied by the wind generators. These two series are very highly autocorrelated. Figures 6c and d are the autocorrelograms of the same series after a filter of first order desautocorrelation. They are now stochastic. Figure 6e is the crosscorrelogram between the two series. It can be seen that the current from the wind generators is simultaneously highly correlated with the wind speed and it is obvious that the behaviour of a wind generator is rather similar to the one of an anemometer.

References

NIHOUL, J.C.J. and RONDAY, F.C., (1975). *Tellus, 27,* 5.

PICHOT, G., DE HAEN, A. and NIHOUL, J.C.J., (1974). *The Belgian automatic oceanographic and meteorological data station,* in *Proc. of the First European Symposium on Offshore Data Acquisition Systems,* Southampton (U.K.), Sept. 1974.

POLLENTIER, A., VANDENBOSSCHE, M. en RIGOLE, F., (1974). *Vektorieel integrerende windmeter voor meteo-oceanografische boeien,* Technical Report 1974/Instrumentation 02, Programme National sur l'Environnement Physique et Biologique, Projet Mer, Ministry for Science Policy.

II

Present state and prospects of data processing

by

Y. ADAM

(Based on work by Y. ADAM, J.P. FOGUENNE, C.J. FRANKIGNOUL, A. POLLENTIER, Y. RUNFOLA, M. VANDENBOSSCHE)

1.- Data treatment : an overview

In the frame of a research program built around a general mathematical model, which is fed by huge amounts of data coming from a great number of laboratories and automatic data acquisition systems, the disponibility of a large and easily accessible data base is obviously a useful tool for the scientists.

The only way to make a compromise between the terrific amount of available data and the accessibility of this information to the scientist, is to build a computerized data base structured with the help of the mathematical model, to develop a set of management and analysis computer programs which will free the scientist from the painful tasks of retrieving data from other laboratories, handplotting his own measurements, performing boring statistical computations and give him a practical tool to easily edit and correct his data, compare them to results of theoretical simulations.

The great variety of data makes this task uneasy; data from automatic acquisition systems (like buoys, current meters) are usually time

series of regularly spaced samples; data issued from *in situ* measurements through laboratories are usually batches of samples collected at different positions and times during a cruise or a survey; some data are counts (*e.g.* number of bacteria), others are decimal numbers (*e.g.* nutrient concentration), some are even synoptic codes (*e.g.* meteorological observations).

One must thus, first design a rather flexible format of data storage, to cope with the variety of data one is faced with; then develop general routines to format, retrieve, access and select every kind of data, each routine being built in such a way that it can easily be tailored by the user to treat the kind of data he is interested in.

2.- Present state of the data base and its associated software

We have described the goal we are aiming at. It must be emphasized that we are still on the first stages of design and development of the data base. The scientists involved in data treatment and information processing have up to now been too busy with other fundamental research (like mathematical models design and optimization, numerical tools creation) or with technological tasks (data acquisition systems implementation) to dedicate their time to the data base.

However, some files already exist and are easily accessible on computer readable storage media (mainly magnetic tape) and an elementary software is able to store, access, edit and visualize these data. The software has no unity and consists in several programs chains, each being specialized in the treatment of a particular type of data. Up to now, mathematical or display tools developed for one type of data cannot be immediately adapted to another type; moreover, computer programs have been designed for particular types of computers and nothing has been made to insure the portability, neither of the software, nor of the data (let us remind that two types of computers, at least, are available in the frame of the program for the data processing : a HP2100A and an IBM 370/158).

The automated data chains handle

1) buoy data,

2) current meter data,

3) meteorological data.

All are time series (data every 15 minutes for current meters, every hour for buoy, every 3 hours for meteo).

The first chain has been implemented in Ostende, the two others in Liège.

2.1.- Meteorological data

The meteorological data handling chain is described in Appendix I. It is the most sophisticated of all because of the complex structure of the time series (28 samples and 14 variables at each time step).

2.2.- Buoy data

The flow diagram of the buoy data handling chain is shown on figure 1.

The first step of the chain is the data acquisition itself, described elsewhere, together with the signal transmission and reception.

In the second step raw data are fed into the computer on paper tape support; the first program (DASS1) stores them on a magnetic tape in a fixed format and updates the catalog of the tape. No correction and no editing are performed on this stage.

In the third step the MT containing the raw data may be

- copied by program MCØPY, for the sake of safety,
- listed by program MLIST,
- edited by program DASS3 (scratches wrong files) and MEDIT (eventually corrects erroneous date or values).

Every file is then tested by program PURIF, which corrects data where erroneous ASCII characters appear, and rewritten at the same place on MT.

In the fourth step a series of programs CH01, CH02, ... decode the information given by every channel of the buoy (CH01 translates channel 1 data, CH02 translates channel 2 data, ...). Results are stored on disc.

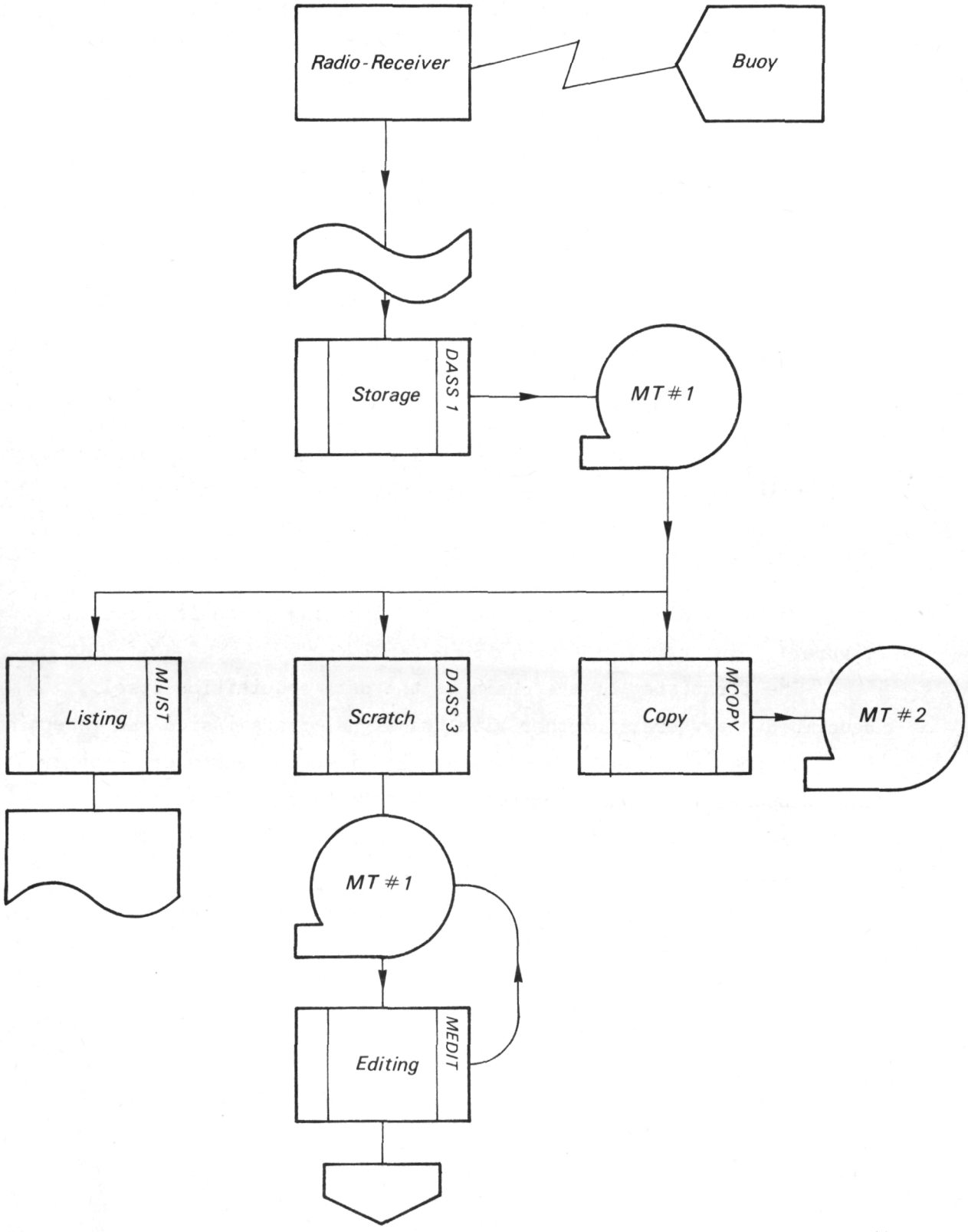

Radio-Receiver
Buoy
Storage
DASS 1
MT #1
Listing
MLIST
Scratch
DASS 3
Copy
MCOPY
MT #2
MT #1
Editing
MEDIT

fig. 1.

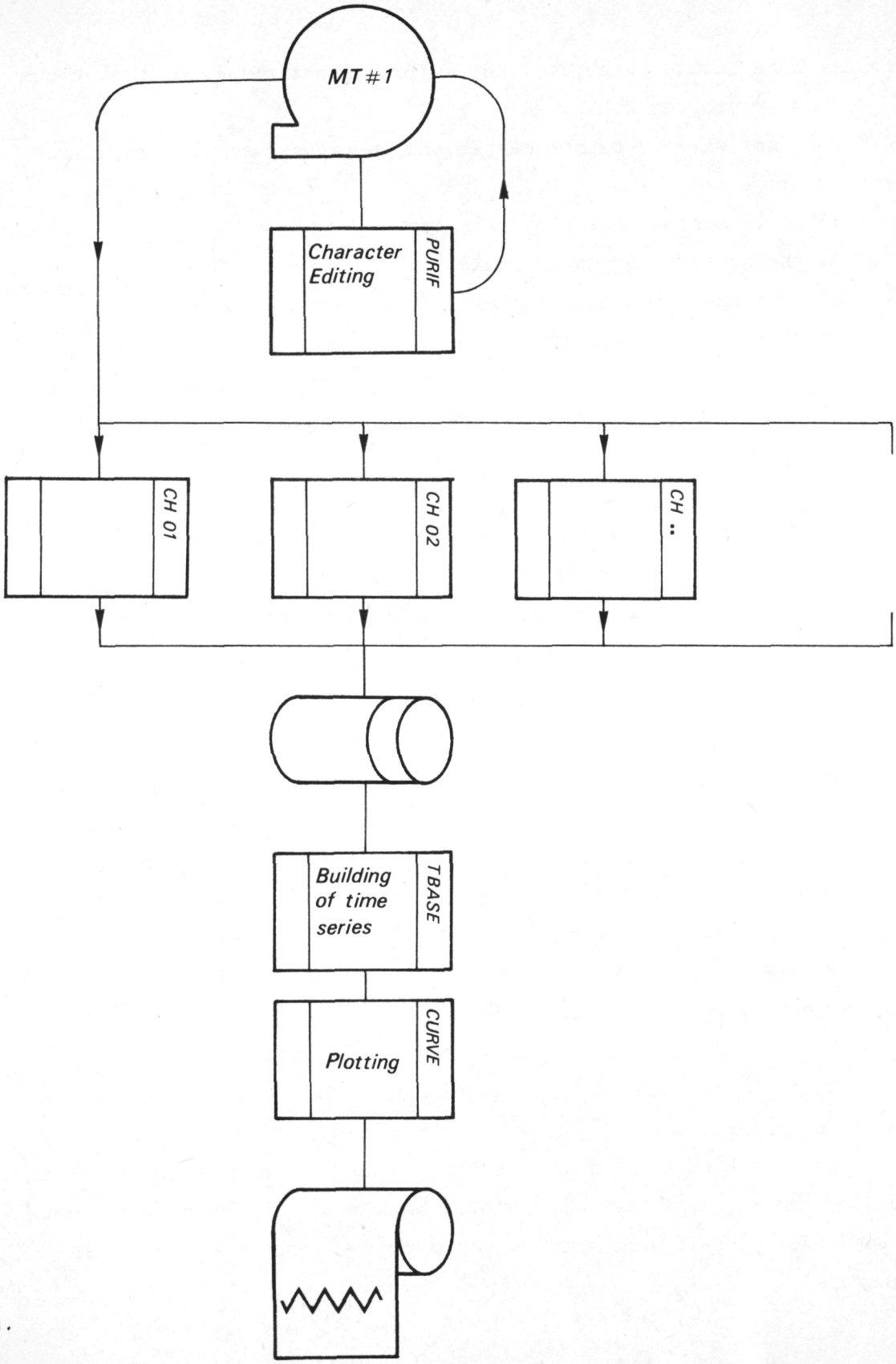

MT #1
Character Editing
PURIF
CH 01
CH 02
CH ..
Building of time series
TBASE
Plotting
CURVE

fig. 1.

Program TBASE builds then from that information time series, which can be plotted by program CURVE.

This software is rather simple and operates fast. Its main drawbacks are :

1) it is exclusively buoy oriented,

2) the storage format is rigid,

3) no actual treatment is performed.

It can be improved in two ways :

1) the first step can be replaced by on line data acquisition. This will be worked out in the near future : signals from the buoy will be immediately stored on disc files (acting as buffers) and then transferred to MT;

2) the last step must be completed by a program which stores the data on a mass storage device in a standard format we will describe later. Buoy information could then be treated by a standard software still to be developed but common to all types of data.

2.3.- Current meter data

This handling chain is the less sophisticated. Current meter data are received in different ways, according to the type of instrument.

VACM data arrive in a ready-to-plot-and-analyse form from WHOI when they have been decoded, edited and pretreated (interpolation of missing values) on a MT written in EBCDIC.

NBA raw data arrive on a paper tape in ASCII characters. No edition or pretreatment has been performed.

Plessey data arrive in Plessey code form (on paper tape or MT); they have to be translated in ASCII or EBCDIC before being available to processing programs.

For each kind of instrument, there exists a program which builds the time series, edits them and stores them on disk-files which serve as input for plotting and analysing programs (namely a Fast Fourier Transform).

3.- Guidelines for the building of the data base and processing software

The utility of a data base and related software in the frame of an interdisciplinary research program has been stressed. We dare not call this structure a data bank, because we do not intend to achieve a very sophisticated software, completely transparent to the users, like some systems used in financial, commercial and banking environments. The software will not be extended so far for two main reasons :

1) environmental data (like oceanographic or meteorological data) present a greater variety of types and structures than business data and need more complex processing. It seems to us to be overweening to design a very sophisticated software which would be computer time greeding with the limited means (material and human) we dispose of;

2) the data base and processing software is intended to be used, not by bank clerks, but by scientists with a minimum experience of computer systems who are assumed to know which kind of information they exactly need and how they want to handle the data. A minimum staff of software specialists would however be necessary to help the scientists in assembling their program chains and to advise them on the choice of computing tools.

This solution has already been experimented in several oceanographic research centers, like WHOI, University of Southampton, and BNDO at the *Centre océanologique de Bretagne*.

The system we aim at will however be flexible enough to enable the storage, retrieval, selection and processing of present and future data sets, whatever be their origin and structure. It will also be designed to facilitate the work of the scientist by giving him standard tools for the analysis of his material and for the validation and comparison of mathematical models and to be easily extended with programs for specific purposes.

Finally, the data storage and the software are thought to be portable (*i.e.* able to be implemented with the least possible modifications) on most families of computer systems in order that the effort made for designing them will benefit the largest number of research groups. This implies that the structure of the programs themselves and of the data

records be compatible with the great majority of the computers used in scientific research centers. We explain later how this can be achieved, for both the software and the storage format.

4.- Requirements for the portability of the storage format and of the software

Computer specialists know very well that almost everything that has been written by any computer system can be read by any other, provided that the 'translation' software exists. The portability of the software is less evident : not all languages are implemented on all computer systems and translating a package from one language to another often needs a lot of time and money. Generally, oceanographic research centers do not have the men needed to work out such a conversion. That is why the software package we are developing is designed to be used, with only a few slight modifications relative to input/output operations, on the great majority of general purpose or scientific computers.

Due to the internal structure of the routines, to the flexible shape of the storage format and to the fact that it is hardly impossible to write data processing programs fully independant from the hardware, the following hardware and software features are needed :

1) a direct memory access to a magnetic tape and disk is available,

2) single precision real words are stored in 2 integer words,

3) a compiler exists for ANSI Fortran IV,

4) records of variable length can be read and written on magnetic tape (eventually through a limited set of special assembly language routines).

ANSI Fortran IV is the most widespread computer language for scientific and technical applications : it is thus the best language to write a scientific package.

As to condition 2), it means that the core storage of a single precision floating point number is twice the core storage of an integer word. That is what happens automatically on 16-bits or 24-bits word

oriented computer, and what can be forced by software on 32-bits or 60-bits word-oriented machines.

The magnetic tape format is portable in the sense that the structure of the records on magnetic tape is the same for all computer systems. It is intended as a data processing and a mass storage format, not as a data exchange format[1]. As such, it uses binary recording mode for compactness and input/output performance, *i.e.* the data on mag-tape are an exact copy of their core storage representation.

A data exchange format should be written in interchange code as EBCDIC or ASCII. Such a code is unsuitable for fast processing and is less compact than binary code.

However, despite the binary recording mode, tapes written by one computer can easily be read by another under several conditions.

1) magnetic tape specifications are compatible on both systems (*i.e.* same number of tracks, same density, same encoding technique, same shape of end-of-record and end-of-file marks);

2) both machines are either 16-bits (word) or 32-bits (byte) oriented; both machines are 24-bits word oriented; both machines are 60-bits word oriented (computers are then called "word compatible");

3) routines exist for the translation of internal formats for real numbers and characters.

Provision is made in the storage format for defining the internal code used to write the numbers and the characters in order that the appropriate routines (condition 3) can be selected. The keys defining these codes can be decoded by any computer word-compatible with the source computer because they are positive integer numbers that have the same format in all systems with the same integer word length.

---

1. Data exchange formats are now being developed by international scientific organizations.

5.- General description of the software

The software being presently on the first stages of development, it cannot be described in detail. It can be defined as an extended subset of the WHOI standard buoy format package, simpler than the latter one under some aspects. The original is being modified to be more general (to treat a greater variety of data structures) and more portable; it will be extended to meet mathematical modelling requirements.

It will consist in :

1) a set of general purpose routines to read, write date records, label and retrieve data files (both on magnetic tape and on disk) and to transfer the data between mass storage and core memory (in arrays accessible to the user), in both directions;

2) a set of data handling programs (using the general purpose routines) to select, edit, list and plot the data in various ways, depending on their structure;

3) a set of mathematical programs to analyse the data and to compare and fit models to experimental features.

6.- The data storage standard format

The format is self-describing : each data file contains in itself every information needed to be read properly whatever be the number of data variables, of samples, their nature, their structure (continuous function of a variable or not), their record type, and the number of records in the file. Magnetic tapes written in standard format also contain at the beginning of the data, an identification file and, after the last data file, an end-of-data file.

Each data file consists of :

1) two label records,

2) data records (in any number).

The first label record has a fixed length and defines :

- the keys for binary data conversion,
- the file creation date,

- the name of the file,
- the number of variables,
- the number of samples,
- the data origin date,
- the type of the second label.

The second label record defines :

- the position where the data were taken (latitude/longitude or other information),
- sampling parameters,
- the initial value of the continuous sampling variable,
- for every variable :
    - its name,
    - its units,
    - the measurement code,
    - the instrument code,
    - the serial,
    - the type in which the data are recorded (integer, real, synoptic),
    - the depth or pressure (if constant),
    - three attributes.

A data record consists of :

- a data file name (to check whether the read data are those described in the first label record),
- the number of samples in the preceeding records,
- the number of samples in the record itself,
- the initial value of the continuous variable,
- the data.

The detailed structure of each record type is described in Appendix II. Only the structure for 16-bits or 32-bits computers is given.

Appendix I -- Specification of the wind field for real-time processing and forecasting

I.1.- Introduction

In a preliminary report [Frankignoul (1971)], the present state of knowledge on wind stress determination was reviewed. Approximate formulae for the drag coefficient in different wind regimes were given, thus allowing to calculate from wind data the surface interaction terms for the ecological model of the Southern North Sea [Nihoul (1973)]. Preliminary information on the practical problem of collecting the required meteorological data was also given.

Arrangements have been made with the *Régie des Voies Aériennes* for real-time transmission via telex of all relevant meteorological data. Regular transmission to Liège University began in May 1973. The system that has been worked out for the specification of the wind field for real-time processing and forecasting is now operational. It is described in the present report. For illustration, computer plots of the observed and geostrophic wind field during the first three days of the JONSDAP experiment in September 1973 are reported. Mention is made of further improvements that will be permitted by an extensive study of the recorded data.

I.2.- Description of the available meteorological data

A number of regular weather stations have been selected for real-time specification of the wind field. These are mainly coastal stations and anchored light vessels within the zone comprised between 50 ° and 54 °N , 0 ° and 5 °E . Location and nature of the stations which are operational now is given in figure 2. A large number of coastal stations have been retained so far, although the relevance of their measurements to marine conditions is often questionable, due to considerable change of surface roughness. Work is undertaken to determine and eliminate those coastal stations that give meteorological data which are too influenced by the disturbing presence of land. Synoptic data is emitted

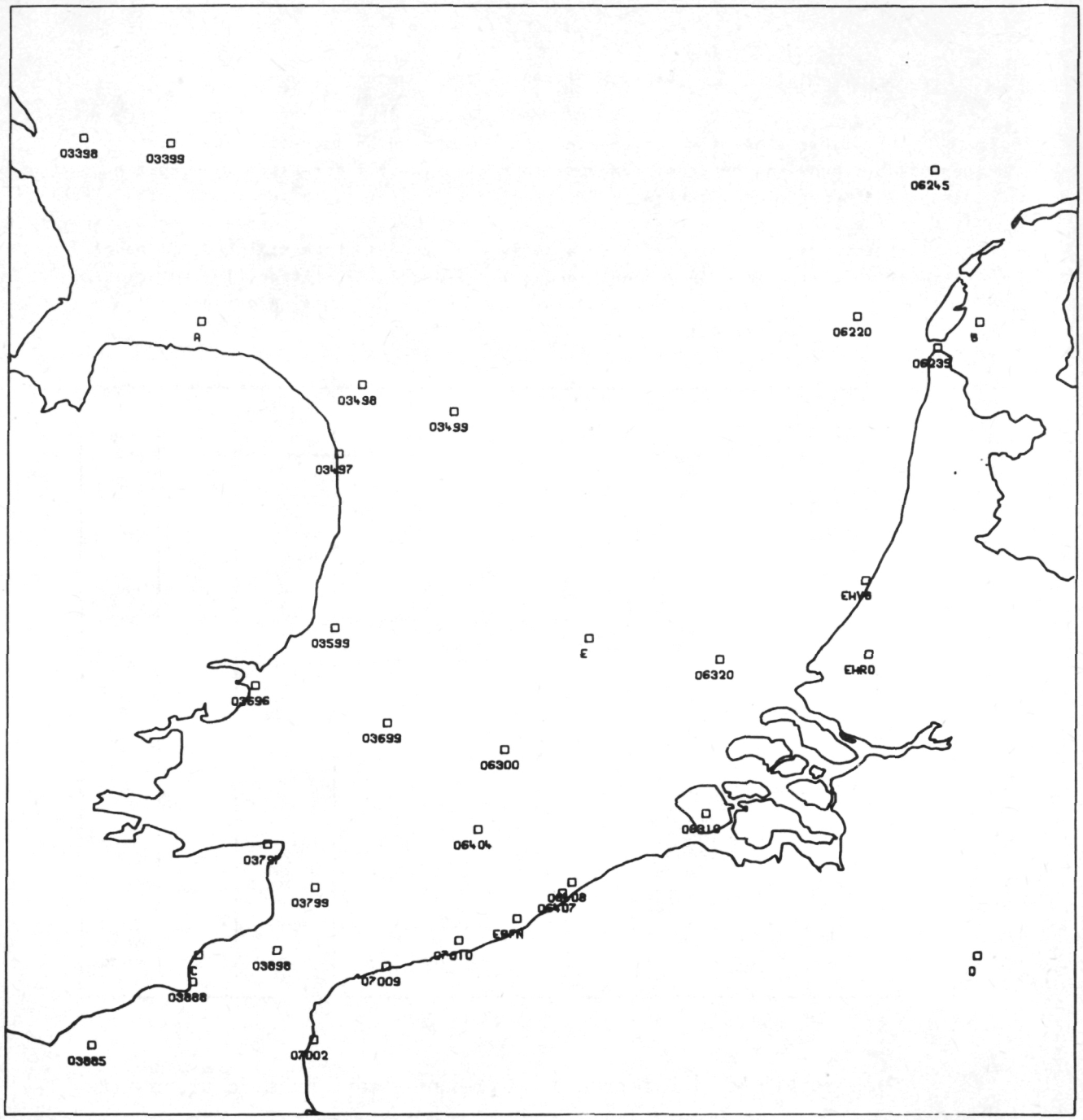


fig. 2.

by most stations every three hours, although some of them show much irregularity. Parameters retained for use in the mathematical model are listed in table 1.

Table 1

List of stored synoptic data

This table shows the various information stored on magnetic tape after the second data handling program. Some stations give their information in "english code", others in "Synop code", others in "Metar code". The set of information varies slightly with the used code. In order to store the information in a standard format, inexistant information is replaced by a dummy code (9999). Some stations, although they use a particular code, do not send all the usual information. The asterisks in the table point the information not always in the messages. A cross denotes an ever-existing information.

Type of data	Unit	English code	Synop code	Metar code
Station name	-	X	X	X
Surface horizontal visibility	meters	X	X	X
Wave height	half-meters	*	9999	9999
period	seconds	*	9999	9999
direction of propagation	tens of degrees	X	9999	9999
Temperature air	degrees °C	X	X	*
sea	degrees °C	X	9999	9999
dew-point	degrees °C	9999	X	*
Barometric pressure	tenths of millibars	*	X	*
Wind (at 10 m height) speed	knots	X	X	X
direction	tens of degrees	X	X	X
Weather present	coded	X	X	9999
past	coded	X	X	9999
Barometric trend	coded	9999	X	9999
Caracteristic of barometric trend	coded	9999	X	9999

Geostrophic wind inferred from pressure maps is also transmitted every three hours, at five locations : 51 °N , 05 °E ; 51° N , 05 °E ; 52 °N , 03 °E ; 53 °N , 01 °E and 53 °N , 05 °E . So far this wind is hand-analysed by experienced meteorologists. In a later stage, the calculation will be computerized at the R.V.A.

Twelve hourly geostrophic wind forecasts at the five locations are similarly transmitted every six hours. More extended forecasts might be used in case of urgency but they are not very reliable at present.

Information coming from ships at random positions and times cannot be handled so far but this is felt to be unimportant, due to the dense distribution of regular stations and the poor quality of ship recorded meteorological data. On the other hand, data from moored buoys is very reliable. A system will be set up to incorporate such data in case of long term mooring. Work will begin on this problem as soon as the first Belgian buoy becomes operational.

I.3.- Data handling

The data is transmitted every three hours via telex from the R.V.A. It is recorded automatically on punched tape in telex code. This punched tape is then stored on a magnetic tape in a chronologic sequence. At regular time intervals (every week or every day, if there is some urgent need) the first program of the data handling chain transfers the results :

a) on another magnetic tape which will be interpreted later;

b) on a listing which provides information for subsequent treatment.

This latter magnetic tape is the input of the second program which interprets the coded messages issued in different codes from the various field stations into numeric values usable by the following programs.

Output of this second step is :

1) data sets on magnetic tape which are stored in chronologic order; there are three kinds of these :
   - data sets containing the results of measurements in field stations;
   - data sets containing 'measured' geostrophic wind at five points;
   - data sets containing predicted geostrophic wind at the same five points.

   Every data set is defined by the time (year, month, day, hour) at which the measurements were made. A data set includes the most complete possible set of observations (even if some are missing or never produced by a particular station) *cf.* table 1, of 28 meteorological stations (27 before January 1st 1974).

2) an optional listing of messages in readable form.

These two first programs form the very first steps of the data processing. These steps must be executed whatever is needed and whatever the following treatment programs are.

The intermediate output is a set of 'crude' data stored in a standard format usable as input by any subsequent program.

It must be emphasized that the rough data from the meteorological stations is only decoded and translated into numerical form. No kind of smoothing, interpolation or debugging has been performed at this point of the treatment. This is intended to store the most original possible measurements; doing so, it will be possible later to determine the eventual bias or systematic errors in data issued by some stations and introduce the corrections in the data handling programs themselves.

I.4.- Observed and geostrophic wind

Weather forecasting provides information on the surface pressure field, which is then converted into a field of geostrophic wind. An important question is then how the surface wind at sea may be derived from the geostrophic wind.

Under ideal conditions (no frontal situation, quasi-steady pressure gradients, weakly curved isobars), the ratio of surface wind speed to geostrophic wind speed depends mainly on the geostrophic wind speed, the stability of the density stratification and the latitude. Hasse and Wagner (1971) have investigated this problem from observations at the German Bight near $54\ ^{\circ}N\ 7^{\circ}E$. The similarity with our test-region and the proximity in latitude of their observation zone suggest the direct applicability of their results. Using standard regression techniques, they found that the relation between the surface wind speed U_{10} and the geostrophic surface wind U_g was (in m/s) :

(1)
- under stable conditions : $U_{10} = 0.56\ U_g + 3.0$
- near neutral : $U_{10} = 0.56\ U_g + 2.4$
- stable : $U_{10} = 0.56\ U_g + 1.5$

with standard deviation 2.1 m/s approximately independent of wind speed in the range $5\ m/s \leq U_g \leq 32\ m/s$. Air-sea temperature difference was

used as stability parameter; the conditions are unstable if

$$\Delta T = T_{air} - T_{water} \ll 0 ,$$

near neutral if

$$\Delta T \simeq 0 ,$$

and stable if

$$\Delta T \gg 0 .$$

The stability can be established readily from the synoptic data, for a number of sea stations. Conditions are considered unstable or stable if the mean temperature difference ΔT is less than $-1.2\ ^{\circ}C$ or greater than $0.7\ ^{\circ}C$ respectively and otherwise neutral.

Wagner and Hasse disregarded all cases where U_g was below 5 mph as the pressure gradient is then too small to be determined reliably. As those cases are of littly dynamical significance, we will use (1) for any value of the geostrophic wind. Note that at small wind speed, U_{10} is larger than U_g mainly because the surface wind is a local variable (influence by grestiness and small scale circulation) whereas U_g is a mesoscale variable.

Under general circumstances, there appear occasionally cases with fronts, noticeable curvatures or marked non stationarities in the pressure field. Curvature effects can be taken into account by computing the gradient wind instead of the geostrophic wind. Approximate formulae for the gradient wind are known. However the work of Neiburger *et al.* (1948) suggests that, over land, the geostrophic wind is more suitable for the determination of the actual wind than the gradient wind. Aagaard (1969) estimates that the error in neglecting curvature is no more than a few percent. Thus it will be neglected although it might play a role at high wind speed [Deacon (1973)]. Formulae (1) will be used, keeping in mind that under general circumstances, the standard error is larger than given.

Formulae (1) describe how to relate the magnitude of observed and geostrophic wind. There is also a small angle between the two vectors which has also to be taken into account. In most studies, the coded directions (in terms of degrees) do not permit a meaningful investigation of this small effect. From the results of Aagaard (1969), Smith (1970)

and Deacon (1973), a reasonable estimate is a $15° - 20°$ counterclockwise rotation of the surface wind U_{10} from the geostrophic wind U_g. We shall adopt

(2) $$\alpha = + 20° .$$

Further test and improvement of relations (1) and (2) will be undertaken using the data whose acquisition system is described.

I.5.- Example of application

As an example of use of meteorological data, we have computed the wind field over the Southern Bight during the first days of JONSDAP survey. The values of wind speed and direction have been interpolated from observed data. The points where the wind field has been calculated are the points of a grid used for tidal computations in the Southern Bight (this grid covers well the studied region). To each point of this computational grid are associated the five nearest meteorological stations. Three of these stations (the nearest ones yielding required information at a given time) are used to compute the value of a function at a point (i,j) of the grid with the formula :

$$f_{ij} = \frac{\sum_{K=1}^{3} \frac{f_K}{d_{ij,K}}}{\sum_{K=1}^{3} d_{ij,K}}$$

where $d_{ij,K}$ is the distance between the (i,j) point and the station K . If the data from any station is obviously wrong, it is then automatically dropped off. Three-hourly information is then integrated over one day in order to get an average daily value. The results of the computation are shown on fig. 3. For the sake of readability, the wind vectors (underlined) are drawn only every two points. The vectors point to the point where the wind is computed and their direction is that of the coming wind.

fig. 3.

WIND FIELD OVER THE SOUTHERN BIGHT

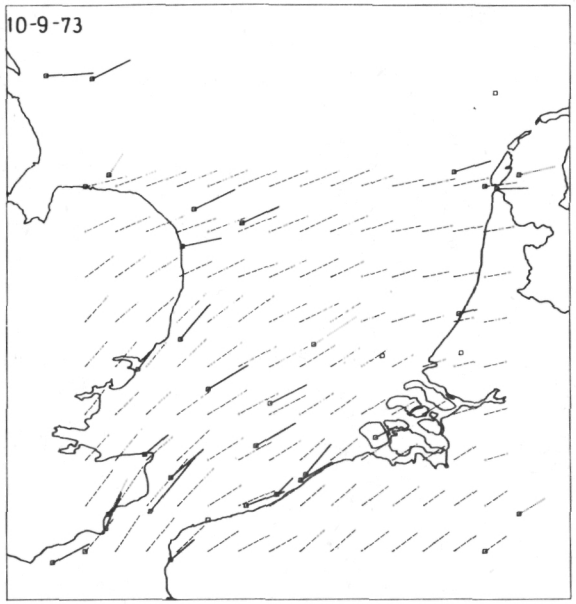
OF THE NORTH SEA DURING JONSDAP 73

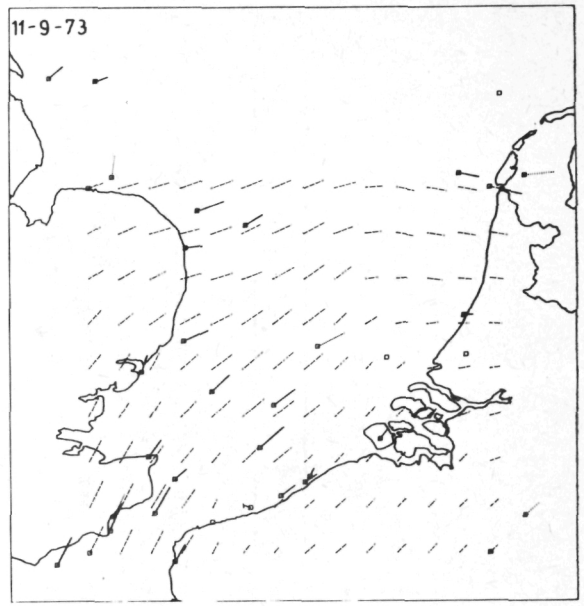
—— OBSERVED WIND

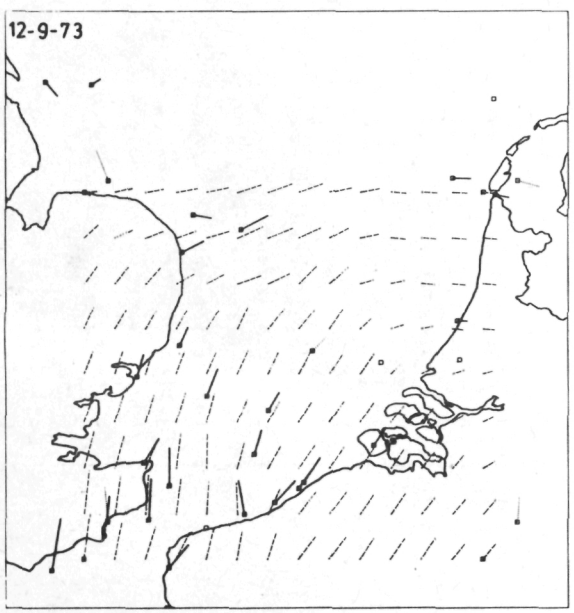
..... OBSERVED GEOSTROPHIC WIND

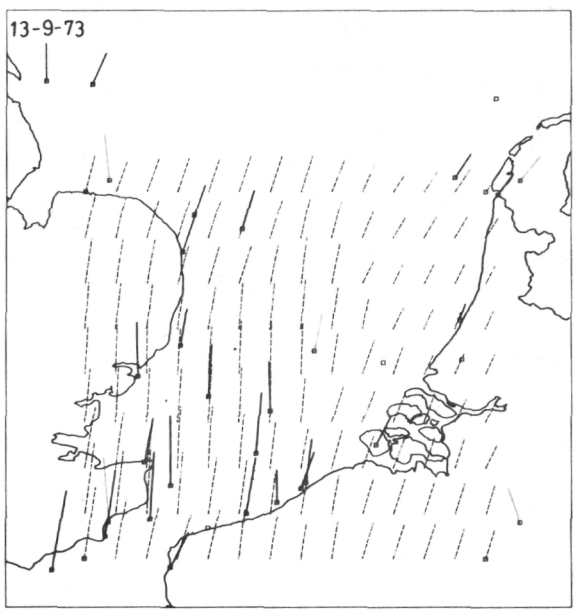
------ INTERPOLATED WIND

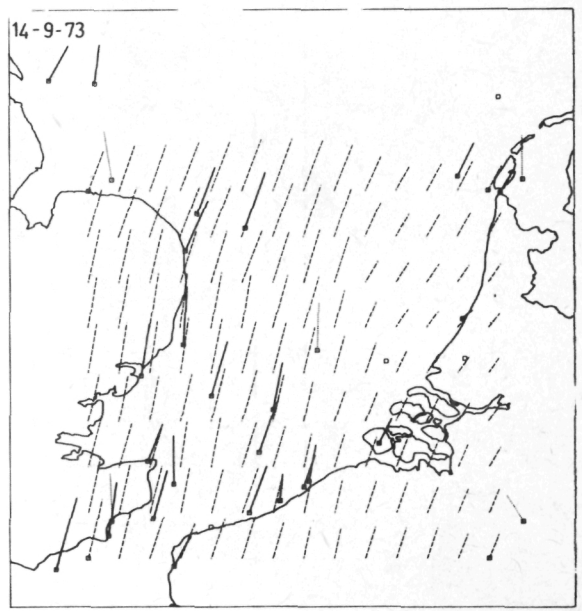
SCALE —— 10 M/S











Appendix II

Label record # 1 (Magnetic Tape format)

Word	Meaning
1	Record length
2	0
3	Record length
4	0
	} this information is needed by some sophisticated Operating Systems
5	Key-word : integer word (value = 1) : defines a Label # 1 record
6	Interchange code (code of the internal character representation) Integer : (1) EBCDIC (2) ASCII
7	Internal code : integer word
8-17	Data Name (20 bytes) - 4 bytes for a mnemonic code (nature of data) - 4 bytes for a station - 7 bytes for the radio identification of the data acquisition support (buoy, bart, ...) - 5 bytes for a mnemonic code (history of data)
18-22	Date of File creation (5 integer words : year-day-hour-minute-second)
23-24	Data source (4 bytes)
25	# variables (integer)
26	# samples (integer)
27	Format of the second Label record (integer) (standard value = 1)
28-32	Date of data origin (5 integer words : year-day-hour-minute-second)
33-104	Comments (144 bytes)

Label # 2

Word	Meaning
1	Record Length
2	0
3	Record Length
4	0
	} see Label # 1 description
5	Keyword : integer word (value = 2) : defines a Label # 2 record
6	of sub samples (integer) (value = 1 if no sub sampling)
7-8	Sampling interval (real word) : meaningfull only for data depending on a continuous variable
9-10	Subsampling interval (real word) : meaningfull only if both former informations are meaningfull
11-12	Julian day or initial value of continuous variable other than time or 0 (no continuous variable)
13-14	Seconds or - 1 or 0
15-18	Latitude : 8 bytes : degrees-min-seconds
19-22	Longitude : idem
23-26	Magnetic variation : idem
	} for standard format 1 Otherwise, 24 bytes available to describe another standard format

Label # 2 (continuation)

Word	Meaning
27-32	Variable name : 12 bytes
33-38	Dimensional units : 12 bytes
39-40	Measure code : 4 bytes
41-42	Instrument code : 4 bytes
43-44	Serial # : 4 bytes
45	Data Type : 2 bytes { 'I' : integer; 'R' : real; 'S' : synoptic }
46	Depth (in meters) or pressure (in mb) or 0 (integer word)
47-48	1st attribute (real)
49-50	2nd attribute (real)
51-52	3rd attribute (real)

This set of information is repeated for every variable in the data file (up to 64)

Data record

Word	Meaning
1	Record length
2	0
3	Record length
4	0

(words 1-4: see Label # 1 description)

Word	Meaning
5	Keyword : integer word (value = 3) : defines a data record
6-15	Data Name (see Label # 1 description)
16	# samples in preceeding data records (integer)
17	# samples in this record
18	Not used
19-20	Julian day or initial value of the continuous variable in this record
21-1172	Data

References

AAGAARD, K;, (1969). Relationship between geostrophic and surface winds at weather ship M, *Journal of Geophysical Research, 74,* 3440-3442.

DEACON, E.L., (1973). Geostrophic drag coefficients, *Boundary-Layer Meteorology, 5,* 321-340.

FRANKIGNOUL, C.J., (1971). Preliminary report on air-sea interaction, *Technical Report N7,* C.I.P.S.

HASSE, L. and WAGNER, V., (1971). On the relationship between geostrophic and surface wind at sea, *Monthly Weather Review*, *99*, 255-260.

NEIBURGER, M., SHERMAN, L., KELLOGG, W.W., GUSTAFSON, A.F., (1948). On the computation of wind from pressure data, *Journal of Meteorology*, *5*, 87-92.

NIHOUL, J.C.J., (1973). *Interactions at the sea boundaries*, in *Proceedings of the 5th Liège Colloquium on Ocean Hydrodynamics*, (Mémoires de la Société Royale des Sciences de Liège).

NIHOUL, J.C.J., (1974). *Réflexions sur la finalité d'une banque de données*, in *Proceedings du Colloque 'Informatique et Environnement'* (Arlon, 1974).

MALTAIS, J.A., (1969). *A nine-channel digital magnetic tape format for storing oceanographic data*. Unpublished manuscript n° 69-55 WHOI.

Chapter IV

Study of the contamination of fish and shell fish

by

P. HERMAN and R. VANDERSTAPPEN

Based on work by Fisheries Research Station, Ostend (Biometry); Institute for Chemical Research, Tervuren (Heavy metals); Station for Phytopharmacy, Gembloux (Pesticides, P.C.B.); all from Ministry of Agriculture (D.G. Research).

1.- Heavy metals

The results mentioned in the present report concern work that has been done in 1974 and that succeeds to the report 1973 *Study of the pollution in sea fish and shell fish.*

Taken in a whole, the activities of 1974 may be subdivised in the continuation of the research of 1973 — observation of the Belgian Coast and study of the Belgian fishery with regard to the contents of heavy metals and organic forms of mercury in the fillets of different species of fish and in shrimps — and in new activities :

- the systematical determination of the contents of methylmercury in different species of fish (fillets) and shrimps;
- determination of heavy metals contents in the liver and the stomach content of different fish species.

The fish and shrimps studied by the Institute of Chemical Research are furnished by the Station for Maritime Fishery that makes biometric studies on them.

- A third activity is the determination of heavy metals contents in organisms collected by the team Van der Ben on the breakwaters of the Belgian Coast.

The results of the work that has been done in 1974 are successively presented as follows.

1.1.- Heavy metals in the fillets

1.1.1.- Determination intended to get together a statistical series of 50 individuals for each species

In shore fishery (Fisheries 1972, 6 species)

Table 1 : mean Hg, Cu, Pb and Zn content in plaice , whiting, sprat, herring and shrimps for n = 50 .

Off shore fishery (Belgian fishery products from July 1972 till end 1973)

Table 2,3 : mean Hg, Cu, Pb and Zn content in plaices and soles of the northern North Sea and the Bristol Channel.

1.1.2.- Evolution of the percentage of heavy metals in fish and shell fish since end 1971 (Initial study)

In shore fishery (Fishing periods from end 1-71 till end 1973)

Table 4 : mean periodical Hg and Cu content (4 fish species and shrimps).

Off shore fishery (Fishing in four regions during the years 1972 and 1973)

Table 5,6 : mean Hg and Cu content per periods 72-73 in plaices and soles (Northern North Sea, Irish Sea, Bristol Channel, English Channel).

1.2.- Methylmercury

First series of determinations on species with different origines (Belgian Coast and other places).

Table 7 : individual relations methylmercury / total mercury.

Table 8 : mean relations methylmercury / total mercury.

1.3.- Heavy metals in the liver, the stomach content and the fillets

Table 9 : Hg and Cu content (individual and mean) in fillets, liver and stomach content of whiting (1974 fishing, Belgian Coast).

1.4.- Heavy metals in marine organisms

Table 10 : mean Hg and Cu contents in marine organisms collected on the breakwaters of the Belgian Coast (1974).

Table 1

Mean levels of Hg, Cu, Pb, Zn (ppm)
Belgian coast : Plaices - Whiting - Cod - Sprats - Herring - Shrimps
(Fisheries 1972)

n = 50	Hg			Cu			Pb			Zn		
	$\bar{X}$	σ	$\sigma/\bar{X}$ (%)	$\bar{X}$	σ	$\sigma/\bar{X}$ (%)	$\bar{X}$	σ	$\sigma/\bar{X}$ (%)	$\bar{X}$	σ	$\sigma/\bar{X}$ (%)
Plaices	0.19	0.08	42	0.77	0.33	42	0.30	0.07	23	6.40	1.60	25
Whiting	0.21	0.10	48	1.07	0.44	41	1.04	0.98	94	10.6	8.82	83
Cod	0.19	0.17	89	0.74	0.39	53	0.33	0.14	42	5.11	1.36	27
Sprats	0.15	0.06	40	1.32	0.49	37	1.67	1.4	84	24.3	5.7	23
Herring (1973)	0.05	0.02	40	0.88	0.26	30	0.28	0.07	25	8.7	2.6	30
Shrimps	0.10	0.03	30	14.6	3.26	22	3.42	3.25	98	26.5	6.47	24

Table 2

Mean levels of Hg, Cu, Pb, Zn (ppm)
Off shore Fisheries (1972) : Plaices

n = 50	Hg			Cu			Pb			Zn		
	$\bar{X}$	σ	$\sigma/\bar{X}$ (%)	$\bar{X}$	σ	$\sigma/\bar{X}$ (%)	$\bar{X}$	σ	$\sigma/\bar{X}$ (%)	$\bar{X}$	σ	$\sigma/\bar{X}$ (%)
Irish Sea	0.35	0.23	66	0.79	0.35	44	0.38	0.47	124	5.98	1.67	28
Bristol Channel	0.20	0.12	60	0.62	0.36	58	0.33	0.22	67	6.58	3.74	57
North Sea	0.20	0.14	70	0.58	0.23	40	0.40	0.58	145	6.33	2.54	40

Table 3

Mean levels of Hg, Cu, Pb, Zn (ppm)
Off shore Fisheries (July 1972 till end June 1973) : Soles

n = 50	Hg			Cu			Pb			Zn		
	$\bar{X}$	σ	$\sigma/\bar{X}$ (%)	$\bar{X}$	σ	$\sigma/\bar{X}$ (%)	$\bar{X}$	σ	$\sigma/\bar{X}$ (%)	$\bar{X}$	σ	$\sigma/\bar{X}$ (%)
Bristol Channel	0.17	0.12	68	0.86	0.46	53	0.38	0.13	34	10.1	6.55	65
North Sea	0.31	0.21	69	1.06	0.65	61	0.38	0.22	59	9.1	3.44	38

Table 4

Mean levels : Hg, Cu (ppm)
Belgian coast : Plaices - Whiting - Cod - Sprats - Shrimps (71-72-73)

Quarter	Plaice			Whiting			Sprats			Cod			Shrimps		
	Hg	Cu	n	Hg	Cu	n	Hg	Cu	n	Hg	Cu	n	Hg	Cu	n
IV/71	0.14	-	46	0.14	-	67	0.14	-	12	0.10	-	34	0.10	-	10
I /72	0.14	0.67	57	0.17	0.84	25	0.15	1.20	23	0.14	0.70	43	0.10	12.2	57
II/72	0.16	0.81	41	0.17	0.86	59	0.11	1.97	9	0.16	0.48	5	0.12	12.5	27
III/72	0.22	0.77	86	0.23	1.49	59	0.17	1.25	16	-	-	-	0.10	16	13
IV/72	0.18	0.90	80	0.18	1.51	107	0.14	1.74	21	0.29	1.09	15	0.09	15	51
II/73	0.19	-	16	0.20	-	30	-	-	-	-	-	-	-	-	-
IV/73	0.12	-	15	0.21	-	10	-	-	-	-	-	-	-	-	-

Table 5

Mean levels of Hg, Cu (ppm)
Off shore Fisheries : Plaices (1972)

Quarter	Southern North Sea			Bristol Channel		
	Hg	Cu	n	Hg	Cu	n
I /72	0.17	0.60	8	0.16	0.73	12
II/72	0.25	0.62	10	0.20	0.76	5
III/72	0.27	0.48	10	0.25	0.70	15
IV/72	0.30	0.78	14	0.23	0.74	14

Table 6

Mean levels of Hg, Cu (ppm)
Off shore Fisheries : Soles (72-73)

Quarter	North Sea			Bristol Channel			English Channel		
	Hg	Cu	n	Hg	Cu	n	Hg	Cu	n
III/72	-	-	-	0.15	0.64	10	-	-	-
IV/72	-	-	-	0.20	1.43	9	-	-	-
I /73	-	-	-	0.15	0.60	33	0.20	0.63	24
II/73	-	-	-	0.13	0.69	13	0.33	0.89	26
III/73	0.35 0.18	1.21 -	22 21	0.20	1.15	40	0.40	1.03	14
IV/73	0.14	-	30	0.16	1.39	13	0.24	-	14

Table 7

Mercury contents and % methylmercury

Species	Hg (total) (ppm)	Methylmercury Hg (total) (%)
Soles North Sea IV/73	0.04	75
	0.05	80
	0.09	66
	0.15	53
	0.16	50
	0.22	63
	0.30	66
Plaices Bristol Channel IV/72	0.11	81
	0.14	100
	0.14	93
	0.15	93
	0.15	86
	0.16	68
	0.21	71
	0.39	56
	0.46	32

Table 7

(continuation)

Species	Hg (total) (ppm)	Methylmercury Hg (total) (%)
Whiting Belgian coast IV/72	0.11	91
	0.13	100
	0.16	100
	0.17	76
	0.34	65
	0.38	53
	0.49	37
Shrimps Belgian Coast IV/72	0.10	60
	0.10	60
	0.10	40
	0.10	40
	0.10	40
	0.13	35
	0.15	27
	0.18	17

Table 8

Mean levels : Mercury contents and % methylmercury

Area	Quarter	Hg (total) (ppm)	Methylmercury Hg (total)	n
Soles				
North Sea	IV/73	0.15 (0.05-0.30)	65 (80-50)	7
Bristol Channel	IV/73	0.22 (0.12-0.30)	44 (65-13)	10
Plaices				
Bristol Channel	IV/72	0.21 (0.16-0.46)	77 (100-32)	10
Belgian coast	IV/72	0.20 (0.12-0.39)	36 (40-20)	13
Whiting				
Belgian coast	IV/72	0.24 (0.13-0.49)	74 (100-37)	10
Sprats				
Belgian coast	IV/72	0.14 (0.09-0.20)	45 (90-26)	10
Shrimps				
Belgian coast	IV/72	0.12 (0.10-0.18)	37 (60-17)	10

Table 9

Fillet - Liver - Stomach content
Belgian coast : Whiting (April 1974)

N° Spec.	Fillet		Liver		Stomach content		
	Hg ppm	Cu ppm	Hg ppm	Cu ppm	Hg ppm	Cu ppm	Nature of the content
49	0.13	1.0	0.16	15.6	0.24	4.2	sprat
50	0.19	0.7	0.11	8	0.17	3.4	!
51	0.10	1.7	0.13	4.2	0.12	2.5	!
52	0.23	0.6	0.09	6.4	0.15	2.2	Shrimps
53	0.23	2.0	0.12	7.1	0.22	4.9	Shrimps
54	0.62	1.2	0.27	4.4	0.11	2.2	!
55	0.17	2.6	0.08	6.4	0.12	3.8	!
56	0.23	1.6	0.10	6.9	0.12	10.2	!
58	0.15	0.8	0.04	5.4	0.13	1.7	!
59	0.19	1.5	0.05	9.6	0.08	3.3	Shrimps
60	0.23	1.8	0.12	6.2	0.10	0.81	!
61	0.20	0.9	0.13	10.1	0.14	3.4	Shrimps
$\bar{X}$	0.22	1.4	0.12	7.5	0.14	3.6	
σ	0.13	0.61	0.06	3.14	0.05	2.4	
$\sigma/\bar{X}$	68	44	50	42	36	67	

Table 10

Average content of Hg, Cu, Zn, Pb
(ppm, dry matter)
Belgian coast : marine organisms (breakwaters - 1974)

Species	n	Hg	Cu	Pb	Zn
Ulva lactuca	12	0.13	8.1	6.3	44
Fucus spiralis	7	0.11	5.5	5	200
Porphyra umbilicalis	2	0.03	22.3	2.4	85
Navicula	1	0.21	86	20.4	127
Asterias rubens	1	0.34	6.1	3.9	210
Mytilus edulis	12	0.44	10	6.8	185
Littorina littorea	13	0.24	73	2.9	80

1.5.- Conclusions

1.5.1.- Heavy metals in fish (fillets) and in shrimps

Factors having an influence

In brief, the conclusions of previous reports have been confirmed : the mean contents of heavy metals may vary between classes and species from one region to the other and according to the period (tables 1, 2, 3 and 10). *In the same species* there is a clear cut correlation between the total Hg content and the age (weight) and the mean contents may be very different according to the regions (tables 2, 3, 4, 6).

The new results strengthen the assumption of a variation of the contents according to the seasons, with higher contents in summer (tables 4, 5, 6). We suggest connecting these fluctuations with those of the primary productivity. Abdullah and Royle (1973) found a similar variation for cadmium in plankton.

Levels of contents

If the Hg levels were already well defined, it is also the case in this moment for Cu, Pb and Zn. It has been confirmed that Zn and Pb contents (25 and 3 ppm) are higher in sprats and shrimps and that shrimps have a higher Cu content (15 ppm).

As for Hg, there should be a fluctuation in function of the seasons.

As for Hg, Cu, Pb and Zn contents of a same species are distributed according to a normal log way, with a variation coefficient of about 50 % . In some species however, such as whiting, plaices, sprats and shrimps (tables 1, 2), this coefficient is nearly 100 % or higher for Pb.

As far as Pb distribution is concerned, we obtain rather curious results : *plaices*, captured in four different regions, have very closely related mean contents (0.3 to 0.4 ppm Pb) but, according to the regions the variation coefficients are very divergent — from 23 % (Belgian Coast) to 145 % (North Sea); *soles*, on the other hand, from three of the same regions have mean contents of the same rate (0.38 to 0.39 ppm of Pb), but the variation coefficients are not very divergent and smaller than those of plaices (tables 1, 2, 3).

In short, same mean Pb content in plaices as in soles, in all cases a correlation between the variation coefficients and the region, 2 to 3 times higher variation coefficients in plaices (in every case there is a series of 50 samples). There seems to be a different physiological reaction.

Cadmium

We have had a great number of cadmium determinations, but notwithstanding several restatements of the question, we are not pleased with the absolute value of the results. The levels we found are nearly 0.2 to 0.4 ppm Cd for soles and 0.7 ppm for whiting; they are considered to be too high and research continues in better conditions on biological material; determination on a great series will follow afterwards.

Nevertheless, the results have a comparative value.

According to the series of 50 samples that have already been analysed, it seems to be evident :

- that for a same species, the means vary in function of the region (soles : North Sea 0.2 ppm; Irish Sea 0.4; Bristol Channel 0.2);
- that the means vary according to the species (soles 0.2 to 0.4 ppm; whiting 0.7 ppm);
- that the variation coefficients vary between 30 and 55 % .

1.5.2.- Methylmercury

Variations according to the species

As appears from table 8, the ratio methylmercury/total mercury differs from one species to another.

In short for the Belgian coast it varies between 36 % for plaices and 74 % for whiting, whereas for the Bristol Channel it varies between 44 % for soles and 77 % for plaices, the total Hg contents being the same. It should be interesting to compare these fluctuations with those of the sulphurated amino acid contents of the same species, those contents may be correlated with the Hg retention.

Variation in the same species

Generally the relation Me-Hg/total Hg varies in inverse ratio to the total mercury contents.

The results are given in table 7.

For *whiting*, the relation reaches 100 % for contents of about 0.1 ppm total Hg and 37 % for ± 0.5 ppm . For *plaices* nearly 100 % for 0.1 ppm total Hg and 32 % for ± 0.5 ppm ; for shrimps 60 % for 0.1 ppm total Hg and nearly 17 % for ± 0.2 ppm . Kosta *et al.* (1974) made a similar observation for a Hg polluted river : "The reduction of total Hg in trout keeps pace with the increase of the methylmercury fraction."

As it is known that the total Hg content is correlated with the age, we may say that the degree of methylmercury increase lessens with the age.

Variations according to the region

For an almost equal mean content of total mercury, a same species may give, according to the regions, totally different relations Me.Hg/ total Hg. Examples are given in table 8.

Plaices of the Bristol Channel and the Belgian Coast have mean contents of total mercury of respectively 0.21 and 0.20 ppm , while the corresponding relation Me-Hg/total Hg are 77 and 36 % , for soles of the southern part of the North Sea and the Irish Sea the contents are 0.40 and 0.37 ppm , the relation 34 and 47 % .

The relative value of the methylation degree of mercury seems important enough to be considered in order to differentiate the regional pollution.

Remarks

After these considerations it becomes apparent that the above mentioned seasonal variations of the total mercury contents should be mainly imputable to the mineral mercury. Indeed, an increase of the content generally keeps pace with a decrease of the methylmercury proportion, while the phenomenon of subsequent elimination of Hg for plaices

is certainly more complicated with methylmercury as CH_3-Hg-proteinate, the half life of which having been rated at 780 days by Hasanen (1973).

In view of the high toxicity of Me-Hg and of the fact that the relation Me-Hg/total Hg presents a high variability, a low content of total mercury, from the point of view of fish consumption, could present the same risks as a higher one.

1.5.3.- Distribution of heavy metals in fillets, liver and stomach content of whiting (Belgian Coast)

These are the first results, for Hg and Cu (table 9) of the new development of our studies.

With regard to the comparison of the contents of the different organs :

- on the average and in most cases copper is more abundant in liver, next in the stomach content;
- on the average and in several cases total mercury is more abundant in fillets.

Those first trials seem to confirm some data of the literature according to which there should be a greater accumulation of Hg in the muscles than in the liver [Gilles *et al.* (1973)] in less polluted areas. A higher Cu-content in the liver is probably not at all an exception, in view of the function of this organ.

The research concerning the relations between the content of the muscle and that of the liver and the stomach content have been unsuccessful, except for Hg between muscle and liver where a correlation $r = 0.75$ implicates a 99 % significative correlation.

New series are already examined, and also new elements such as Me-Hg.

1.5.4.- Marine organisms captured on the breakwaters

This study, started in 1974, is based upon four campaigns during which marine organisms (sea-weed, diatoms, mussels, littorines, etc.) are captured on the breakwaters of the Belgian coast. Only heavy metals are studied.

Table 10 gives the mean contents, calculated on the dry material (the water content is generally ± 70 %).

Concerning the three animal species that already have been studied (mussels, littorines and star-fish), we may admit that, pro element, the Hg-, Cu-, Pb- and Zn-contents are nearly the same; nevertheless an exception should be made for littorines with a Cu-content of 73 ppm and for mussels and starfish with a Zn-content of ± 200 ppm .

Compared with the heavy metal contents in fish and shellfish, calculated on dry material (nearly 3.5 times the values calculated on fresh material), the Hg and Pb contents are nearly the same. The contents are higher for copper in littorines (that contain hemocyanine) and rank above those of shrimps (nearly 73 against 50 ppm). Starfish and mussels have a nearly three times higher Zn content than the high value found for this element in sprats and shrimps.

2.- Pesticides and P.C.B. [Henriet]

As for the heavy metals — continuation of the determination of pesticides and P.C.B. intended to get together a statistical series for each studied species (plaice, sole, whiting, cod, sprats, shrimps, herring) and different fishing groups — the results confirm that the contents are relatively low and there is no differentiation between regions. The means are : pp'DDT : 0.004 ppm ; DDD : 0.002 ppm ; DDE : 0.002 ppm ; Lindane : 0.003 ppm ; Dieldrine : 0.002 ppm ; P.C.B. : 0.04 ppm .

For recall the amounts of the different kinds of pesticides and P.C.B. are clearly higher in the sprats.

References

ABDULLAH, M.I., ROYLE, L.G., (1973). *Cadmium in British coastal waters environments*, C.E.C. Luxembourg European Colloquium .

KOSTA, L. *et al.* (1974). Fate and significance of mercury residues in an agricultural ecosystem, *Proceedings and report of research coordination meetings ISPRA 1972*, organized by FAO/IAEA, Vienna.

HASANEN, E., (1973). *Mercury pollution in Finland,* C.E.C. Luxembourg European Colloquium.

GILLES, G. *et al.* (1973). *Etat de la contamination par le mercure des poissons de mer et d'eau douce,* C.E.C. Luxembourg European Colloquium.

Chapter V

Inventory of the water- and sediment pollution

by

J. BOUQUIAUX and P. HERMAN

The inventory of the coastal zone and of the rivers, realised in 1974, has been assembled in an advancement report composed of eleven parts, a summary of which is given in the next pages.

New activities

Mr and Mrs Van der Ben, of the Royal Institute for Natural Sciences, have been associated to the inventory work. This made the following extensions possible :

- the study of the phytoplanktonic biomass of the mixing zone of the sea;
- the study of the contamination of marine organisms, caught on four breakwaters of the Belgian coast (vegetal and animal macro-specimens, diatomea).

Pursued inventory

- further study of the coastal zone;
- new studies of the river Meuse and of some rivers of its hydrographic bassin; idem for the rivers Ijzer, Schelde and Sure;
- a particular study of the rivers at the frontier point, only according to the water analysis (twenty-six places);
- a study of sediments of the Ghendt-Terneuzen Channel is going on.

Circumstantial results

It should be noted that all the results, just as the informations according to the places and data of the sampling are put on slips; exemplars of them exist in the Data Compiling Center. The complete list of the slips, kept since the beginning of the inventory and classified in alphabetical order of the sampling places, are given, for the coastal zone and per hydrograph basin, in an annex to the present report.

Studies

In 1973, a monography has been devoted to the river Ijzer; a second, that will be published during the first trimester of 1975, will refer to the river Vesdre.

I

Coastal zone

1.- Emissions (towards the sea)

1.1.- Chemical study of the water

(Based on work by J. BOUQUIAUX, K. DE BRABANDER, C. BOELEN, R. DE BOECK, H. VANDEPUTTE, J. VAN DIJCK, Mrs VERHOEVEN - Staff of the Institute of Hygiene and Epidemiology of the Department of Public Health; Mr. BULTYNCK, director of the T.V.Z.A.K.)

The study of the emission of pollutants into the sea concerned in 1974 the composition of the sewage, thrown out by the drains of Blankenberge and Nieuport during the whole month of July.

When the results 1974 of Blankenberge are compared with those of the summer 1972, we find a remarkable similitude for the organic pollution; on the other hand, the concentration of metals in the water varies from one year to the other : in 1974, the Cu- and Pb-contents are beneath the detection-limit, those of Cr, which are very constant, approach the 20 ppb.

In Nieuport the water undergoes a primary epuration and the organic pollution is not as important as in Blankenberge; for the metal contents there is a similitude, except for Cr that has not been found in Nieuport. By extrapolation of the pollutant load of July 1974, it was possible to make a crude estimation of the pollutants that are annually trained off into the sea by the drains of Blankenberge and Nieuport.

Table 1

	Blankenberge		Nieuwpoort	
	t/day	t/year	t/day	t/year
BOD	1.82	664	0.59	219
COD	3.76	1372	2.42	883
Susp. mat.	1.90	693	1.63	594
N_{tot}	0.46	168	0.45	165
N_{amm}	0.42	153	0.44	163
NO_2^-	0.038	14	0.185	67
NO_3^-	0.041	15	0.197	72
PO_4^{---}	0.094	34	0.070	26
Cl^-	7.045	2573	1.50	549
SO_4^{--}	1.065	389	0.87	316
Det. an.	0.060	22	0.0012	4
Cd	$0.109\ 10^{-3}$	0.040	-	-
Cu	-	-	-	-
Fe	$2.504\ 10^{-3}$	0.914	$2.72\ 10^{-3}$	0.992
Hg	$<0.002\ 10^{-3}$	-	-	-
Mn	$0.495\ 10^{-3}$	0.18	$0.229\ 10^{-3}$	0.084
Ni	-	-	-	-
Pb	-	-	-	-
Zn	$1.571\ 10^{-3}$	0.573	$1.458\ 10^{-3}$	0.532

1.2.- Bacteriology

(Based on work by Mrs DE MAYER, J. BARBETTE, J.P. DAUBY, J. DEMANET, J.M. SEBA - Institute for Hygiene and Epidemiology)

This year the control of the emissions of bacteriological pollutants in the North Sea was entirely devoted to the analysis of the material thrown out by the drains of Nieuport and Blankenberge during the month of July.

On the basis of 10 samples for Nieuport and of 11 samples for Blankenberge those samples are mean samples taken over a period of 3 days or 72 hours, we proceeded to a counting of total, coliform, faecal coliform and faecal streptococcic germs. The number of germs found in the samples varied very little during the sampling period. There is a remarkable similitude between the number of germs in July 1973 and 1974, as it appears from the following table concerning the situation in Blankenberge.

Table 2

(col./100 mℓ)

	July 1973	July 1974
coliform germs	10^9	5.10^8
faecal coliform germs	5.10^8	10^8
faecal streptococcic germs	10^6	5.10^6

It is nearly impossible to make a repartition of the number of germs per equivalent inhabitants, there is too big a fluctuation of the inhabitants of the two stations during the observation period, and this makes the comparison with a stationary population impossible. According to these results, the influence of the primary epuration in Nieuport is not very important. The difference with Blankenberge is maximum of a factor 10 and negligible with regard to the number of germs in the sewage.

It should be noted that each of the samples corresponds to 72 h of sampling; owing to the working conditions it is unfortunately impossible to make analyses every day.

1.3.- Sediments

(Based on work by P. HERMAN, R. VANDERSTAPPEN, K. MEEUS-VERDINNE, P. HANISET, J. ISTAS, J. CORNIL, G. LEDENT, R. VAN DER ZEYP, G. NEIRINCKX, H. STRUELENS, P. HEIMES - Institute for Chemical Research of the Ministry of Agriculture)

The deposits in sea of the outlets (sewage systems and channels) have been recalculated for the drains of Blankenberge and Nieuport. The

pollution by material in suspension and, in some degree, by the decantation mud, is very variable in the time, nevertheless we find important Ag-, Ba-, Bi-, Cu-, Hg- and Sn-contents in Blankenberge and Nieuport. From one year to the other the Pb- and Zn-values vary from very low to very high. The comparison of samples, taken in Blankenberge in summer and in winter, taking into account the variations of discharge and of material in suspension, reveals that the Cr-, Ni-, Cu- and Sn-contamination is more important during the summer.

The pollution of the "Spuikom" (where the overflow of the drain-system is discharged in periods of floods) is closely related with that of the sea in front of Blankenberge (most polluted place of the coast; there is a greater pollution of organic matter, of total sulphur and especially of crude).

2.- Immixture (mixing zone in the sea)

2.1.- Chemical study of the water

(Institute for Hygiene and Epidemiology, cf. § 1.1)

The first five series of samples, taken at the usual 12 sampling points have been completed by two new series bearing the numbers 6 and 7 and also taken at the same points. From the seven series of results one may draw the following conclusions :

Profile of the dissolved oxygen :

- increasing from Oostduinkerke till Middelkerke
- decreasing from Mariakerke till Heist
- increases lightly in Knokke.

The *nitrate* contents of the stations in the SW of Ostend are considerably below the average value. In Ostend they approach this value while in the NE we always find higher values, the difference being sometimes very important (as in Heist, for example).

For *phosphates*, on the other hand, we find only small deviations from the general average, except in Knokke.

Table 3

Mean concentrations of nutrients
(general average for the coastal zone)

	Units	Min	Max	$\bar{X}$	$\bar{X}$ [1]
N_{tot} [2]	mg N/ℓ	1	2.5	1.67	1.67
N_{amm}	mg N/ℓ	1	0.47	0.17	0.17
NO_2^-	mg NO_2^-/ℓ	0.04	0.07	0.05	0.015
NO_3^-	mg NO_3^-/ℓ	1.99	6.89	3.98	0.90
PO_4^{---}	mg PO_4^{---}/ℓ	0.20	1.00	1.22	0.38

1 Mean expressed in mg N/ℓ of mg P/ℓ .

2 Total nitrogen : organic nitrogen + ammoniacal nitrogen, with the exception of nitrites and nitrates.

Table 4

Mean heavy metal concentrations (µg/ℓ)

	Min	Max	$\bar{X}$
Cd	<1	<1	<1
Cu	13	19	14
Fe	81	153	136
Hg	0.09	0.24	0.14
Mn	54	100	68
Pb	14	22	18
Zn	27	49	39

Remark : the measurements are carried out by A.A.S. on decanted no filtered raw water.

The remark concerning the phosphate concentration applies also to Cu- and Pb-concentrations for which the deviation of the general average is very small. Contrary to what has been observed for nitrates, heavy metals are generally homogeneously distributed all along the Belgian Coast.

Superficial and deeper waters

In order to estimate the possible divergence between the values found in superficial and deeper waters, we took four double samples, no significant difference has been found.

2.2.- Bacteriology

(Institute for Hygiene and Epidemiology, cf. § 1.1)

The report mentions the results found in four sampling points, spread over the Belgian coast. These points are Lombardsijde, Mariakerke, Heist and Knokke.

2.2.1.- Bacteriological situation in the different stations

With reference to the faecal coliforms, the greatest number of germs has been found in the zone of Mariakerke in February, April, June, October and November (superficial and deeper waters) and also in August (deeper water).

In Lombardsijde we observed a serious increase of the number of germs in April and September.

In Heist we found a very high number of germs (superficial and deeper waters) in February.

2.2.2.- Bacteriological evolution as influenced by sampling period

There are two main contamination periods, the first one in spring, the other one in October-November. As no samples have been taken in September and October in Heist and Knokke, it is impossible to draw a conclusion concerning these two points. The number of germs, found in samples of deeper water, seems also to be greater than in superficial water. This difference could be ascribed to the influence of the tides and particularly of the current in this part of the water.

The same observations can be made concerning the number of faecal streptococci, which are unquestionable factors of human pollution.

In any case, the regularly most contaminated zone, from a bacteriological point of view, seems to be the zone of Mariakerke. Knokke, on the

other hand, notwithstanding the two higher values in April and October (superficial water) and in October (deeper water), has a low faecal coliform content and seems to be the less polluted zone.

Table 5

Faecal coliforms in superficial water

Stations	Febr.	April	May	June	July	Aug.	Sept.	Oct.	Nov.
Lombardsijde	200	1980	< 10	50	< 10	< 10	1100	290	880
Mariakerke	1200	1700	< 10	600	50	60	550	1100	1600
Heist	8200	400	10	300	50	< 20	-	1400	-
Knokke	800	150	10	< 10	10	< 10	-	320	-

Table 6

Faecal coliforms in deeper water

Stations	Febr.	April	May	June	July	Aug.	Sept.	Oct.	Nov.
Lombardsijde	600	800	10	50	< 10	< 10	1600	420	1440
Mariakerke	2200	3900	< 10	500	100	20	700	1800	3800
Heist	2800	150	30	300	100	20	-	1750	-
Knokke	2200	50	10	< 10	40	10	-	350	-

2.2.3.- Conclusions

a) The precise mechanism that governs the bacteriological situation of the water depends on different factors :

- the permanent and/or sporadic coastal supply with sewage. Nevertheless, nothing allows us to say that the touristic season has an influence on the pollution of the sea;

- the bacteriological effect of the sea-water on non-resistant germs;

- the influence of the general content (physical, chemical and biological) on the resistant germs.

b) The western part of the Belgian coast is more polluted at the beginning of the year.

c) On the other hand, the central part, with Mariakerke and Heist, is more polluted in October.

3.- Organisms on the breakwaters

Samples of mussels, periodically taken on four breakwaters by Mrs. Van der Ben have been studied. The results of the analyses were very irregular and to draw conclusions it will be necessary to expect the results of new samplings.

3.1.- Biomass

(Based on work by Mrs VAN DER BEN and Prof. I. ELSKENS, V.U.B.)

Estimation of the chlorophyll content of the sea-water of the Belgian coast in connection with the evolution of silica and NH_4^+ , NO_2^- , NO_3^- and PO_4^{---} ions. Every month samples have been taken at four of the twelve stations and inventorized by the group : Lombardsijde, Mariakerke, Heist and Knokke, both in superficial and deeper water.

3.1.1.- Results and discussion

Comparison between the stations

Water samples rarely have the same chlorophyll concentration at all stations and those differences are unequal from one station to another. Only the April concentrations, in superficial water, are alike in the four sampling points.

In function of the sampling period, the stations of Lombardsijde and Mariakerke present, in superficial and deeper waters, a comparable evolution with two classical maxima, the first one in the spring, the other one at the end of the summer.

On the contrary, the graphics concerning Heist and Knokke are not classical at all; they do not present a spring peak in the superficial

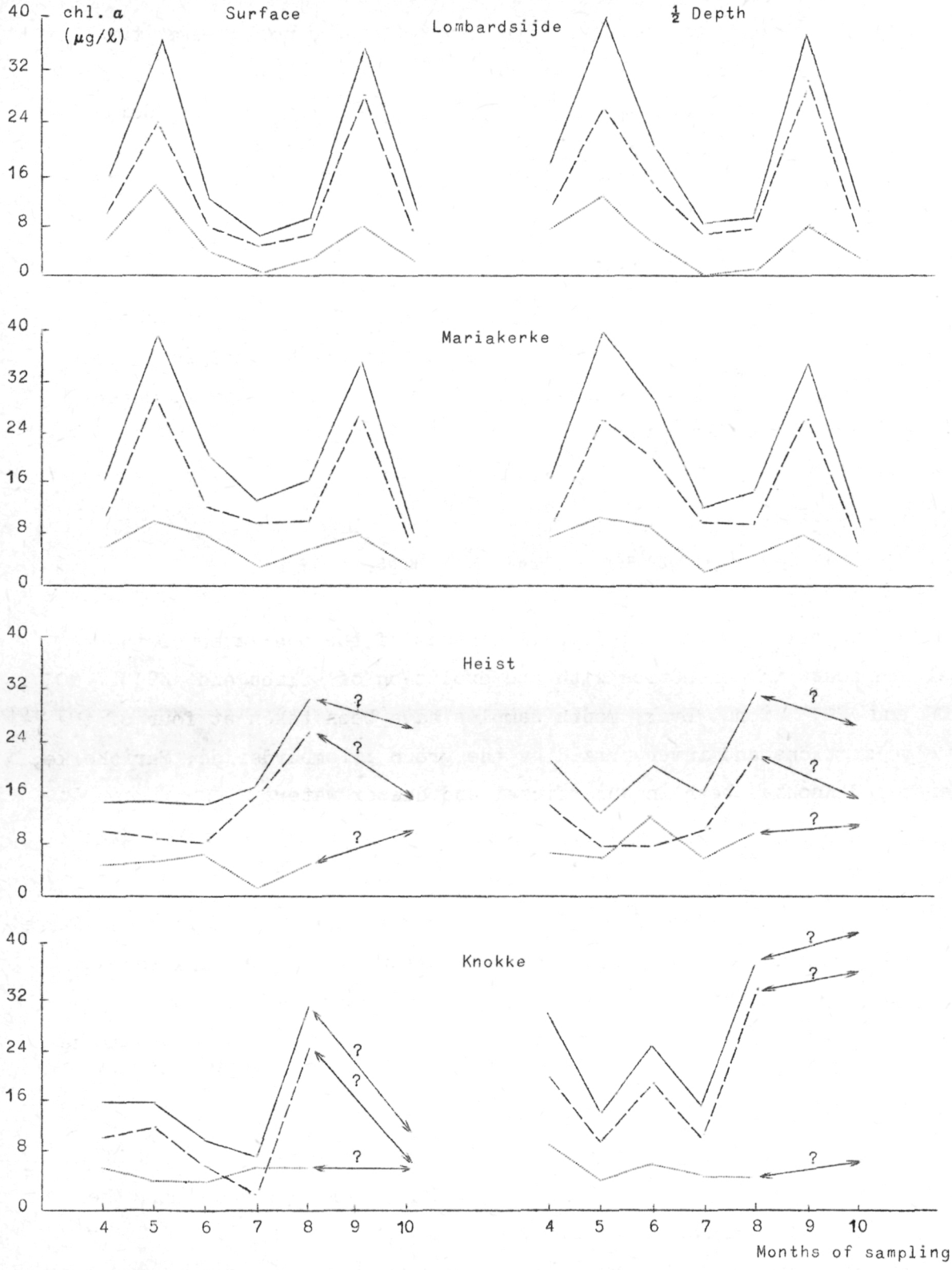


fig. 1.

Variation of the chlorophyll-*a* content between April and October 1974 (monthly campaigns).

——— total plankton – – – – – net-plankton ——— nanoplankton

water; the superficial water of Heist had a particularly constant chlorophyll content for the sampling period of April, May and June.

Comparison between the superficial and the deeper waters

The chlorophyll-a concentration coming from the total plankton are often greater in the deeper than in the superficial waters; the greatest differences are found in Knokke (April, June, July and principally October).

Comparison between the chlorophyll contents given by the nano- and netplankton

The calculation of the chlorophyll-a concentration relations nanoplankton/netplankton, during the period April to August, led to very variable results : in 11 cases out of 40 this relation is nearly 0.5 . The other values vary between 0.5 and 6 on the one hand (13 cases out of 40) and between 0.5 and 0.1 on the other hand (16 cases out of 40).

3.1.2.- Chemistry

Globally, the general chemical situation of the waters, during the period April to August, may be described as follows :

Nitrates : important falling of the concentration between April and July, with local anomalies in Heist (deeper water) and Knokke (deeper water). The situation is less clear in August.

Ammonia : the ammonia-content falls lightly during the same period. August may be considered as a period with a low ammonia-content.

Nitrites are found everywhere in small quantities.

Phosphates : as for the nitrates they fall from April till July and vary in August. The phosphate content becomes a bit higher in all stations during the month of June (except in the deeper water in Lombardsijde and in the superficial water in Heist).

Silice : varies strongly according to the sampling period, but the variations are in the same way in all stations (except in Lombardsijde (superficial water) and Heist (superficial water), where the peak does not appear in June.

3.1.3.- Conclusions

As the number of campaigns does not even cover a complete annual cycle, it is evident that every serious interpretation of the results is impossible at this moment. Actually there seems to be a different behaviour of the water in the SW and the NE zones :

- in the SW-zone (Lombardsijde and Mariakerke), the chlorophyll content according to the sampling periods evolves on the classical way;
- in the NE-zone (Heiste and Knokke) this evolution seems to be subjected to important perturbations.

3.2.- Organisms on the breakwaters

(Mr. VAN DER BEN; I.C.R.: quantitative analyses of heavy metals; I.H.E.: bacteriology and pesticides)

Four campaigns with, for each of them, collecting of seven organisms on four breakwaters (Nieuport, Raversijde, Heist and Knokke).

3.2.1.- Collected organisms

1) Plants : green algae : *Ulva lactuca* L.
brown algae : *Fucus spiralis* L.
red algae : *Porphyra umbilicalis* (L.)
diatoms : *Navicula grevillei* AG. and *Navicula mollis* SM mixed (Diatoms of the "Schizonema-type")

2) Animals : starfish : *Asterias rubens* L.
mussels : *Mytilus edulis* L.
winkles : *Littorina littorea* L.

At this moment we cannot take into consideration the diatoms (Navicula) and starfish, samples of them having been taken only once.

3.2.2.- Results and discussion

a) Only the results concerning the analysis of the specimen caught during the first three campaigns were available at the end of 1974 and are discussed in this paper.

Table 7

	Hg				Cu			
	n	min	max	$\bar{X}$	n	min	max	$\bar{X}$
Ulva lactuca	12	0.03	0.23	0.13	12	5.8	12.5	8.3
Fucus spiralis	6	0.03	0.22	0.08	6	2.3	7.7	5.3
Porphyra umbilicalis	3	0.03	0.03	0.03	3	10.1	34.4	22.1
Navicula	1	-	-	0.21	1	-	-	85.9
Asterias rubens	1	-	-	0.34	1	-	-	6.1
Mytilus edulis	12	0.14	0.77	0.45	12	6.3	20.6	9.7
Littorina littorea	13	0.13	0.41	0.24	13	40.1	138.7	62.7

	Pb				Zn			
	n	min	max	$\bar{X}$	n	min	max	$\bar{X}$
Ulva lactuca	12	3.13	13.88	6.39	12	24.2	89.5	45.5
Fucus spiralis	6	1.13	8.12	4.58	6	95.4	328.4	192.6
Porphyra umbilicalis	3	2.03	3.66	2.79	3	67.0	140.3	103.16
Navicula	1	-	-	20.4	1	-	-	127.4
Asterias rubens	1	-	-	3.9	1	-	-	210.2
Mytilus edulis	12	4.30	14.13	6.97	12	120.5	316.9	191.2
Littorina littorea	13	0.51	4.42	2.78	13	46.8	134.9	79.03

The lowest mean contents are always found in plant (material : Hg and Pb in *Phorphyra*, Cu in *Fucus*, Zn in *Ulva*; the highest mean contents are especially detected in animal material : Hg, Pb and Zn in mussels, Cu in winkles (which naturally contain copper in their hemocyanine). Nevertheless, two high means are found in plants : Pb in *Ulva* and Zn in *Fucus*.

b) When we only consider the plants (Naviculae excepted) we find the highest concentration of elements that do not play a physiological role (Hg and Pb) in *Ulva lactuca*; we find the lowest concentration in *Porphyra*.

c) When we only consider the animals, mussels have the highest concentrations of those two metals.

These results are discussed in function of the literature and the water- and sediment-contents of the same coastal zone.

3.2.3.- Tentative of conclusions

- The absolute levels, found for Hg, Cu, Pb and Zn are superior to what could be considered as normal, but do not seem to be excessive. Nevertheless a comparison with the literature is difficult due to the different levels of drying.

- The increasing contamination from the SW to the NE-stations, detected by the other teams of the Inventory Group, is found again in the organism, with a greater contamination however in Heist (Leopold channel) than in Knokke where some minima are revealed.

- Heavy metals are strongly concentrated by the organisms and truly reflect the situation of those metals in the water, especially with regard to the elements that do not play a physiological role. The best contamination detection are the algae. The species that should be specially studied are *Ulva lactuca*, *Fucus spiralis*, *Porphyra umbilicalis* and *Mytilus edulis*.

- Concerning the bacteria in the mussels and the pesticides in *Ulva lactuca* it is necessary to wait for more results.

3.3.- Sediments

(I.C.R., cf. § 1.3)

The pollution degree of the coastal zone and the correlation between this pollution and the proportion of fine particles of sediments have been confirmed. The part of the coast NE from Ostend is more polluted (especially Blankenberge and Ostend). On the whole, the sediments, samples of which have been taken in 1974, include less fine particles and since the pollutant contents are relatively lower than the preceeding years. Sediment pollution in the neighbourhood of the breakwater, also function of the quantity of fine particles, is very small.

Table 8

Sediments - Synthesis of the results
Coastal zone (immixture)
(6 campaigns from 1971 till 1974)

	Units	n	min	max	$\bar{X}$
< 37 μ	%	67	0	92	42.06
P/F : 110 - 550 °C	%	66	0.21	15.41	4.29
550-1000 °C	%	66	1.44	16.95	7.20
Org. mat. ($K_2Cr_2O_7$)	%	54	0.04	5.8	2.37
Al_2O_3	%	54	2.28	10.83	6.03
Fe_2O_3	%	54	0.53	3.96	2.16
TiO_2	%	54	0.05	0.55	0.30
P_2O_5	%	3	0.07	0.30	0.17
CaO	%	54	3.61	16.41	10.60
MgO	%	54	0.14	2.15	0.97
K_2O	%	54	0.85	1.97	1.40
Na_2O	%	3	1.03	2.24	1.51
S_{tot}	%	54	0.02	1.27	0.5
Cl	%	54	0.01	0.25	0.14
Ag	ppm	62(17)	< limit	2	0.7
Ba	ppm	7	56	140	110
Bi	ppm	65(63)	< limit	16	10
Co	ppm	65	0.3	14	3
Cr	ppm	65	4	120	42
Cu	ppm	65	0.6	58	14
Ga	ppm	65	0.8	22	6
Ge	ppm	65(20)	0.7 !!	8	3 !!
Hg	ppm	57	0.01	1.77	0.48
Mn	ppm	65	70	1488	496
Ni	ppm	65	0.4	27	11
Pb	ppm	65	10	280	80
Sn	ppm	65	0.3	18	7
Sr	ppm	54	115	660	301
V	ppm	65	0.8	105	29
Zn	ppm	65	15	271	120
Zr	ppm	65	33	370	176
Crude	mℓ/100g	96	0	0.22	0.008

Be, Cd, In, Li, Mo, Sb, Tl : inferior to the detection limit.
() : number of results used for the calculation of the mean value.

Table 9

Comparison of the sediments classified according to their granulometry
(6 campaigns from 1971 till 1974)

	Un.	Sand				Mud				Remarks
		n	min	max	$\bar{X}$	n	min	max	$\bar{X}$	
Org. mat.	%	18	0	0.8	0.2	36	1.02	58	3.4	
Al_2O_3	%	18	2.3	4.5	1.2	34	5.7	10.8	7.73	2 samp. mud : 3.16 & 3.9
Fe_2O_3	%	18	0.53	1.35	0.74	36	1.45	3.96	2.85	
TiO_2	%	18	0.05	0.22	0.11	36	0.25	0.55	0.4	
CaO	%	18	3.61	8.96	5.53	36	9	16.41	12.74	
MgO	%	18	0.14	0.65	0.29	36	0.8	2.14	1.32	
K_2O	%	18	0.85	1.25	1.04	36	1.02	2	1.59	*
S_{tot}	%	17	0.02	0.32	0.11	36	0.38	1.27	0.89	1 samp. sand : 0.48
Co	ppm	26	0.3	2	1	39	2	14	4	
Cr	ppm	26	4	23	12	39	32	120	56	
Cu	ppm	26	0.6	10	2	39	4	58	22	
Ga	ppm	25	0.8	3	2	39	3	22	8	1 samp. sand : 12
Hg	ppm	18	0.01	0.28	0.08	37	0.11	1.77	0.68	2 samp. sand : 0.38 & 0.45
Mn	ppm	26	70	330	126	39	230	1500	725	
Ni	ppm	25	0.4	7	3	39	4	27	16	1 samp. sand : 15
Pb	ppm	25	10	39	22	39	40	280	120	1 samp. sand : 59
Sn	ppm	24	0.3	4	2	39	1	18	9	2 samp. sand : 16 & 7
Sr	ppm	17	115	220	147	39	223	660	382	1 samp. sand : 240
V	ppm	26	0.8	17	7	39	17	105	44	
Zn	ppm	16	15	61	38	35	60	271	166	2 samp. sand : 178 & 217 1 samp. mud : 36
Zr	ppm	26	33	270	138	39	88	370	201	*

* For K_2O and Zr : partition less sharp.

II

Rivers

1.- Hydrographic basin of the river Meuse

1.1.- Chemistry of the water

(Institute for Hygiene and Epidemiology, cf. § 1.1, part I)

1.1.1.- River Meuse at the Dutch frontier

According to the analyses effectuated up to this day, the Meuse at the point where it leaves Belgium, carries an organic charge that may become important at certain moments, and a rather large quantity of nutrients. The large fluctuations of the chloride and sulphate contents are probably due to an up-river pollution. The metal-pollution is rather important; the Cd-content is, moreover, alarming owing to the high toxicity of this metal; the Fe- and Zn-contents are nearly always very high. The pesticide concentrations are low.

1.1.2.- Other frontier-points

In 1974 we started a study of all the frontier points.

1.1.3.- Tributaries

The *direct tributaries of the river Meuse* have characteristics that are similar to the characteristics of the Meuse in Hastière. None of them presents pesticides in demonstrable quantities. They are weakly or not polluted, except a light organic charge in the Semois.

The same situation appears in the *tributaries of the Sambre* (except that in these we find traces of lindane), while the *Sambre*

Table 10

Frontier points - Bassin of the Meuse

	Date	O_2 %	COD mg/ℓ	BOD mg/ℓ	S.M. mg/ℓ	N_{tot} mg/ℓ	N_{amm} mg/ℓ	NO_2^- mg/ℓ	NO_3^- mg/ℓ	PO_4^{---} mg/ℓ
French frontier - Meuse and tributaries										
Houille in Felenne	10-06-74	102.7	4	5.6	12	4.1	0.05	-	0.90	0.40
Viroin in Mazée	10-06-74	85.2	11	0.3	4	2.1	0.05	-	1.92	0.67
Meuse in Hastière	10-06-74	100	15	5.0	16	3.4	<0.005	-	1.05	0.15
Semois in Bohan	24-06-74	98.9	18	16.8	20	-	0.05	0.04	0.77	0.89
Sambre and tributaries										
Hantes in Leval Chaudev.	11-06-74	87.1	11	7.5	12	4.2	0.26	0.26	11.3	0.52
Hantes in Montig. St-Chris.	11-06-74	100.9	18	6.5	16	3.3	0.05	0.14	10.3	0.46
Thure in Bersillies	11-06-74	87.1	7	5.7	12	3.4	0.23	0.26	10.8	0.95
Sambre in Erquelinnes	11-06-74	24.5	33	8.0	12	4.7	2.01	0.04	0.07	1.07
Chiers and tributaries										
Ton in Lamorteau	24-06-74	50.1	134	5.2	30	-	0.57	0.29	2.62	2.15
Chiers in Torgny	24-06-74	49.5	7	4.4	15	-	0.19	0.55	7.87	0.67
Ton in Harnoncourt	24-06-74	77.5	4	9.7	15	-	0.43	0.28	3.97	1.17
Dutch frontier - Meuse and tributaries										
Geer in Kanne	25-06-74	-	17	10.7	10	4.0	3.30	0.05	0.03	4.08
Geer in Kanne	18-07-74	77.4	16	5.0	10	9.4	9.40	<0.01	4.2	37.7
Warmbeek in Achel	18-07-74	86.1	24	7.0	15	7.1	7.1	<0.01	< 0.01	1.23
Warmbeek in Achel	01-10-74	89.7	24	4.5	-	3.3	0.18	0.17	12.4	0.28
Itterbeek in Kinrooi	01-10-74	119.2	10	3.3	-	7.8	0.17	0.17	16.65	0.28
Dommel in Neerpelt	19-06-74	85.6	21	4.2	40	2.2	0.57	0.31	3.90	1.72

itself has an important organic charge and a deficit of dissolved oxygen; this is confirmed by the presence of free ammonia, representing more than 40 % of the total nitrogen.

In January of this year we took a new series of samples in the *Rulles*, the *Laclaireau* and the *Ton*. The influence of the paper-mill of

Table 10

(continuation)

	Cl^- mg/ℓ	SO_4^{--} mg/ℓ	Det.an. mg/ℓ	Cd ppb	Co ppb	Cr ppb	Cu ppb	Fe ppb	Hg ppb	Mn ppb	Ni ppb	Pb ppb	Zn ppb
French frontier - Meuse and tributaries													
Houille	8	14	0	< 1	< 5	11	8	300	0.15	40	6	13	85
Viroin	16	22	0	< 1	< 5	10	< 5	270	<0.01	55	16	22	175
Meuse	20	42	0.08	1	< 5	17	< 5	420	<0.01	92	12	5	237
Semois	10	16	0.16	-	-	13	-	-	0.24	95	-	-	70
Sambre and tributaries													
Hantes	24	28	0.08	< 1	< 5	< 5	< 5	390	<0.01	40	< 5	< 5	187
Hantes	22	34	0	< 1	< 5	< 5	< 5	120	<0.01	40	12	< 5	200
Thure	16	30	0.05	< 1	< 5	9	< 5	260	<0.01	71	< 5	< 5	225
Sambre	34	64	0.12	< 1	< 5	10	9	200	<0.01	128	8	< 5	235
Chiers and tributaries													
Ton	152	128	0.17	-	-	13	-	-	0.19	550	-	-	100
Chiers	44	44	0.04	-	-	17	-	-	0.13	145	-	-	70
Ton	12	96	0.15	-	-	8	-	-	0.03	35	-	-	240
Dutch frontier - Meuse and tributaries													
Geer	44	68	0.03	2.2	< 5	22	7	2300	<0.01	95	48	13	130
Geer	106	68	0.18	1.3	< 5	2.5	2.5	75	<0.02	36	17	17	225
Warmbeek	82	83	0.25	< 1	< 5	2.5	4.5	1280	<0.02	80	26	15	250
Warmbeek	46	98	0.04	< 1	< 5	< 0.5	5	960	0.03	250	< 3	6	120
Itterbeek	38	56	0.03	< 1	< 5	< 0.5	< 2	590	0.03	60	< 3	< 4	40
Dommel	46	58	0.04	5.4	1	29	8.4	380	0.21	75	16	10	1230

Harnoncourt on the pollution level of the *Ton* is evident. It is expressed by a considerable increase of the organic charge and of the chlorides-, sulphates- and Mn-concentrations, by an oxygen deficiency, and also by the presence of 80 ng/ℓ of lindane and of 12 ng/ℓ of its δ isomer.

The conclusions drawn concerning the *Rulles* in 1973, saying that this river was clear, are confirmed by the new samples. Downstream the *Mellier*, on which a wood distillery has been constructed, we find small quantities of phenol-products.

In December 1973 new series of samples has been taken in the *Mehaigne*. For the two campaigns we find a small organic pollution that increases in Ambresin and Huccorgne. The oxygen-saturation is only lightly affected by this pollution. The nitrates are very high on the whole flow of the river, except in the neighbourhood of Ambresin where they decrease, especially in spring. We never found high phosphate concentrations. In winter we note higher chloride-concentrations and also an important increase of sulphates. Important lindane-concentrations have been found, especially in Branchon, as in 1973.

This year a very detailed study has been made of the *Vesdre*. The results of this study will be published in a special report.

At the frontier with the Netherlands, two series of results refer to the *Yeker* and the *Warmbeek*. In July the *Yeker* is strongly polluted by nutrients (39 mg/ℓ of NO_3^-), while in June the nutrient pollution is more normal; the Fe, Ni and Cr-contents allow to suppose a contamination by a discharge. Pesticides are not found in it. The *Warmbeek* presents a light organic pollution and a small concentration of lindane and of its α-isomer.

The *Itterbeek* is caracterized by a light supersaturation of dissolved oxygen and a rather high nitrates content, while the *Dommel* is principally polluted by Cd, Cr and Zn.

1.2.- Pesticides

(Mr. GORDTS and Mr VANDEZANDE : I.H.E.)

Some pesticides are not taken into account because they are not demonstrable in the basin of the river Meuse. It concerns Aldrin, Heptachlor, pp' DDT, DDE, DDD, α- and β-endosulfan, endrine, HCB and β-HCH.

No pesticides at all have been found in the *Laclaireau*, *Chiers*, *Semois*, *Houille*, *Thure*, *Sambre*, *Yeker*, *Dommel*, *Warmbeek* and *Meuse*. Attention must be drawn to the fact that only one sample has been taken on each river, at the frontier.

In the *Ton*, lindane has only been found in Harnoncourt (80 ng/ℓ).

An exception should be made for the *Mehaigne* where relatively high concentrations of lindane were found. From Huy to Ambresin the lindane-concentration increases linearly with a maximum of 840 ng/ℓ ; downstream from this place the concentration decreases and at the confluence with the *Meuse* we still find 60 ng/ℓ . We find a higher concentration in summer (840 ng/ℓ) than in winter (95 ng/ℓ). This is probably due to the fact that the river runs through an agricultural area.

Concerning the *Vesdre* we refer to the special report.

1.3.- Hydrobiology

(G. VAN HOOREN and H. DE SCHUTTER, I.H.E.)

1.3.1.- River *Meuse* at the French frontier

The new results of 22.9.1973, found in Heer, confirm a former conclusion, namely a low degree of pollution of the *Meuse* where it enters Belgium (*Mathematical Model, Annual Report, III*, chapter V).

1.3.2.- River *Meuse* at the Dutch frontier

Referring to the results of 1972-1973 (*Mathematical Model, Annual Report, III*, chapter V), the water of the *Meuse* is liable to periodical pollutions that are not necessarily related to seasons. After the small pollution period of July-August 1973, the situation is becoming worse and arrives at a maximum in December 1973, January, February and March 1974 (α-mesosaprobe). Then follows a restoration period till June 1974, ending with a moderate pollution.

1.3.3.- Tributaries

Ton and *Laclaireau* : the results of 1973 are confirmed, here too the *Laclaireau* is a pure river, but after its confluence with the *Ton*

it is highly polluted in Dampicourt, a pollution that still increases in the neighbourhood of Harnoncourt (α-meso- till poly-saprobe).

Semois and tributaries : in the surroundings of Habay-la-Neuve the *Semois* is very pure. In Rulles, however, we observe an important pollution.

Mehaigne : this river presents the characteristics of an organic pollution. The situation varies between a moderate and a high pollution but is not alarming. The worst situation is observed in the neighbourhood of Mehaigne and the pollution degree decreases towards the confluence with the *Meuse*.

Vesdre : downstream from Eupen the *Vesdre* is little polluted. The saprobity index varies between a β-meso- and an α-meso-saprobe situation, according to the places and the data. In Pepinster, however, the pollution is important.

In general the results correspond with those found in 1972 (*Mathematical Model, Annual Report, III*, chapter V).

1.4.- Bacteriology

(Institute for Hygiene and Epidemiology, cf. § 1.1, part I)

1.4.1.- River *Meuse* at the Dutch frontier

In 1974 the *Meuse* has been examined three times on faecal pollution at the point it leaves Belgium.

Table 11

Dates	Places	Total germs /mℓ	Coliforms /100 mℓ	Faecal coliforms /100 mℓ	Faecal streptococci /100 mℓ
25-6-74	Lanaye	252.000	780.000	18.000	200
18-7-74	Lanaye	281.000	670.000	4.000	700
10-9-74	Lanaye	99.000	200.000	6.000	550

Compared with last year the pollution was much more important in June and July. At that moment a stem of Salmonella bredeney has indeed been isolated. On the contrary, the sampling of September indicates a considerable regression of the coliforms.

1.4.2.- Other points of river *Meuse*

As, for most of the points, we only dispose of one result, it is difficult to draw conclusions after this first year of sampling.

1.4.3.- Tributaries

We note, however, that the *Sambre* is considerably more polluted than the *Meuse*. On the *Hantes*, Salmonella panama has been isolated in Leval-Chaudeville.

Semois and *Chiers* are still little polluted.

Laclaireau and *Ton* : this year a new series of samples has been taken in the rivers *Laclaireau* and *Ton*. Such as last year the faecal pollution of *Laclaireau* is very small. After its confluence with the *Ton*, the pollution strongly increases; this appears specially in front of the paper-mill of Harnoncourt. Salmonella Typhi-murium has been isolated in Dampicourt.

The *Rulles*: at its source, the *Rulles* is little polluted; this pollution considerably increases from the distillery of Marbehan. In Marbehan, Salmonella infantis and S. brandenburg have been isolated.

The *Mehaigne* : this river presents an important pollution. There are more faecal streptococci than Esch. coli. Four stems of Salmonella have been isolated : S. manchester, S. brandenburg, S. worthington and S. derby.

At the Dutch frontier, the *Yeker* carries a lot of coliforms.

1.5.- Sediments

(Institute for Chemical Research, cf. § 1.3, part I)

The sediments of the rivers accumulate the pollution and generally this accumulation does not depend on the granulometry, contrarily to what

is observed in the sea where the proportion of particles smaller than 37 µm gives an idea of the quantity of pollutants.

Among the sediments of the *Ourthe*, for instance, some of them, rather rough (45 % , < 37 µm) , are very polluted (Angleur), while others, very small (85 % , < 37 µm) , are considerably less polluted (Chênée).

It is worth remembering that there exists a very good concordance between the conclusions drawn from the water analysis (instantaneous pollution) and those drawn from the sediments (integrated pollution).

1.6.- Research work

1.6.1.- River *Meuse*

According to the degree of pollution, the course of the *Meuse* has been divided into three parts (*Mathematical Model, Annual Report, III*).

a) from Heer (French frontier) to Tihange : small pollution;

b) from Flémalle-Haute to Herstal : highest degree of pollution (region of Liège, confluence with the Ourthe);

c) downstream from Herstal : the pollution decreases but does not reach the degree of the first section again.

1.6.2.- Frontier points

The new results concern the frontier points of the course of the *Meuse* : Heer and Lanaye. They confirm that the *Meuse* is more polluted when it leaves our country than when it enters it.

1.6.3.- Tributaries

This year several tributaries have been studied : *Laclaireau, Ton, Rulles* (tributary of *Semois*), *Mehaigne, Ourthe* and *Vesdre*. The study of *Laclaireau* and *Ton* allowed to say that a paper-mill had little influence on the pollution of sediments, except on Mn (the water analysis revealed on organic pollution and a higher Fe- and Mn-concentration). The pollution of the sediments in the *Ton* is due to its tributary the *Chavette*.

Rulles : the contribution to the sediments of the *Rulles* from the *Mellier*, a tributary contaminated by a wood saw-mill, is very clear,

although of rather little importance : crude, Pb, Hg, total S, Cu, organic matter. The analysis of the water samples, taken at the same place (downstream from the confluence), reveals only an increase of the COD.

The little degree of pollution of the sediments of the *Mehaigne* is constant on the whole course of the river, just as that of the water, except in the neighbourhood of its confluence with the *Meuse* (sugar works) where we find small Sn, Zn and crude-contents in the sediments.

The sediments of the *Ourthe*, polluted upstream from its confluence with the *Vesdre* (among others by Cr), undergo the influence of this affluent particularly for Cd, Cu, Hg, Zn and crude, the contents of which reach record levels. There is also a considerable increase of water pollution, especially when the metal concentrations are concerned.

The pollution of the *Vesdre* justified a more detailed study for the whole course of this river. In 1974 the number of samples has been multiplied in order to make it possible to publish a report similar to that made for the Yser. This study will group the results of the inventory since 1972, the nature of the activities and the characteristics of the hydrographic basin. The study will be published at the beginning of 1975.

2.- Hydrographic basin of the river *Scheldt*

2.1.- Chemistry of the water

(Institute for Hygiene and Epidemiology, cf. § 1.1, part I)

2.1.1.- River *Scheldt* and tributaries at the French frontier

At the French frontier, several small tributaries, such as the *Grande Honnelle*, the *Aunelle*, the *Hogneau* and the *Trouille* join the *Scheldt*; they have a mean or even small organic pollution.

The *Trouille* is lightly supersaturated with dissolved oxygen. The nitrate-concentrations are always higher than 10 mg/ℓ .

The *Aunelle*, contrarily to the other tributaries, is lightly polluted with pesticides.

Table 12

Frontier points - Basin of the Scheldt

	Date	O_2 %	COD mg/ℓ	BOD mg/ℓ	S.M. mg/ℓ	N_{tot} mg/ℓ	N_{amm} mg/ℓ	NO_2^- mg/ℓ	NO_3^- mg/ℓ	PO_4^{---} mg/ℓ
French frontier										
Grande Honnelle in Autreppe	11-06-74	93.6	15	10	8	2.6	0.45	0.39	11.0	1.13
Aunelle in Marchipont	11-06-74	96.3	7	5	8	2.2	0.07	0.29	13.9	1.17
Hogneau in Quiévrain	11-06-74	77.4	15	10	8	2.7	0.63	0.72	10.0	0.22
Channel of Condé in Hensies	11-06-74	90.0	37	11.5	12	2.4	0.18	0.27	9.7	0.43
Trouille in Civry	11-06-74	126.5	15	8.9	12	2.4	0.05	0.26	13.8	0.92
Scheldt in Blécharies	17-06-74	24.4	51	27	20	-	17.2	1.7	2.1	2.15
Channel Espierres	17-06-74	15.9	66	2.8	200	-	9.5	0.2	0.34	1.75
Espierres in Leers Noord	17-06-74	0	904	320	1050	-	22.0	0.3	0.47	5.21
Lys in Ploegsteert	02-07-74	0.	7.6	40	4	8.4	5.6	< 0.005	< 0.01	4.9
Lys in Ploegsteert	20-08-74	0	82	16	30	7.0	6.25	0.20	0.32	1.93
Lys in Ploegsteert	01-10-74	0	40	8.4	35	7.2	1.94	0.03	< 0.01	3.36
Dutch frontier										
Scheldt in Doel	19-06-74	22.8	472	7.6	570	5.6	4.7	0.97	3.3	2.24

The *Condé canal* has the same characteristics as the other rivers, but a higher organic pollution and important quantities of PCB (more than 1500 ng/ℓ).

The metal pollution is negligible in the *Aunelle* and the *Hogneau*, but we find Cr and Ni in the *Grande Honnelle* and high Cr and very high Pb concentrations in the *Trouille*.

On the other hand, the situation of the *Scheldt* at the French frontier is far frop being satisfactory. We find an important deficiency of dissolved oxygen, high COD and BOD values, a great quantity of ammoniacal nitrogen, but a low metal pollution (except 20 ppb Ni and Pb), and finally an important pesticide concentration (> 5000 ng/ℓ).

During the former years we already mentioned the catastrophic situation of the *Espierres* and the new samples confirm the high pollution

Table 12

(continuation)

	Cl^- mg/ℓ	SO_4^{--} mg/ℓ	Det.an. mg/ℓ	Cd ppb	Co ppb	Cr ppb	Cu ppb	Fe ppb	Hg ppb	Mn ppb	Ni ppb	Pb ppb	Zn ppb
French frontier													
Grande Honnelle	28	63	0.10	< 1	< 5	15	< 5	290	<0.01	50	18	5	200
Aunelle	26	47	-	< 1	< 5	< 5	< 5	200	<0.01	<15	< 5	< 5	181
Hogneau	28	57	0.05	< 1	< 5	< 5	9	330	<0.01	55	< 5	< 5	231
Channel of Condé	64	156	0.02	< 1	1	11	13	150	<0.01	142	< 5	< 5	212
Trouille	28	51	0.04	< 1	< 5	41	< 5	260	<0.01	21	< 5	100	225
Scheldt	110	167	0.01	1.2	8.5	12	8	590	0.27	315	24	20	400
Channel Espierres	180	146	0.20	2.4	2.4	12	24	4000	0.63	250	30	95	495
Espierres	236	293	4.72	-	-	210	-	-	0.04	495	-	-	630
Lys	92	120	0.27	0.8	3.5	< 2	7	430	0.02	190	25	6	80
Lys	114	69	0.10	< 1	< 2	< 5	< 3	100	0.05	190	10	< 5	30
Lys	76	158	0.80	< 1	< 5	13	13	290	0.38	180	8	10	100
Dutch frontier													
Scheldt	8700	1172	1.39	1.5	4	-	41	5900	0.30	430	26	32	160

COD of about 1000 mg/ℓ , more than 1000 mg/ℓ material in suspension, 200 ppb of Cr, 4000 ppb of Fe, and nearly 2000 ng/ℓ of PCB.

The situation of the *Espierres canal* is better although the pollution degree is important.

Finally we took three samples of the water of the *Lys* and in none of them found any trace of dissolved oxygen. At the French frontier this river seems to be in a permanent state of anaerobiose, with COD values varying between 40 and 80 mg/ℓ . The metal pollution on the contrary is relatively low; the situation is the same for pesticides, the quantities of which are inferior to the detection limits.

2.1.2.- River *Scheldt* at the Dutch frontier

At the Dutch frontier the situation of the Scheldt is worse than at the French frontier, with a COD value of nearly 500 mg/ℓ . The metal

concentrations, on the other hand, are nearly the same, except for Fe which has a concentration of 6000 ppb , ten times the value found at the French frontier.

We did not find any trace of pesticides at the Dutch frontier.

2.2.- Pesticides

(Mr GORDTS and Mr VANDEZANDE, I.H.E.)

Some pesticides are not taken into account because they are not demonstrable in the whole Scheldt basin (Aldrin, pp' DDT, DDD, α- and β-endosulfan, endrine and HCB).

2.2.1.- Tributaries of the river *Scheldt*

No pesticides have been found in the *Hogneau*, the *Espierres canal*, the *Lys* and the *Trouille*

The *Espierres* is undoubtedly the most polluted river. This confirms the results mentioned in the *Annual Report III* (α- and γ-HCH, 400 ng/ℓ). On 15.10.73 lindane and its β- and δ-isomers have been found in Estaimpuis and in Espierres (700 ng/ℓ , 365 ng/ℓ , 750 ng/ℓ). A great concentration of dieldrin has also been found (905 ng/ℓ). At the frontier-point on the *Espierres* we found PCB (1800 ng/ℓ) and also dieldrin (50 ng/ℓ).

In the *Condé canal* PCB has been found many times (1730 ng/ℓ). This could indicate some industrial pollution.

Concerning the *Dyle* we refer to the *Annual Report III*.

2.2.2.- River *Scheldt*

Generally the *Scheldt* is low polluted with pesticides (*Annual Report, III*). In Doel (Dutch frontier), no pesticides have been found but at the French frontier captan has, exceptionally, been found in a high concentration (5850 ng/ℓ) . This is probably due to an accidental contamination. We also observe the influence of the tributary *Espierres* in Helkijn (Lindane, β- and δ-HCH : 160 ng/ℓ , 80 ng/ℓ , 95 ng/ℓ) .

2.3.- Hydrobiologie

(Mr VAN HOOREN, Mrs DE SCHUTTER, I.H.E.)

2.3.1.- River *Scheldt*

The results of the immersed slides show clearly that the *Scheldt* has a high degree of pollution at the place where it enters in Belgium. Contrarily to the chemical results, the hydrobiologic results show that the pollution decreases gradually till Ghent.

2.3.2.- Tributaries of the river *Scheldt*

Espierres : from a hydrobiological point of view, this river is heavily polluted, as there exist no more vegetal and animal organisms. Due to the preponderating presence of bacteria, bacteriophytes such as *Sphaerotilus natans* and *Zoogloea-ramigera*, the environment can be considered as hypersaprobe.

Dyle : during the period from 19.8.1973 to 3.10.1973, samples of plankton have been taken over the whole course of the *Dyle* and analyses have been made.

Where the results of the plankton analyses do not give a clear idea of the situation of the *Dyle*, the results of the immersed slides may be considered as characteristic.

At already a few kilometers from its source the *Dyle* is polluted. This pollution increases gradually and attains a first maximum in Gastuche (downstream a paper-mill). In Florival we observe a serious reduction of the biological development on the immersed slides, probably due to toxic effect of the water. Downstream from Louvain the pollution degree is extraordinarily high and we observe a tendency to hypersaprobity. In Wijgmaal a predominant population of Mycophytae shows an obvious hypersaprobe environment. After dilution of the *Dyle* with the water from the *Demer*, this hypersaprobe situation decreases, although the tendency to hypersaprobity continues to exist till the confluence with the *Zenne*.

As compared with the fluctuation of the chemical pollution index according to Prati and Pavanello (Annual Report II) the slidings of saprobity index numbers, taking into account the tendency to hypersaprobity

nearly agree. Nevertheless, the optimistic picture of the pollution, given by the pollution index of Froti, does not seem to agree with the reality.

2.4.- Bacteriology

(I.H.E., cf. § 1.1, part I)

As for the Meuse, we started in 1974 with a study, at the frontier points, of the tributaries of the river Scheldt.

2.4.1.- River *Scheldt* and tributaries at the French frontier

At the French frontier the *Scheldt* receives a lot of little tributaries such as the *Grande Honnelle*, the *Aunelle*, the *Hogneau* and the *Trouille*. On their entering in Belgium these small rivers have already a high degree of pollution; especially when coliforms are concerned.

The *Espierres* and the *Lys* have a very important, if not catastrophic degree of pollution. In Leers-Nord Salmonella brandenburg has been isolated in the *Espierres*.

2.4.2.- River *Scheldt* at the Dutch frontier

The situation of the *Scheldt* in Doel is, of course, dependent on the faecal pollution of all its tributaries.

2.5.- Sediments

(I.C.R., cf. § 1.3, part I)

At the end of 1973 a complete study has been made of the course of the *Scheldt* and samples of sediments have been taken in the *Espierres*, the *Dyle* and the *Ghent - Terneuzen canal*.

2.5.1.- River *Scheldt*

The study of the *Scheldt* confirmed the former observations. The pollution of the Scheldt sediments, observed at the French frontier point,

increases considerably after the confluence with the *Espierres* (*e.g.* crude, Cr, Hg, Cu and organic matter) and at Kerkhove (Pb, Zn, Sr). The same can be observed for the water.

The pollution downstream from Ghent to Doel is high and constant, except for Cr and Zn the contents of which diminish in the sediments.

2.5.2.- Tributaries of the river *Scheldt*

It is confirmed that the contribution of the *Dendre* and of the *Rupel* maintain the pollution level of water and sediments, but do not aggravate it.

The pollution of the sediments of the *Espierres*, already very important at the frontier, increases till the confluence with the *Scheldt* and this explains the influence on the pollution of the river. The sediments of the *Espierres canal* are also polluted but not in as high a degree as in the river.

The *Dyle*, which is not polluted at its source, has, on its course, several polluted zones, the pollution being observed as well in the water as in the sediments. Out of these zones the pollutant contents of the sediments are low.

The first contamination is observed in Ways. Afterwards, in the region of Wavre, from Limal to Gastuche, we find a characteristic Hg, Mo, crude and principally Cr and Ni pollution, probably due to paper-mills. In Florival the influence of an important accumulator factory finds an expression in the very high Pb-contents of the sediments (very abundant Pb and Fe in the water, local suppression of the aquatic life). The agglomerations of Louvain and, particularly, of Mechelen, contribute to the increase of the pollution level. The pollutant contents are particularly high in the sediments in Muizen and Mechelen (broad arm of the Dyle); they diminish then till the confluence with the *Zenne*.

In the *Ghent-Terneuzen canal*, a study is undertaken on the sulfur-components in the sediments. The sulfur components are abundant and seem associated — in a stable way — with the organic matter.

3.- Hydrographic basin on the river *Yser*

3.1.- Chemistry of the water

(I.H.E., cf. § 1.1, part I)

The new results confirm former conclusions : important eutrophication, especially in summer (*cf.* monography concerning the river *Yser*, 1973).

The situation is very similar in the *Berghes canal* and the *Duinkerke canal*, but with a considerably higher organic charge. The metal pollution is nearly the same as in the *Yser*. It is of little importance, except for Cr in the *Duinkerke canal*.

The *Yser* and its tributaries are not polluted by pesticides; only the *Yser* reveals some traces of dieldrin.

3.2.- Hydrobiology

(Mr VAN HOOREN and Mrs DE SCHUTTER, I.H.E.)

During the year 1974 samples have been taken four times in the basin of the river *Yser*.

Compared with 1973, the *Heidebeek* reveals a considerably higher coliform pollution but a lower faecal Streptocci pollution.

The situation is nearly the same in the *Berghes* and *Duinkerke canals*.

4.- Hydrographic basin of the river *Rhine*

4.1.- Chemistry of the water

(I.H.E., cf. § 1.1, part I)

During the year 1974 samples have been taken of the river *Sûre* in Martelange.

The analysis of those samples revealed a quasi-inexistant pollution degree; only one abnormality : the presence of 17 ppb of Cr. No

pesticides have been found. According to the same samples there seems to be little bacteriological pollution in the river *Sûre*.

III

General conclusions

1.- Progress of works

The first task of the inventory group is an analytical one. The whole question is to improve gradually the description of the pollution degree of the Belgian superficial waters.

Within this cadre, the advancement may be presented under three aspects :

1) The *determination of new parameters*, which were not yet considered until to-day, what is the case for the immixion zone of the sea where, thanks to the work done by the newly associated team Van der Ben, it was possible to start with the study concerning the phytoplanktonic biomassa and with that of the bio-indicators.

Attention should also be drawn on a comparative inventory of the deeper water on the twelve places where, in 1971, superficial samples had been taken. No significant difference has been found.

2) The study of samples taken at *new places* that had not yet been inventorized. It concerns especially some tributaries of the river Meuse, the rivers at the frontier-points, the sediments of the Ghent - Terneuzen canal and, for the sea, the sediments in the neighbourhood of the breakwaters. On the whole nothing special has to be mentioned.

3) *Repeated measurements* at previously inventorized places in order to collect a reasonable number of data allowing to describe a situation based on means and to follow its evolution. This "further work", concerned the twelve places where samples were taken in the immixion zone of the sea, the outlets of the coast and some rivers.

The second task of the inventory group, which is a synthetical one, consists of establishing balances starting from the whole lot of the analytical data and of making their interpretation. Those balances can be found in each of the ten advancement reports in the form of *tables of mean and extreme values*. In another connection we already said that a monography of the pollution of the Vesdre, especially with heavy metals and pesticides, will be published in 1975.

Since a long time the problems of a *balance of "inputs" in the immixion zone of the sea* is exercising our minds. The solution of this problem comes up against the difficulty presented by the measurement of the outlets. We hope that a new approach, based upon the study of the discharge in the sea of the rainwater, will allow us to progress. According to recent information, this 'input" should reach some two hundred million of m^3 per year.

2.- General synthesis of the results

It is impossible to give in a few lines a general idea of the results and once more we refer to the ten reports.

At the best we can try to synthesize the results concerning the *immixture zone of the sea* which, in opposition to the rivers, is characterised by a coherent whole.

The pollution level of this zone, previously defined as superior to a normal pollution and to that found in "open sea" has been confirmed not only by the campaigns but also by the contamination of marine organisms found on the breakwaters. In this case of course it concerns only a tendency deduced from the first results.

The new acquisitions of 1974 also allow to confirm that the pollution degree is higher from the NE of Ostend to Blankenberge. On the other hand, according to a cycle unfortunately still incomplete, the evolution of the biomass should be different and even abnormal in this part of the immixture zone.

Concerning the bio-indicators of the pollution, the macroscopic algae seem to give the best results.

For the *rivers* we merely point out that the pollution of the *Mehaigne* is typical for the agricultural activities and that the detailed hydrobiologic study of the *Dyle*, made in 1974, was particularly instructive.

3.- Further studies

Concerning the *coastal zone* :

- continuation of the actual research and determination of all kinds of other information allowing the elaboration and publication of a general study, as complete as possible, at the end of 1975.

Concerning the *rivers* :

- publication of two monographies, the first one concerning the Vesdre at the beginning of 1975, the other one concerning the Dyle after a study of this river during the year 1975.
- the inventory of the rivers at the frontier points.

IV

Appendix

List of record cards

1.- Sea and coastal area

Immixtion area, approaches of breakwaters, beaches, fairways and channels, sewers emitting in the sea.

- Blankenberge (sea, channel, sewers, Spuikom), - Bredene (sea), - E. Heist (sea), - Heist (sea, breakwater, beach, Channels of Schipdonk and Zelzate), - Knokke (sea, breakwater, beach), - Lombardsijde (sea), - Mariakerke (sea), - Middelkerke (sea), - Nieuwpoort (breakwater, fairway, channels of Plassendaal, Veurne, Ijzer, sewers), - Oostduinkerke (sea), - Oostende (sea, fairway, channels of Brugge-Oostende, Noord Eede), - Raversijde (breakwater - Wenduine (sea), - Zeebrugge (W. Heist) (sea, beach, channel).

2.- Water courses, by basins and rivers

2.1.- Basin of the Meuse

Albert (channel), Berwinne, Bocq, Chiers, Dison (river of), Dommel, Geer-Jeker, Hantes, Helle, Hoegne, Houille, Hoyoux, Itterbeek, Julienne, Laclaireau, Lesse, Mangombroux (Biez of), Marche-en-Famenne (river of), Membrette, Mehaigne, Meuse-Maas, Molignée, Ourthe, Rebais, Rulles, Ruyff, Sambre, Samson, Semois, Thure, Ton, Vesdre, Vierre, Viroin, Vresse (river of).

2.2.- Basin of the Scheldt

Aunelle, Condé (channel), Dendre-Dender, Dijle, Escaut-Schelde, Espierres, Espierres (channel), Ghent-Terneuzenchannel, Gete (Grote), Haine, Hofstade (lake of), Hogneau, Honnelle (grande), Lys-Leie, Rupel, Trouille.

2.3.- Basin of the Yser

Bergues-Veurnechannel, Blankaart, Dunkerke-Nieuwpoort channel, Handzame-vaart, Hanebeek, Haringebeek, Heidebeek, Ieperkanaal, Ieperlee, Kemmel-beek (Grote), Lovaart, Poperingevaart, Robaartbeek, Warmbeek, Yser-Ijzer.

2.4.- Basin of the Rhine

Sûre.

Comment

All the record cards can be transmitted when requested to the "Centre de Documentation (Liège University), I.H.E. (Bruxelles) or I.R.C. (Tervuren).

Chapter VI

Physiological effects of some pollutants

by

A. DISTECHE

(Based on work by G. PERSOONE, F. BENIJTS, C. CLAUS, P. SORGELOOS, L. VANHECKE-SARLET, Gent University; J.P. VANDEN BOSSCHE, Ch. PERPEET, M. VLOEBERGH, Brussels ULB University; A. DISTECHE, J.M. BOUQUEGNEAU, F. LAMBOT, Ch. GERDAY, Liège University)

1.- Phytoplankton

1.1.- Effect Hg^{++}, Pb^{++}, Cu^{++}, Zn^{++}, Cd^{++} on the growth of the phytoflagellate *Dunaliella viridis* and the diatom *Phaeodactylum tricornutum* [Benijts *et al.* (1974c)]

The organisms are grown under laboratory controlled conditions (light, aeration, CO_2, temperature) in artificial sea water (150 cm^3) prepared following Dietrich and Kalle (1963). Salinity is 30 ‰, the water is filtered through a 45 µm membrane filter; it is used either with or without addition of Vlasblom growth stimulating medium [Walne (1956)] containing $FeSO_4$, NaH_2PO_4, $NaNO_3$, $MnCl_2$, glycine.

The heavy metals are added as chlorides and the growth of the algae during 120 h is compared to the growth in absence of pollutants. The growth curves are drawn and integrated using Bode's formula. The ratio $\frac{\text{integrated growth curve test experiment}}{\text{integrated growth curve blank experiment}}$ allows to express the %

inhibition due to the addition of the heavy metal ions, either in presence or absence of culture medium.

The results are shown in figures 1 to 4.

It is obvious that the two test organisms react differently and that the toxicity scales are as follows : *Dunaliella viridis* :

$$Pb^{++} \gg Cu^{++} \gg Zn^{++} , \quad Hg^{++} , \quad Cd^{++}$$

in absence of added culture medium,

$$Pb^{++} \geq Hg^{++} \gg Zn^{++} , \quad Cu^{++} \gg Cd^{++}$$

in presence of added culture medium; *Phaeodactylum tricornutum* :

$$Hg^{++} , \quad Cu^{++} \gg Zn^{++} , \quad Cd^{++} > Cu^{++}$$

in absence of added culture medium,

$$Hg^{++} \gg Pb^{++} , \quad Zn^{++} , \quad Cu^{++} = Cd^{++}$$

in presence of added culture medium.

It should be noticed that the addition of growth stimulating medium considerably decreases the toxic effect of the heavy metals.

These results show how difficult it is to rely on "test" organisms to evaluate water quality[1]. Different phytoplanktonic organisms react differently and the observed effects are sensitive to the presence of phosphates, nitrates, iron, amino-acids, substances favouring eutrophication, but found in a very wide range of concentrations in natural conditions.

1.2.- Kinetics of adsorption and intake of Zn^{++} by *Dunaliella viridis* and *Phaeodactylum tricornutum* [Benijts *et al.* (1974b)]

The phytoplankton cells are grown as described above in artificial sea water enriched with Vlasblom medium (plus 0.03 mg/ℓ Na_2SiO_3 when diatoms are grown). The growth is followed with a Coulter counter and samples are retrieved to analyse the total Zn content using atomic

---

1. Marine Algal assay Procedure Bottle test : Eutrophication and Lake Resteration Branch National Environmental Research Center, Corvallis, december 1974.

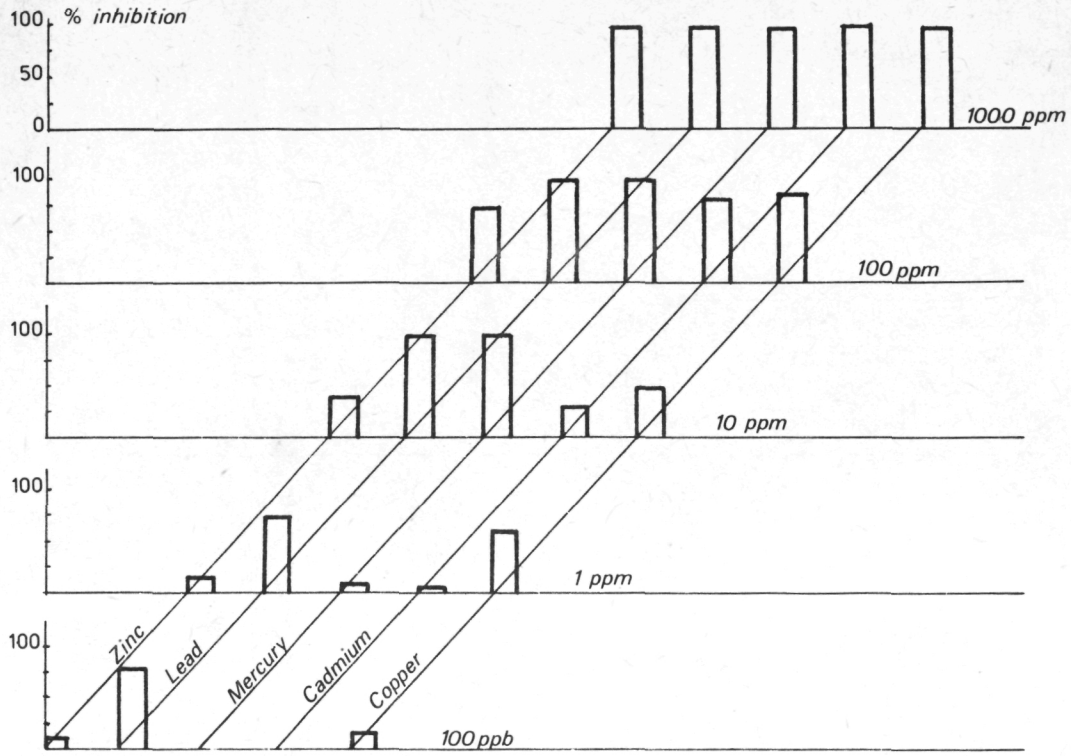


fig. 1.
Dunaliella viridis without addition of culture medium.

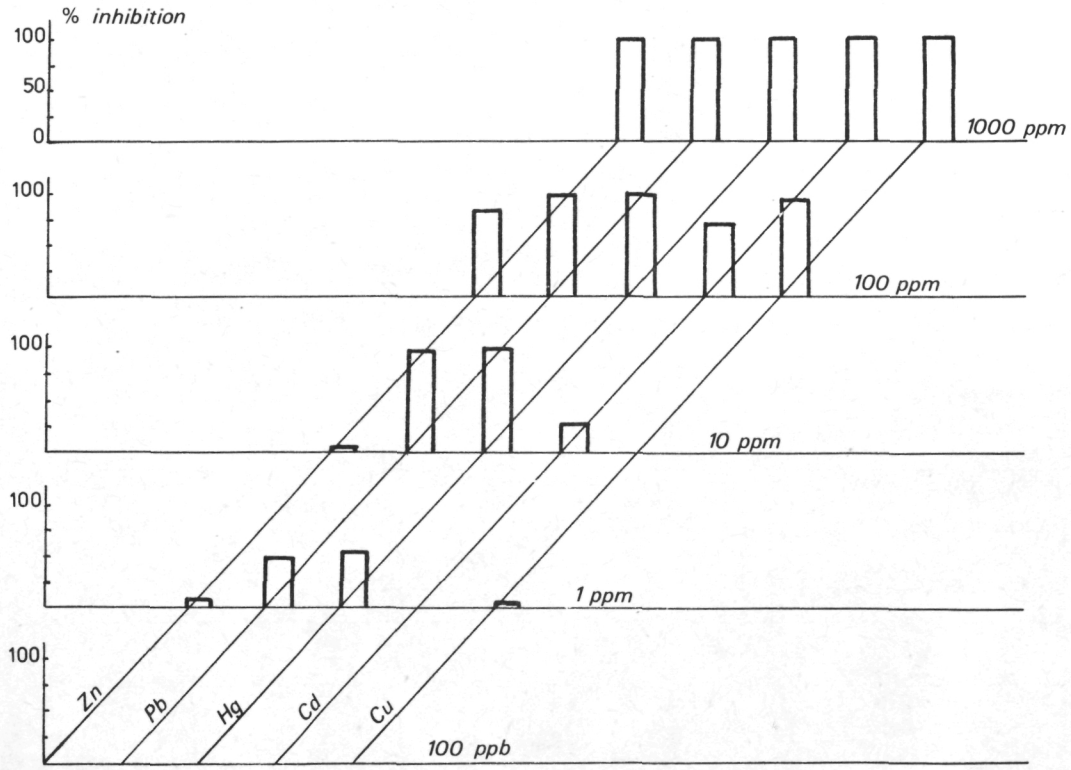


fig. 2.
Dunaliella viridis with addition of culture medium.

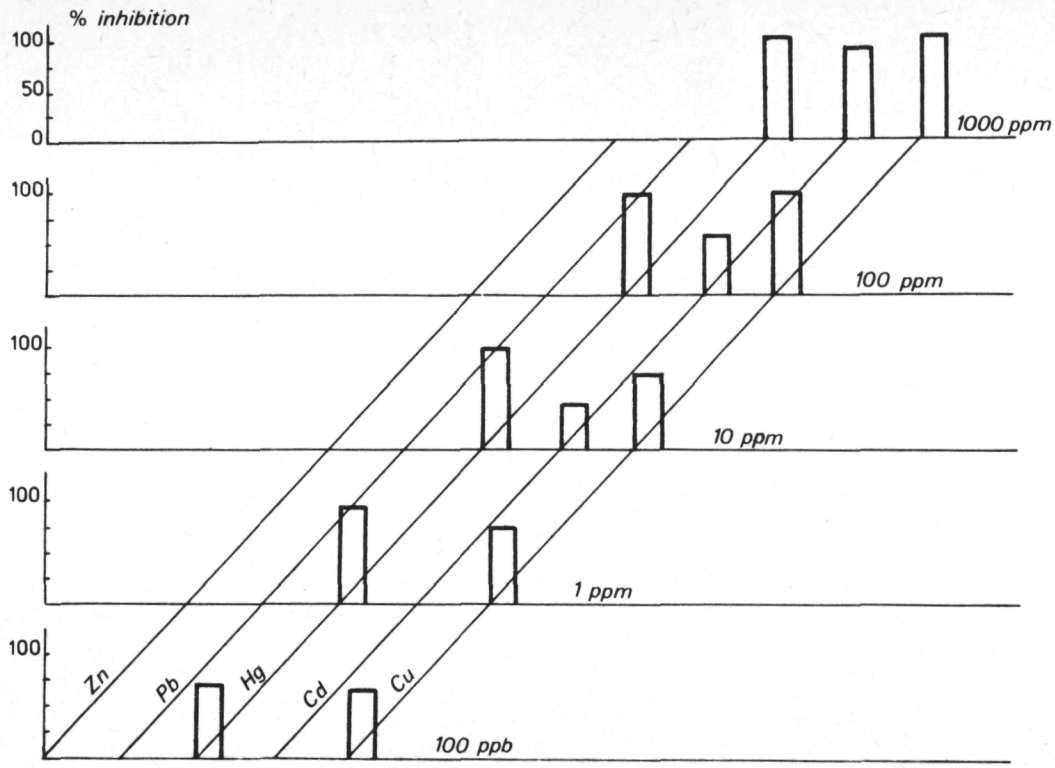


fig. 3.
Phaeodactylum tricornutum without addition of culture medium.

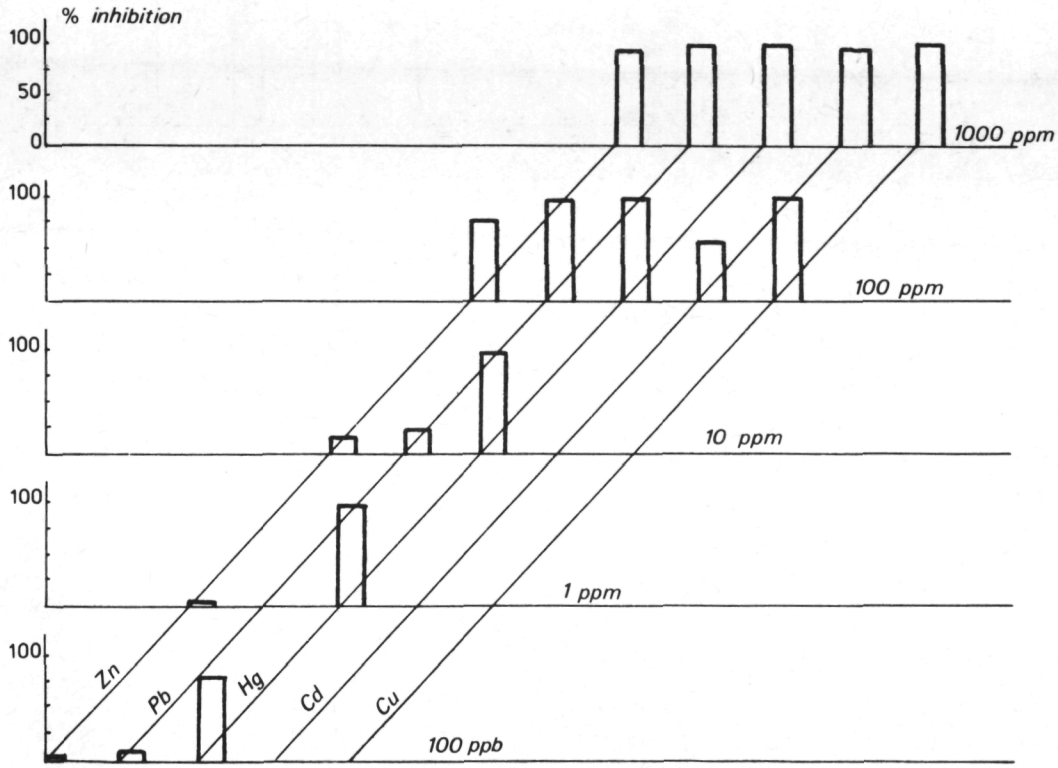


fig. 4.
Phaeodactylum tricornutum with addition of culture medium.

absorption [the centrifuged cells are mineralized in HNO_3 (65 % vol. conc.) + $HClO_4$ (70 % vol. conc.), 1/1].

Figures 5 and 6 show the effect of increasing Zn concentration on the growth curve of the two test organisms, figures 7 and 8a,b give the total amount of Zn, either adsorbed on the cell walls or entered in the protoplasm, as a function of time, expressed in 10^{-9} mg Zn per cell.

Without going into a detailed examination of the curves it is clear that the results are again quite different depending on the test organism :
a) in *Dunaliella* cultures the total Zn content per cell measured after one hour is almost the same whatever the amount of Zn^{++} added to the sea water; in *Phaeodactylum* cultures the Zn content varies enormously after one hour depending on the Zn^{++} concentration (with the exception of the 100 ppm case).
b) *Dunaliella* cells accumulate more Zn in function of time when the Zn^{++} concentration increases (not taking into account the exception at 100 ppm) and the curves show that higher accumulation can be correlated with a slowing down of the population growth.

Phaeodactylum cells which show high Zn contents at the early stages, lose Zn during the active phase of their growth curve (with the exception of what happens at 80 ppm , for which no explanation is given).

Table 1 shows the total Zn content of the cells after 7 days.

Table 1

Zn^{++} added (ppm)	Zn (10^{-9} mg) per cell	
	Dunaliella	Phaeodactylum
1	0.12	0.09
10	0.47	0.19
30	0.97	0.70
50	2.23	1.82
80	2.22	5.84
100	0.80	0.22

The amount of Zn per cell after 7 days increases although there is a large difference in the shape of the accumulation curves versus time,

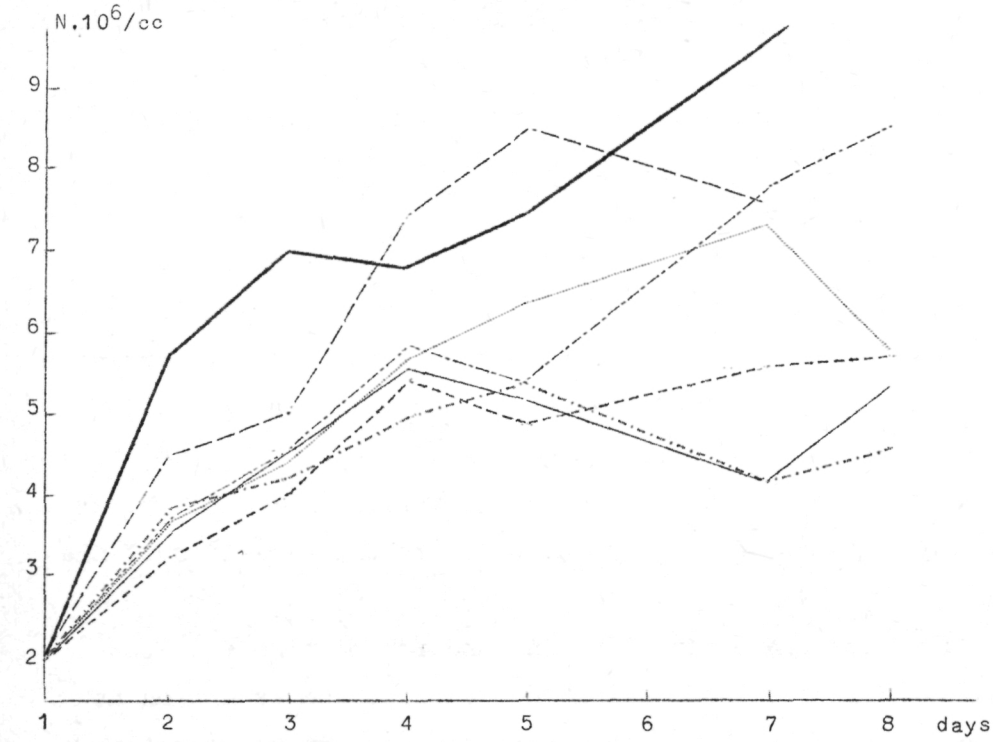
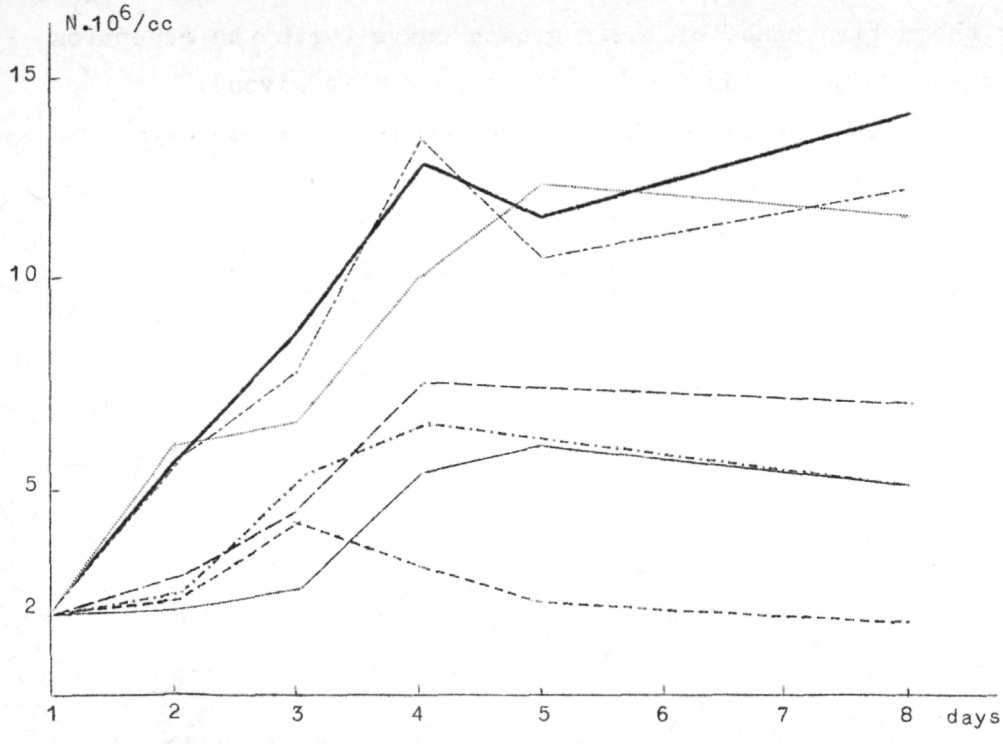


fig. 5.
Dunaliella viridis growth curve.



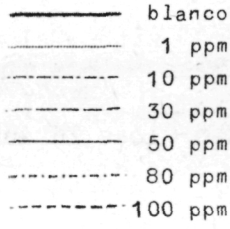


fig. 6.
Phaeodactylum tricornutum growth curve.

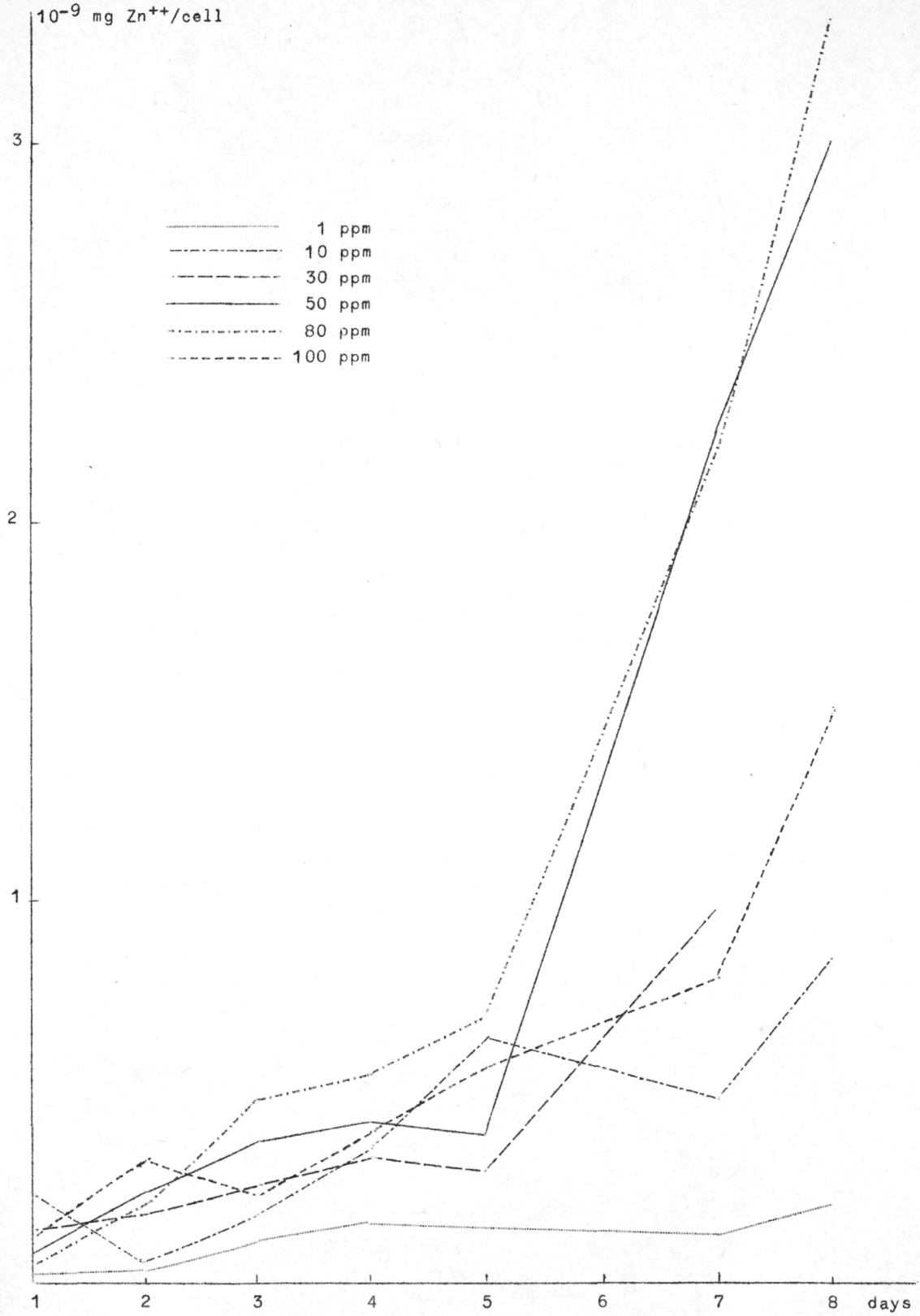


fig. 7.
Zn ad-absorption/cell unit by Dunaliella viridis.

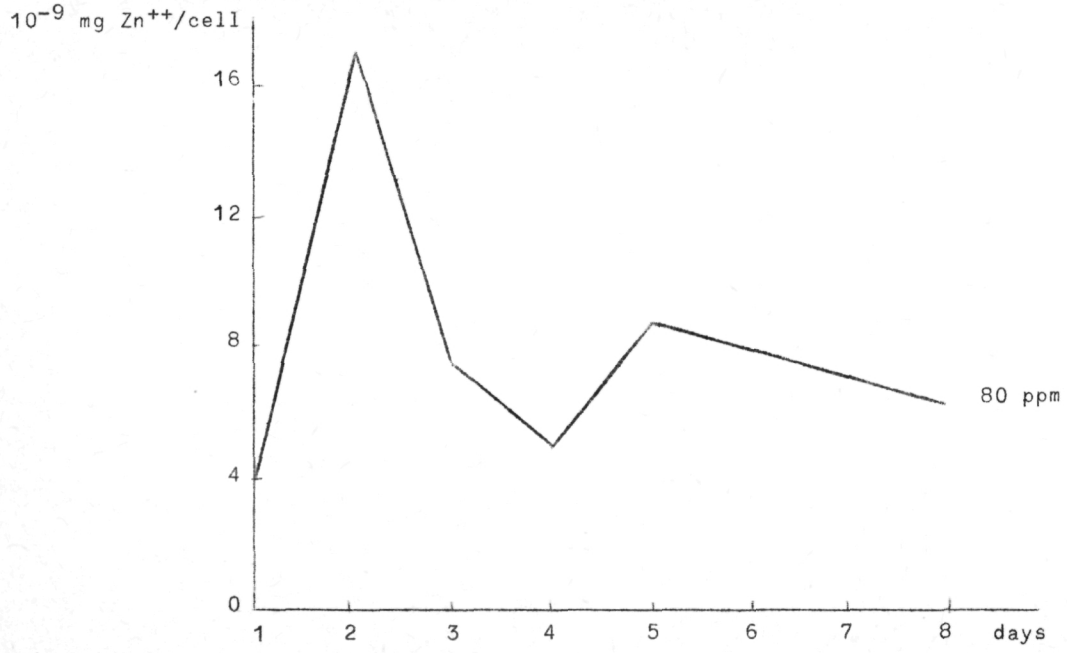


fig. 8a.

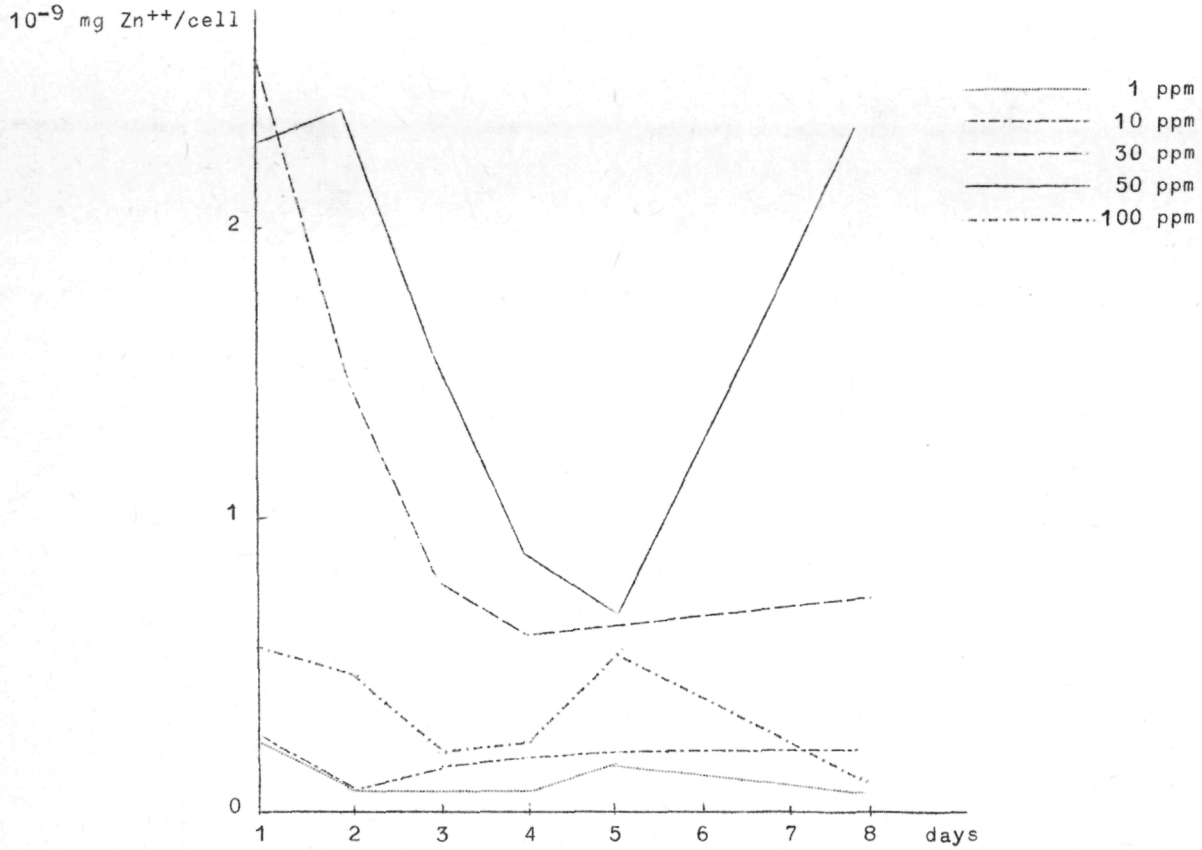


fig. 8b.
Zn ad-absorption/cell unit by Phaedactylum tricornutum.

with increasing Zn^{++} initial concentration in the sea water. A maximum is attained at 80 ppm . At 100 ppm the growth is at least for *Phaeodactylum* strongly inhibited and seems to be correlated to a marked decrease of the Zn content; the effect is less obvious for *Dunaliella* since the growth curves flatten at 50 , 80 and 100 ppm .

So it looks as if during active growth a decrease in the growth rate could be related to an increase in Zn content, but that strong growth inhibition has the opposite result and very much decreases the apparent Zn uptake.

The interpretation of these results is not easy since no distinction can be made between the Zn adsorbed on the cell walls or incorporated in the protoplasm without the use of radio-isotopes, besides the authors have made no attempt to evaluate mortality. Dead cells might behave differently compared to living ones.

The work however shows that the burden per cell can reach rather large values, and that there is a marked difference between naked cells and those having a silica shell.

If the amount of Zn adsorbed on the cell walls is large compared to what enters the cell and varies in time, toxicity experiments become difficult to interpret, although the input to the food chain can still be assessed.

A further complication arises from the fact that the amount found on and in the cells becomes in dense cultures large enough to alter the initial Zn^{++} concentration in the sea water. At 1 ppm , 88 % of the Zn is found bound to the cells after 7 days in *Dunaliella* cultures, dropping to 11.7 % at 80 ppm and 4.5 at 110 ppm . Similar effects are found in *Phaeodactylum* suspensions.

Strict control of the amount of toxic substances to which organisms are exposed, although at first sight a perequisite, seems to have been overlooked by many people. The above findings rightly draw attention to this important problem.

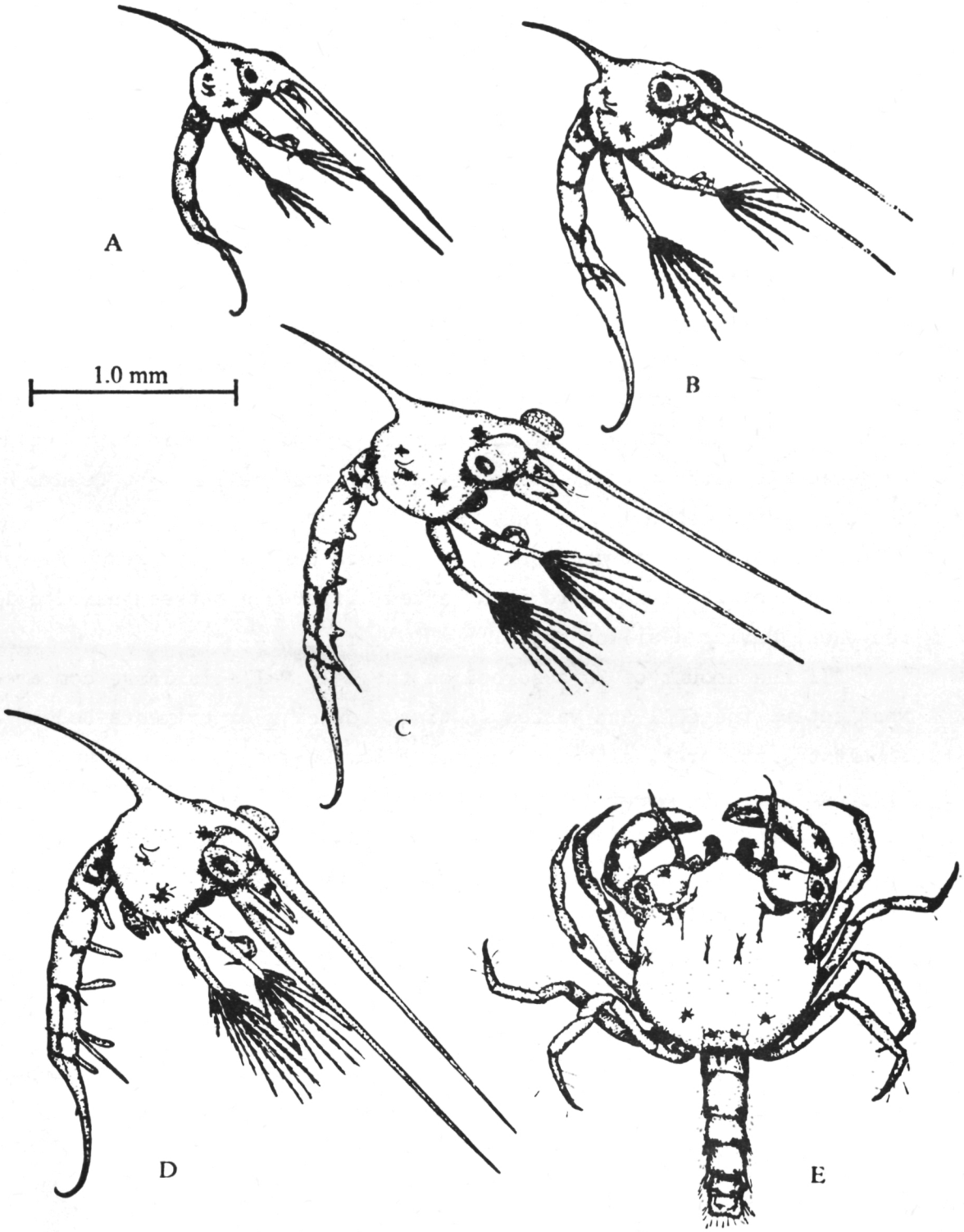


fig. 9.
Zoeal stages one through four (A, B, C, D) and megalops (E) of the R. harrisii.

2.- Invertebrates

2.1.- Combined effects of Zn^{++} and Pb^{++} on the larval development of the mudcrab *Rithropanopeus harrisii* [Benijts *et al.* (1974a)]

Costlow *et al.* (1971) have shown that the little mudcrab *Rithropanopeus harrisii* can rather easily be reared in laboratory conditions and that high survival conditions can be obtained.

The hatched larvae are kept in 20 ‰ sea water in small glass scales; they are fed with Artemia-larvae; the temperature is kept at 23.5 °C , the animals are reared 12 h in the dark and 12 h under controlled light conditions. The larvae go through 5 zoeal stages (fig. 9); at the megalops stage each is kept in isolation to avoid cannibalism. The development is followed until the first crab-stage. Zn^{++} and Pb^{++} are added as chlorides and a series of concentrations pairs is tested (0 , 25 , 50 ppb) . Per concentrations pair 5 parallel experiments with 10 larvae are carried out. The average development duration is calculated, the combination 0 ppb Zn^{++} and 0 ppb Pb^{++} being the blank experiment for which a development duration of 14.35 days is found.

The results after statistical treatment are displayed in figure 10 showing the contours of equal mean time of development as a function of both the Zn^{++} and Pb^{++} concentration.

The graph shows a significative optimum combination at about 30 ppb Zn^{++} and 25 ppb Pb^{++} leading to a shortening of the larval development to 13.95 days.

It can further be shown that an increase of the Pb^{++} concentration from 0 to 50 ppb increases the development duration following a quadratic law. At 50 ppb Pb^{++} and 0 ppb Zn^{++} the duration is 14.35 days. An increase of the Zn^{++} concentration from 0 to 50 ppb has no significative effect. Lead is more toxic than zinc.

The "dramatic" synergism described for Zn^{++}, Pb^{++} and Hg^{++} in the growth of the marine ciliate *Cristigera* by Gray and Ventilla (1973) in the range 0-100 ppb Zn^{++} and 0-188 ppb Pb^{++} , the effects of both these metal ions being more important than that of Hg^{++}, is not observed in the present case, on the contrary.

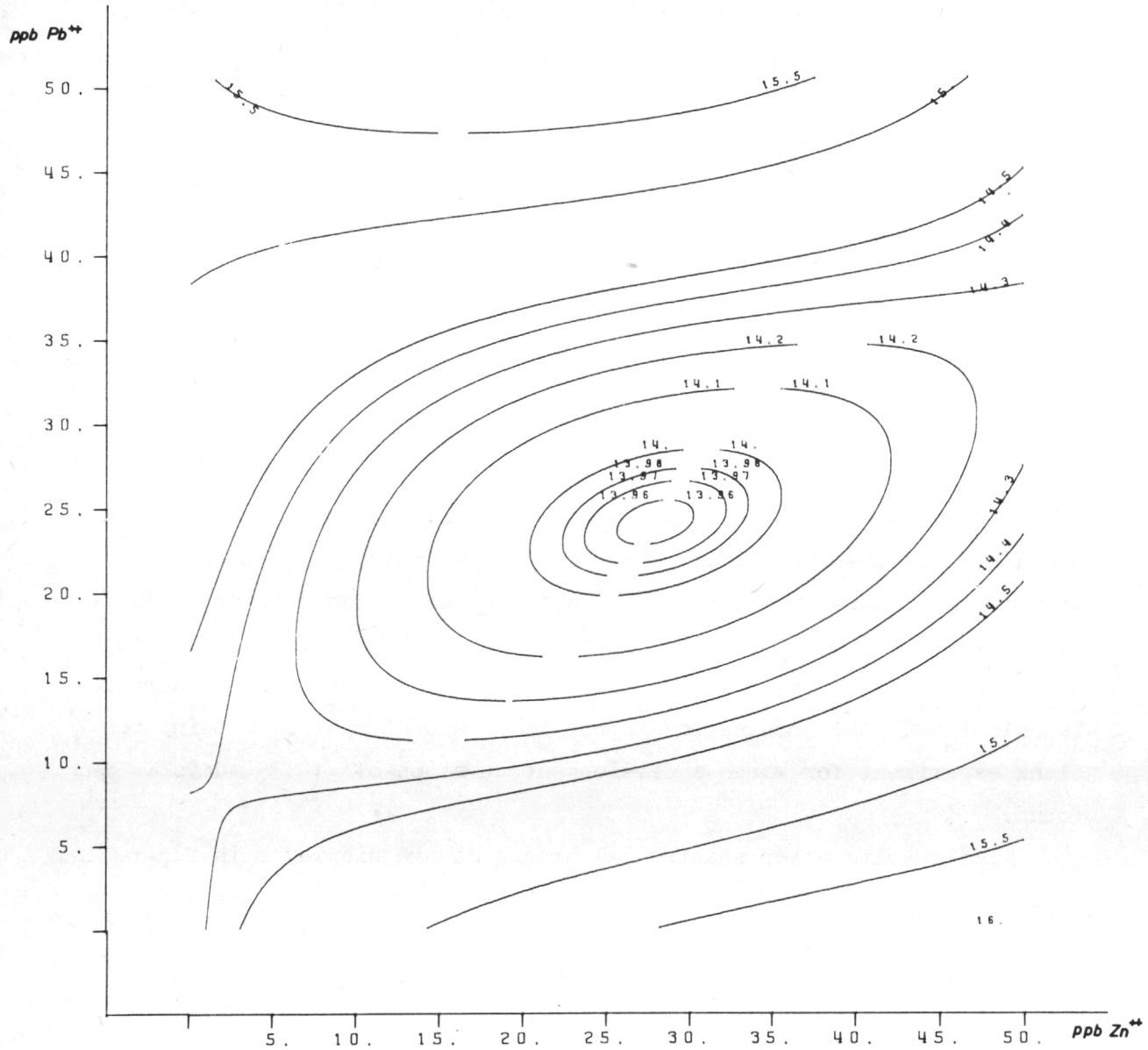


fig. 10.
Mean time of development of Rithropanopeus harrisii from hatch to megalops in days (5 replicates).

Again the choice of the test organisms is crucial and certainly there must exist species, especially at very low metal concentrations like in these experiments, where one might well be in the range where metal ions play an essential role in some metabolic pathways and therefore enhance biological processes instead of inhibiting them.

Whatever the result however the method used by Benijts *et al.* with its type of display, is an elegant tool to show synergisms either positive

or negative of importance either in normal physiological conditions or in acute intoxications.

2.2.- Effect of Hg^{++} on *Mytilus edulis* and *Asterias rubens* [Perpeet, Vloebergh (1974)]

2.2.1.- *Mytilus edulis*

a) Distribution of ^{203}Hg in the organs

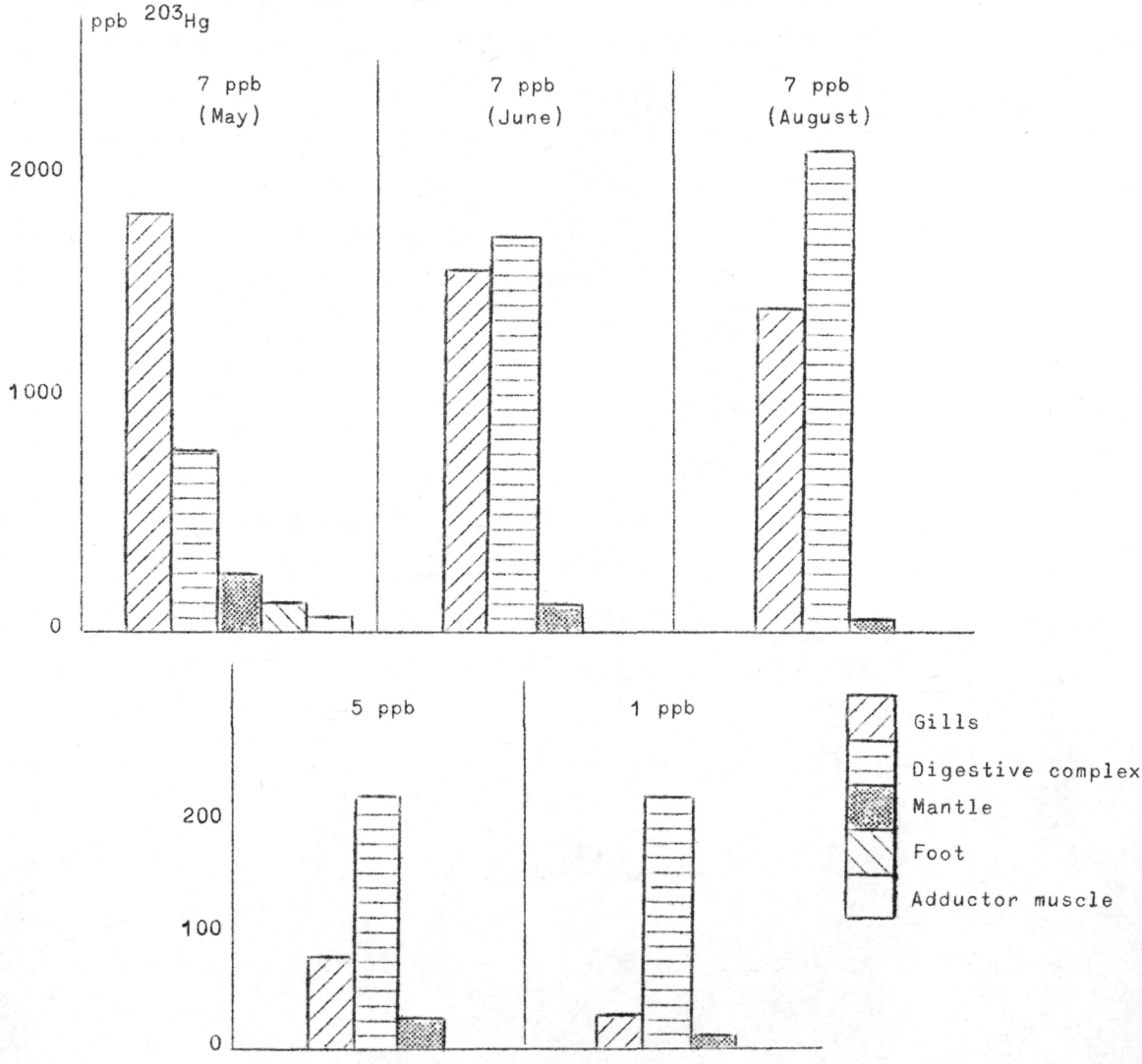


fig. 11.

Hg content of the organs of Mytilus edulis exposed to sea water containing 7, 5 and 1 ppb Hg.

Mussels (20 specimens) are placed during 24 h in 51 artificial (32 ‰) sea water contaminated with 7 ppb ^{203}Hg (0.005 µCie)($HgCl_2$) , the radioactivity in the gills, the digestive tract and related organs, the mantle, the adductor muscle and the foot is measured using a liquid scintillation technique (Packard Tri-Carb 3375). The tissues are dissolved in 1 cm^3 Soluene 350 (50 °C , 2 h) ; 10 cm^3 Dimilume are then added. The experiments are carried out in May, June and August. In May the mussels are sexually mature and have used most of their stored glucids and lipids. Figure 11 shows that in May accumulation is highest in the gills, it remains important in June and August, but becomes even higher in the digestive tract. The adductor muscle contains 30 times less Hg , the mantle and the foot are a little more contaminated.

At 1 ppb and 7 ppb , during sexual resting period, the distribution follows the same pattern, but the amounts of Hg found are much reduced. It seems that there is a threshold concentration between 5 and 7 ppb where accumulation increases sharply.

b) Kinetics of the ^{203}Hg accumulation in the organs at 5 and 1 ppb

The sea water is replaced every day during 7 days. Figure 12 shows the rate of intake of ^{203}Hg in the various organs. Accumulation is faster the higher the Hg concentration.

Figure 13 indicates the effect of salinity : the gills accumulate at a lower initial rate in 16 ‰ sea water containing 5 ppb ^{203}Hg .

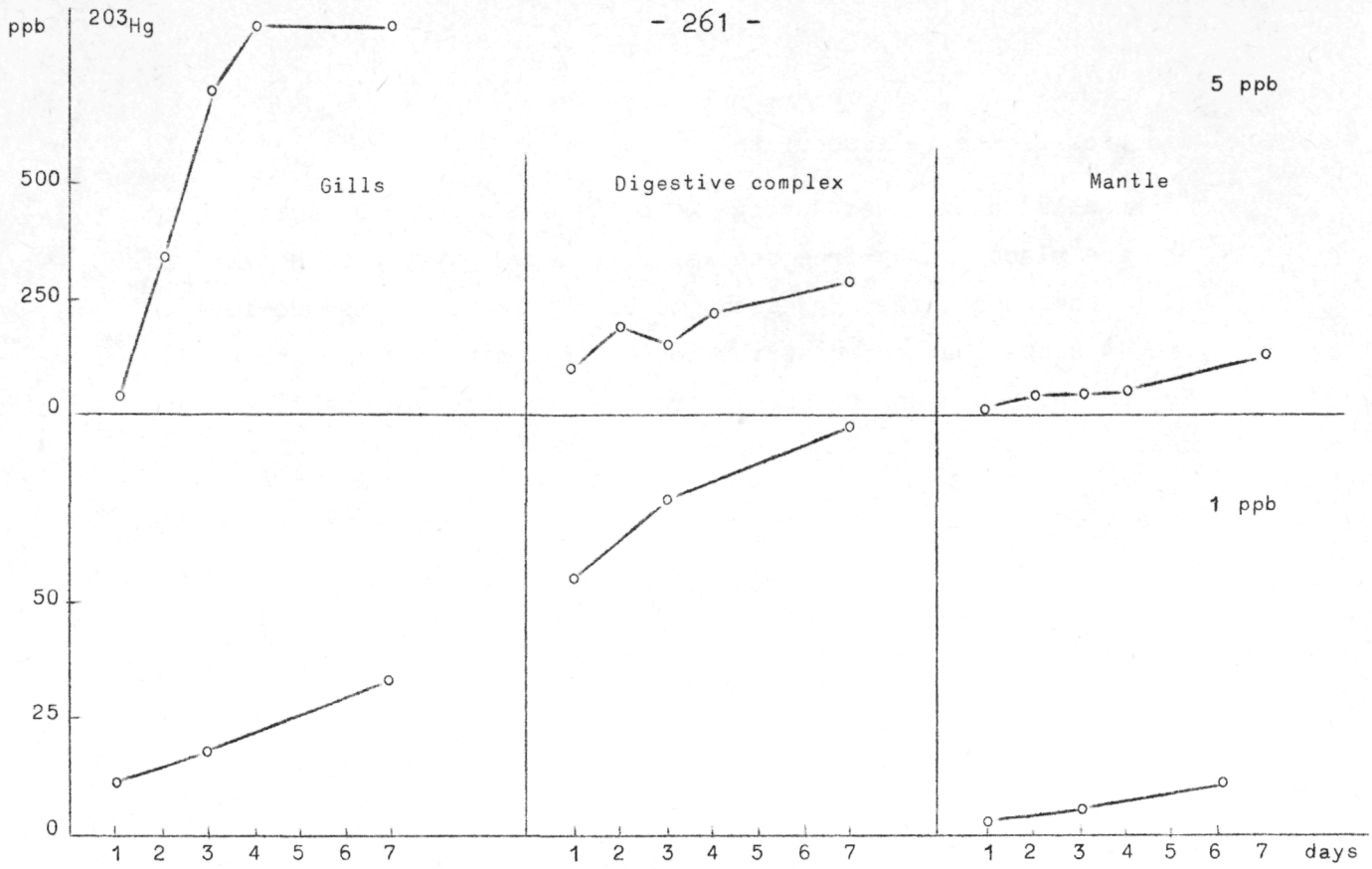


fig. 12.

Kinetics of accumulation of Hg in Mytilus edulis exposed to sea water containing 5 and 1 ppb Hg.

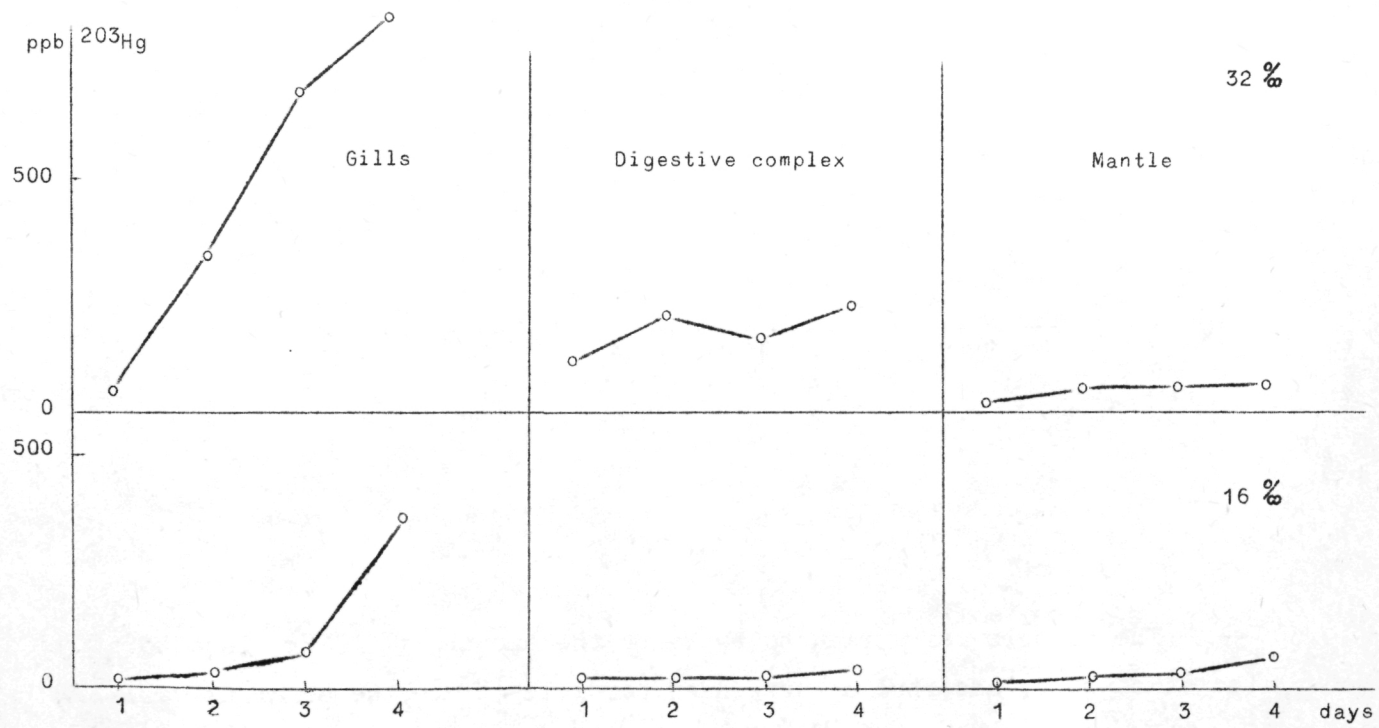


fig. 13.

Effect of salinity on the uptake of Hg by Mytilus edulis exposed to sea water containing 5 ppb Hg.

c) Kinetics of the release of the ^{203}Hg burden

Mussels intoxicated during 24 h in sea water containing 7 ppb ^{203}Hg are placed in Hg-free sea water, changed every day. No Hg is found in the water, the Hg seems to be eliminated in pseudo-feces. Figure 14 shows that a redistribution of the initially incorporated ^{203}Hg probably happens before its release, fastest in the digestive organs.

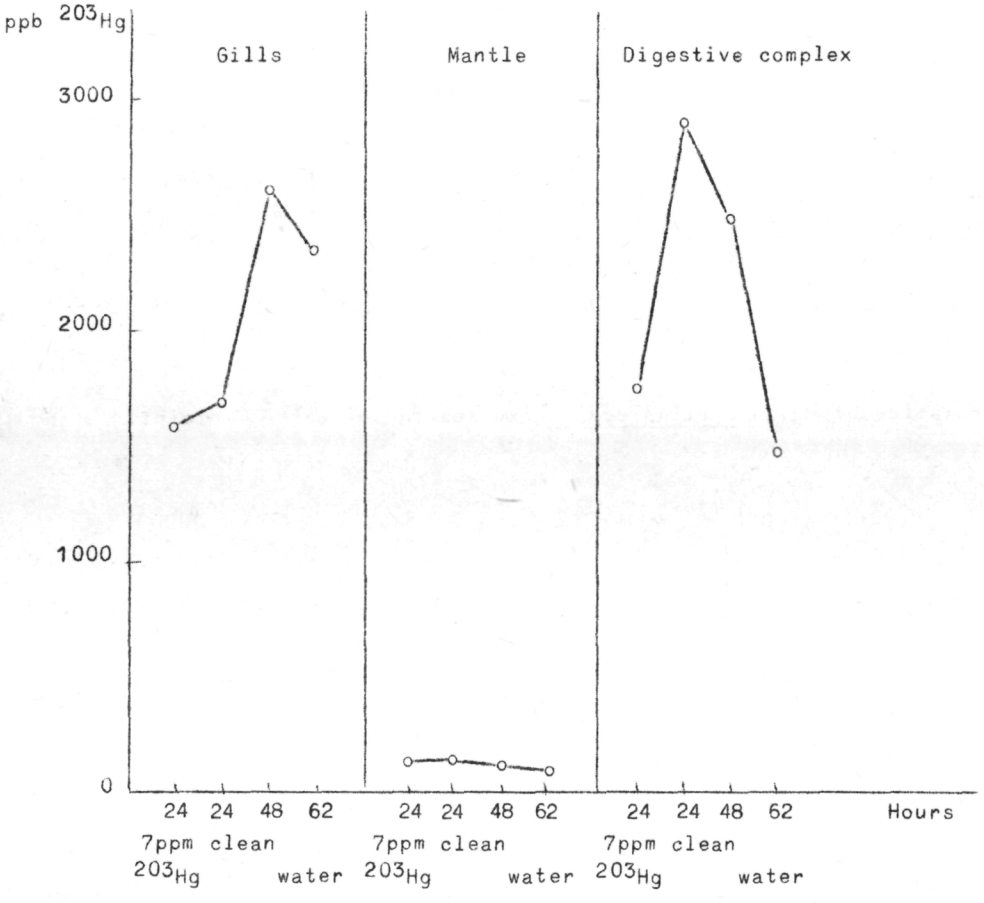


fig. 14.
Release of Hg by Mytilus edulis kept in non contamined sea water after initial intoxication (7 ppb Hg).

The authors have tried to evaluate the amount of ^{203}Hg lost to the atmosphere, adsorbed on suspended particles or on the aquarium walls. In natural sea water their results show that a large proportion of the added ^{203}Hg is quickly adsorbed on particulate matter. They use an

aquarium forming a closed system with traps at the air inlet and outlet (acid $KMnO_4$ solution). Starting at 10 ppb Hg in solution, they end at 8.6 ppb after 65 min ; 9.5 ppb Hg are found on the particles retained on a millipore filter.

With artificial sea water, in presence of mussels, fine particulate matter is formed which adsorbs part of the mercury. Evaporation represents however the most important loss. After 8 days, under these conditions at an initial concentration of 23 ppb the mussels however contain 2.3 ppm ^{203}Hg in the average.

2.2.2.- *Asterias rubens*

Five specimens are exposed in 5 ℓ sea water contaminated with $HgCl_2$ containing ^{203}Hg . The results are expressed as if the total amount of mercury was radioactive.

a) Distribution of ^{203}Hg in the organs (1 ppm Hg in the sea water)

Figure 15 shows that the podia and various parts of the skin accumulate large quantities of Hg . After 15 h the animals are in very bad physiological condition (swelling of disc and arms, loss of pigmentation, cessation of movements). This severe intoxication explains probably the loss of Hg initially accumulated and its release in the water. Digestive organs do not participate at this Hg concentration.

b) Release of ^{203}Hg from *Asterias rubens* initially intoxicated in sea water containing 0.2 ppm Hg

The animals first intoxicated at 0.2 ppm Hg during 24 h are in much better condition than in presence of 1 ppm Hg .

The digestive tract and the podia accumulate Hg ; as in the case of Cu^{++} it seems that at high concentrations the heavy metals block the respiratory system, which limits the entry in other organs. At low concentration the Hg is distributed in organs other than the podia.

Figure 16 shows the release of the Hg load which is fast from the podia and the skin, but the situation is quite different for the stomach and the pyloric caeca, showing a redistribution of the toxic material.

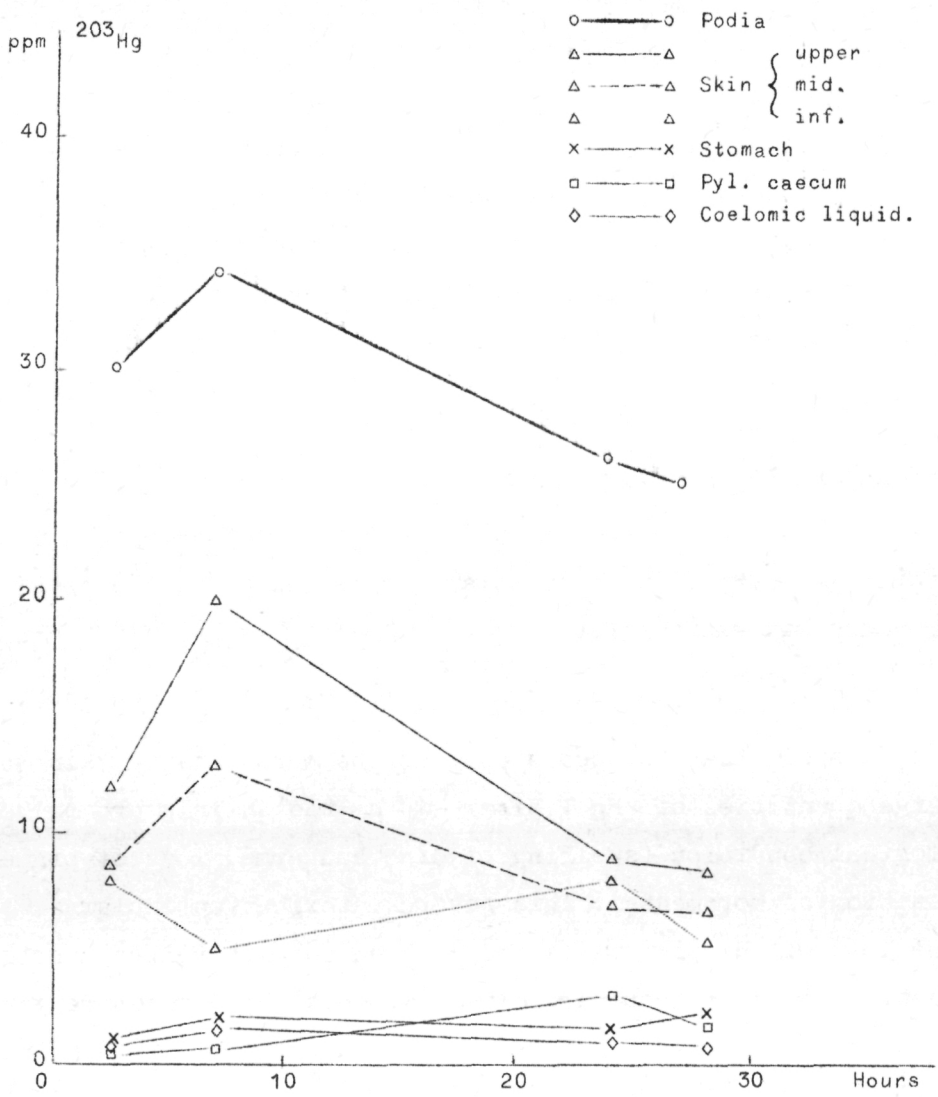


fig. 15.
Uptake of Hg by Asterias rubens exposed to sea water containing 1 ppb Hg.

c) Intoxication of *Asterias rubens* fed on contaminated mussels

Preliminary experiments show that one mussel contaminated in sea water containing 0.8 ppm Hg and fed to one *Asterias rubens* produces an increase of radioactivity in the stomach and the pyloric caeca. The podia and the skin are little affected. The starfish contains about 10 times less Hg than the mussel per gram.

When fed with one mussel exposed to 5 ppb Hg , the starfish accumulates progressively Hg in the pyloric caeca as shown in table 2.

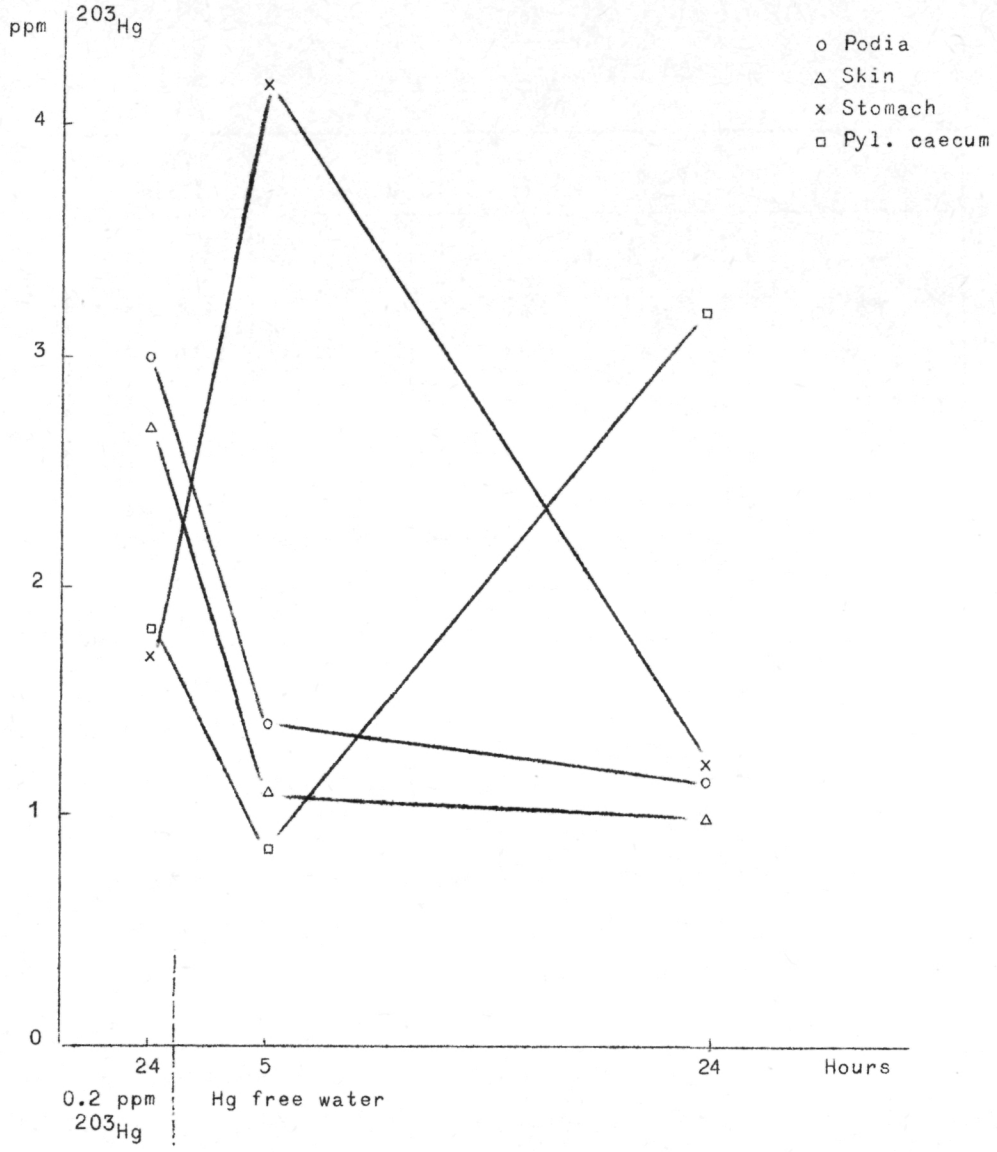


fig. 16.

Release of Hg by Asterias rubens kept in non contamined sea water after initial intoxication (0.2 ppm Hg).

Mucus is formed by the starfish, containing as much as 13 ppb Hg . This process might prove to be an unexpected excretory pathway.

The experiments performed with ^{203}Hg allow to study the effect of very low concentrations of Hg . They show that direct intoxication is more effective than intoxication by ingestion of contaminated food in the case of *Asterias rubens*. They also show how fast Hg is taken from water in the gills of mussels. Conditions similar to those created

Table 2

^{203}Hg content (ppb) in the organs of Asterias rubens fed with contaminated mussels

Organs	Controls		48 hours digestion		106 hours digestion		127 hours digestion	
Podia	0.27	0.51	0.98	0.48	1.47	2.34	0.85	1.22
Skin	1.11	0.54	0.98	1.24	0.63	1.55	1.48	0.87
Stomach	0.17	0.41	0.91	1.80	1.29	13.37	1.50	0.60
Pyl. caecum	0.09	0.17	6.20	4.65	10.10	3.89	55.17	14.13
Rect. caecum	0.32	1.50	2.29	1.04	1.65	6.79	13.60	6.50
Gonad	0.14	0.33	1.39	5.00	0.80	-	6.40	0.39

in the laboratory are seldom found in natural environment, since Hg is probably adsorbed on particulate matter in the water column or in sediments where anaerobic conditions might lead to very stable forms but where bacteria might also produce dangerous methylated forms. However, direct intoxication is a very fast process, which exists even at very low concentrations of free ions and it cannot be overlooked as one of the important entry routes of heavy metals in marine animals, many of which filter continuously enormous amounts of water through their respiratory system. Some do also retain suspended matter eventually loaded with heavy metals. Release of mercury in the sea results probably in most cases in local effects, because of fast adsorption on particulate matter : mussels collected at 3 km from an outlet have been found to contain 0.93 ppm Hg [Fimreite *et al.* (1971)], the specimens found at 11 km distance contained only 0.11 ppm Hg .

d) Cr, Cd, Cu, Pb, Mn, Zn and Fe content of *Mytilus edulis* collected in the Scheldt [Vanden Bossche (1975)]

The mussels have been collected, 100 at a time and grouped 4 by 4 in function of their length (varying between 2 and 6 cm) downstream, at Perkpolder, Terneuzen and Hoofdplaat. The specimens have been taken in January and May to show eventual seasonal effects in connection with sexual maturity (May).

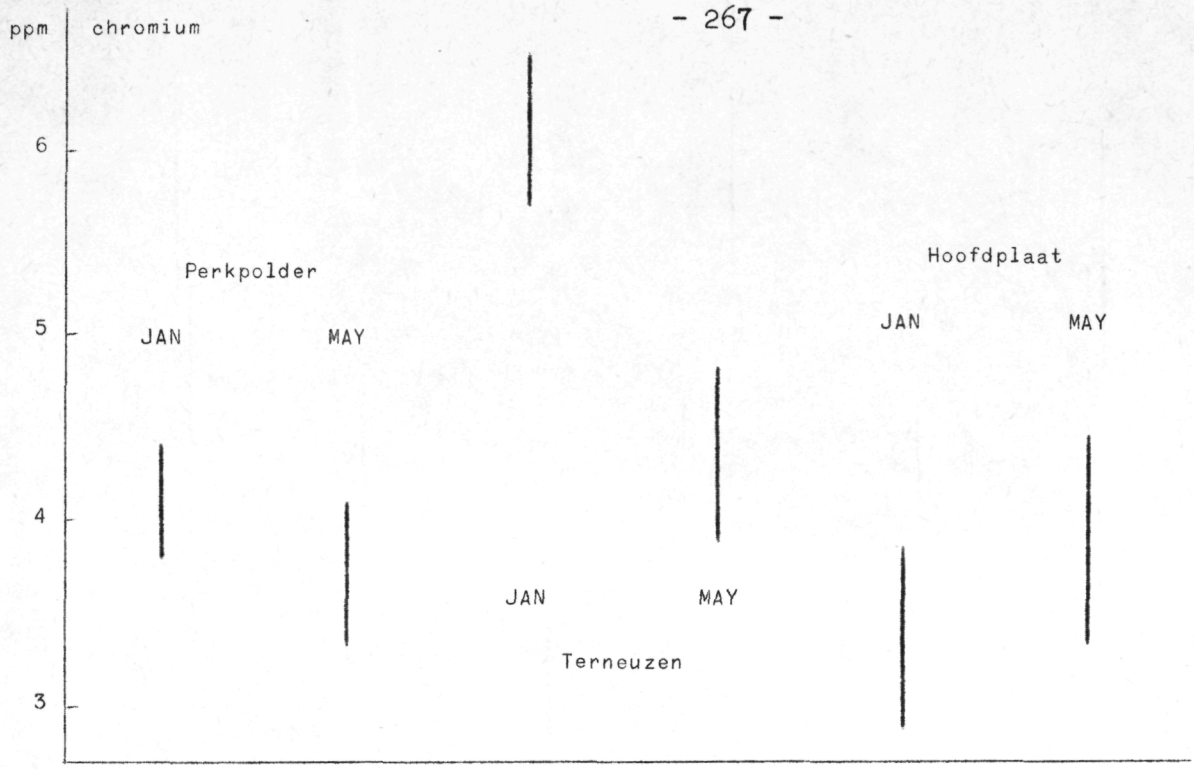

ppm
chromium
6
5
4
3
Perkpolder
JAN
MAY
Terneuzen
JAN
MAY
Hoofdplaat
JAN
MAY

fig. 17.

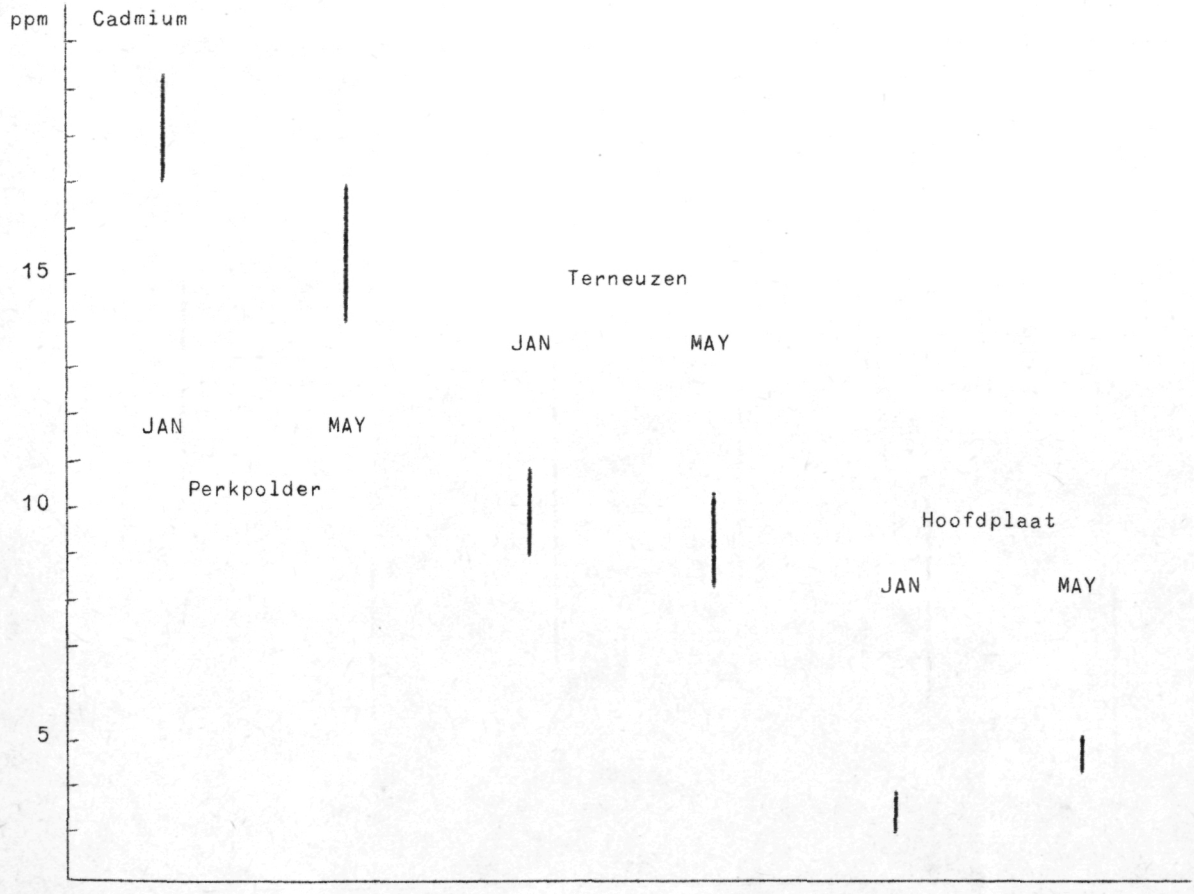

ppm
Cadmium
15
10
5
Perkpolder
JAN
MAY
Terneuzen
JAN
MAY
Hoofdplaat
JAN
MAY

fig. 18.

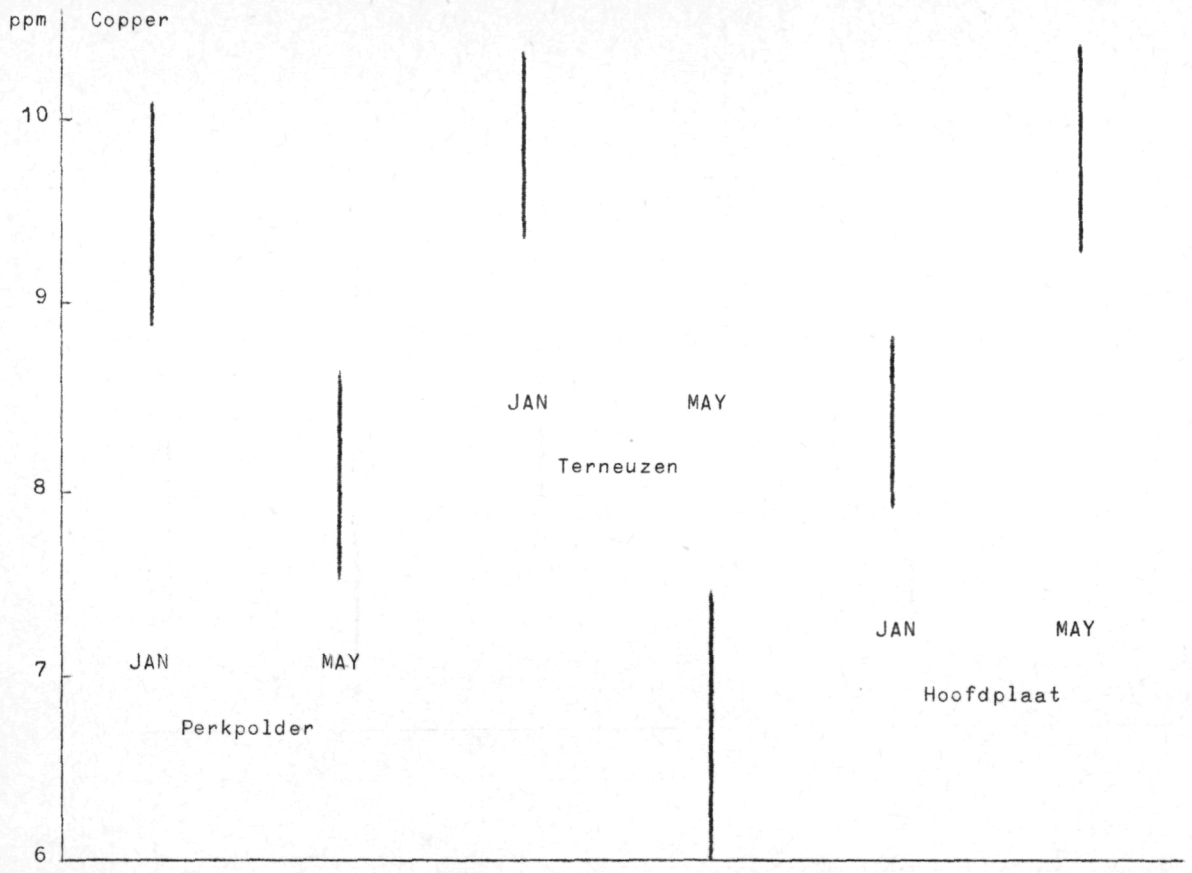

ppm
Copper
10
9
8
7
6
JAN
MAY
Perkpolder
JAN
MAY
Terneuzen
JAN
MAY
Hoofdplaat

fig. 19.

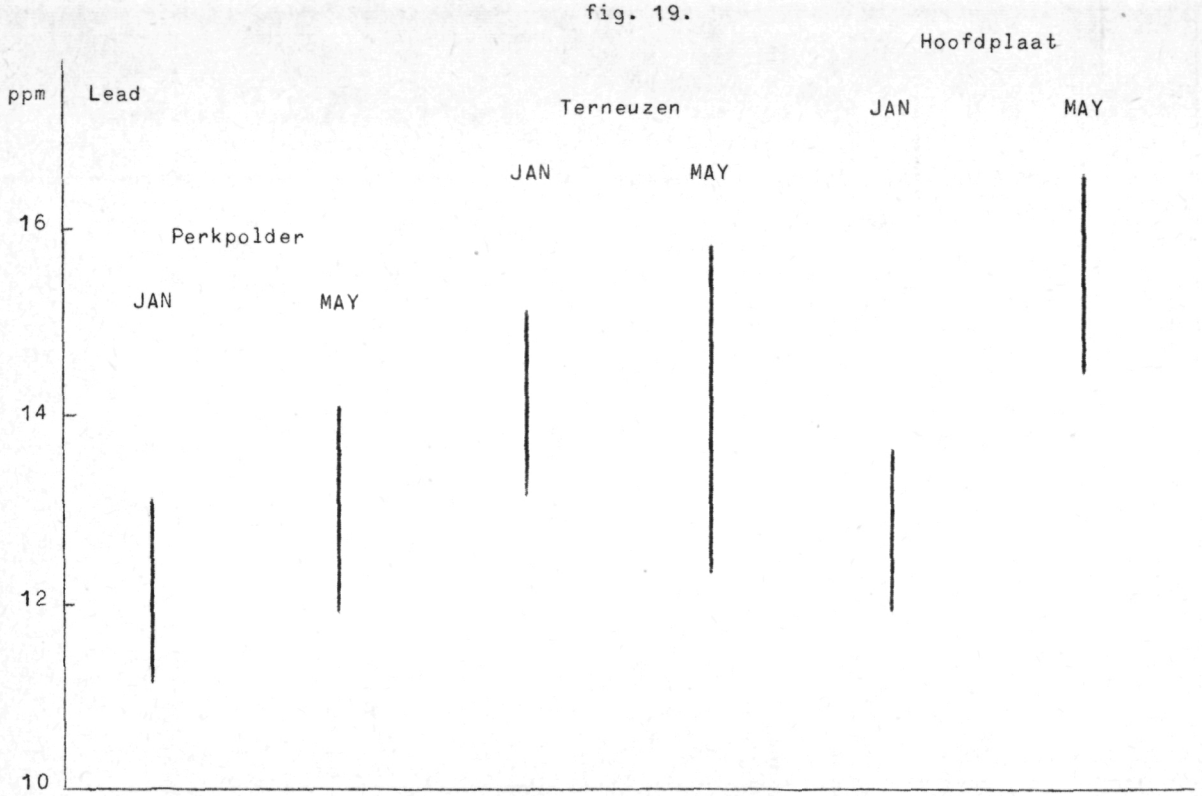

ppm
Lead
16
14
12
10
Perkpolder
JAN
MAY
Terneuzen
JAN
MAY
Hoofdplaat
JAN
MAY

fig. 20.

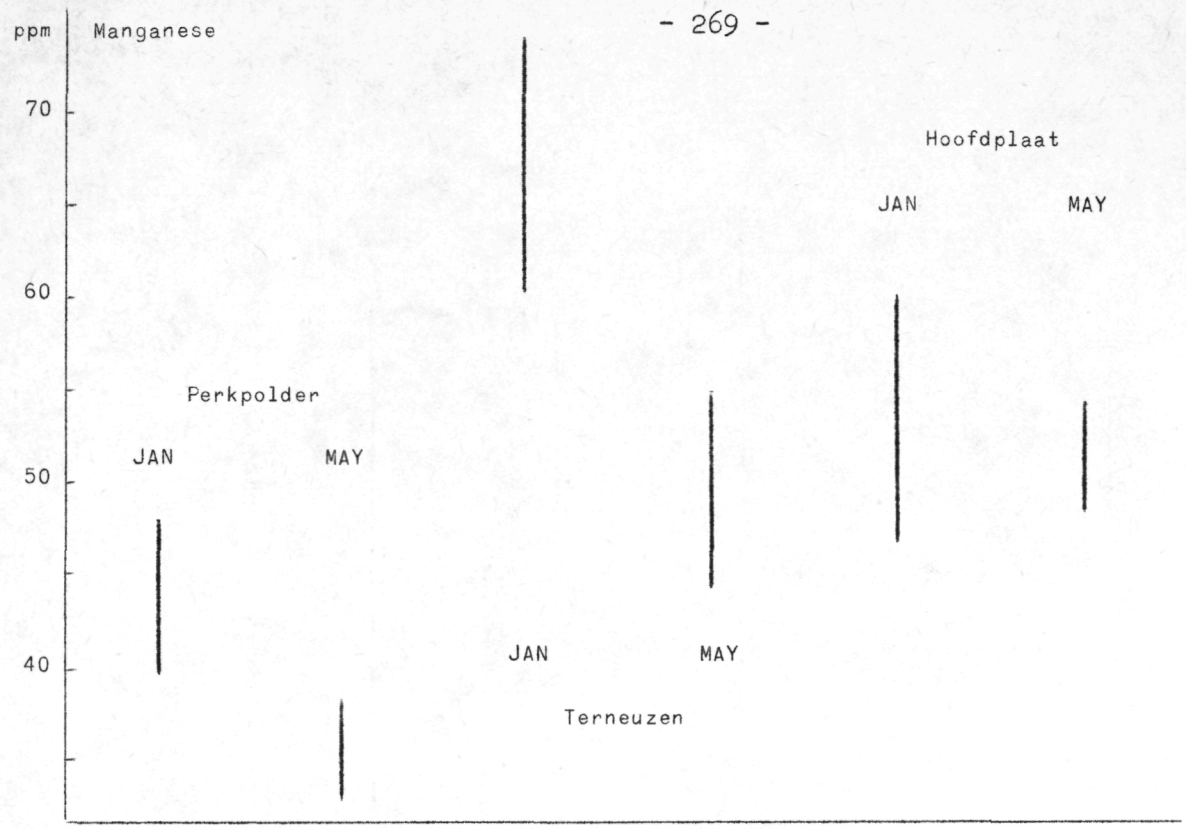

ppm
Manganese
70
60
50
40
Perkpolder
JAN
MAY
JAN
MAY
Terneuzen
Hoofdplaat
JAN
MAY

fig. 21.

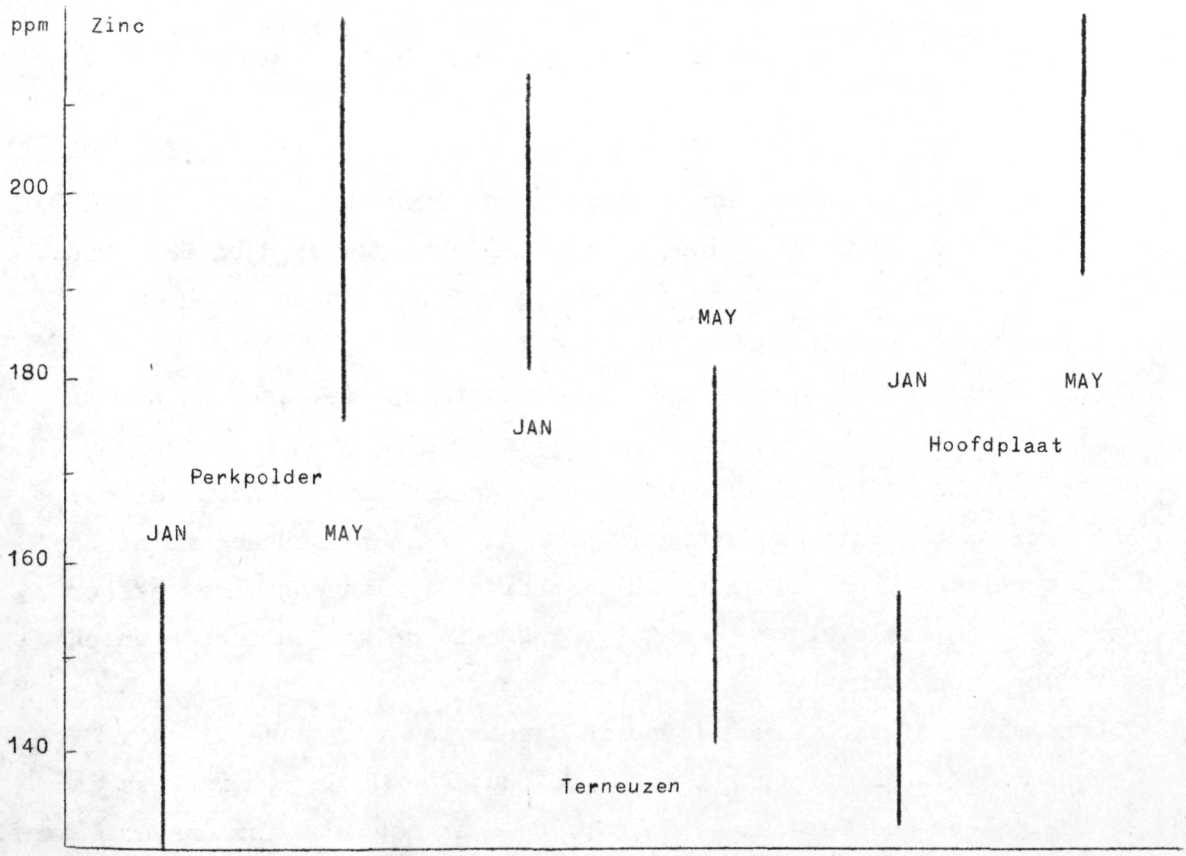

ppm
Zinc
200
180
160
140
Perkpolder
JAN
MAY
JAN
MAY
Terneuzen
JAN
MAY
Hoofdplaat

fig. 22.

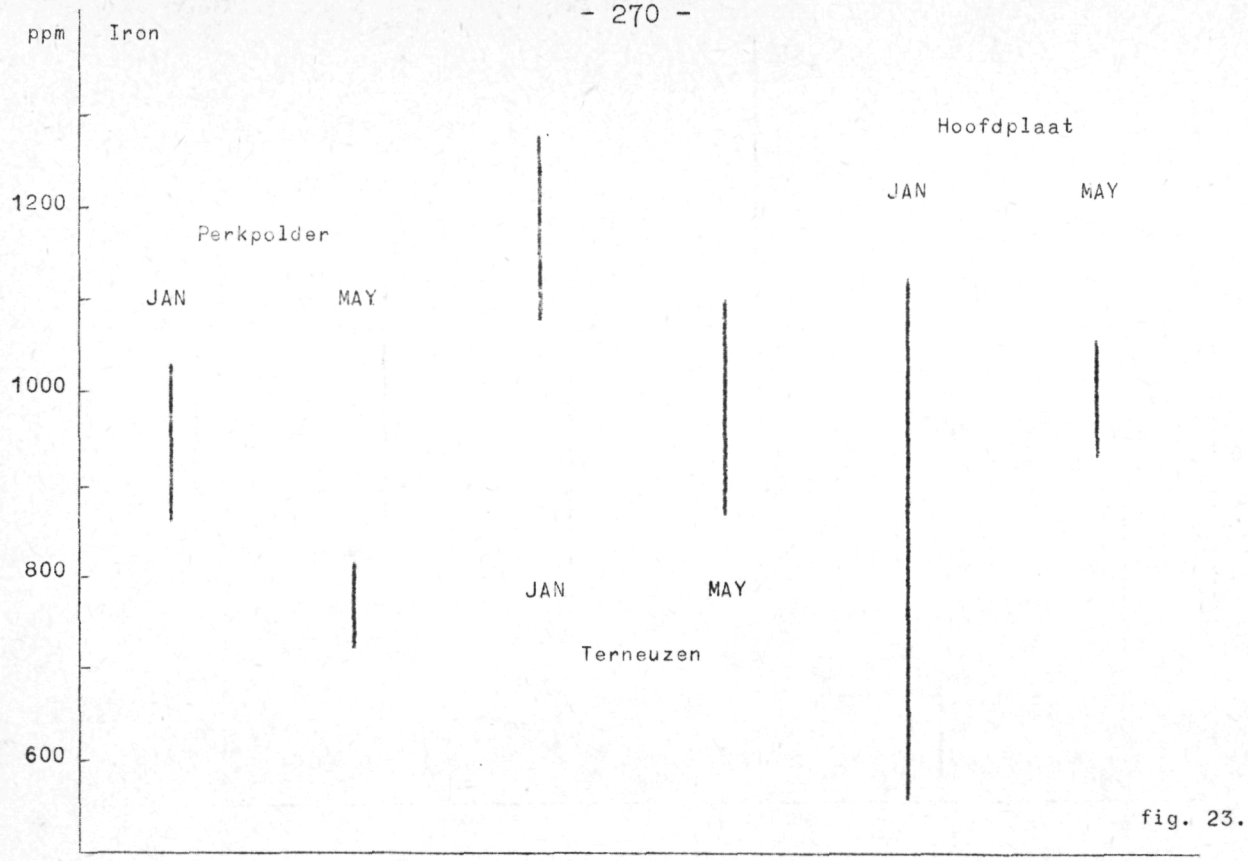


fig. 17-23.
Cr, Cd, Cu, Pb, Mn, Zn, Fe content of Mytilus edulis collected in the Scheldt.

The mussels kept in deep freezer are dried at 115 °C during 24 h, ashed at 450 °C. The ashes are suspended in 3 cm^3 HCl and 1 cm^3 HNO_3. After heating and slight dilution, the solution is filtered on Sartorius 25 mm Ø SM 12804 filters and brought to 25 cm^3. It is analysed by atomic absorption (Perkin Elmer 303).

The results are indicated in figures 17 to 23 expressed in ppm dry weight (µg/g).

There seems to be no correlation between the metal concentrations and the size of the animals. There is no sign of increased accumulation in older specimens. None of the results show a simultaneous increase or decrease of all metals at one locality. There is no way to decide which place is more contaminated.

Comparison of the values found in January and May however shows some regularity : the concentration of Cd, Cu, Fe, Mn and Cu is less in May at Perkpolder and Terneuzen. This is however not true for Zn and Pb at Perkpolder.

It is to be noted that the results at Hoofdplaat in January might be too low because of the use of a different filtering technique; the Cd concentrations at Perkpolder in January are probably too low because of a defect of the Cd lamp : the mean value should be around 16 ppm .

The results confirm the finding of Perpeet and Vloebergh (1973) regarding the absence of correlation with size; the date for Cu, Zn, Fe are lower than theirs, the data for Pb, Cd and Cr are in the same range.

The fact that lower concentrations are found in May might indicate the existence of some excretory mechanism, but this is only speculation since no data are available about the metal concentrations in the water, in the sediments, in suspended matter, at the same localities, at the same time in the year.

3.- Vertebrates (fish)

3.1.- Accumulation and excretion of Hg by *Myoxocephalus scorpius* (scorpion fish) [Bouquegneau (1975)]

Myoxocephalus scorpius, also called *Cottus scorpius* is of little importance as food resource, but plays an important ecological role. It is extremely voracious, feeding on crustaceans, fish eggs and larvae. It is found along the North Atlantic and the North Sea coasts.

The fishes are kept in natural sea water and exposed to sublethal doses of 0.1 ppm and 1 ppb Hg ($HgCl_2$ or CH_3HgCl). The water is changed every day. The methodology is the same as described in the previous work on the eel *Anguilla anguilla* [Bouquegneau (1973a)].

3.1.1.- Total Hg burden and body distribution in non-intoxicated fish

Table 3 shows the distribution of Hg in specimens from the region of Ostend and Den Helder (Netherlands). No significant difference is found between the fish originating from these two localities, but the total body burden is very high (1.1 ppm Hg), most of which located in the muscles.

Figure 24 indicates that there exists a correlation between the muscle content and the body weight, but no correlation is found between

Table 3

Distribution of Hg in non-intoxicated Myoxocephalus scorpius

Organs	Weight (g)	Concentration of Hg (ppm)					Hg burden (µg)
		(1)	(1)	(2)	(2)	$\bar{m} \pm ES$	
Muscles	71.5	0.9	1.3	1.7	1.4[1]	1.3 ± 0.2	93.0
Skin	10.5	0.4	0.6	0.5	0.2	0.4 ± 0.1	4.2
Stomach	5.1	0.4	0.7	0.7	0.6	0.6 ± 0.1	3.1
Gills	4.6	0.7	0.8	1.1	0.9	0.9 ± 0.1	4.1
Bones	3.2	-	0.4	0.8	0.9	0.7 ± 0.2	2.2
Liver	2.4	0.5	1.5	2.2	1.0[2]	1.3 ± 0.4	2.6
Gonads	0.8	-	0.4	0.4	0.7	0.5 ± 0.1	0.4
Intestine	0.7	0.4	0.5	0.9	0.8	0.7 ± 0.1	0.5
Kidney	0.4	0.8	1.0	1.0	0.7	0.9 ± 0.1	0.4
Bile	0.3	-	0.3	-	0.4	0.4 ± 0.1	0.1
Spleen	0.2	0.5	0.7	1.0	0.8	0.8 ± 0.1	0.2
Heart	0.2	0.4	0.8	0.9	0.3	0.6 ± 0.1	0.1
Brain	0.1	-	1.4	1.3	0.8	1.2 ± 0.2	0.1
Body weight	100	Total amount of Hg in 100 g fish					111.0 µg 1.1 ppm

(1) : 2 living specimens from the Fisheries Institute in Ostend.
(2) : 2 living specimens from the Marine Station of Den Helder.
1 Including the 25 results from fig. 1 [Bouquegneau (1975)].
2 Including the 25 results from fig. 2 [Bouquegneau (1975)].

the liver Hg concentration and the body weight. Correlation however does exist between muscle and liver burden : the more Hg in the muscles, the more in the liver.

3.1.2.- Total Hg burden and body distribution in fish intoxicated during one month in sea water containing 1 ppb Hg ($HgCl_2$ or CH_3HgCl)

Table 4 gives the distribution of Hg in fish kept during one month in sea water containing 1 ppb Hg ($HgCl_2$ or CH_3HgCl) . The results clearly demonstrate the accumulation of Hg in the various organs, the gills being especially affected in the case of HgCl ,

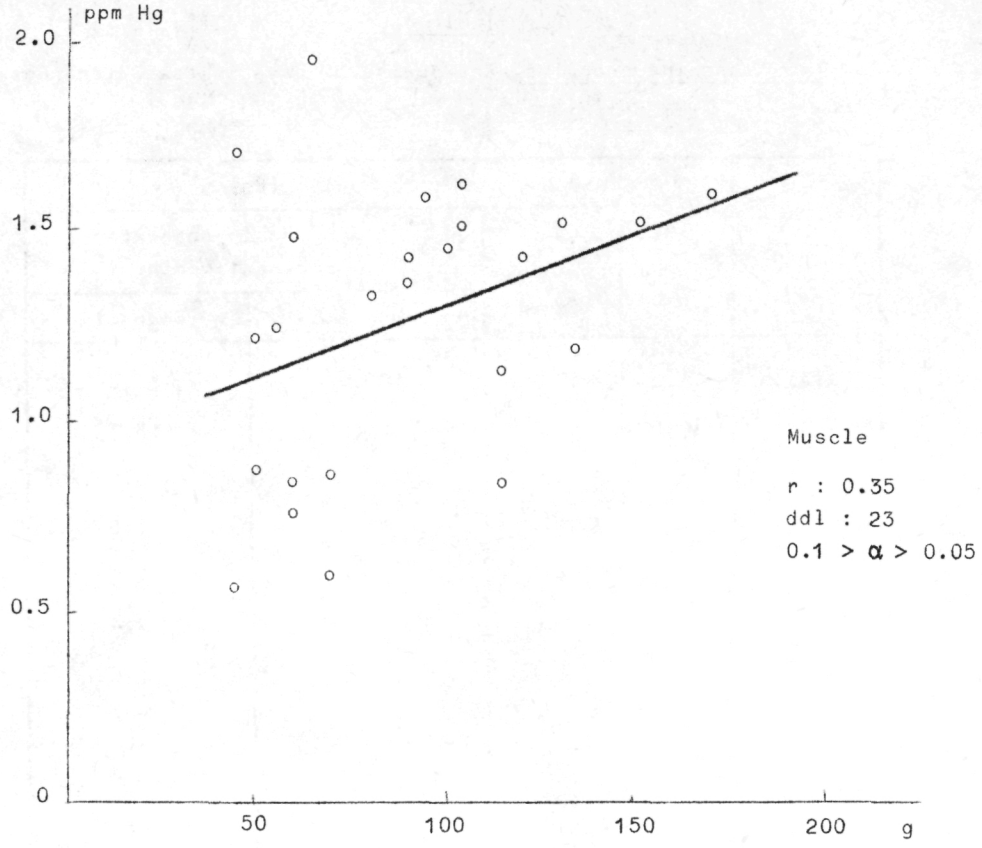


fig. 24.
Relationship between the concentration in muscles from Scorpion fish and body weight.

as observed in sea water adapted eels. The overall effect is more important with CH_3HgCl , but the distribution differs from that observed in the case of $HgCl_2$.

3.1.3.- Kinetics of Hg accumulation and excretion

Fish are first kept during 24 days in sea water containing 0.1 ppm Hg ($HgCl_2$) ; some specimens are placed in non-contaminated water after 8 days and the Hg content of the main organs is followed in both batches.

Figure 25 shows the kinetics of accumulation and release in muscle, liver and gills.

Table 4

Hg burden in Myoxocephalus scorpius kept during 30 days in sea water containing 1 ppb Hg ($HgCl_2$ or CH_3HgCl)

Organs	Weight (g)	Hg burden (µg)		
		Controls	1 ppb Hg in sea water during 1 month	
			$HgCl_2$	CH_3HgCl
Muscles	71.5	93.0	100.1	135.9
Skin	10.5	4.2	4.2	13.7
Stomach	5.1	3.1	3.1	5.1
Gills	4.6	4.1	12.0	11.5
Bones	3.2	2.2	1.9	2.6
Liver	2.4	2.6	4.6	7.4
Gonads	0.8	0.4	0.4	1.0
Intestine	0.7	0.5	0.5	0.8
Kidney	0.4	0.4	0.6	0.8
Bile	0.3	0.1	0.3	0.4
Spleen	0.2	0.2	0.2	0.5
Heart	0.2	0.1	0.2	0.5
Brain	0.1	0.1	0.2	0.2
Body weight	100			
Hg body load		111.0 µg	128.3 µg	180.4 µg
Hg body concentration		1.1 ppm	1.3 ppm	1.8 ppm
Concentration factor		-	$(1.3 - 1.1).100 = \underline{200}$	$(1.8 - 1.1).100 = \underline{700}$

The Hg distribution has been followed as shown in table 4 for the other body parts. The total concentration factor reaches 51 , 75 and 98 respectively after 8 , 16 and 24 days in presence of 0.1 ppm Hg ($HgCl_2$) , it falls to 46 and 35 when the fish is kept, after 8 days intoxication during 8 and 16 days in non polluted water.

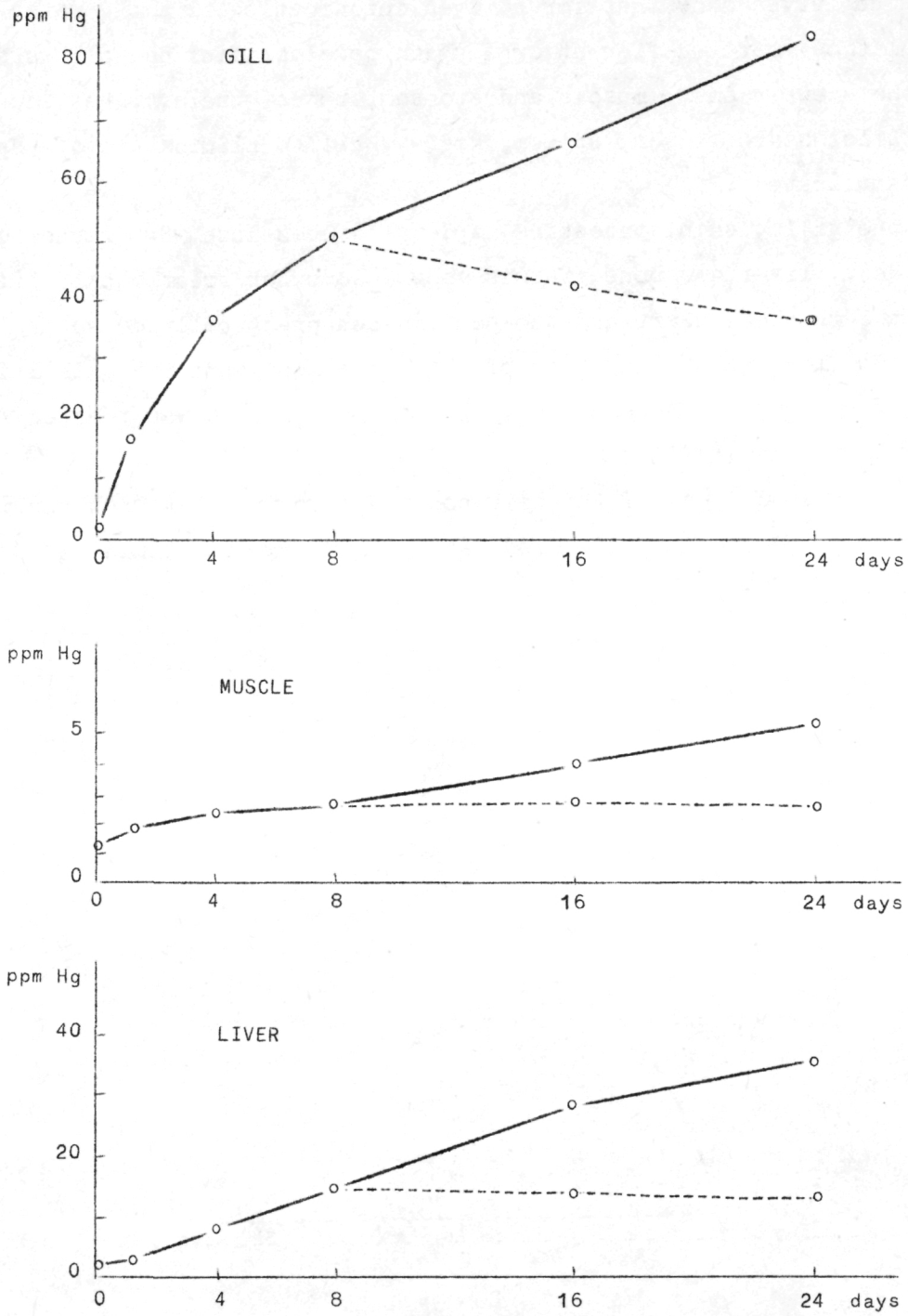


fig. 25.

Accumulation of Hg in the gills, muscles and liver of Scorpion fish kept in sea water containing 0.1 ppm Hg (heavy line).
Increase of Hg concentration when the fish are kept in non contamined water after 8 days intoxication (dotted line).

The curves show that for a given intoxication time the rates of accumulation in the different organs can be classified as follows starting with the slowest one : muscle and stomach, bones, brain, intestine and skin, bile, heart, liver, spleen, kidney, gills. Elimination of Hg is more complicated :

a) the gills, skin, intestine, spleen tissues lose Hg rather quickly; the kidney, liver and bone tissues show a somewhat greater half life.

b) the muscles, heart and stomach tissues practically do not release their Hg load within the time of the experiment, and the half life of Hg is very long in these organs. The same conclusion was reached for eels [Bouquegneau (1973a)].

c) the Hg content of the bile continues to increase when the intoxicated fish is decontaminated, indicating that Hg is eliminated from the liver.

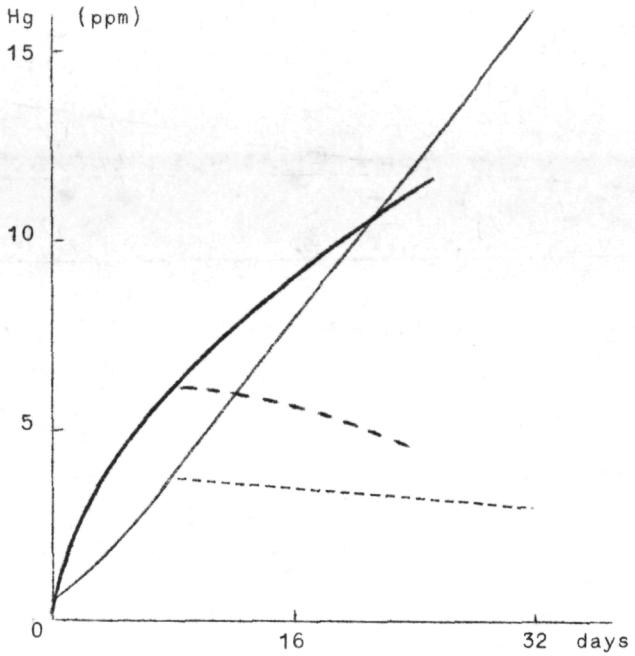


fig. 26.
Accumulation and release of mercury by Scorpion fishes (heavy lines) and sea water adapted eels (thin lines). Both are intoxicated in sea water containing 0.1 ppm Hg ($HgCl_2$).

It is possible from the different accumulation and release curves to construct a diagram showing the kinetics of intake and removal of Hg in

the total body as shown in figure 26, together with the results obtained for sea water adapted eels [Bouquegneau (1973a)]. It is obvious that the scorpion fish accumulates Hg much faster than eels at the start of the experiment; elimination is also faster.

The above results reveal that *Cottus scorpius* has an abnormally high burden of Hg in natural conditions. The intoxication experiments indicate that Hg accumulates in muscles and is stored there with an extremely long half life; liver is more active, accumulates and releases Hg much faster.

The fact that the amounts found in fish living in normal conditions are of the same order of magnitude in both liver and muscle indicate that the polluting levels at Ostend and Den Helder are rather the same regarding Hg.

Direct accumulation, through the gills, is very important and although intoxication through the food chain cannot be discarded and is difficult to ascertain, both effects cumulate.

The fact that the scorpion fish accumulates and eliminates Hg faster than eels is related to the difference in the relative weight of muscles, gills and liver in both fishes : respectively 71.5 % and 84.8 % , 4.6 % and 1.9 % , 2.4 % and 0.9 % .

It also seems evident that the excretory mechanisms are more efficient in *Cottus scorpius* than in *Anguilla anguilla* : the Hg concentration in the kidney still increases in eels submitted to desintoxication [Bouquegneau (1973a)] and remains stationary in scorpion fish.

3.2.- The mechanism of resistance of fish to Hg-poisoning [Bouquegneau *et al.* (1975)]

It has been shown by Bouquegneau (1973a) that eels intoxicated by Hg at sublethal doses of $HgCl_2$, accumulate large quantities of Hg and become resistant to otherwise lethal concentrations.

This type of adaptation mechanism can be identified as being related to the formation in different organs of the eel of metallothionein-like proteins.

Eels adapted to sea water are exposed to 0.4 ppm Hg ($HgCl_2$) during two weeks. The organs of control animals and intoxicated

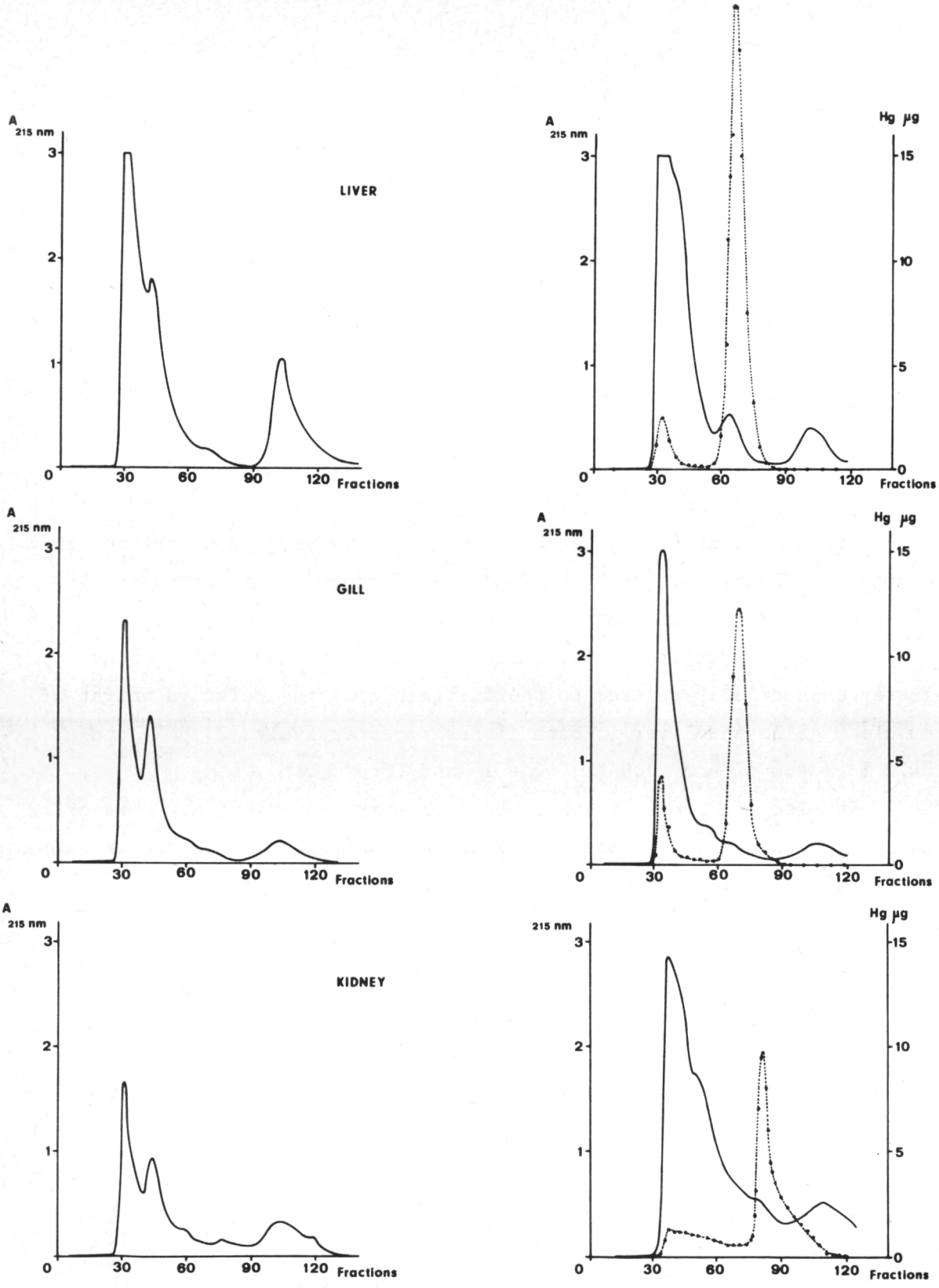

A
215 nm
LIVER
Hg µg
Fractions
GILL
KIDNEY
0
30
60
90
120
1
2
3
5
10
15

fig. 27.

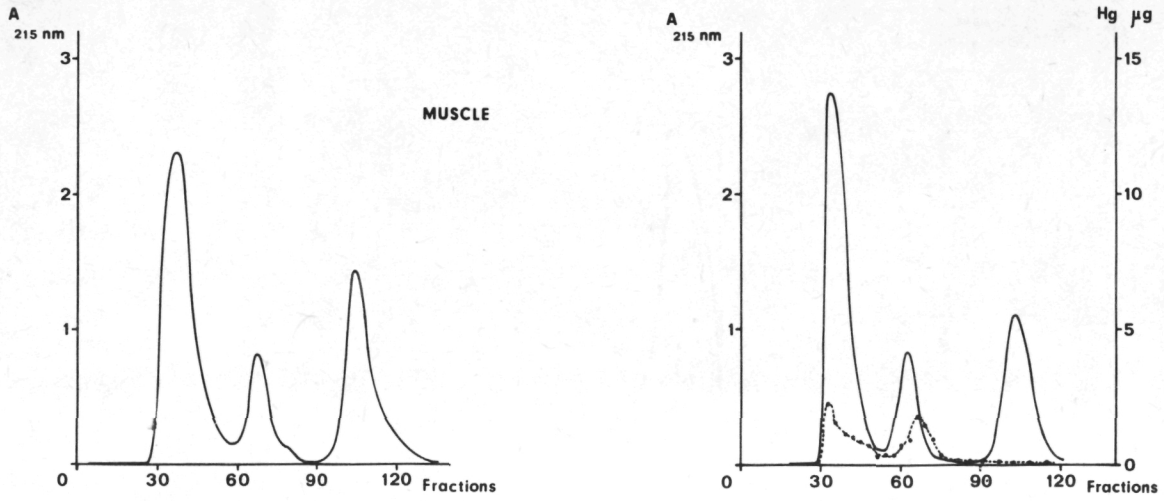


fig. 27.

Elution profiles on Sephadex G 75 columns (5 x 50 cm) of the extracts of different eel tissues. Left side, control fish; right side, intoxicated fish. Hg concentration is expressed in µg/9 mℓ fractions (dotted line).

specimens are homogenized in 3 volumes of 0.5 M sucrose, the extracts are centrifuged and chromatographied on Sephadex G75 columns equilibrated in NH_4HCO_3 0.05 M . Elution is monitored at 254 nm ; the amount of Hg is determined in the fractions as described earlier [Bouquegneau (1973a)]. Amino acid analyses are made using the procedure of Benson and Patterson (1965) and a Beckman amino acid analyser Model 120 B.

Figure 27 shows the typical distribution of Hg in the various fractions obtained from liver, gill, kidney and muscle of chronically intoxicated eels.

Except in the muscle sample most of the Hg is found bound to a protein fraction having a molecular weight close to 10000 daltons.

The mercury carrying fraction of liver extracts shows an unusual protein spectrum, similar to those produced by metallothioneins (fig. 28). Removal of Hg (70 %) by dialysis against chelating agents produces a spectral change also typical of these proteins.

Table 5 shows the amino acid composition of the Hg binding protein from eel liver. The low level in aromatic amino acid residues and the high content in cysteine residues is also characteristic of metallothioneins although the amount of cysteine is smaller than in the proteins extracted from kidney and liver of mammals and birds exposed to Cd and Hg intoxication.

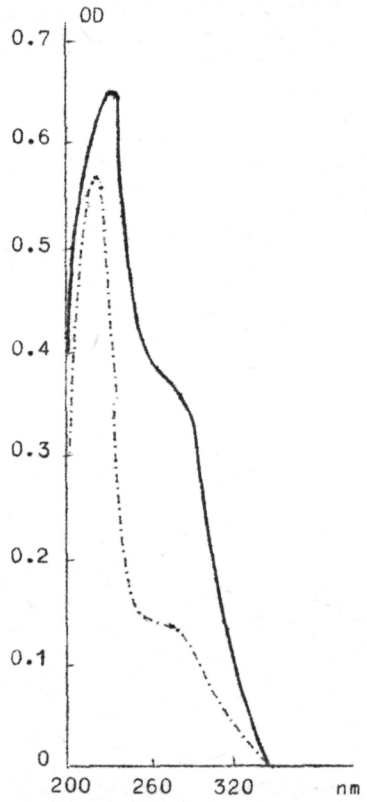
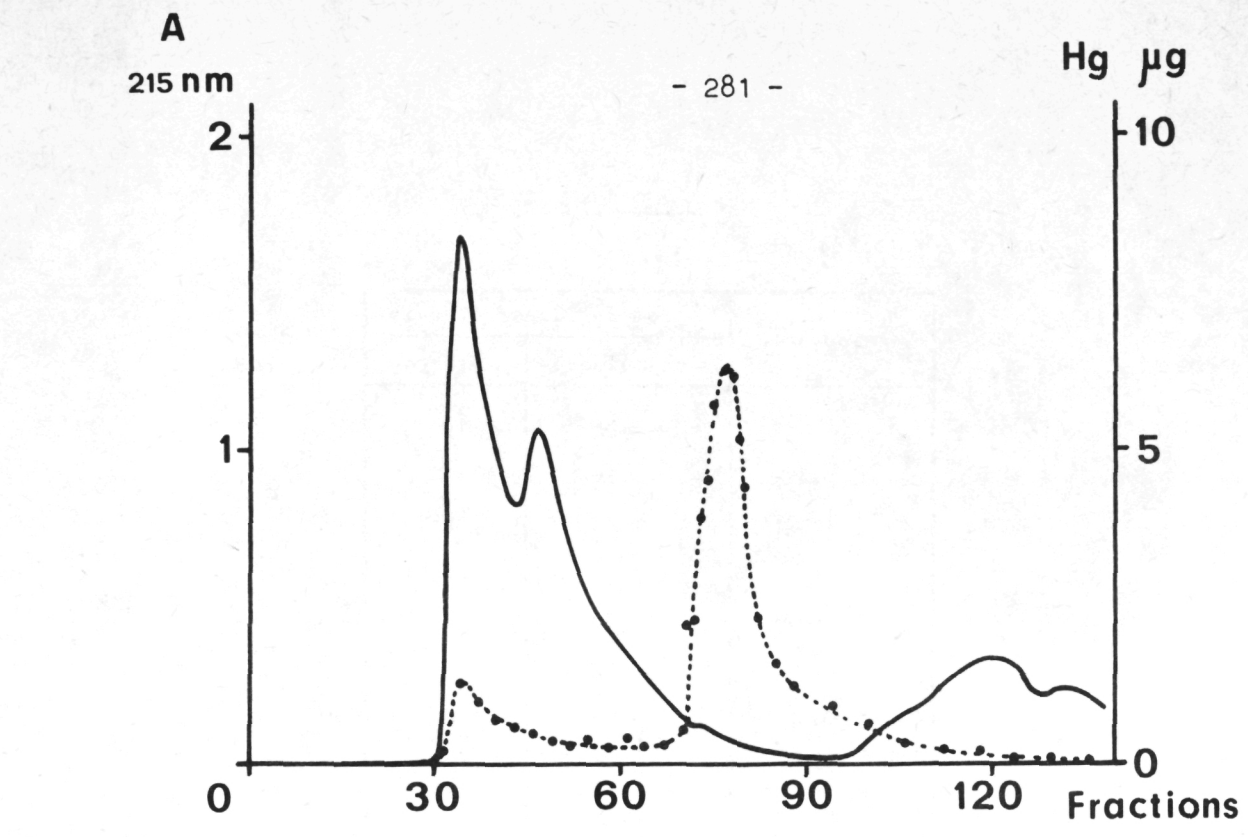


fig. 28.

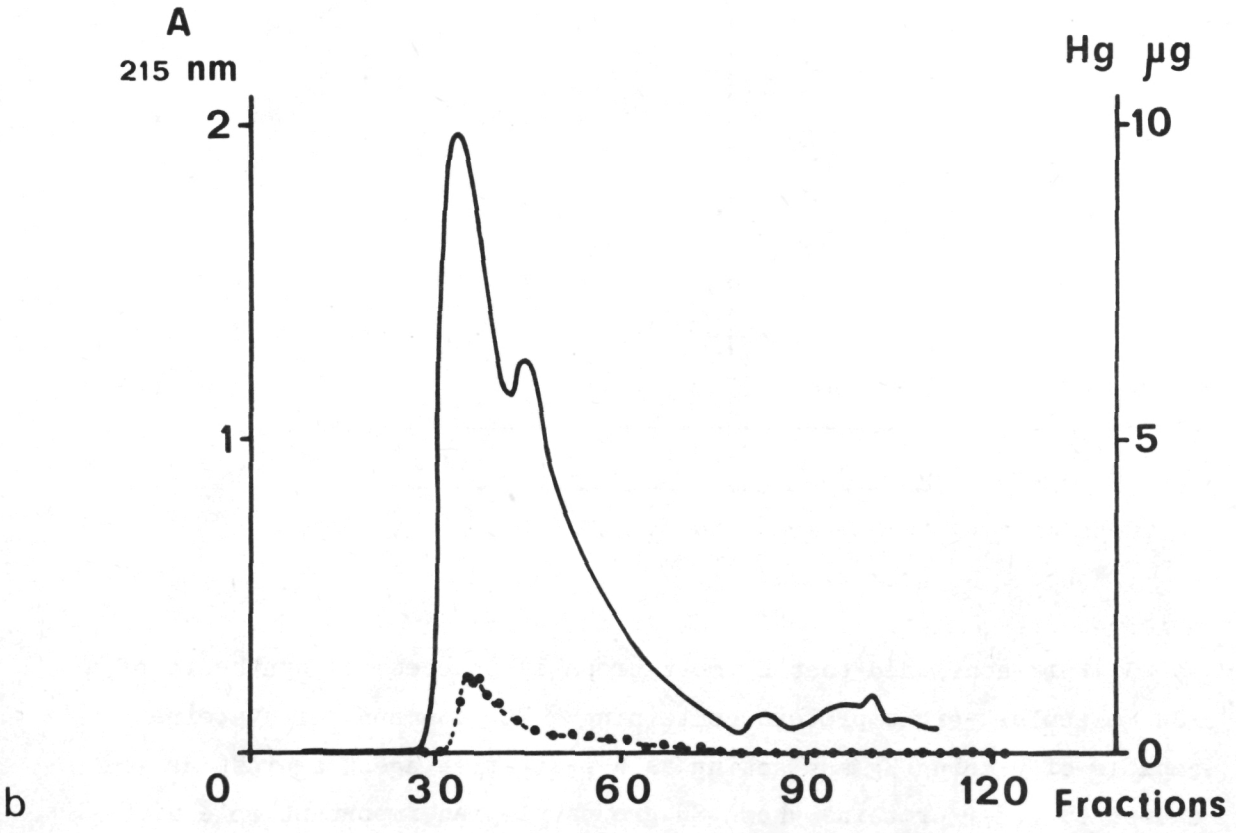
Ultra-violet absorption spectra in NH_4HCO_3 0.05 M of the Hg binding protein of eel liver in presence (———) and absence (·-·-·-·-) of mercury (see text).

To test the role of these proteins in the adaptation mechanism developed by chronically intoxicated eels, the Hg distribution in the different gill protein fractions obtained from eels exposed to 0.4 ppm Hg during 8 days has been compared to the Hg distribution in extracts from acutely intoxicated eels (10 ppm — 5 h) .

Figure 29 shows the elution profiles indicating that in acutely poisoned eels, the Hg is absent in the low molecular weight proteins, revealing that the amount of metallothionein is extremely low. In this case one gram tissue contains 61 µg Hg ; 46 µg are found in the insoluble fraction, the rest in the supernatant is bound to high molecular weight proteins. At sublethal doses one gram tissue contains after 8 days 120 µg Hg ; 23 µg in the insoluble fraction, 97 µg in the supernatant, 78 µg bound to the metallothionein fraction.



a



b

fig. 29.

Elution profiles on Sephadex G 75 columns (5 x 50 cm) of the gill extracts prepared from 1 g gill tissue of chronically (a) and acutely (b) intoxicated eels. Hg concentration is expressed in µg/9 mℓ fractions.

Table 5

Amino acid composition of Hg binding protein in eel liver

Amino acid	N_o of residues/molecule	
	calculated	assumed
Lys	9.60	10
His	1.10	1
Arg	1.70	2
Asp	8.08	8
Thr	6.50	7
Ser	7.60	8
Glu	10.20	10
Pro	10.20	10
Gly	11.10	11
Ala	11.20	11
* Cys (half)	8.60	9
Val	4.80	5
** Met	0.83	1
Ile	3.10	3
Leu	4.60	5
Tyr	0.00	0
Phe	1.06	1
Trp	-	-
Total	100.30	102.0

* determined as cysteic acid

** determined as methionine sulfone

It is concluded that Hg most probably induces the synthesis of a low molecular weight protein containing a large amount of cysteine capable of binding Hg and acting as a protective agent against damage caused to other proteins where SH groups play an important role with respect to their enzymatic activity, linked for instance to the active transport of Na. It is known [Bouquegneau (1973b)] that acutely intoxicated eels die from disruption of the osmotic balance, the Na content of the blood increasing drastically.

3.3.- The effect of Cd on eels (*Anguilla anguilla*) adapted to sea water [Lambot (1975)]

Sea water adapted eels are exposed to natural sea water containing varying concentrations of Cd ($CdCl_2$) . The tissues are mineralized in HNO_3 65 % (2.5 cm^3 per g fresh tissue). The diluted extract is analysed using atomic adsorption techniques (Perkin-Elmer 103 and 303); samples with low Cd content are analysed by polarography after dry mineralization under activated oxygen (Tracer-lab 600). Mineralization with $HNO_3 + H_2O_2$ and extraction (APDC-MIBK) have also been used.

3.3.1.- Mortality curves

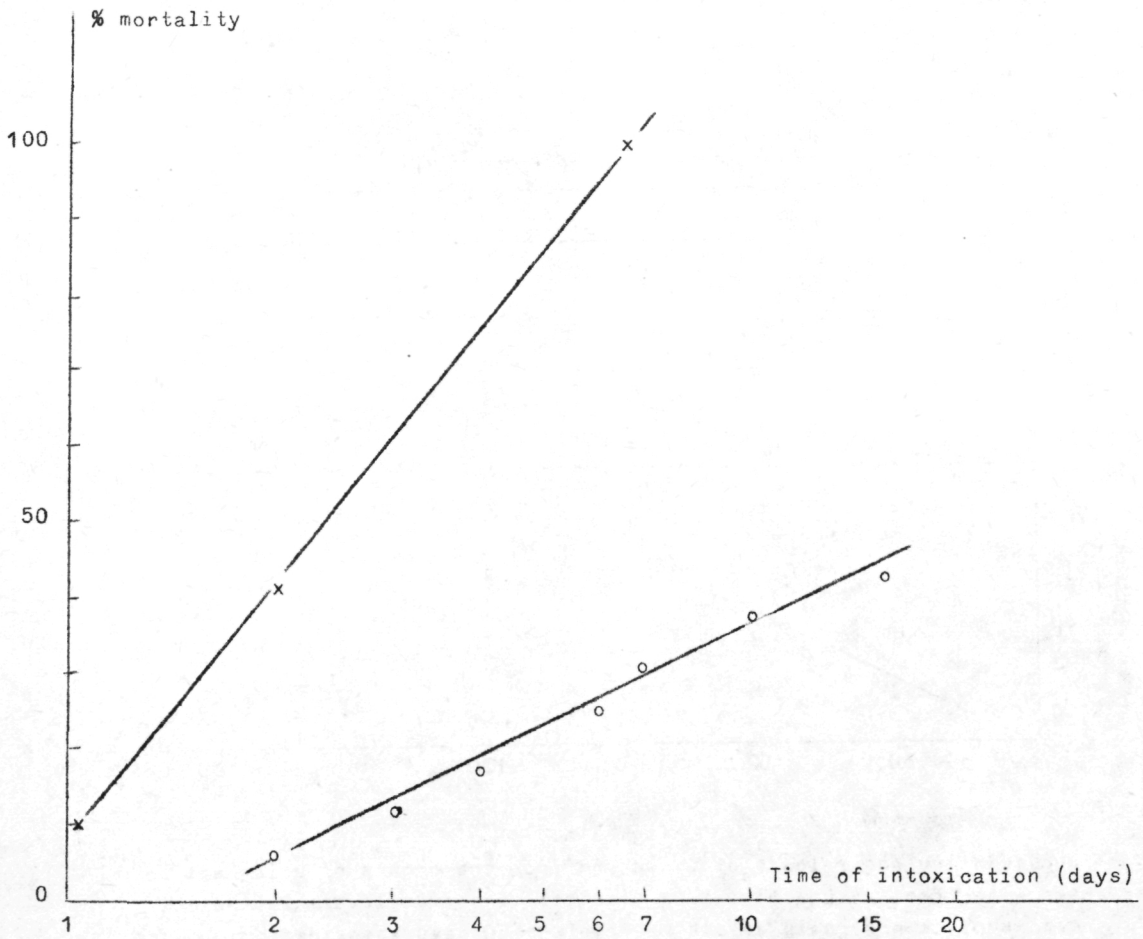


fig. 30.
Mortality curves for eels intoxicated in sea water containing 30 ppm Cd (o) or 80 ppm Cd (x).

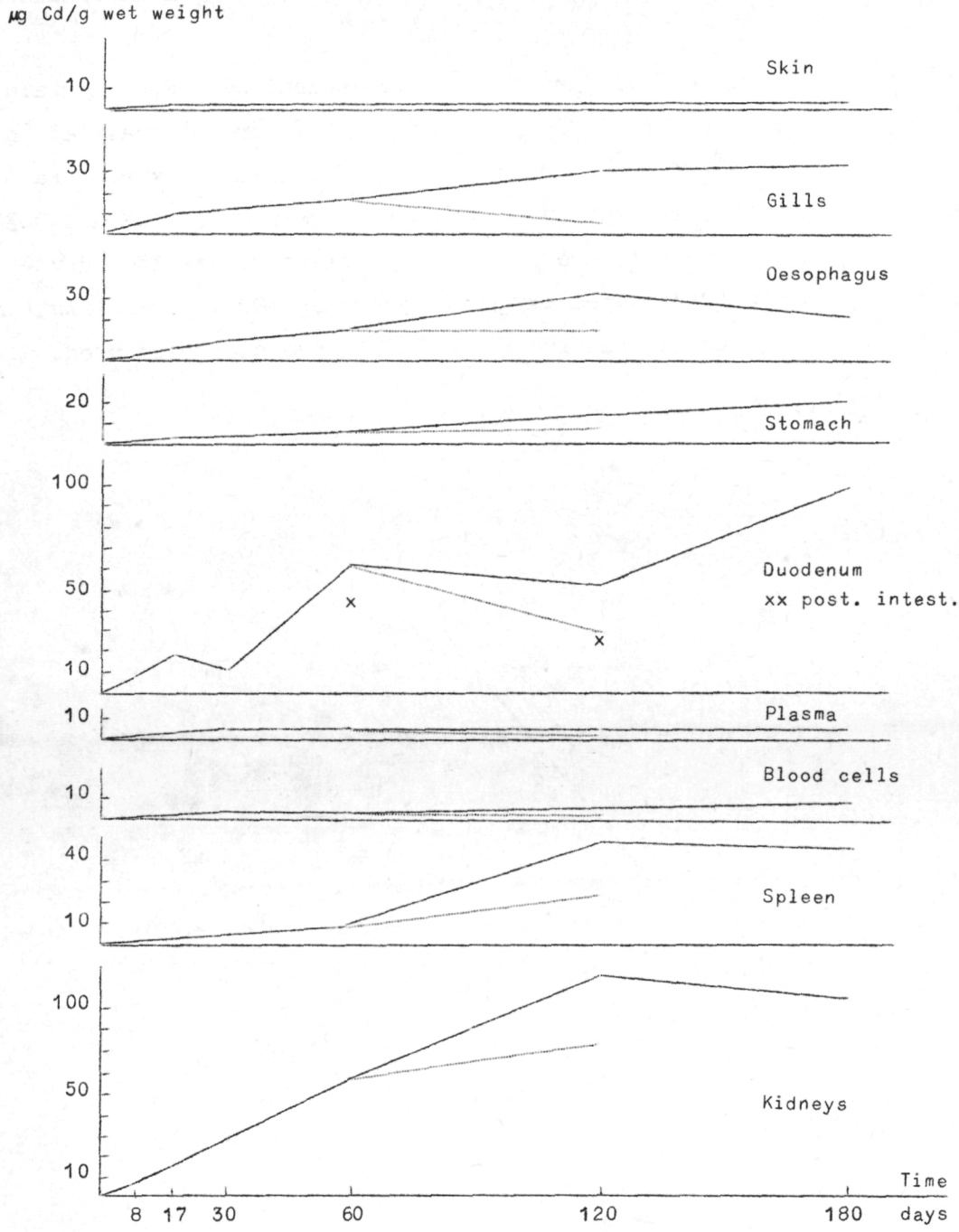


fig. 31a.

Accumulation and release of Cd in and from the organs of eels kept in sea water containing 13 ppm Cd (dotted line : Cd levels in the animals kept in non polluted sea water after 60 days intoxication).

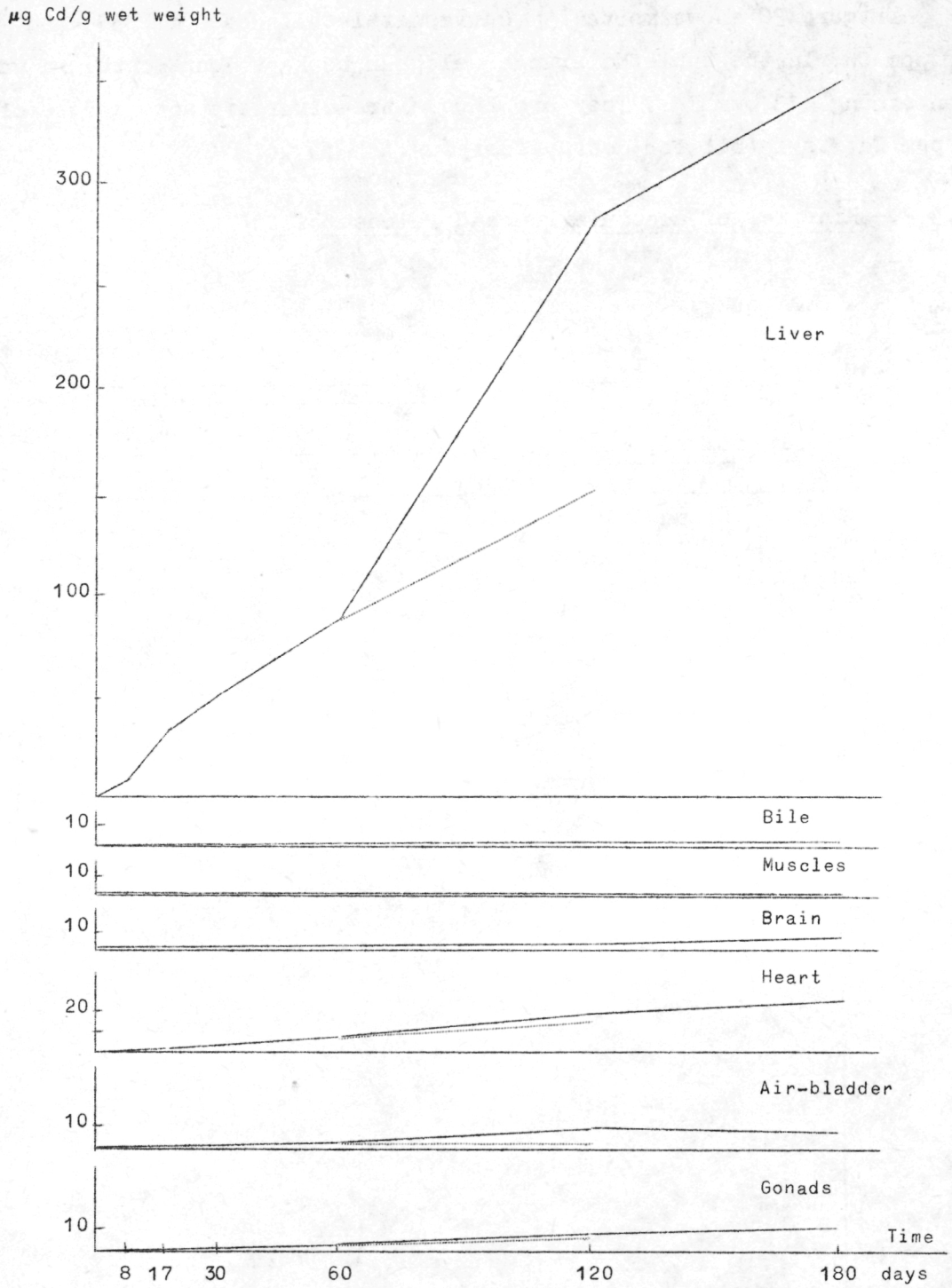


fig. 31b.

Accumulation and release of Cd in and from the organs of eels kept in sea water containing 13 ppm Cd (dotted line : Cd levels in the animals kept in non pelluted sea water after 60 days intoxication).

Figure 30 shows mortality curves at lethal doses of 30 and 80 ppm Cd. In the sublethal range eels can be kept four months in water containing 13 ppm Cd . They are thus extremely resistant; a dose of 5 ppm Cd is lethal for *Cottus scorpius*.

3.3.2.- Kinetics of accumulation and release of Cd

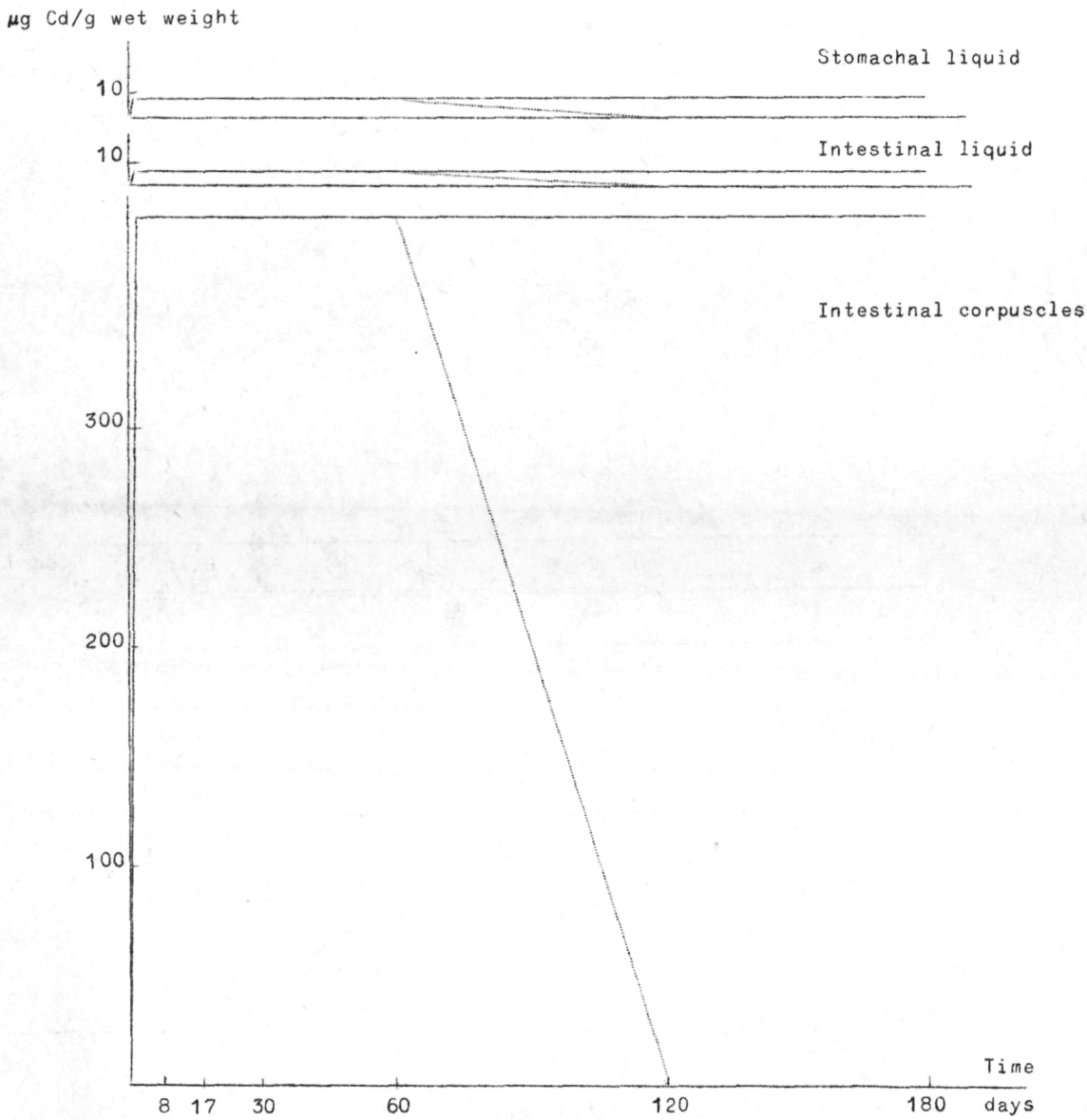


fig. 31c.
Accumulation and release of Cd in and from the organs of eels kept in sea water containing 13 ppm Cd (dotted line : Cd levels in the animals kept in non polluted sea water after 60 days intoxication).

Figure 31 (a,b,c) shows the accumulation of Cd in different organs and body fluids of eels exposed to 13 ppm Cd , some of the animals being kept in non contaminated water after 60 days intoxication.

Accumulation is highest in the liver, kidneys and duodenum. Release is negligible when the loaded animals are kept in normal sea water.

The case of intestinal corpuscles will be dealt with later in this report.

Table 6 gives the distribution of Cd in animals kept during 60 days in sea water containing 0.013 , 0.13 and 13 ppm Cd . Concentration

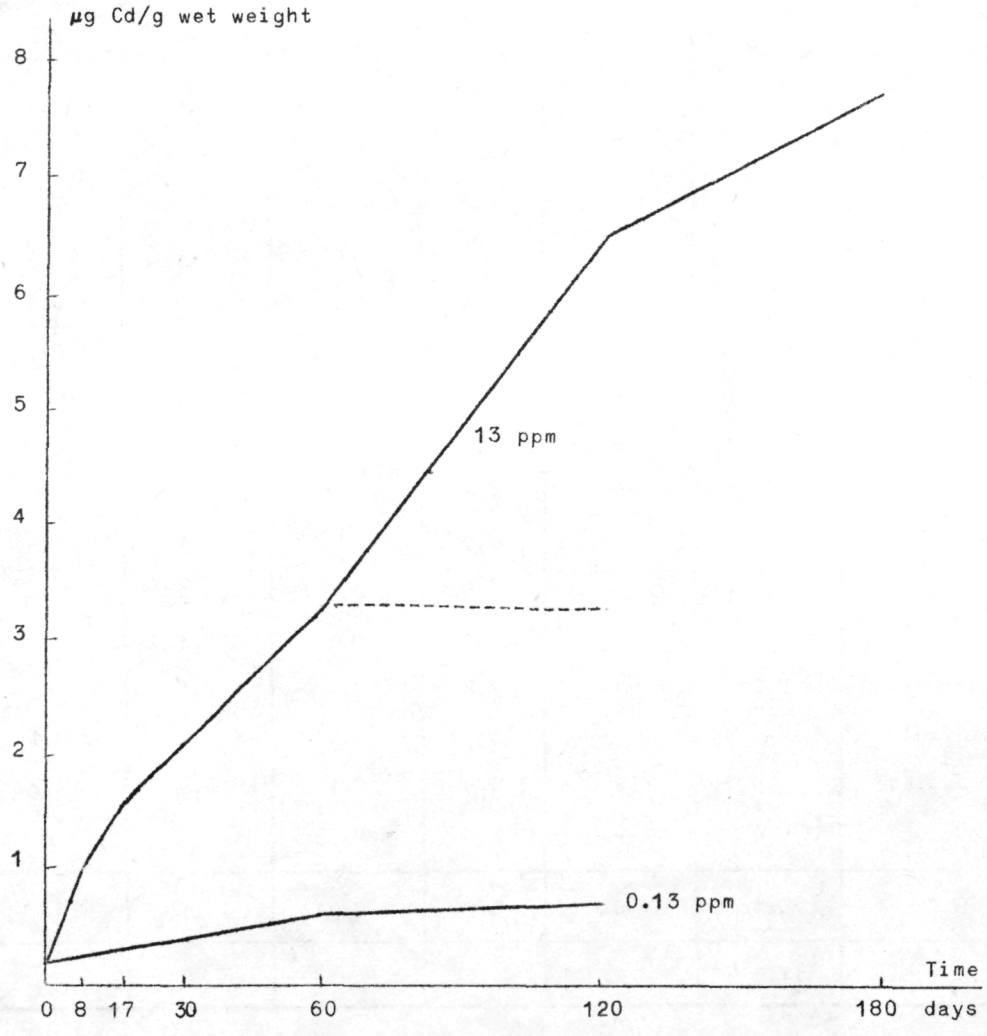


fig. 32.

Accumulation and release of the total Cd load in eels exposed to sea water containing 13 ppm and 0.13 ppm Cd (dashed curve : Cd load in animals kept in non polluted water after initial intoxication).

Table 6

Distribution of Cd in eels intoxicated during 60 days in sea water containing 0.013 , 0.13 or 13 ppm Cd

Cd concentration in sea water	0.013 ppm	0.13 ppm	13 ppm		0.013 ppm	0.13 ppm	13 ppm
Organs	Cd concentration ppm (wet weight)*			Weight of organs(g)	Total amount of Cd (µg)		
Muscles	< 0.5	< 0.5	0.6	75.5	7.5 ?	15.1 ?	43.0
Skin	0.2	0.4	1.2	10.6	2.1	4.2	12.7
Bones	-	-	-	6.6	0.7 ?	1.3 ?	3.8 ?
D.T. Oesophagus	< 0.3	1.5	14.5				
Stomach	< 0.3	-	5.2	Σ = 2.1	1.9	17.4	65.3
Duodenum	2.2	19.2	60.8				
Post. intest.	0.9	4.3	43.8				
Liver	0.9	6.0	88.3	1.2	1.1	7.2	106.0
Kidneys	1.6	21.8	56.2	0.7	1.1	15.3	39.3
Gonads	< 0.2	0.5	3.2	0.7	< 0.1	0.3	2.2
Plasma	0.1	0.3	3.1	0.6	< 0.1	< 0.1	1.8
Gills	0.7	2.6	16.5	0.5	0.3	1.3	8.2
Intest. liquid	< 0.1	< 0.5	5.6	0.4	< 0.1	< 0.1	2.2
Blood cells	0.5	0.3	2.6	0.3	0.1	0.1	0.8
Spleen	0.5	1.7	9.7	0.2	0.1	0.3	1.9
Air bladder	0.4	-	2.5	0.2	< 0.1	-	0.5
Bile	0.4	0.4	1.2	0.1	< 0.1	0.1	0.1
Heart	< 0.2	-	7.8	0.1	< 0.1	-	0.8
Stomachal liquid	-	-	9.7	0.1	< 0.1	< 0.1	1.0
Intest. corpuscles	2.0 ?	22.0	396.0	0.1	0.2	2.2	39.6
Brain	< 0.3	0.5	1.8	< 0.1	-	-	-
Total body	0.15	0.63	3.29	100	15.1	63.5	329.2
Concentration factor	11.6	4.9	0.25				

* 1 ppm = 1 µg/g .

factors $\frac{\text{ppm Cd in tissue or animal}}{\text{ppm Cd in water}}$ are higher the lower the Cd concentrations of the sea water.

Figure 32 shows total body burden versus time at 13 ppm and 0.13 ppm .

It can further be shown that at 13 ppm , after 120 days exposure, the muscles (0.6 ppm Cd) only contain 7 % of the total Cd body load, although they represent 75 % of the body weight. The liver with a weight corresponding to 1 % of the body contains 50 % of the total Cd.

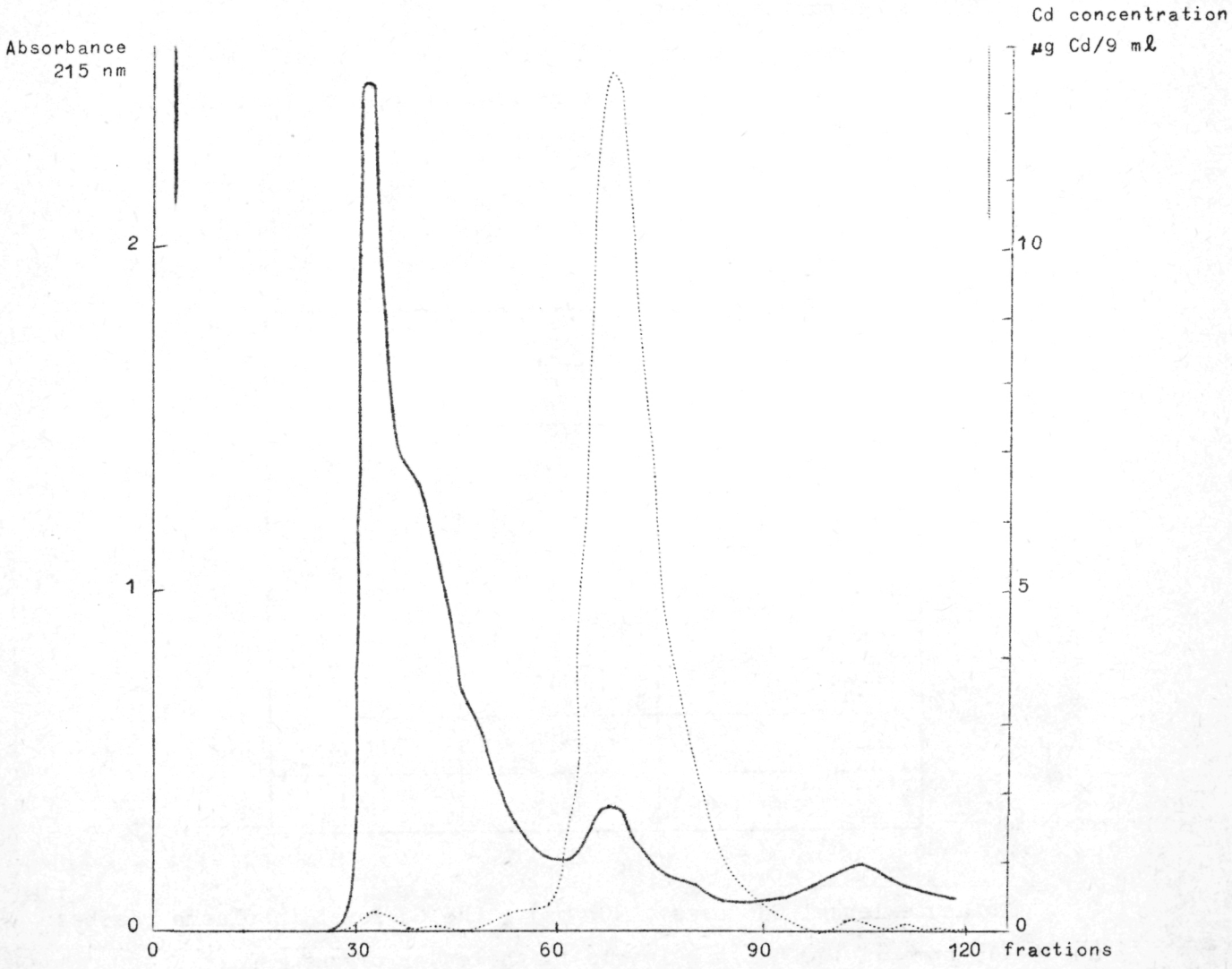


fig. 33.
Eel intoxicated during 120 days in sea water containing 13 ppm Cd . Absorbance and Cd distribution in fractions collected from liver extracts passed on Sephadex G 75 [see Bouquegneau et al. (1975)].

Figure 33 shows that Cd is bound, as Hg, to a metallothionein, the existence of which has also been recently demonstrated in plaice (*Pleuronectes platessa*) by Coombs (1974).

At lower doses (0.13 ppm) the kidneys, the liver and the digestive tract contain 50 % of the total Cd body burden but the duodenum and the kidneys contain more Cd than the liver. In non-intoxicated fish where the total amount of Cd is 0.1 - 0.2 ppm the concentration is also maximum in the kidneys. Storage in the liver seems to happen only at high Cd concentration ranges.

Comparison with Hg intoxicated eels is shown in table 7 and shows how different the two metals are distributed between the organs.

Table 7

Comparison between the distribution of Hg and Cd in the organs of eels exposed to contaminated sea water

Organs	0.13 ppm Cd 60 days	0.1 ppm Hg 32 days
	Total Cd in µg	Total Hg in µg
Muscles	15.1	1136.3
Skin	4.2	163.6
Digestive tract	17.4	36.3
Gills	1.3	126.7
Liver	7.2	43.7
Kidneys	15.3	92.6
Total body	63.5	1614.4
Concentration factor	4.9	162

At acute lethal Cd doses (90 ppm), the Cd level in plasma reaches about 15 ppm in 10 h, the levels in the other organs remain below or are equal to those observed during prolonged sublethal actions.

3.3.3.- Intestinal corpuscles

Both in sea water adapted eels and scorpion fishes, white mucus corpuscles (~ 1 μ diam) are observed in the intestine. They are also present in fresh water eels.

In eels intoxicated with Cd these corpuscles are found to contain enormous amounts of Cd (see table 8).

Table 8

Cd content of intestinal corpuscles from eels intoxicated at different Cd concentrations

Cd concentration in sea water (ppm)	Cd concentration in the intestinal corpuscles (ppm) (wet weight)			Maximum concentration factor
	Min	Max	m	
0.005 (= SW from the aquarium)			< 4	
0.013			< 4	< 307
0.13	5	27	22	207
0.9	7	71	55	79
13.0	141	859	396	66
90	33	3397	942	38

Although their weight fraction is very small (0.1 g) they carry after 8 days intoxication at 13 ppm half the total Cd found in the animal. After 120 days the corpuscles carry as much Cd as all the muscles.

Corpuscles from non intoxicated eels retain Cd *in vitro* : put into distilled water containing 90 ppm Cd , they contain 2.188 ppm Cd after 6 h treatment. The same is observed in sea water.

The corpuscles taken after 6 h from eels exposed to 90 ppm Cd contain about the same amount (3000 ppm Cd) as found in corpuscles directly exposed to a solution containing identical Cd concentration. The same is true at other Cd concentrations and it thus seems that Cd is simply adsorbed on the corpuscles directly from the sea water ingested by the animal. The effect is to considerably lower the Cd concentration in

the intestine : in one experiment at 90 ppm Cd in the sea water, the Cd concentration was found to be 45 ppm in the stomacal liquid and only 1.3 ppm in intestinal liquid; the corpuscles carried 3000 ppm Cd . The presence of corpuscles would therefore protect the intestinal wall and greatly limit the entry of Cd by this route.

Table 9

Composition of intestinal corpuscles of sea water adapted eels

Element	ppm (dry weight)
Mg	126,000
Ca	75,000
Na	20,500
S	5,400
K	1,300
Sr	700
P	600
Si	150
As	74
Zn	46
Ti	31
Fe	27
F	20
Al	15
Cr	11
Br	10
Ba	5
Sb	5

The average composition of the corpuscles is given in table 9. Their content in Ca and Mg is very high, and these metals are probably present under the form of carbonates, precipitated in an organic matrix formed from mucous secretions and cellular debris.

The Cd concentration observed in muscle animals in non contaminated sea water (1 - 5 ppb Cd) is of the order of 0.03 - 0.10 ppm, rising sometimes to 0.4 ppm . After 120 days in sea water containing 13 ppm Cd, the concentration in the muscles only reaches 0.6 ppm . Direct intoxication by Cd has thus probably little effect in natural conditions on the average level found in fish muscles. However it is obvious that the

viscera although their weight fraction is small can carry an important part of the total burden and their Cd content should be controlled. Whether ingestion of contaminated food has a bearing on the Cd level in fish remains an open question and awaits further experimentation.

Fish seem to be protected against the toxic effects of Cd by the formation of metallothionein at least in the liver and also by the presence of intestinal corpuscles capable of adsorbing large amounts of Cd, subsequently eliminated.

4.- General conclusions

1) Whether in invertebrates or vertebrates, and in the case of diatoms direct intoxication quickly rises the heavy metal burden of exposed animals or plants; the release when back in non-contaminated water, at least in animals, seems to be a comparatively slow process involving the redistribution of the heavy metals within the body, the half life being largest in muscle. With diatoms Zn seems to quickly adsorb on the cell walls; its subsequent fate depends strongly on the growth aptitude retained under intoxication.

2) Marine species seem in general extremely resistant in presence of heavy metals and are capable of accumulating large amounts of these, becoming a potential danger to man as food. The resistance can be explained in the case of fish by the production of low molecular weight proteins containing large amounts of SH groups having high affinities for heavy metals like Hg, Cd, etc. These metallothioneins normally control the cell content in essential metals like Zn and Cu. Their synthesis is enhanced when large amounts of heavy metals are present in water. It should be interesting to look for these proteins in marine invertebrates. If the aquatic animal life is capable of synthetizing more rapidly large amounts of such proteins then terrestrial animals or plants do, then the danger of consuming contaminated marine food at a rate greater than the rate at which mammals for instance are capable of producing metallothionein might be the final due to determine tolerable contamination levels in aquatic

animals. The whole problem of tolerable doses would boil down to an estimate of the defense capacity of terrestrial animals first, in terms of the kinetics of their protective proteins production. By no doubt many marine species can accumulate enormous doses of heavy metals, lethal to man, without difficulties. Little damage is therefore expected to be caused to marine life by dumping heavy metals in the sea. The danger of eutrophication, with all its ecological changes, appears far more important.

Both types of pollution have an impact on man, the former because it lowers the quality of marine food, the other because it lowers the amount of consumable food produced. On the other hand, in heavily eutrophicated regions heavy metals easily bind to organic suspended matter and sediments, anoxic conditions lead to stable compounds and the potential danger of heavy metals is lowered. Regression of eutrophication might lead to the release of heavy metals and subsequent direct contamination of marine life at all levels. The kinetics of intake are generally fast compared to the release mechanisms : to trap heavy metals in eutrophicated areas and subsequently to release them by suddenly controlling PO_4 , NO_3 , etc. sources, would simply substitute to continuous dumping a sort of square wave action which obviously should be avoided by determining the optimal rate of reversal to normal conditions.

3) Water quality tests either using phytoplankton, larvae, fish, etc. will all give different results depending on how the test is carried out and the type of organism used. The author believes that field surveys are far more efficient to determine the intensity of pollution and its type.

4) Direct intoxication is obviously important for marine species ingesting or filtering great amounts of water; the effect of pollutants moving through the food chain is still difficult to assess, although many results seem to indicate that direct contamination is more effective. Further studies are needed to clarify this point.

5) Adsorption and desorption of heavy metals on particulate matter, organic or inorganic, on living cells, on particles inside animals (like

those formed to bind large amounts of Cd in fish) are to be studied more carefully; in the case of phytoplankton, at least for diatoms, this process might prove to be an important entry route not only for heavy metals but for other pollutants.

6) More studies are needed on the benthic fauna physiology with respect to accumulation of toxic substances and possible rate of release in correlation with local substrate and water quality.

7) Efforts should be continued to obtain kinetic data as required for modelling marine systems [Nihoul (1975)] at all levels of marine life and to try and group animals and plants with respect to their main physiological behaviour (oxygen and CO_2 consumers or producers, filter feeders, scavengers, detritus feeders, predators, etc.) to try and evaluate the rate of energy flow through the globalized system together with the fate of the toxic substances resulting from man's impact on the marine ecosystem.

References

BENIJTS, F., CLAUS, C., SORGELOOS, P., (1974a). Belgian Nat. R.D. Progr. Environment – Water – Sea Project – *Technical Report 1974/PHYSIOL. SYNTHESE 03.*

BENIJTS, F., VANHECKE, L., PERSOONE, G., (1974b). Belgian Nat. R.D. Progr. Environment – Water – Sea Project – *Technical Report 1974/PHYSIOL. SYNTHESE 01.*

BENIJTS, F., VANHECKE-SARLET, L., PERSOONE, G., (1974c). Belgian Nat. R.D. Progr. Environment – Water – Sea Project – *Technical Report 1974/PHYSIOL. SYNTHESE 02.*

BENSON, J.V. and PATTERSON, J.A., (1965). *Analyt. Chem., 37,* 1108-1110.

BOUQUEGNEAU, J.M., (1973a). Belgian Nat. R.D. Progr. Environment - Water - Sea Project - *Technical Report 1973/PHYSIOL. SYNTHESE 06.*

BOUQUEGNEAU, J.M., (1973b). *Bull. Soc. Roy. Sc. Liège, 9-10,* 447-455.

BOUQUEGNEAU, J.M., (1975). Belgian Nat. R.D. Progr. Environment - Water - Sea Project - *Technical Report 1975/PHYSIOL. SYNTHESE 01.*

BOUQUEGNEAU, J.M., GERDAY, Ch. and DISTECHE, A., (1975). Belgian Nat. R.D. Progr. Environment - Water - Sea Project - *Technical Report 1975/PHYSIOL. SYNTHESE 03.*

COOMBS, T.L., (1974). Nato Sc. Com. Conf. on Eco-Toxicity of Heavy Metals and Organo-Halogen Compounds.

COSTLOW *et al.*, (1971). *4th European Marine Biol. Symp.*, Ed. Crisp, Cambridge University Press, 211-220.

DIETRICH, G. and KALLE, K., (1963). *General Oceanography*, Interscience, New-York.

FIMREITE, N. *et al.*, (1971). *The Canadian Field Naturalist, 85* (3), 211.

GRAY, J. and VENTILLA, R., (1973). *Ambio, 2* (4), 118-121.

LAMBOT, F., (1975). Belgian Nat. R.D. Progr. Environment - Water - Sea Project - *Technical Report 1975/PHYSIOL. SYNTHESE 02.*

Marine Algal assay Procedure Bottle Test : Eutrophication and Lake Resteration Branch National Environmental Research Center - Corvallis - December 1974.

NIHOUL, J.C.J. (ed.), (1975). *Modelling of Marine Systems*, Elsevier, Oceanogr. Series.

PERPEET, Ch. and VLOEBERGH, M., (1973). Belgian Nat. R.D. Progr. Environment - Water - Sea Project - *Technical Report 1973/BIOL. SYNTHESE 05.*

PERPEET, Ch. and VLOEBERGH, M., (1974). Belgian Nat. R.D. Progr. Environment - Water - Sea Project - *Technical Report 1974/PHYSIOL. SYNTHESE 01.*

VANDEN BOSSCHE, J.P., (1975). Belgian Nat. R.D. Progr. Environment - Water - Sea Project - *Technical Report 1975/PHYSIOL. SYNTHESE 04.*

WALNE, P. (1956). *Fish. Invest. Lond. Soc., 20* (9).